

School of Applied Science

Department of Applied Physics

Measurement of Lead Isotopes in Snow and Ice from Law Dome and other sites in Antarctica to characterize the Lead and seek evidence of its origin

Paul Travis Vallelonga

This thesis is presented as part of the requirements for the award of the Degree of Doctor of Philosophy of the Curtin University of Technology.

September 2002

Abstract

Human activities such as mining and smelting of lead (Pb) ores and combustion of alkyllead additives in gasoline have resulted in extensive global Pb pollution. Since the late 1960's studies of polar ice and snow have been undertaken to evaluate the extent of anthropogenic Pb emissions in recent times as well as to investigate changes in anthropogenic Pb emissions in the more distant past. The polar ice sheets have been used to investigate Pb pollution as they offer a long-term record of human activity located far from pollution sources and sample aerosol emissions on a hemispheric scale. Lead isotopes have been previously used to identify sources of Pb in polar snow and ice, while new evaluations of Pb isotopic compositions in aerosols and Pb ore bodies allow more thorough evaluations of anthropogenic Pb emissions.

Lead isotopic compositions and Pb and Barium (Ba) concentrations have been measured in snow and ice core samples from Law Dome, East Antarctica, to produce a detailed pollution history between 1530 AD and 1989 AD. Such a record has been produced to evaluate changes in anthropogenic Pb emission levels and sources over the past 500 years, to determine when industrial (anthropogenic) activities first began to influence Antarctica and also to investigate natural Pb fluxes to Antarctica. Additional samples were also collected from Law Dome snow and ice cores to respectively investigate seasonal variations in Pb and Ba deposition, and the influence of the 1815 AD volcanic eruption of Tambora, Indonesia.

All samples were measured by thermal ionisation mass spectrometry, for which techniques were developed to reliably analyse Pb isotopic compositions in Antarctic samples containing sub-picogram per gram concentrations of Pb. Particular attention was given to the quantity of Pb added to the samples during the decontamination and sample storage stages of the sample preparation process. These stages, including the use of a stainless steel chisel for the decontamination, contributed ~5.2 pg to the total sample analysed, amounting to a concentration increase of ~13 fg g⁻¹. In comparison, the mass spectrometer ion source contributed typically 89 ± 19 fg to the blank, however its influence depended upon the amount of Pb available for analysis and so had the greatest impact when small volumes of samples with a very low concentration were analysed. As a consequence of these careful investigations of the

Pb blank contributions to the samples, the corrections made to the Pb isotopic ratios and concentrations measured are smaller than previously reported evaluations of Pb in Antarctica by thermal ionisation mass spectrometry.

The data indicate that East Antarctica was relatively pristine until ~1884 AD, after which the first influence of anthropogenic Pb in Law Dome is observed. “Natural”, pre-industrial, background concentrations of Pb and Ba were ~ 0.4 pg/g and ~ 1.3 pg/g, respectively, with Pb isotopic compositions within the range $^{206}\text{Pb}/^{207}\text{Pb} = 1.20 - 1.25$ and $^{208}\text{Pb}/^{207}\text{Pb} = 2.46 - 2.50$ and an average rock and soil dust Pb contribution of 8-12%. A major pollution event was observed at Law Dome between 1884 and 1908 AD, elevating the Pb concentration fourfold and changing $^{206}\text{Pb}/^{207}\text{Pb}$ ratios in the ice to ~1.12. Based on Pb isotopic systematics and Pb emissions statistics, this was attributed to Pb mined at Broken Hill and smelted at Broken Hill and Port Pirie, Australia. Anthropogenic Pb inputs to Law Dome were most significant from ~1900 to ~1910 and from ~1960 to ~1980. During the 20th century, Ba concentrations were consistently higher than “natural” levels. This was attributed to increased dust production, suggesting the influence of climate change and/or changes in land coverage with vegetation.

Law Dome ice dated from 1814 AD to 1819 AD was analysed for Pb isotopes and Pb, Ba and Bismuth (Bi) concentrations to investigate the influence of the 1815 AD volcanic eruption of Tambora, Indonesia. The presence of volcanic debris in the core samples was observed from late-1816 AD to 1818 AD as an increase in sulphate concentrations and electrical conductivity of the ice. Barium concentrations were approximately three times higher than background levels from mid-1816 to mid-1818, consistent with increased atmospheric loading of rock and soil dust, while enhanced Pb/Ba and Bi/Ba ratios, associated with deposition of volcanic debris, were observed at mid-1814 and from early-1817 to mid-1818. From the results, it appeared likely that Pb emitted from Tambora was removed from the atmosphere within the 1.6 year period required to transport aerosols to Antarctica. Increased Pb and Bi concentrations observed in Law Dome ice ~ 1818 AD were attributed to either increased heavy metal emissions from Mount Erebus, or increased fluxes of heavy metals to the Antarctic ice sheet resulting from climate and meteorological modifications following the Tambora eruption.

A non-continuous series of Law Dome snow core samples dating from 1980 to 1985 AD were analysed to investigate seasonal variations in the deposition of Pb and Ba. It was found that Pb and Ba at Law Dome do exhibit seasonal variations in deposition, with higher concentrations of Pb and Ba usually observed during Summer and lower concentrations of Pb and Ba usually observed during Autumn and Spring. During Autumn-Spring 1985, however, this seasonal pattern was apparently reversed, with high concentrations during the Autumn and Spring seasons. At Law Dome, broad patterns of seasonal Pb and Ba deposition are evident however these appear to be punctuated by short-term deposition events or may even be composed of a continuum of short-term deposition events. This variability suggests that complex meteorological systems are responsible for the transport of Pb and Ba to Law Dome, and probably Antarctica in general.

Acknowledgements

I would first like to acknowledge the support of my supervisor, Prof. Kevin Rosman, for providing guidance, inspiration, wisdom and enthusiasm at the necessary times and for believing in me. Hearty thanks go to Dr. Jean-Pierre Candelone for giving generously of his knowledge and time and principles, and putting up with me and freezing for months at a time. The staff of the John de Laeter Centre of Mass Spectrometry, particularly Dr. Robert Loss, Dr. Andreas Bollhöfer and Dr. David Nelson, are also generously thanked for their knowledge, valuable assistance and interest. While Mr. Graeme Burton also falls in that category, he is additionally acknowledged for keeping us all caffeinated, stocked with the necessary bottles and laboratory supplies and for keeping the mass spectrometer going consistently and reliably, an achievement in itself. Thanks also to Dr. Katja Van de Velde, a great person to work with and an inspiration in the lab. Very little of this work would have been possible without the assistance of Mr. Peter Brooker and Mr. David Prior, for maintaining, fixing and creating many things mechanical and electrical, respectively. My thanks also go to the many students of the John de Laeter Centre of Mass Spectrometry who have put up with my ramblings on so many Friday afternoons, particularly Adam Frew. To keep the acknowledgements to *only* two pages, I will broadly thank the secretary and staff of the Department of Applied Physics, the postgrads and the School Support Unit – you know who you are. Finally, I would like to extend my utmost gratitude to Emeritus Professor John de Laeter for his efforts in the Centre of Mass Spectrometry group and in the Physics Department, to support and nurture the continuing growth of physics and inspire us with his humility and incredible capacity for research, publication and hockey.

The staff and students of the Antarctic Co-operative Research Centre, particularly Mr. Vin Morgan, Dr. Tas van Ommen, Dr. Mark Curran and Dr. Barbara Smith, and the C.S.I.R.O. Marine Laboratories are thanked for their knowledge, support and guidance and for making Hobart a nice place to visit.

This research has been supported by grants from the Australian Research Council (A39938047) and the Antarctic Science Advisory Committee (No. 1092) in the Glaciology Section. My undertaking of this research was made possible by a Teaching Assistanceship granted by the Curtin University of Technology Office of Research and Development and supported by the Department of Applied Physics,

while its completion was made possible by special funding provided by Professor John de Laeter.

I would like to thank all of my family for supporting me and for accepting my extended absence. I would like to thank my friends for supporting me and for accepting my extended presence. And I would like to thank Alison, for making the end worthwhile.

Thesis scope within that of Australian Research Council Grant A39938047

This research was undertaken within the scope of a larger research program involving the collaboration of laboratories in Australia, France, Italy and the United Kingdom. Funding was provided for the evaluation of Pb pollution records at three locations in Antarctica: Law Dome, Victoria Land and Coats Land. Through personal communication with Professor Kevin Rosman, chief investigator of the research program, access has been provided to the pollution records produced for Coats Land and Victoria Land, however these data do not represent part of the thesis research. **This thesis is solely concerned with the production and evaluation of data pertaining to Law Dome, Antarctica.** Data from Coats Land and Victoria Land are only included to assist in the interpretation of the record produced here for Law Dome, and to hypothesize on potential fluxes of Pb and Ba to Antarctica in general. The Victoria Land data has not yet been published, while the Coats Land data is currently in press [(Planchon et al. 2002b), subsequently published in 2003, v.67, pp.693-708].

The Law Dome samples were obtained by the Australian Antarctic Division and supplied to Curtin University through the Antarctic CRC, while the Victoria Land samples were obtained by the Italian National Program for Antarctic Research and supplied to the Department of Environmental Sciences in Venice. The Coats Land samples were obtained by the British Antarctic Survey and supplied to the Laboratory of Glaciology and Environmental Geophysics in Grenoble, France.

Thesis structure and presentation of research articles

This thesis is presented in a somewhat unconventional structure. It consists of four main chapters - Introduction, Methods, Literature Review and Results. From the research undertaken, three papers (research articles) have been written and submitted to peer-reviewed internationally-recognized journals:

- One paper documenting the techniques and procedures utilized in the analysis of the Law Dome samples (Published in *Analytica Chimica Acta*, 2002, v.453, pp.1-12)
- One paper documenting the Law Dome Pb and Ba record for approximately the past 500 years (In press to *Earth and Planetary Science Letters* at the time of writing, subsequently published 2002, v.204, pp.291-306)
- One paper documenting fluxes of Pb, Ba and Bi to Law Dome during the eruption of Tambora, a volcano in Indonesia, in April 1815 AD (Submitted to *Earth and Planetary Science Letters* at the time of writing, subsequently accepted).

These papers were written through the course of the research. Each features a particular analysis of one aspect of the project and provides its own background and summary material regarding that topic. They have been incorporated into the structure of the thesis in their published or submitted forms. In accordance with the form of a thesis by publications, substantial literature review and results sections have been prepared. In contrast, the introduction and methods sections have been prepared with a view to providing balance to the content of the thesis by documenting topics which are of importance to this research but were not adequately described in the research articles.

Table of Contents

Abstract	i
Acknowledgements	iv
Thesis scope within that of Australian Research Council Grant A39938047	vi
Thesis structure and presentation of papers	vii
Table of Contents	viii
List of Tables	x
List of Figures	xi
Chapter 1. Introduction	1
1.1 Lead	1
1.2 History of Pb production and its use	3
1.3 Natural and anthropogenic emissions of Pb into the atmosphere	6
1.4 Atmospheric transport of aerosols	8
1.5 Polar ice cores	9
1.6 Analyses of heavy metals in polar snow and ice	13
1.7 Research objectives	15
Chapter 2. Methods	16
2.1 Ice cores	16
2.2 Ice core decontamination procedure	19
2.3 The Femtolab	28
2.4 The VG 354 thermal ionisation mass spectrometer	35
2.5 RESEARCH ARTICLE: Recent advances in measurement of Pb isotopes in polar ice and snow at sub-picogram per gram concentrations using thermal ionisation mass spectrometry.	45
Chapter 3. Literature Review	58
3.1 The first reliable evaluation of Pb concentrations in polar snow and ice	61
3.2 Studies of heavy metals in ice and snow: 1969 to 1981	68
3.3 Studies of Pb concentrations in Antarctica: 1983 – 1993	75
3.4 Evaluations of heavy metals emissions: 1980 to the present	86
3.5 Analyses of Pb in Greenland ice and snow: 1991 to the present	96
	viii

3.6 Analyses of Pb in Antarctica: 1993 to the present	145
Chapter 4. Results & Discussion	185
4.1 Changes in Pb and Ba concentrations and Pb isotopes at Law Dome over the past 500 years	185
4.2 RESEARCH ARTICLE: The lead pollution history of Law Dome, Antarctica, from isotopic measurements on ice cores: 1500 AD to 1989 AD	190
4.3 Comparison of Law Dome and Coats Land pollution records	207
4.4 Evaluation of Pb and Ba concentrations and Pb isotopes at Victoria Land since 1891 AD	218
4.5 Natural Pb and Ba inputs at Law Dome, Coats Land and Victoria Land.	225
4.6 RESEARCH ARTICLE: Lead, Ba and Bi in Antarctic Law Dome ice corresponding to the 1815 AD Tambora eruption: an assessment of emission sources using Pb isotopes.	231
4.7 Natural Pb deposition in Antarctica, and the influence of Mount Erebus.	265
4.8 Seasonal variations of Pb in Law Dome snow, 1980 – 1985 AD.	267
Chapter 5. Conclusions & recommendations	276
Chapter 6. References	279
Appendices	291
1. Law Dome, Coats Land and Victoria Land data	
2. Lead and Ba isotopic tracer solution calibration	
3. Research Article: Lead fluxes and Pb isotopic compositions from Masaya Volcano, Nicaragua.	

List of Tables

Table 1.1. Worldwide emissions of Pb from natural sources.

Table 1.2. Natural versus anthropogenic emissions of trace metals to the atmosphere in 1983.

Table 2.1. Physical characteristics of Law Dome ice cores studied.

Table 3.1. Averaged concentrations of sea salt- and dust-related elements in ice samples from Greenland and Antarctica.

Table 3.2. Amount of Pb (in 10^3 tonnes) smelted or burned each year since 1750 AD.

Table 3.3. Past and present-day deposition fluxes of heavy metals to the Greenland ice cap.

Table 3.4. Annual Pb emissions from major Southern Hemisphere sources, 1925-1986.

Table 3.5. Measurement of the Pb concentration and isotopic composition of a sample using a ^{205}Pb spike.

Table 3.6. Measurements on selected samples reflecting the measurement precision achieved by Chisholm et al. (1995).

Table 3.7. Trace metal concentrations and Pb isotopic compositions in Taylor Dome ice samples.

Table 3.8. Trace metal concentrations expected in ice, as contributions from rock and soil dusts present in Taylor Dome ice samples.

Table 4.1. Average Ba concentrations in various Antarctic sites, 1530 – 1994.

Table 4.2. Calculation of contributions of dust- and Mount Erebus-type Pb in Victoria Land samples, assuming a binary mixture.

Table 4.3. Summary of crustal Pb inputs at various locations in Antarctica.

List of Figures

- Figure 1.1. The radiogenic growth curve for terrestrial Pb: $^{207}\text{Pb}/^{204}\text{Pb}$ vs $^{206}\text{Pb}/^{204}\text{Pb}$.
- Figure 1.2. World Pb production during the past 5500 years.
- Figure 1.3. Recent historical changes in mine production and anthropogenic emissions of lead to the atmosphere.
- Figure 1.4. Diagram illustrating the trapping process for air bubbles in snow and ice strata near the close-off layer.
- Figure 2.1. Locations of some ice-core sites at Law Dome, East Antarctica, with inset showing locations of Law Dome, Dome C and Vostok in Antarctica.
- Figure 2.2. Layout of decontamination equipment on a bench in the CSIRO semi-clean room during acid-cleaning.
- Figure 2.3. A set of chisels within their custom-made carrying box.
- Figure 2.4. The lathe and other ice core decontamination equipment prepared in the laminar-flow clean hood prior to the decontamination.
- Figure 2.5. The decontamination technique used to remove the ice core veneers.
- Figure 2.6. Scoring an extremity of the inner core section with a chisel.
- Figure 2.7. Collection of an inner core piece.
- Figure 2.8. The new lathe designed for decontamination and high-resolution sampling of long ice cores.
- Figure 2.9. Plan of the femtolab.
- Figure 2.10. Airflow in the femtolab.
- Figure 2.11. A quartz chamber used for the sub-boiling distillation of Milli-Q quality water.
- Figure 2.12. A TeflonTM chamber used for evaporating the samples.
- Figure 2.13. Diagram showing the arrangement of the three Re filaments used for analysis of the samples.
- Figure 2.14. The VG 354 thermal ionisation mass spectrometer.
- Figure 2.15. Radial and axial focusing of a magnetic sector mass spectrometer with oblique beam entrance and exit.
- Figure 2.16. Schematic of a Daly collector.
- Figure 2.17. Results of measurements of the NIST SRM 981 common lead isotopic standard over twenty months.

- Figure 2.18. Mass spectra of a ^{205}Pb tracer, a common Pb sample and a tracer-sample mixture such as would be prepared for isotope dilution analysis.
- Figure 3.1. Increase of industrial Pb pollution in Camp Century snow with time since 800 BC.
- Figure 3.2. Variations of Pb concentration across the Wisconsin/Holocene boundary in the Dome C ice core.
- Figure 3.3. World Pb smelter production and alkyllead production since 1750 AD.
- Figure 3.4. Changes in Pb concentrations in Greenland ice and snow.
- Figure 3.5. Changes in Cd, Zn and Cu concentrations in Summit snow from 1967 to present.
- Figure 3.6. Changes in the $^{206}\text{Pb}/^{207}\text{Pb}$ ratio in Greenland snow between 1967 and 1988.
- Figure 3.7. Concentrations of Pb in Greenland snow from principal source regions and US Pb consumption in gasoline as a function of time.
- Figure 3.8. The isotopic composition of Pb in Summit snow, and USA and Eurasian aerosols for the years 1971-1989.
- Figure 3.9. The LDPE lathe described by Candelone et al. (1994) for decontamination of snow and ice cores.
- Figure 3.10. Changes in worldwide Pb production over the past 5500 years and Pb concentrations and Pb crustal enrichment factors in central Greenland ice from 2960 to 470 years ago.
- Figure 3.11. Changes in Pb concentrations in snow/ice deposited at Summit, central Greenland, from 1773 to 1992.
- Figure 3.12. Observed changes in $\delta^{18}\text{O}$ isotopes, Pb, Cu, Zn and Cd concentrations and Pb/Al, Cu/Al, Zn/Al and Cd/Al ratios in Summit, Greenland, ice from 149,100 to 8,250 years ago.
- Figure 3.13. Lead/Al, Cu/Al, Cd/Al and Zn/Al ratios measured in 24 ice core sections dated from 149,100 to 8,250 years ago vs Al concentrations in the sections.
- Figure 3.14. Changes in heavy metal fallout fluxes and heavy metals/Al concentration ratios in Greenland ice from 18,910 to 7,260 years ago.
- Figure 3.15. Representation of the inner core samples collected by Hong et al. (1996b) from a section of a Summit snow/ice core from 67.1-68.025 m depth.

Figure 3.16. $^{206}\text{Pb}/^{207}\text{Pb}$ isotopic ratios and Pb concentrations in Greenland ice from 962 B.C. to 1523 A.D.

Figure 3.17. Lead isotopic compositions in Greenland ice between 7313 BC and 1523 AD.

Figure 3.18. Depth profiles of Cd, Zn, Cu and Pb concentrations in Greenland snow from winter 1989 to summer 1990.

Figure 3.19. Lead in Greenland from 1955 to 1990, comparison of data sets of Boutron et al. (1991) and Boyle et al. (1994).

Figure 3.20. The isotopic composition and concentration of Pb in fresh surface snow collected at Dye 3 during 1988 and 1989.

Figure 3.21. Seasonal changes in the isotopic composition of Pb in fresh surface snow from Dye 3 and snow core samples representing the years 1970 to 1988.

Figure 3.22. $^{206}\text{Pb}/^{207}\text{Pb}$ isotope ratios and Pb concentrations in a Summit snow pit.

Figure 3.23. Lead isotopic compositions from a Greenland snow pit (1981-1990).

Figure 3.24. Intra-annual variations in Pb and Cd concentrations in Greenland firn core sections dated from ~1780 to ~1788, and from 1698-1700.

Figure 3.25. Lead isotopic compositions of Antarctic surface waters collected in 1987 and 1988.

Figure 3.26. Lead concentrations in snow from a pit in Coats Land, Antarctica.

Figure 3.27. Statistics for Pb-emitting processes, 1920-1990.

Figure 3.28. Measurement of Pb concentrations of Milli-Q water, high purity water and the silica gel/phosphoric acid activator.

Figure 3.29. Results of analyses of 100 pg samples of the NIST SRM 981 isotopic standard after correction for isotopic fractionation by 0.24 ± 0.06 %/a.m.u.

Figure 3.30. Sampling sites and $^{206}\text{Pb}/^{207}\text{Pb}$ ratios in Antarctic snow blocks collected in 1983 and a Dome C ice core section dated to ~7500 years BP.

Figure 3.31. The inverse of the Pb concentration versus the $^{206}\text{Pb}/^{207}\text{Pb}$ ratio for Antarctic seawater measured by Flegal et al. (1993).

Figure 3.32. Lead isotope ratios in recent Antarctic snow and ice compared to Antarctic seawater, South Atlantic Ocean pelagic sediments and gasoline.

Figure 3.33. Lead concentrations in Antarctic (Victoria Land) snow from 1965 AD to 1991 AD.

- Figure 3.34. Comparison of the temporal trends of Pb concentrations in the Atlantic sector (Coats Land) and the Pacific sector (Victoria Land and Adelie Land) of Antarctica with gasoline Pb consumption in South America and Oceania.
- Figure 3.35. REE patterns for volcanic ash layers, continental desert dust and Antarctic ice core dust.
- Figure 3.36. Theoretical mixing hyperbolae constructed for combinations of Antarctic dust sources, Antarctic and continental dust sources and continental dust sources.
- Figure 3.37. Seasonal position of the core sections analyzed by Hong et al. (1998) relative to an idealized $\delta^{18}\text{O}$ profile.
- Figure 3.38. A three-isotope plot for ice from Law Dome and Dome C and Australian petrol.
- Figure 3.39. Lead isotopic compositions and concentrations in selected samples from Law Dome.
- Figure 3.40. Comparison of the isotopic composition of ice at Summit, central Greenland, with Law Dome, Antarctica.
- Figure 3.41. The isotopic ratios of Pb in Antarctic ice.
- Figure 3.42. Differences in metal concentrations in the successive thick exterior concentric shells trimmed from cylindrical core segments and in the final axial samples.
- Figure 4.1. Lead concentrations and $^{206}\text{Pb}/^{207}\text{Pb}$ ratios at Law Dome, 1530 AD to 1989 AD.
- Figure 4.2. Barium concentrations and Pb/Ba ratios at Law Dome, 1530 AD to 1989 AD.
- Figure 4.3. Comparison of Pb concentrations at Law Dome and Coats Land.
- Figure 4.4. Comparison of Ba concentrations at Law Dome and Coats Land.
- Figure 4.5. Comparison of Pb/Ba ratios at Law Dome and Coats Land.
- Figure 4.6. Comparison of $^{206}\text{Pb}/^{207}\text{Pb}$ ratios at Law Dome, Coats Land and Victoria Land (dated using the ice flow model of Udisti et al. 1999).
- Figure 4.7. Comparison of $^{206}\text{Pb}/^{207}\text{Pb}$ ratios at Law Dome, Coats Land and Victoria Land (dating adjusted to match the c.1900 pollution event to those of Law Dome and Coats Land).
- Figure 4.8. Comparison of Pb concentrations at Law Dome, Coats Land and Victoria Land.

Figure 4.9. Comparison of Ba concentrations at Law Dome, Coats Land and Victoria Land.

Figure 4.10. $^{206}\text{Pb}/^{207}\text{Pb}$ ratio vs $^{208}\text{Pb}/^{207}\text{Pb}$ ratio plot of pre-industrial Law Dome and early Coats Land and Victoria Land samples.

Figure 4.11. $\delta^{18}\text{O}$ values for two Law Dome Summit cores, DSS-W2k and DSS-W0k over the period summer 1979/1980 to summer 1985/1986.

Figure 4.12. $\delta^{18}\text{O}$ values and Pb concentrations measured in DSS-W2k core sections dating from summer 1979/1980 to summer 1985/1986.

Figure 4.13. $\delta^{18}\text{O}$ values and Ba concentrations measured in DSS-W2k core sections dating from summer 1979/1980 to summer 1985/1986.

Figure 4.14. $\delta^{18}\text{O}$ values and Pb/Ba ratios measured in DSS-W2k core sections dating from summer 1979/1980 to summer 1985/1986.

Figure 4.15. $\delta^{18}\text{O}$ values and $^{206}\text{Pb}/^{207}\text{Pb}$ ratios measured in DSS-W2k core sections dating from summer 1979/1980 to summer 1985/1986.

Figure 4.16. $^{206}\text{Pb}/^{207}\text{Pb}$ ratio vs $^{208}\text{Pb}/^{207}\text{Pb}$ ratio plot of Law Dome DSS-W2k samples dating from 1980 to 1985 and pre-industrial Law Dome ice.

Declaration

This thesis contains no material which has been accepted for the award of any other degree or diploma in any university.

To the best of my knowledge and belief this thesis contains no material previously published by any other person except where due acknowledgment has been made.

Signature:

Date:

Chapter 1: Introduction

1.1 Lead

Lead (Pb) is one of the seven metals of antiquity, its discovery predating historical records. In remote antiquity, Pb ore was valued as an eye paint and ornamental material, and the earliest known Pb artifact, found in Turkey, dates to 6500 BC (Nriagu 1983). The chemical symbol for lead, Pb, is derived from its Latin name, *plumbum*. It is a very soft, low-melting metal, solid at room temperature and recognized for its blue-grey colour, malleability and fairly high density. Lead melts at 327°C and boils at 1751°C. Lead is a trace element in the Earth's crust, with a mean abundance of ~13 ppm, but it can be present in large quantities as galena (PbS) and co-mineralized with copper, silver, gold, zinc, tin, arsenic and antimony (Greenwood and Earnshaw 1984). Lead ores are widely distributed and commercially produced in over fifty countries, the largest producers being the USA, the former USSR, Australia, Peru, China and Canada. Approximately 5 million tonnes of Pb are produced annually, however secondary sources of Pb production are becoming dominant over primary production (Sangster et al. 2000). The main uses of Pb are batteries, pigments and chemicals, gasoline antiknock additives, cable sheathing, solder and other applications (Greenwood and Earnshaw 1984). Lead is a toxic metal and high levels of emission in the urban environment have resulted in a major public health problem, particularly in developing nations (Nriagu et al. 1996). At high levels of human exposure to Pb, damage results to almost all organs and organ systems, most importantly the central nervous system, kidneys and blood, while at lower levels, blood synthesis and other biochemical processes are affected and biological and neurological functions are impaired, among other effects (Tong et al. 2000).

Lead has four stable naturally occurring isotopes, ^{204}Pb , ^{206}Pb , ^{207}Pb and ^{208}Pb , which are produced by stellar nucleosynthesis and by terrestrial radiogenic decay of Uranium and Thorium. Of the stable Pb isotopes, ^{206}Pb , ^{207}Pb and ^{208}Pb are end products of the radioactive decay chains of ^{238}U ($T_{1/2}=4.5\times 10^9$ y), ^{235}U ($T_{1/2}=7.1\times 10^8$ y) and ^{232}Th ($T_{1/2}=1.4\times 10^{10}$ y), respectively (Faure 1986). In addition to nucleosynthesis, ^{204}Pb is produced radiogenically by the double β -decay of ^{204}Hg , however due to the

low probability of this type of radioactive decay, the terrestrial abundance of ^{204}Pb essentially remains constant.

Representative atomic abundances of each of the stable Pb isotopes, ^{204}Pb , ^{206}Pb , ^{207}Pb and ^{208}Pb are 1.4%, 24.1%, 22.1% and 52.4%, respectively (Rosman and Taylor 1998). These abundances vary in terrestrial samples due to the different rate of radiogenic production for each isotope, with the isotopic composition of Pb in the Earth's crust steadily changing. However, the isotopic composition of Pb in an ore body does not change and remains identical to that at the time of formation of the ore body, because the Pb is separated geochemically from the parent U and Th (Faure 1986). This heterogeneity between Pb isotopic compositions in different ore bodies is important in geological and environmental research, as the Pb isotopic compositions of ores from different regions with different geological histories can be distinguished. Geochemists commonly use this information to establish rock ages, while environmental scientists employ Pb isotopes to identify sources of Pb pollution on local, regional and hemispheric scales. Generally, it is found that younger ores and crustal material have higher $^{206}\text{Pb}/^{207}\text{Pb}$ ratios >1.20 compared to older ores, (which can be as low as ~ 1), as can be extrapolated from Figure 1.1. Differences in the isotopic compositions of Pb emitted by natural and anthropogenic processes are essential for the identification and evaluation of pollution in natural archives using isotopic analyses.

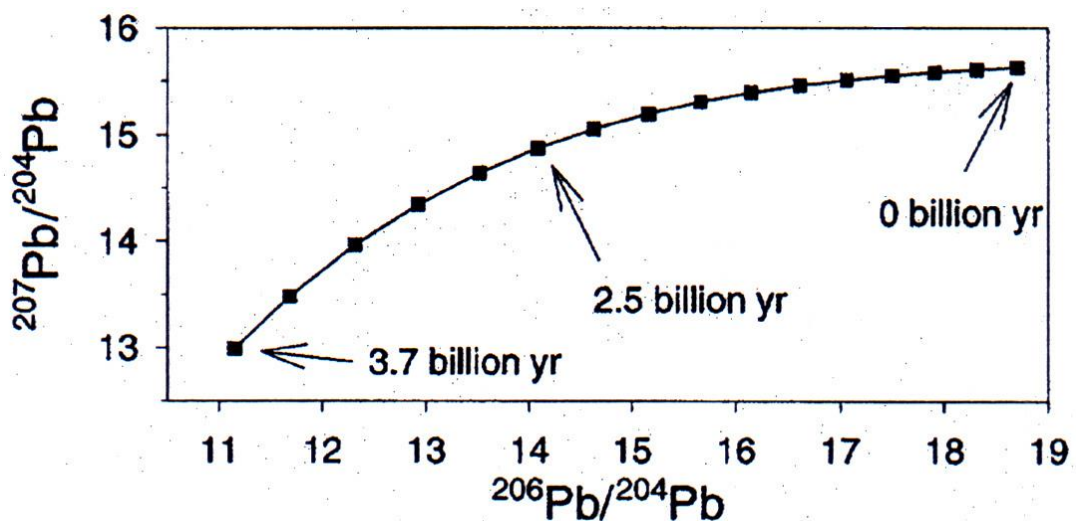


Figure 1.1. The radiogenic growth curve for terrestrial Pb: $^{207}\text{Pb}/^{204}\text{Pb}$ vs $^{206}\text{Pb}/^{204}\text{Pb}$, from (Sangster et al. 2000). Ages in the plot are given as years before present.

1.2 History of Pb production and its use

Lead Production prior to 1500 AD

Lead has been known since antiquity, however its use did not become significant until the Bronze Age, from 2100 BC to 1200 BC, during which time approximately 9.5 million tons of Pb was produced (Nriagu 1983). The different rates of Pb production over time are shown in Figure 1.2. Silver (Ag) was a valuable commodity in ancient times and until the decline of the Roman Empire, Pb was principally obtained as a by-product of Ag production. In antiquity, the primary process for desilvering Pb ores was cupellation, which was probably discovered about 4000 BC. In the process of cupellation, the argentiferous Pb ore is melted in a shallow furnace and exposed to a blast of air, which results in the oxidation of Pb and other base metals that can then be removed from the surface as slag. The Pb oxides could then be used as white Pb or resmelted to recover the Pb. Nriagu (1983) notes that cupellation was a very effective technique for separating Pb and Ag, even in the most crudely-designed furnaces, with ancient coins and artifacts commonly assayed at >98% Ag. In antiquity, Pb had many uses, in alloys and coinage, as a colourant in glass, for pottery glazes and enamels, and also as a cosmetic. The corrosion resistance and formability of Pb saw it extensively used in plumbing, building and ship construction, and it has been noted that sheet Pb was employed to retain moisture in the hanging gardens of Babylon (Greenwood and Earnshaw 1984). Early (Copper Age) production of Pb was mainly located in Asia Minor, however later centres of Pb production moved east to the Aegean and Greece (from 2100-1200 BC) and the Iberian Peninsula (1200 BC to 500 AD), through the successive Greek, Carthaginian and Roman Empires (Nriagu 1983).

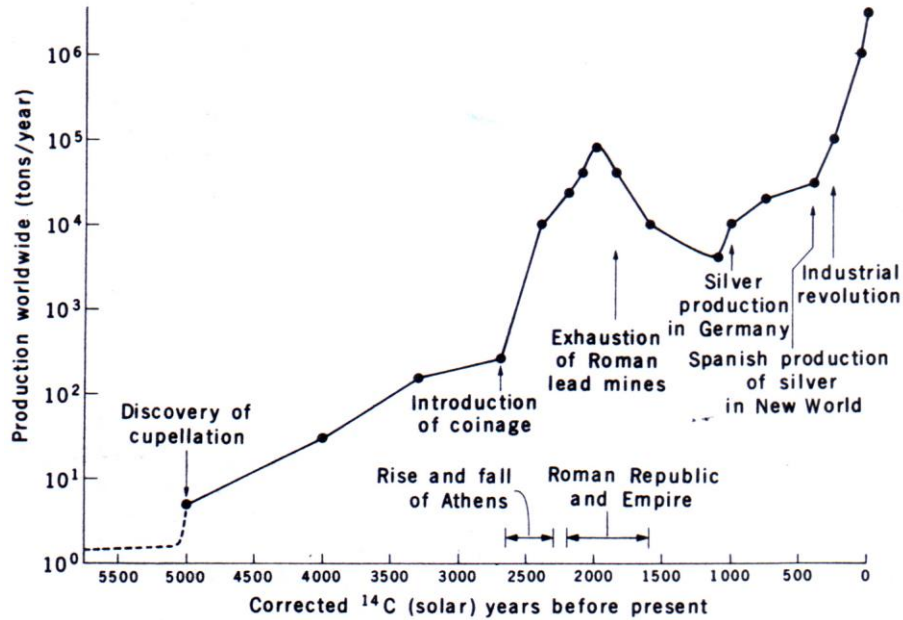


Figure 1.2. World Pb production during the past 5500 years, from Settle and Patterson (1980).

The main Pb producing regions operated by the Carthaginian and Roman Empires were located in Spain, however Pb production operations were undertaken throughout Europe and Asia Minor mainly for the recovery of Ag. At the height of the Roman empire, ~2000 years before present, approximately 80,000 tons of Pb were produced per year by cupellation, with emissions of Pb fume calculated to be ~5% of total Pb production (Hong et al. 1994). Following the collapse of the Roman Empire, Pb production slowed to less than 10,000 tonnes per year. Lead production was later stimulated with the opening of mines in central Europe ~1100 AD, and has been steadily growing up to the present. Prior to ~1500 AD, the majority of Pb production and consumption had been located within Europe, however other significant producers of Pb in antiquity were India and China (Nriagu 1983).

Lead production since 1500 AD

Since 1500 AD, world Pb production has increased in response to new technologies and applications, for example the main contemporary application of Pb, the battery, was not invented until 1800 AD. Colonization has also led to greater rates of Pb

production. The colonization of the Americas produced a boom in Ag and Pb production (Settle and Patterson 1980), while the two largest producers of Pb, the USA and Australia, are both colonies established after 1500 AD. After the 16th century, with the development of large furnaces with tall smoke stacks, Pb emissions were emitted higher into the atmosphere and capable of being routinely transported further. The quantity of Pb emissions also increased as Nriagu (1996) notes that ‘the Industrial Revolution brought about unprecedented demand for metals and an exponential increase in the intensity of metal emissions...’. During the 20th century, demand for Pb and other metals has continued to increase, with ~90% of total mine outputs consumed during the 20th century (Nriagu 1996). The discovery of alkyllead additives for gasoline in the 1920’s and their subsequent introduction worldwide has seen another increase in demand for Pb in the 20th century, and has also significantly increased the quantity of Pb emitted to the atmosphere (Bollhöfer and Rosman 2000). This is shown in Figure 1.3.

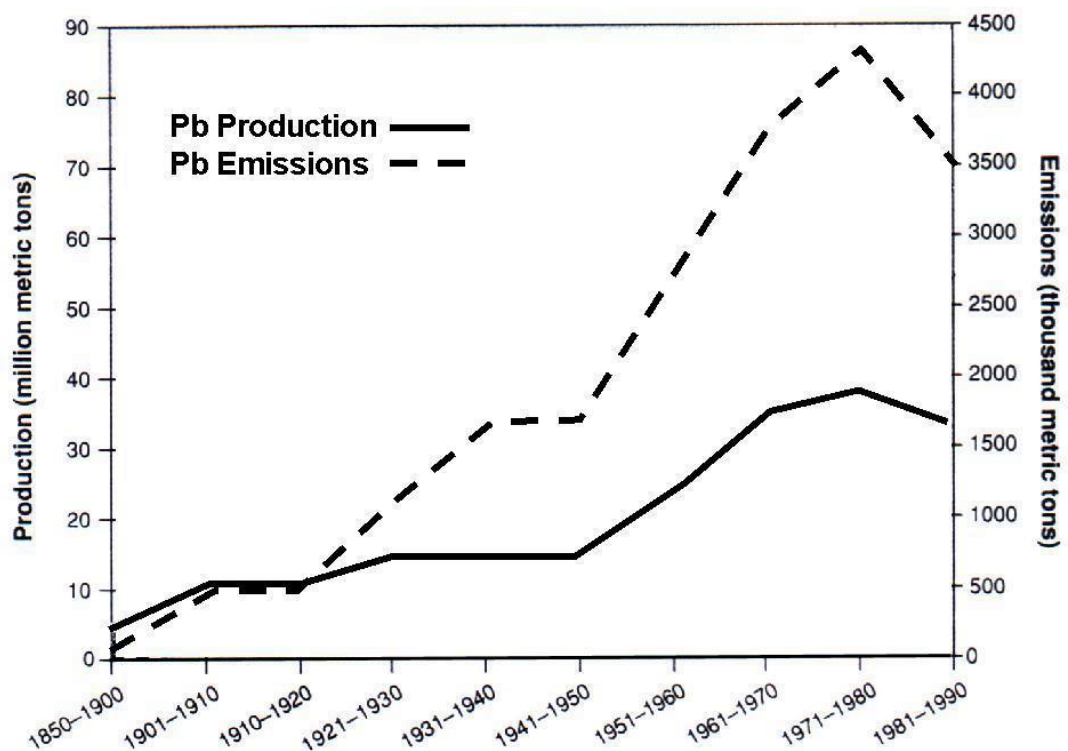


Figure 1.3. Recent historical changes in mine production and anthropogenic emissions of Pb to the atmosphere, redrawn from Nriagu (1996).

1.3 Natural and anthropogenic emissions of Pb into the atmosphere

The predominant natural sources of Pb emission are wind-blown rock and soil dust and volcanoes, as shown in Table 1.1. The relative importance of each of these sources depends upon the geographical location being considered, however. In the Northern Hemisphere, large arid areas such as the Sahara and deserts in North America, the Middle East and central Asia all contribute greatly to dust emission. In comparison, arid areas in the Southern Hemisphere are fewer and smaller, including the Patagonian loess plains and deserts in southern Africa and central Australia (Basile et al. 1997). Volcanoes are recognized as a source of Pb emissions through quiescent degassing or from explosive or effusive eruptions. Concentrations of Pb and other heavy metals are enriched in volcanic plumes relative to crustal levels (Hinkley et al. 1994), and volcanoes have been attributed as a significant source of local Pb emissions (Zreda-Gostynka and Kyle 1997, Monna et al. 1999). While concentrations of Pb in the open oceans are generally quite low, there has been some argument over the possibility of concentrating Pb in the thin oil-layer on the ocean surface. The enrichment of Pb in sea spray has been most recently evaluated at ~200 times greater than mean ocean Pb concentrations (Nriagu 1989). However, evaluations of the natural emission of Pb from ocean spray have been somewhat undermined by the presence of anthropogenic Pb in surface ocean waters and the potential for long-range transport of anthropogenic Pb through deep-ocean currents (Alleman et al. 2001). Biological emissions of Pb also play an important role, with continental and marine biota emitting a median total of $\sim 2 \times 10^3$ tonnes of Pb per year. The sources of these emissions are not well-studied however, and their dispersion and potential seasonal variations are still to be established.

Table 1.1. Worldwide emissions of Pb from natural sources, from Nriagu (1989).

Emission sources	Pb emissions ($\times 10^9$ g.yr ⁻¹)		
	Range	Median	
Wind-borne soil particles	0.3-7.5	3.9	
Seasalt spray	0.02-2.8	1.4	
Volcanoes	0.54-6.0	3.3	
Wild Forest fires	0.06-3.8	1.9	
	Total	10.50	10.50
Biogenic sources			
Continental particulates	0.02-2.5	1.3	
Continental volatiles	0.01-0.38	0.20	
Marine biogenic sources	0.02-0.45	0.24	
	Total	1.74	1.74
	Total		12.24

The various proportions and quantities of natural Pb emissions have varied greatly over the history of the earth, particularly as a result of past glacial periods. As revealed by ice core records, the quantities of dust emitted during past ice ages have been well in excess of current interglacial levels (Petit et al. 1999). Particularly, the cooler climate and changing meteorological patterns are considered to have been more conducive to the production of dust in arid areas and transport of that dust to the polar ice caps (Chylek et al. 2001). Less atmospheric water vapor would have also decreased the quantity of dust washed out of the atmosphere by rainfall, while the changing distribution of vegetation and likely enlargement of arid regions would have also assisted the increased production of dust (Basile et al. 1997). There is no evidence to indicate that the quantity of Pb emitted due to volcanism has significantly changed over the period of natural history recorded by ice core records (~400 ky), however.

As described in the previous section, the sources of anthropogenic Pb emission have varied over time. Currently, however, consumption of alkyllead gasoline additives and mining and production (including smelting) of non-ferrous metals remain

significant emission sources of anthropogenic Pb. Within the urban environment, coal burning and incineration are also important Pb emission sources (Nriagu and Pacyna 1988). Of these various emission sources, alkyllead burning and non-ferrous metal emissions are mostly responsible for long-range dispersion of Pb aerosols. This is mostly due to the fine size of the organolead particles emitted from combustion engines, and the tall smoke stacks from which smelter fume is released. Smaller combustion sources, such as incineration and coal burning, are more localized in their extent, but may result in significant levels of local pollution.

1.4 Atmospheric transport of aerosols

Lead is transported through the air as particulates, and as such its transport is dependent upon the size, shape, mass and other physical and chemical properties of the particle or particle distribution emitted. Lead is effectively sequestered in the hemisphere in which it is emitted, on account of the ~10 day mean atmospheric residence time for anthropogenic Pb aerosols (Patterson and Settle 1987) and the approximate 1-year period required for significant exchange of aerosols between the Northern and Southern Hemispheres (Levin and Hesshaimer 1996). As ~85% of Pb emissions occur in the Northern Hemisphere (Bollhöfer and Rosman 2000), quite different quantities of Pb pollution are observed in Antarctica and Greenland. It has been estimated that ~70% of alkylleads produced each year are emitted into the atmosphere, predominantly through combustion, but also with associated losses during manufacture and gasoline handling (Nriagu 1978). Aerosols are routinely monitored by satellite, and have been observed to travel between continents within a few days. The troposphere and stratosphere are generally well separated, with only the most violent volcanic eruptions being able to transport significant quantities of Pb to the stratosphere. Studies of seasonal snow deposition in Greenland have identified that the origins of air masses vary through the year, with greater influence of Pb from North America from autumn to winter, and more influence from Eurasia in the spring to mid-summer period (Rosman 1998a). These findings, based on Pb isotopic analyses, were found to be in good agreement with calculations based on air mass back-trajectory models. Evaluations of Pb isotopes in various urban centers by Bollhöfer and Rosman (2001) have indicated that it is likely that western Europe is influenced by Pb emissions from Russia and eastern Europe and that the atmosphere

above western North America may be influenced by Pb aerosols emitted from China and transported across the North Pacific.

Geochemical evaluations have also been employed to identify the patterns of intercontinental transport of particulates. Grousset et al. (1992) and Basile et al. (1997) studied Sr and Nd isotopes in Antarctic Dome C and Vostok ice dating to the past glacial stages 2, 4 and 6, dated to ~20, ~60 and ~120 ky BP. They found that the dust deposited in Antarctica during the glacial stages was composed of a mixture of predominantly Patagonian dust and a 10-15% contribution from arid regions in southern Africa and Australia. Studies of recent snow (Bory et al. 2002) and ancient ice (Svensson et al. 2000) from Greenland have found that the majority of dust deposited in Greenland originates from the arid desert regions in central Asia.

1.5 Polar ice cores

The polar ice caps have been extensively studied in the 20th century as an abundant and relatively accessible natural archive of past atmospheric conditions. The Antarctic and Greenland ice sheets, respectively representing the atmospheres of the Southern and Northern hemisphere, consistently accumulate snow each year and are permanently frozen due to their location in the high altitudes and latitudes. As the polar ice caps receive only minor quantities of liquid H₂O, they are classified as deserts, with only low-lying coastal areas of Greenland and Antarctica receiving occasional rain events or subject to melting of surface snow during the summer. Reliable snow and ice archives require that the snow deposited each year is not remelted and percolated through previously deposited snow strata, thus maintaining the sequential annual stratification of the snow (Wolff 2000). Other aspects of snow deposition, such as variations in the amount of snowfall through the year, the quantity of snow drift, and the surface roughness of the bedrock underlying the ice sheet all influence the regularity of the snow and ice strata, and so influence the applicability of a particular location for accurately representing past atmospheric characteristics. Long-term records of past changes in temperature, dust levels, CH₄ and CO₂ concentrations have been produced from ice cores drilled at Summit (Greenland) and Vostok (Antarctica) which respectively sample the past 110 ky and

~400 ky of snow deposition (Petit et al. 1999), or approximately the past four glacial cycles.

Although surface snow is not very dense, the successive years of frozen snow strata deposited on the polar ice sheets result in the compression of underlying snow. Surface snow usually has a density of approximately 350 kg/m^3 , and a porosity of 0.6 to 0.7. Denser snow is termed *firn*, which consists of any snow strata that have not been so compressed as to become ice. Eventually, the weight of the overlying snow and firn is sufficient to close all channels with the air trapped in the firn above, at densities greater than $\sim 800 \text{ kg/m}^3$, as shown in Figure 1.4. The depth at which this occurs is known as the close-off depth, and normally occurs between 60 – 100 m below the snow surface (Wolff 2000). It is classified as such because that is the depth at which bubbles of air are trapped within the ice and are no longer free to mix with the overlying, less-dense, firn. While Pb is deposited as particles and so is not mobile in the snow, chemical species such as methane sulphonic acid (MSA), Oxygen isotopes and major ions can diffuse through snow strata (Wolff 2000). This diffusion results in the gradual attenuation of seasonal variations in these signals as they are smoothed between successive snow and ice strata. The gradual movement of the ice sheets over the buried land surfaces of Greenland and Antarctica result in further thinning of the ice layers and hence degradation of seasonal signals.

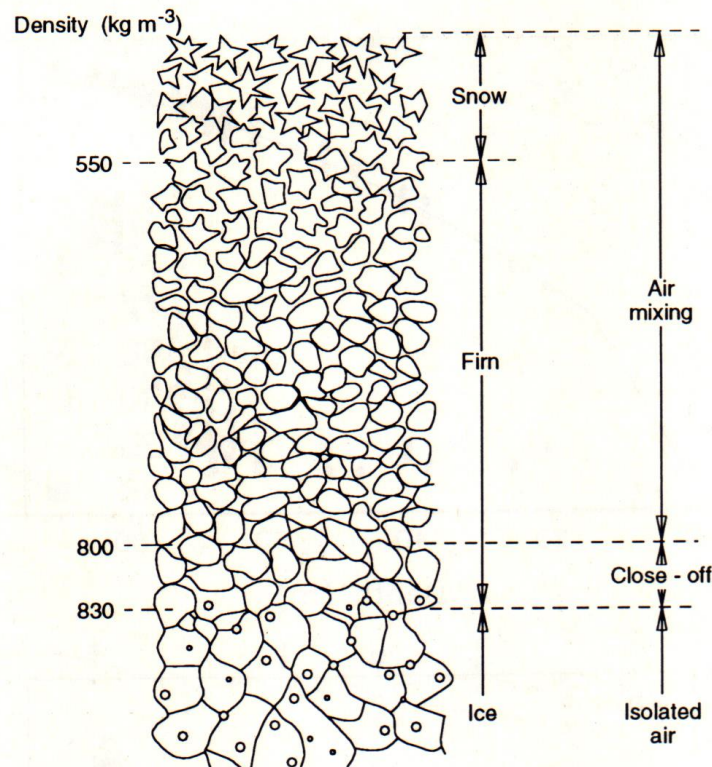


Figure 1.4. Diagram illustrating the trapping process for air bubbles in snow and ice strata near the close-off layer, from Legrand et al. (1994).

Ice cores may be dated in a variety of ways, including the counting of annual signals, the observation of historical features, ice flow modeling, and correlation with other ice core records (Wolff 2000). The counting of annual signals is arguably the most reliable method for relative dating, and as such it is dependent upon the retention of these signals with depth. However, when possible, this method can provide a near-definitive core dating, with minimal uncertainty. As discussed in the previous paragraph, various conditions of meteorology and snow deposition are required for annual signals to be retained over a significant period in an ice core record. Annual signals commonly identified in ice core records include isotope ratios of H and O and concentrations of peroxide, SO_4^{2-} , MSA and sea salts. Variations in the isotopic compositions of H and O are essentially temperature-dependent and so vary systematically between Winter and Summer, while peroxide concentrations can be related to the semi-annual variation in levels of sunlight at the poles. Variations in the emission of sulphate and MSA (related to marine biological productivity) and sea salts can be seasonal in nature (Curran et al. 1998).

The identification of historical features allows particular strata to be dated accurately, however it leaves the remainder of the ice core dating record to be interpolated between these accurately dated strata. Accurate historical records of volcanic eruptions are usually only available for events occurring within the past ~2000 years. Features that can be observed in ice core records include volcanic eruptions (identified by electrical conductivity and identification of acidic species, currently valid to >10 ky BP) and nuclear weapons testing (identified by β^- radioactivity peaks, enables determination of ~1954 AD and ~1964 AD snow strata). At sites with very low snow accumulation, seasonal signals are not retained and horizon dating is not possible in the deeper sections, so ice flow modeling must be employed (Wolff 2000). This technique is essentially based upon assumptions on the rate of thinning of the ice layers, but can be improved by taking into account the changes in snow accumulation over time (related to temperature variations) as well as ice mass-balance changes and different regimes of ice flow over time. This method of dating is essential for constructing a time-scale at low snow accumulation sites such as in central Antarctica.

Finally, ice core signals can be matched to those in other records for which an independent dating has been established (Wolff 2000). While inter-comparison of volcanic signals in ice core records is common, this method is particularly useful for the deep ice cores for which the only other dating technique available is ice flow modeling. The deeper sections of these ice cores can be compared to other core records which contain corresponding data that can be measured. For example, atmospheric methane concentrations or ice volume records can be determined from ice cores and also from marine sediment cores, so by correlation of these patterns in the sediment and ice core records, the dating obtained for the sediment core record can be applied to that obtained from the ice core record (Wolff 2000). By matching the phenomena observed in polar ice core records to those observed in marine sediment cores, the bottom-most ages of these ice core records can be established. However, the possibility of identifying a phase-shift between the snow and marine sediment is eliminated by assuming *a priori* that they are contemporaneous (Wolff 2000).

1.6 Analyses of heavy metals in polar snow and ice

Most of the investigations of heavy metals in snow and ice have been undertaken in the remote regions of Greenland and Antarctica, as the snow and ice strata contain relatively few impurities compared to other environmental media, are the simplest matrix available for analysis, and sites can be chosen to minimize the influence of human activity or local natural sources (rock outcrops, sea water) (Wolff 1990). Also, the accumulation rate of snow in Antarctica and Greenland is such that the past few centuries of snow deposition can be relatively easily accessed, and it is this period which is most commonly sought for pollution studies. Studies of Pb have demonstrated varying levels of Pb in Antarctica and Greenland, in response to changing sources and locations of anthropogenic Pb emissions over time (Rosman et al. 1999). This work has essentially developed from the research reported by Murozumi et al. (1969), who attributed significantly increasing Pb concentrations in Greenland ice from ~2800 BP to 1964 AD to increasing levels of anthropogenic Pb emissions. As will be described in detail in the literature review, work undertaken on Greenland snow and ice during the 1990's has identified the relative sources of these emissions and also determined the history of anthropogenic Pb emissions in the Northern Hemisphere to ~5,500 years before present. Investigations of Antarctic snow and ice have been challenged by lower Pb concentrations (regularly <1 pg/g). The Pb pollution history of Antarctica has only been evaluated for Pb concentrations from ~1925 AD to ~1992 AD. Although investigations of isotopes of Pb and other metals have assisted in determining the main natural sources of Pb emissions in the Southern Hemisphere (Rosman 2001), many questions still remain regarding the history of anthropogenic Pb emissions in the Southern Hemisphere.

For other metals, emissions from anthropogenic sources are not so severe, and in some cases the geochemical cycle is still dominated by natural sources, as shown in Table 1.2. Concentrations of Cu, Cd and Zn have been measured in Antarctica (Boutron et al. 1993, Wolff et al. 1999) and Greenland (Candelone et al. 1995, Hong et al. 1996) and linked to variations in anthropogenic and natural emission sources. Rhodium, Pd and Pt have been investigated in Greenland and Alpine snow and ice and increasing concentrations of these metals during the late 20th century have been associated with the introduction and development of catalytic converters (Barbante et

al. 2001). Bismuth has been measured in Greenland and Antarctica, with volcanism confirmed to be the main emission source (Chisholm et al. 1997, Ferrari et al. 2000). Techniques have been reported for the measurement of a variety of metals, such as Co, Cu, Zn, Mo, Pd, Ag, Sb, Pt, Bi and U, by ICP-MS, and these techniques have been applied to Greenland and Antarctic samples (Barbante et al. 1997, Planchon et al. 2001, 2002a). Techniques for measuring Cd, In, Tl and Ag in Ancient Antarctic ice by thermal ionisation mass spectrometry have also been reported (Matsumoto and Hinkley 1997).

Table 1.2. Natural versus anthropogenic emissions of trace metals to the atmosphere in 1983, from Nriagu (1989). All figures are in units of 10^9 g/yr.

Trace metal	Anthropogenic source	Natural Source	Total emission	Natural/Total emissions
As	19 (12-26)	12 (0.86-23)	31 (13-49)	0.39
Cd	7.6 (3.1-12)	1.3 (0.15-2.6)	8.9 (3.2-15)	0.15
Cr	30 (7.3-54)	44 (4.5-83)	74 (12-137)	0.59
Cu	35 (20-51)	28 (2.3-5.4)	63 (22-105)	0.44
Hg	3.6 (0.91-6.2)	2.5 (0.10-4.9)	6.1 (1.0-11)	0.41
Mn	38 (11-66)	317 (52-582)	355 (63-648)	0.89
Mo	3.3 (0.79-5.4)	3.0 (0.14-5.8)	6.3 (0.93-11)	0.48
Ni	56 (24-87)	30 (3.0-57)	86 (27-144)	0.35
Pb	332 (289-376)	12 (0.97-23)	344 (290-399)	0.04
Sb	3.5 (1.5-5.5)	2.4 (0.07-4.7)	5.9 (1.6-10)	0.41
Se	6.3 (3.0-9.7)	9.3 (0.66-18)	16 (2.5-24)	0.58
V	86 (30-142)	28 (1.6-54)	114 (32-220)	0.25
Zn	132 (70-194)	45 (4.0-86)	177 (74-280)	0.34

In order to evaluate changes in the emissions of Pb and other heavy metals as determined from concentrations in ice and snow samples, it is necessary to evaluate the transfer of these impurities to the polar ice sheets. The two methods normally considered regarding the deposition of impurities into polar snow are dry deposition and wet deposition (Wolff 1990), where dry deposition is the process by which wind-borne particulates are deposited on the snow surface independent of snowfall, so the

efficiency of particle transfer by dry deposition is determined by such factors as (snow and particle) surface roughness, particle mass and the vicinity of emission sources. It appears that dry deposition may be important for the largest-sized locally-generated aerosols and at locations with low snow accumulation rates, however at other locations wet deposition appears to be more important (Davidson et al. 1981). Wet deposition is the process by which impurities are transferred to the surface in snow, and the aerosols often act as ice nuclei from which ice crystals grow. Different impurities will have different efficiencies for each of the types of deposition, and indeed these may also vary where some impurities have different means of anthropogenic emission. These factors, which dictate the deposition of anthropogenic and natural particles to the polar ice sheets, are important to determining how representative ice core records are for characterizing the extent of, and variations in, anthropogenic activities that cause significant levels of pollution.

1.7 Research objectives

The primary objectives of this research are as follows:

- To produce a detailed history of Pb isotopes and Pb and Ba concentrations at Law Dome, Antarctica, covering the past 500 years.
- From this record, to determine how anthropogenic Pb inputs to Antarctica have varied over time and establish when they first became significant.
- To attempt to identify the main anthropogenic Pb emission sources in the Southern Hemisphere from Pb isotopes.
- To evaluate if different Antarctic locations sample emissions from different regions in the Southern Hemisphere, by inter-comparison of the Law Dome record with newly available pollution records from two other Antarctic locations.
- To identify the predominant natural sources of Pb to Law Dome and evaluate any spatial variation in natural Pb sources across Antarctica.
- To observe and account for the extent of natural variations in Pb isotopic compositions at Law Dome.
- To evaluate seasonal variations in the deposition of Pb at Law Dome.

Chapter 2: Methods

2.1 Ice cores

All samples were obtained from sections of ice cores drilled near the summit of Law Dome, situated on the coast of Wilkes Land, East Antarctica. Law Dome is a small coastal ice cap approximately 200 km in diameter with a maximum altitude of ~1400 m a.s.l. (Morgan et al. 1997). It is situated on an Antarctic coastal prominence and predominantly receives easterly airflow from low-pressure cyclonic air masses that center about 65°S. The Law Dome summit has been evaluated as an excellent location for obtaining reliable and well-dated ice cores, on account of the high snow accumulation and the relatively regular quantity of snowfall received throughout the year (McMorrow et al. 2002). Mean wind speeds at Law Dome are low at ~8.3 m/s, with minimal influence from katabatic winds at the summit. Also, mean annual temperatures are approximately -22°C , contributing to minimal loss of snow during the summer. A map of Law Dome, also showing the location of the DSS drilling site (labelled 'DSS') is shown in Figure 2.1.

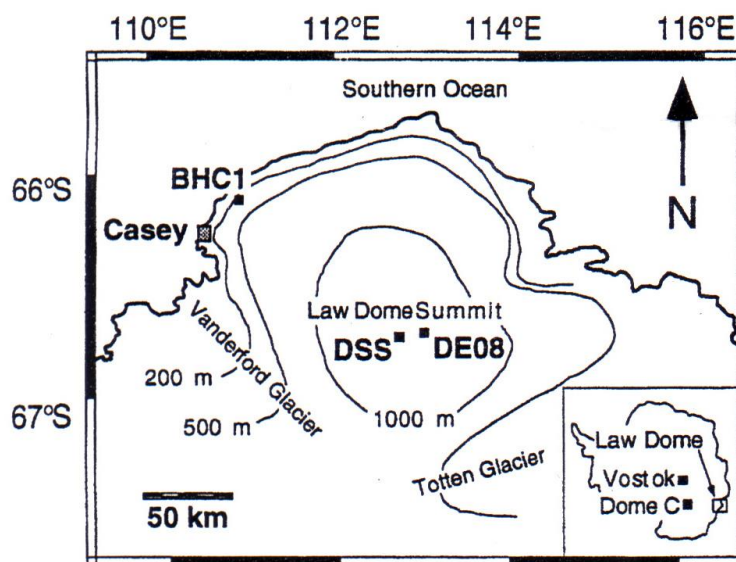


Figure 2.1. Locations of some ice-core sites at Law Dome, East Antarctica, with inset showing locations of Law Dome, Dome C and Vostok in Antarctica, from Edwards et al. (1998).

The most thoroughly investigated Law Dome core is the Dome Summit South main (DSSmain) ice core. The core is located at latitude 66°46'11"S, longitude 112°48'25"E and altitude 1370 m a.s.l., approximately 4.6 km south-southwest of the Law Dome summit. Drilling of the core commenced in 1988 and was completed by 1993, when bedrock was reached 1200 m below the surface, with the bottom-most core layers corresponding approximately to the last interglacial ~110,000 years BP. The core location features a high snow accumulation rate of ~600 kg/m²/yr. The core was drilled using an electromechanical drill, in a fluid-filled hole. The core has been accurately dated by counting of annual $\delta^{18}\text{O}$ layers to a depth of 399 m, corresponding to 1304 AD, with two ambiguous seasonal $\delta^{18}\text{O}$ cycles leading to a maximum uncertainty of ± 1 year prior to 1776 AD (Palmer et al. 2001). Beyond this depth, the dating has been established from ice flow models constrained by spot measurements of fine-detail $\delta^{18}\text{O}$ and peroxide measurements (Morgan et al. 1997). Volcanic events, identified by SO_4^{2-} signals, have been observed and accurately dated in the DSSmain core, as described by Palmer et al. (2001).

The majority of the core samples analyzed were obtained from two Law Dome cores, DSS-W20k and DSS99, with the remaining samples obtained from other cores, DSSmain, BHD and DSS-W2k, also located near the Law Dome summit. A summary of details for the various cores analyzed is included in Table 2.1. Samples obtained from the DSS-W20k core corresponded to the periods 1692 AD – 1858 AD and 1933 AD – 1977 AD, while the period 1852 AD – 1939 AD was sampled from the DSS99 core. Four sections of the DSSmain ice core were sampled, comprising the earliest part of the record, with these samples dated to 1605 AD, 1530 AD, 68 AD and 6500 BP. One sample from the BHD core was obtained to link the pollution record at 1650 AD, while the DSS-W2k core was sampled to provide the most recent samples, from 1980 – 1989 AD. Five DSS-W2k core sections were sampled at high-resolution to study seasonal variations in Pb deposition, while two cores were sampled at lower resolution for inclusion in the main Law Dome pollution record. With the exception of the DSS-W20k core, all of the ice cores sampled were located within 2 km of the DSSmain drilling site and were all dated using approximately similar methods. A different dating method was

applied to the DSS-W20k core, so it will be discussed separately. All core sections were stored in sealed polyethylene bags at approximately -25°C in a cold storage facility in Hobart, Tasmania, prior to decontamination.

Table 2.1. Physical characteristics of Law Dome ice cores studied, from Vallelonga et al. (2002b).

Ice Core Designation	Drilling method	Core Depth (m)	Date of drilling	Surface Accumulation (kg/m ² /yr)
DSS	Electromechanical, Fluid-filled hole	1200	Summer 1988 to Summer 1993	640
DSS99	Thermal, Dry hole	125	January 1999	640
DSS-W2k	Hand-drilled corer	20	January 2000	600
DSS-W20k	Electromechanical, Dry hole	70	December 1997	160
BHD	Thermal, Dry hole	475	Summer 1977	650

Due to their location near the Law Dome summit, the DSSmain, DSS99, DSS-W2k and BHD cores were all primarily dated by counting of annual $\delta^{18}\text{O}$ signals. By comparison of the $\delta^{18}\text{O}$ signals observed in each core with those observed in the DSSmain core, each of these cores could be dated with an annual layer uncertainty of approximately ± 1 year. The DSS-W2k core was hand-drilled in January 2000 to a depth of 20.3 m, at a location 2 km west of the DSSmain drilling site. The DSS99 core was thermally drilled in March 2000 at a site located at $66^{\circ}46'14.23''\text{S}$, $112^{\circ}48'25.00''\text{E}$, approximately 100 m south of DSSmain. The core was drilled to ~ 125 m depth. The BHD core was thermally drilled in October 1977 to a depth of 475 m. The core was located at $66^{\circ}43'13''\text{S}$, $112^{\circ}50'10''\text{E}$, approximately 1 km north of DSSmain.

The DSS-W20k core was electromechanically drilled in December 1997. The core was located approximately 20 km West of DSSmain drilling site, at $66^{\circ}46'27''\text{S}$, $112^{\circ}21'26.1''\text{E}$. The core was drilled to 70 m, comprising of 73 core sections. Due to the

location of the DSS-W20k core site on the lee of the Law Dome Summit, seasonal variations in $\delta^{18}\text{O}$ signals are not retained in the ice core record. As such, the core dating was originally based on calculations of the snow-accumulation rate and associated models of the ice densification, producing a snow accumulation rate estimate of $\sim 200 \text{ kg/m}^2/\text{yr}$. The snow accumulation rate was constrained by determination of the close-off depth from measurements of trapped-gas species ($\sim 150 \text{ kg/m}^2/\text{yr}$, V. Morgan, pers. comm.) and by observation of SO_4 signals indicating the presence of volcanic debris in the ice core strata. From measurements of electrical conductivity and, later, SO_4^{2-} concentrations, snow strata corresponding to the deposition of ash and dust erupted during the 1815 AD Tambora (Indonesia) volcanic eruption and 1808 AD (unidentified location) eruption were identified in the core at $\sim 42 \text{ m}$ and $\sim 43.3 \text{ m}$ depth, respectively. The dating associated with the volcanic debris strata observed in the DSS-W20k samples was tied to the dating of corresponding SO_4^{2-} signals observed in the DSSmain core, located 20 km to the east. The dating of volcanic strata in the DSS-W20k core further constrained the dating of the core (snow accumulation rate $\sim 155 \text{ kg/m}^2/\text{yr}$) and confirmed the snow accumulation rate determined by trapped-gas measurements. As such, the accuracy dating of the DSS-W20k core is evaluated to be $\pm < 5$ years between 1977 and 1750 AD, and ± 15 years in the oldest sample, dated to 1692 AD (Vallelonga et al. 2002b).

The collection and dating of the Coats Land samples is described by Planchon et al. (2002b) and Wolff and Suttie (1994). Lead and Ba concentrations and Pb isotope data for the Coats Land and Victoria Land samples were obtained via personal communication with Kevin Rosman. Additional information regarding Victoria Land and dating of snow cores from that location have been published by Barbante et al. (1997), Maggi and Petit (1998) and Stenni et al. (1999, 2000).

2.2 Ice core decontamination procedure

The drilling and subsequent storage of ice cores exposes them to surface contamination from the drilling fluid, the drilling equipment and urban air containing significant levels

of anthropogenic Pb. Candelone et al. (1994) described a technique for the removal of contaminated surface layers from ice cores by the sequential chiselling of concentric ice veneers from the core while it was suspended in a plastic lathe. This technique was adopted for the preparation of samples from Law Dome ice core sections, the full procedures of which are given by Vallelonga et al. (2002a). Apparatus used for the ice core decontaminations were cleaned and stored in the semi-clean laboratory in the CSIRO Marine Laboratories in Hobart, Tasmania. The ice cores were decontaminated within a laminar-flow bench supplied with high-efficiency particulate arresting (HEPA)-filtered air, located within cold room operated at -12°C , at the Antarctic Co-operative Research Centre (Antarctic CRC) in the University of Tasmania, in Hobart. Following an ice core decontamination, the ice core samples and all equipment were taken to the CSIRO Marine Laboratories semi-clean laboratory for aliquotting of samples, and cleaning of apparatus. One core section was decontaminated each week, with the apparatus cleaned in sequences of acid baths between the decontaminations. Two sets of chisels, melting bottles and scoops were used on a fortnightly cycle, with one set used for a decontamination while the other set was cleaning. All cleaning was undertaken using either Analytical grade (BDH AnalaR[®]) or sub-boiling quartz-distilled (designated “ultra-pure” or “UP”) nitric acid (HNO_3) and Milli-Q (MQ) or sub-boiling quartz-distilled (“ultrapure”, “UP”) water. A picture of some of the apparatus cleaned in the CSIRO semi-clean laboratory is shown in Figure 2.2. Within the semi-clean room, lint-free laboratory smocks, head covers and overshoes were worn, in addition to disposable polyethylene gloves. In the Antarctic CRC, one-piece Tyvek coveralls were worn over insulated clothing. Shoulder-length polyethylene gloves were worn during the decontamination, over which were worn disposable polyethylene gloves. Gloves were regularly changed to ensure that contamination was not entrained to the equipment or core samples during cleaning, transport or decontamination. The decontaminated samples were stored frozen at -25°C and sent to Perth, Australia, in an insulated box containing dry ice for mass-spectrometry.

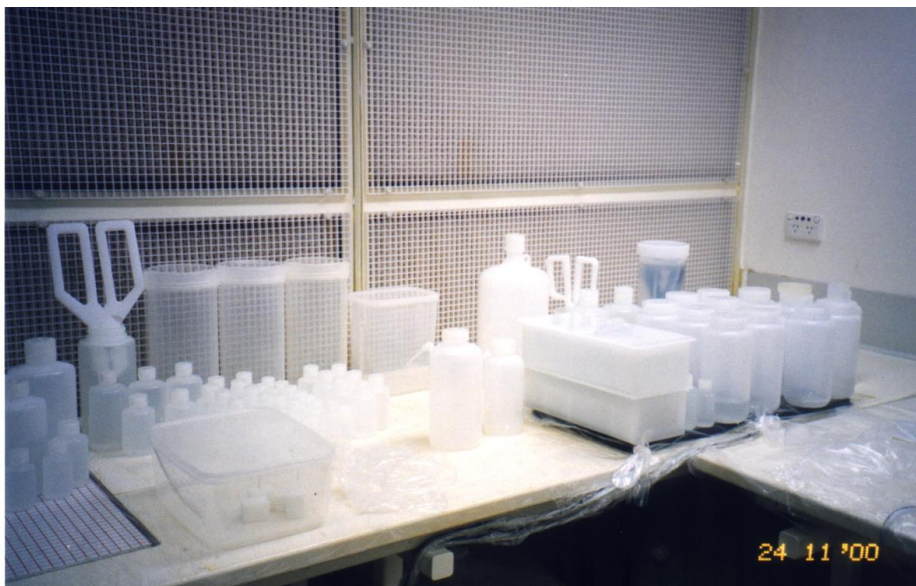


Figure 2.2. Layout of decontamination equipment on a bench in the CSIRO semi-clean room during acid-cleaning. Note the HEPA-filters in the background. Stainless steel chisels are located on the (black) heating-pads in rectangular boxes, as are the melting bottles for collecting core layers and innercore pieces. Tongs for manipulating the inner core, and bottles for aliquotting the samples can also be seen. Photo by P. Vallelonga.

Apparatus used in the decontamination procedure was categorized depending upon its role in the procedure, which determined the type of cleaning that would be undertaken. The lathe parts were of low cleaning priority, as they were not intended to contact the core except for the exterior, contaminated, ends of the core, and so were cleaned at room temperature in a bath of dilute AR grade HNO_3 and MQ water for 24 hours, then stored in another bath of dilute UP HNO_3 and MQ bath. All other equipment (Stainless steel chisels, melting bottles, collecting scoops, innercore tongs) was of high cleaning priority, so they were cleaned with heated solutions of dilute UP HNO_3 . The 5 stainless steel chisels were cleaned, stored and transported in a frame within a custom-made polyethylene box, as shown in Figure 2.3. On the day prior to the decontamination, the lathe pieces and chisels were rinsed with MQ and UP water, respectively, packed in three acid-cleaned polyethylene bags which were heat-sealed airtight, and transported to the Antarctic CRC cold room. In the airstream of the laminar-flow bench within the cold

room, the bags were opened and the lathe pieces and chisels were placed inside the bench. The lathe was then assembled and the chisels left inside the bench for the decontamination of the ice core the following day.



Figure 2.3. A set of chisels within their custom-made carrying box. The box was also filled with acid and heated, when the chisels were to be cleaned. Photo by P. Vallelonga.

On the day of a decontamination, the remaining decontamination apparatus were rinsed with UP water, packed in three acid-cleaned polyethylene bags (also heat-sealed airtight) and transported to the Antarctic CRC cold room. The apparatus was packed such that the melting bottles and scoops used for the exterior layers were all contained in one bag, and the tongs, melting bottles and scoops used for the innermost layer and inner core were all contained in another bag. On arrival at the Antarctic CRC, warm clothing was put on, and the equipment was transferred into the cold room. Once within the cold room, coveralls and polyethylene gloves were put on. Scoops and melting bottles for the first (external) and second (next-to-external) layers were removed from their bags and placed within the bench. The ice core section, transferred to the cold room a few days prior to the decontamination, was removed from its polyethylene bag and, if necessary, parts of the cross-section were removed for analyses of major ions and/or $\delta^{18}\text{O}$ analyses using a bandsaw situated within the cold room. For decontaminations of the DSSmain, DSS99,

W2k and BHD cores, $\delta^{18}\text{O}$ data were obtained earlier to establish the location of a full annual cycle of deposition within the core, so as to avoid any potential bias in the results which may be caused by seasonal variations in the Pb concentrations and/or Pb isotopic compositions of Law Dome snow.

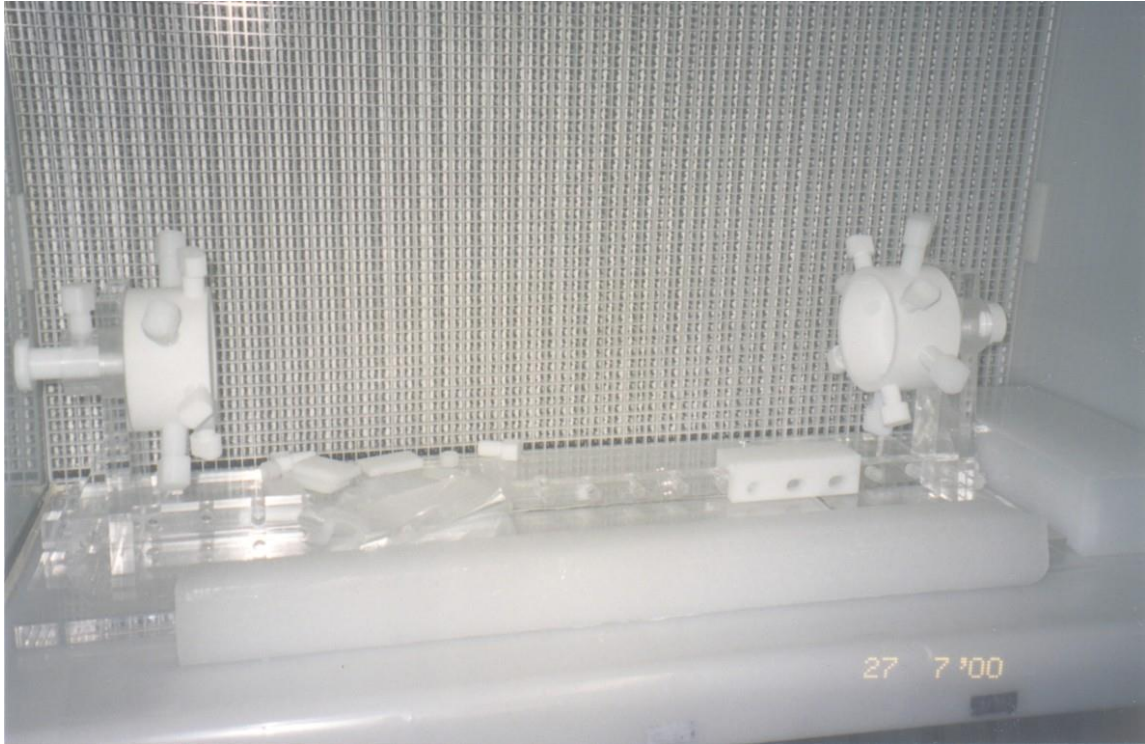


Figure 2.4 The lathe and other ice core decontamination equipment prepared in the laminar-flow clean hood prior to the decontamination. Note the core in the foreground, and chisel box to the far right. Photo by P. Vallelonga.

The core was then held in the airstream of the bench, but not within the bench, and using Chisel #1, a layer of ice was removed from the core and discarded onto the cold room floor. The studies of Candelone et al. (1994) and Chisholm et al. (1995) have shown that the external layer of a core is usually highly contaminated, and so the removal of this exterior layer of ice prior to collection was assumed to assist the establishment of reliable data for the outermost collected layer of ice. Following removal of this layer, Chisel #1 was placed in an unused polyethylene glove and not touched for the duration

of the decontamination. The core was then held within the lathe by one operator, while the other fixed the core ends in the lathe holders (a circular tumbler, with radial screws for securing the core). With the core secured in the lathe, it was free to be rotated, and the collection of ice core layers commenced.



Figure 2.5. The decontamination technique used to remove the ice core veneers, with one operator chiselling the ice core, and the other collecting the chips in a plastic scoop. Photo by T. van Ommen.

The collection of each core layer was standardised, with the core being chiseled along its length by one operator, and the other operator catching the falling chips and slowly rotating the core. This is shown in Figure 2.5. Chiselled chips of ice were caught with a polyethylene scoop (for the innermost layer, a Teflon FEP scoop was used) made by removing sections from a 1 L Nalgene bottle. Occasionally, these chips would be transferred into a melting bottle (a polyethylene 1L Nalgene widemouth bottle) by pouring the chips through the mouth of the bottle. The bottle cap was placed over its mouth to act as the handle of the scoop during the collection of chips. For each layer, a new chisel was used so as to minimize the transfer of contamination from one layer to

the next via the chisel, so chisel #2 was used for the first layer, chisel #3 was used for the second layer, chisel #4 was used for the third layer and chisel #5 was used for the inner core. After the first two layers were collected, the scoops were returned to their polyethylene bags, while the melting bottles (containing the chips) were kept within the bench. The bag containing the tongs, melting bottles and scoops for the third layer and inner core were then transferred into the bench, and the third layer was collected in a similar manner as with the previous two layers.

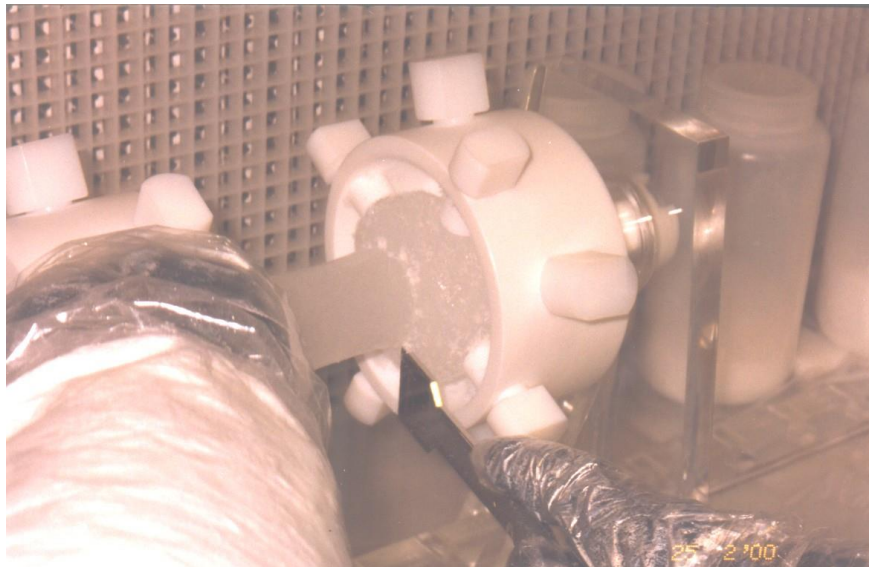


Figure 2.6. Scoring an extremity of the inner core section with a chisel, prior to breaking the core at that point and removing the core holder, to permit collection of the inner core pieces. Photo by P. Vallelonga.

After the third layer was collected, the final chisel (#5) was used to score, or cut, grooves into the sections of the inner core where it would be broken, as shown in Figure 2.6. While the core was always broken at both extremities, its length determined the number of pieces it would be broken into, on account of the length of the widemouth bottles (~15 cm) used to collect the inner core pieces. Usually, the cores were cut into two pieces, with the inner core divided into equal halves, however in the longer cores (usually DSS99 cores), the inner core was usually divided into four pieces of equal length. While one operator supported the inner core using the tongs, the inner core was

broken at one extremity by striking it firmly with the chisel at the location where it had been scored. After the core was broken, the ice core holder was removed and a widemouth bottle was placed around the exposed inner core section, as shown in Figure 2.7. The inner core was broken at the next point at which it had been scored, and the core section was caught in the widemouth bottle. This was repeated for each core section to be collected, with each core section caught within a different widemouth melting bottle. With the final inner core section collected, the decontamination was complete and the apparatus could be returned to the semi-clean laboratory for cleaning. The capped, airtight, polyethylene widemouth bottles containing the ice core layers inner core pieces were sealed airtight in acid-cleaned polyethylene bags and stored in the cold room overnight, and were melted and aliquotted the following day. The samples in the widemouth melting bottles were melted at room temperature within the semi-clean laboratory and then poured into Nalgene™ polyethylene bottles that had been cleaned for several months in sequentially-dilute baths of UP HNO₃ and UP water. For each of the inner core sections, aliquots were also made for collaborating laboratories in Grenoble, France, and Venice, Italy. All aliquots were stored in acid-cleaned polyethylene bags and transported frozen to Perth, Australia.

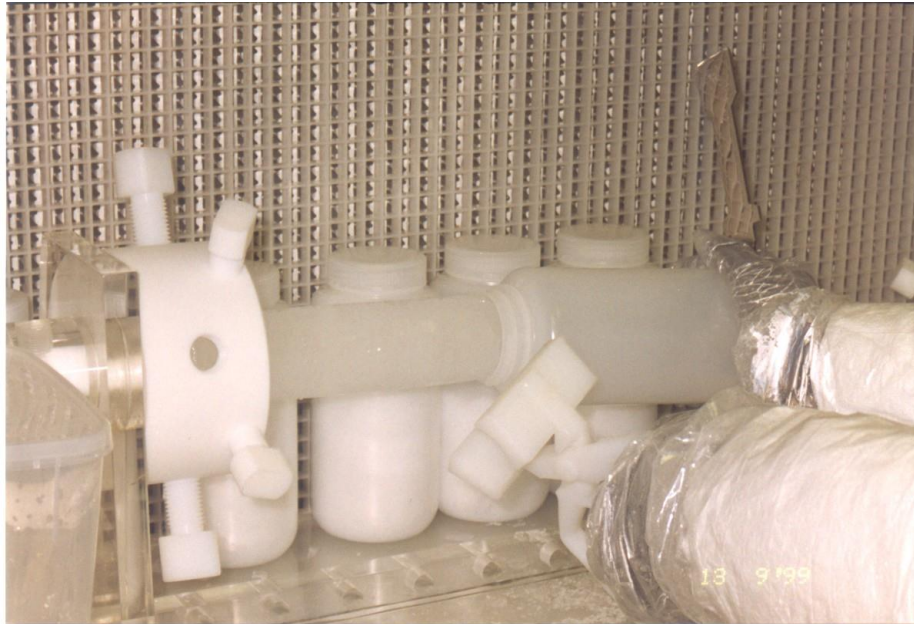


Figure 2.7. Collection of an inner core piece, showing the inner core being inserted into a Nalgene 1 L widemouth bottle. Widemouth bottles in background contain previously collected core layers and/or inner core pieces. Photo by P. Vallelonga.

While the techniques described above were followed for most decontaminations, some variations were adopted for particularly long cores. An extension was built to increase the length of the lathe base to accommodate cores up to 80 cm in length, as shown in Figure 2.4. This extension was secured to the existing lathe base by means of a polyethylene bridge, which was also useful as a resting place for the chisel during the collection of the inner core sections. This polyethylene bridge was cleaned in the same manner as the collecting scoops. For the high-resolution sampling of the DSS-W2k cores (for evaluating seasonal variations in the Law Dome snow record), a new lathe design was adopted, in which the core was cantilevered, or only suspended at one end. This design enabled shorter inner core sections to be collected from long pieces of ice more easily than the lathe technique described above, and is shown in use in Figure 2.8. After approximately half of the core length had been sampled (that is, the core was approximately similar in length to normal core sections), the lathe technique described

above was employed as it was found to be easier for collecting inner core sections from shorter pieces of ice.



Figure 2.8. The new lathe designed for decontamination and high-resolution sampling of long ice cores. Photo by P. Vallelonga.

2.3 The Femtolab

The femtolab is a class 100 clean laboratory located at Curtin University of Technology in Perth, Australia, designed for the preparation of samples containing small (picogram-size) amounts of Pb (Loss and Rosman 1987). The laboratory features an antechamber containing a fridge and freezer and is supplied by air that has been filtered through several stages of HEPA filters. Positive air pressures are maintained within the laboratory and antechamber to ensure that any gaps in the structure of the laboratory do not allow contaminated air to enter. This positive air pressure gradient also ensures that air is directed from the laboratory into the antechamber and from the antechamber to the outside while operators enter or leave the laboratory. All critical work was carried out on

a centrally located bench directly underlying a bank of HEPA filters, including the weighing, spiking and preparation of samples as well as their loading onto Rhenium mass spectrometer filaments. Samples were evaporated under infrared lamps located near the central bench. Lead fallout rates measured in Teflon PFA beakers (Savillex Corp.) were $0.03 \pm 0.01 \text{ pg cm}^{-2} \text{ day}^{-1}$ on the central bench and $0.14 \pm 0.02 \text{ pg cm}^{-2} \text{ day}^{-1}$ near the infra-red lamps. Within the laboratory are also facilities for producing ultrapure water (by sub-boiling distillation in quartz) and for cleaning plastic apparatus in nitric acid baths. A plan of the femtolab is shown in Figure 2.9.

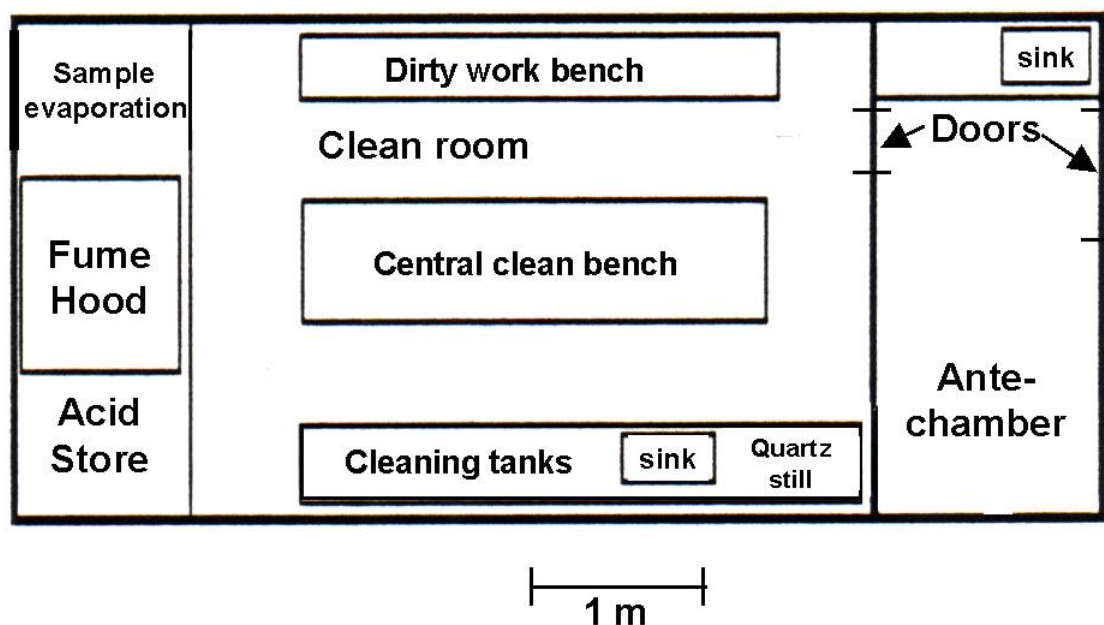


Figure 2.9. Plan of the femtolab, showing the antechamber and laboratory layout and the location of the clean bench, redrawn from Loss and Rosman (1987).

Air circulation

Air supplied to the femtolab undergoes a number of filtration stages before it is directed onto the clean bench, to minimize the probability that Pb-bearing particles remain within the airstream by the time the air is directed onto the central bench. Outside air is collected by an exterior intake fan, passed through a rough particulate filter and an activated charcoal filter and is then chilled by an air conditioning unit to $\sim 22^\circ\text{C}$. This air

enters the Femtolab antechamber after being pumped through a HEPA filter above the doorway into the antechamber. The air in the antechamber is then pumped into the Femtolab through another HEPA filter that directs air downwards over the doorway by which the Femtolab is accessed. Within the Femtolab, circulation of the air from the ceiling to the floor is maintained by false wall plenums covered by rough particulate filters, which allow air to be drawn in at the bottom of each wall and passed up the wall plenums to the ceiling. At the ceiling, the air is passed again through a HEPA filter situated directly above the central bench and directed down directly onto the bench. Air within the laboratory continues along this circular regime until it reaches the far end of the laboratory, where it is ejected through an air outlet. Airflow in the femtolab is shown in Figure 2.10.

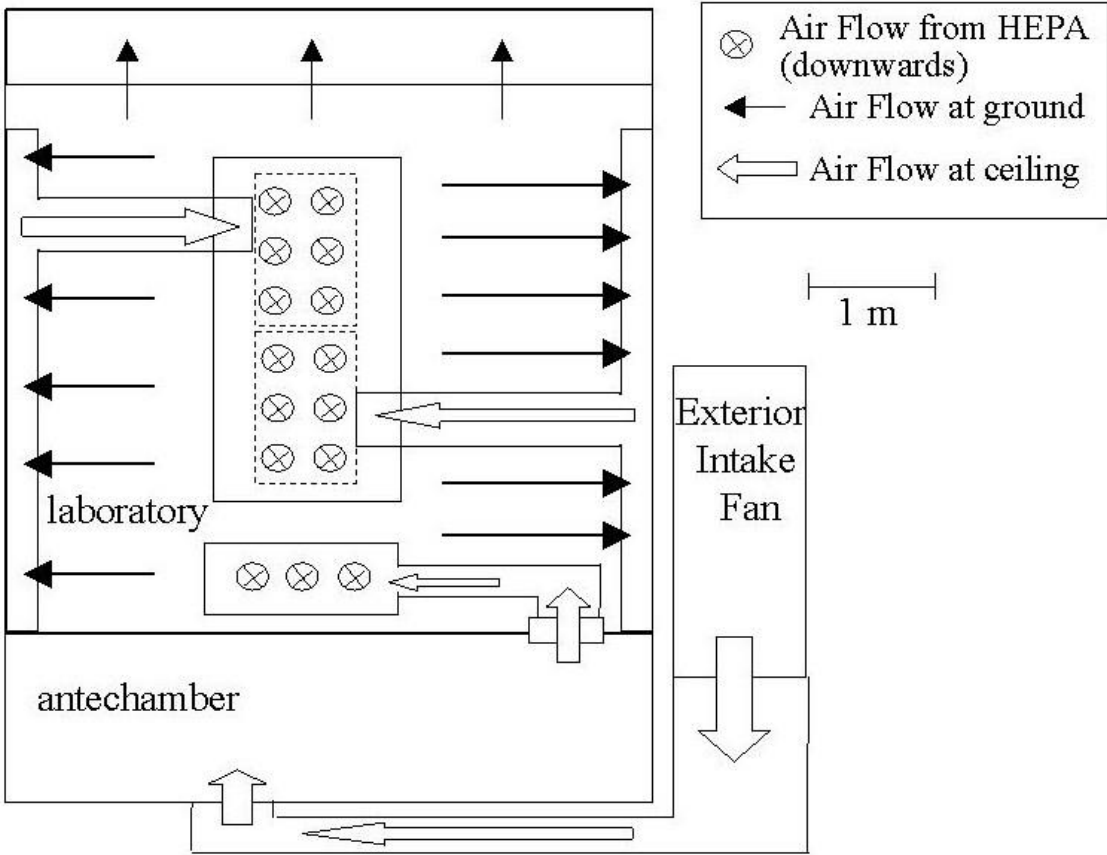


Figure 2.10. Airflow in the femtolab. Note that the sizes of the arrows do not represent air velocity.

Water purification

Filtered deionised water was used at all stages of samples preparation, with highest-purity water used for the most contamination-sensitive procedures such as the dilution of reagents and cleaning of apparatus. Milli-Q grade water (~ 0.05 pg Pb/g) is transferred to the femtolab by polyethylene tubing from an adjacent clean laboratory, in which a water purification system consisting of an IBIS™ Reverse Osmosis system and a USFilter™ water polishing unit is operated. In the femtolab, this water was further polished using a custom-made quartz chamber, in which the water is purified by sub-boiling distillation. The quartz still in the Femtolab is shown in Figure 2.11. The technique of sub-boiling distillation has been described in detail by Kuehner et al. (1972), involving the sub-boiling evaporation of water and its collection on a water-cooled quartz condensation tube. The MQ water is fed into the bottom of the chamber and is heated, as it rises to the water surface, by two filaments heated by an electric current and supported in sealed quartz tubes above the condensation tube and surface of the water. When it arrives at the surface, the water is at a sufficient temperature to undergo sub-boiling evaporation before it is discharged through a tube that collects water from the surface. In this way, the water that remains at the surface retains higher levels of impurities than that which is evaporated, but is steadily removed through the discharge tube, so a surface of pure water is constantly exposed to the heating elements. The pure water collected from the condensation tube has been analysed to contain much lower levels of Pb, ~ 0.005 pg/g, compared to the water supplied to the still, with the method of determination described in section 2.5. Water produced using the quartz still in the femtolab has been designated *ultrapure water* (UPW), to distinguish it from less-pure grades of water used for some acid baths and other initial cleaning applications.

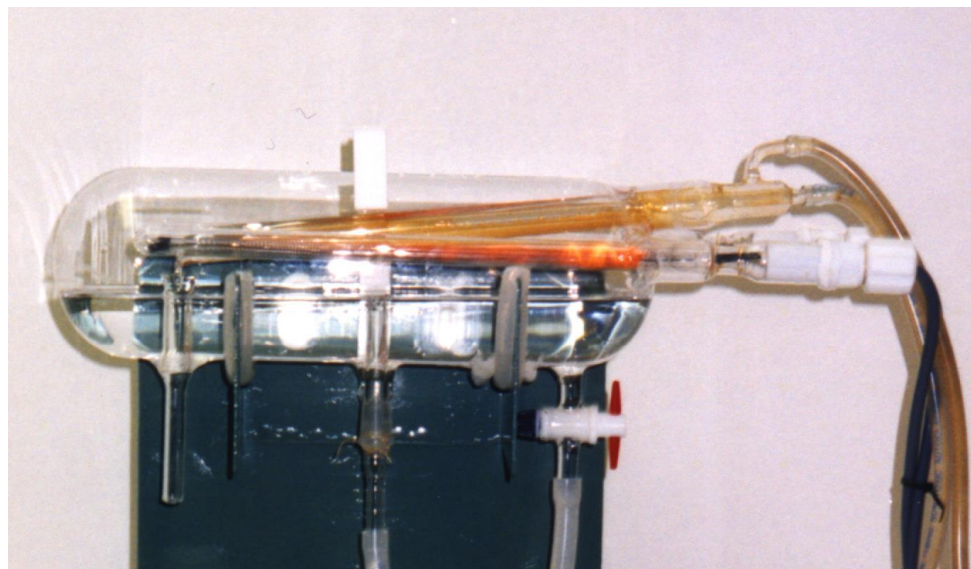


Figure 2.11. A quartz chamber used for the sub-boiling distillation of Milli-Q quality water. This still is used in the CSIRO cleanlab, and is similar in design to that used in the femtolab. Photo by P. Vallelonga.

Mass spectrometer sample preparation

On account of the low levels of Pb present in the samples, minimal sample preparation was undertaken. Essentially, sample preparation procedure involved the transfer of Antarctic samples into Teflon PFA (Savillex Corp.) beakers, weighing, addition of reagents and ionisation enhancers, evaporation and transfer onto a mass spectrometer filament. With the exception of the evaporation stage, all of these procedures were undertaken on the central bench within the Femtolab.

Prior to transfer into the beakers, samples were melted in their storage bottles at room temperature on the Femtolab bench. 15 mL and 45 mL Teflon PFA (Savillex Corp.) beakers were used to prepare samples, and were preconditioned by filling them with UPW, 50 μ L conc. UP HF, 50 μ L conc. UP HNO₃ and 50 μ L dil. H₃PO₄ and heating them in Teflon™ chambers under an infra-red lamp. The Teflon™ chamber features Teflon PTFE walls with a base consisting of two Teflon PFA layers and with clear Teflon FEP film providing an airtight covering over the top of the chamber. A Teflon™

chamber is shown in use in Figure 2.12. As the sample is heated in the pot, evaporating reagents creates an over-pressure in the chamber, and the vapour condenses on the coolest part of the chamber – its walls and the Teflon PFA base. As the chamber is closed to air entering from above and features an over-pressure, the sample can be evaporated under the lamp with minimal likelihood of sample contamination from the lamp or surrounding air. Water vapour condensing on the walls and base collect in the space between the two Teflon PFA layers in the base of the chamber, through drain holes drilled into the upper Teflon PFA layer.



Figure 2.12. A Teflon™ chamber used for evaporating the samples, located under an infrared lamp. The beaker containing the sample is placed within the pot, on the Teflon PFA base, while the chamber is covered with clear Teflon FEP film. Photo by P. Vallelonga.

After 2 hours the preconditioned beaker was emptied and the fully melted sample was shaken vigorously and approximately 10 to 20 mL of sample was tipped into beaker directly from its storage bottle. The sample was weighed on a two-decimal place electronic balance, and 10 μL conc. UP HNO_3 , 3 μL Si gel- H_3PO_4 solution, 6 μL dilute

Al solution (~200 ng) and 6 μL of a mixed $^{205}\text{Pb}/^{137}\text{Ba}$ (~3 pg/64 pg) spike solution were added. Nitric acid was used to ensure that the Pb in the sample did not diffuse into the walls of the Teflon PFA beaker, while the silica gel and Al solution, and phosphoric acid were found to enhance the ionisation efficiency of the samples and assist the evaporation of the sample into a small, easily-located spot, respectively. The addition of the Pb and Ba tracers enables both their concentrations to be determined in the same aliquot by IDMS. The solution was evaporated to dryness at $\sim 80^\circ\text{C}$ in a Teflon chamber placed under an infrared lamp, with a 20 mL sample requiring approximately 15 hours to evaporate completely. The μL -quantities of reagents were dispensed into the samples using an Eppendorf micropipetter, and "metal-free" tips which had been cleaned in a heated acid bath of dilute UP HNO_3 . After evaporation, the samples were transferred to degassed, zone-refined triple-Re filaments using an additional 3 μL of Si gel- H_3PO_4 solution. The design of the filament beads is shown in Figure 2.13. The filaments are supported in a perspex mount, which includes two electrical contacts which enable a current to be supplied to the central filament, onto which the sample is transferred. A low current is passed through the filament to dry the deposit, then the filament temperature is slowly increased to red heat to evaporate the H_3PO_4 , leaving a faint white deposit. The samples are then packed in an airtight box and arranged in the mass-spectrometer carousel, ready for loading.

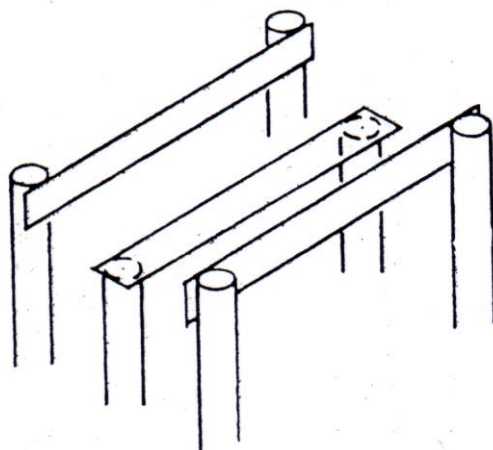


Figure 2.13. Diagram showing the arrangement of the three Rhenium filaments used for analysis of the samples. The sample was loaded on the central filament (~1 cm long).

2.4 The VG 354 thermal ionisation mass spectrometer

A FISIONS Instruments (now Micromass) VG 354 thermal ionisation mass spectrometer was used to measure Pb isotopic compositions and Pb, Bi and Ba concentrations. The VG 354, shown in Figure 2.14, is a 90° magnetic sector thermal ionisation mass spectrometer, with 9 Faraday collectors and one Daly collector. Solid samples are loaded onto filaments, which are then placed into bead holders and assembled on a carousel, which can hold up to 16 samples. The carousel is then loaded into the VG 354 source chamber and pumped down to a pressure suitable for analyses to commence, normally $<5 \times 10^{-8}$ Torr ($<5 \times 10^{-6}$ Pa). Through the holders, a current can be passed through the side or central filaments of the Re bead, to degas the samples prior to measurement or to heat the samples until they undergo thermal ionisation. Degassing of the samples removes hydrocarbons and other forms of molecular interference from the bead block and sample surface, and was undertaken by applying a 4 A current to the side filaments (resulting in a filament temperature of approximately 1400°C) and a 1 A current to the central filament (resulting in a filament temperature of approximately 900°C) of each sample prior to analysis. During measurement, only the central filament was heated, with a current of approximately 2.5 A resulting in a filament temperature of 1250 to 1350°C. The VG 354 includes the mass spectrometer instrument, with a sample source chamber, magnetic analyser and collector arrays, and associated vacuum and electronic systems controlled by a Hewlett-Packard computer.



Figure 2.14 The VG 354 thermal ionisation mass spectrometer, operated within the School of Applied Physics at Curtin University. Photo by G. Burton.

Thermal ionisation

In the VG354, ions are liberated from the solid sample by thermal ionisation, a process first applied to mass spectrometry by Dempster (1918). This technique involves heating a sample on a highly refractory metal filament until atoms in the sample begin to evaporate. As the atoms evaporate off the filament, there is a probability that an electron will be liberated from the atom, and so it will be ionised. The probability of an atom being ionised depends upon the temperature of the filament, the work function of the filament and the ionisation potential of the sample, and is semi-quantitatively described by the Saha-Langmuir equation, shown below, where n^+/n^0 is the ratio of ionised to neutral species, e is the electronic charge, W is the work function of the filament, IP is the ionisation potential of the sample, k is the Boltzmann constant and T is the surface temperature of the filament (de Laeter, 2001).

$$\frac{n^+}{n^0} \propto \exp \frac{e(W - IP)}{kT}$$

The process of thermal ionisation is not fully understood (Kessinger et al. 2001), as the addition of certain ionisation enhancers to the sample can act to substantially improve the probability of ionisation beyond that described by the Saha-Langmuir equation. For example, the addition of suspensions of silica gel to Pb samples, as described by Cameron et al. (1969) and Gerstenberger and Haase (1997), increase the ionisation efficiency of Pb heated on a Re filament by several orders of magnitude. These developments allow pg amounts of Pb to be measured by thermal ionisation mass spectrometry. The technique described by Gerstenberger and Haase (1969) was employed, allowing ion currents of $\sim 1 \times 10^{-15}$ A to be generated from a 1-pg sample loaded on a triple-Re filament and heated to temperatures between 1250 and 1350°C. An optical pyrometer was used to measure the temperature of the filament. The process of thermal ionisation results in isotopic fractionation of the ionised sample, which must be corrected if accurate measurements of isotopic compositions are to be accomplished (de Laeter 2001). The problem of instrumental mass fractionation in the VG 354 TIMS is discussed later.

Following ionisation, the ions were accelerated through an electric potential of ~ 8 kV, and passed through a collimator stack, by which the ion beam could be focussed and directed down the flight path. The energy E imparted to the ions, of mass m and charge e , is described by the equation given below:

$$E = eV = \frac{1}{2}mv^2$$

where V is the accelerating voltage acting upon the ion and v is its velocity. One advantage of the thermal ionisation technique is that all ions are singly charged (White and Wood 1986), so ions of the same mass will have the same velocity, as shown in the equation above. The various plates and lenses in the collimator stack were used to focus the beam in the vertical (z) and lateral (y) planes. Additional focusing in the vertical z -plane was accomplished by the mass spectrometer geometry, which directed the ion

beam into the magnetic sector at an angle of 26.5° to the perpendicular of the magnetic field, as shown in Figure 2.15. This increases the sensitivity of the mass spectrometer by focussing the vertically-dispersing ion beam into the collector slit, as described by Cross (1951). An additional benefit of this extended ion-deflection geometry is the doubled dispersion length (source slit-to-magnet and magnet-to-collector slit lengths) of 540 mm, equal to twice the radius of curvature of the magnetic sector, allowing a larger beam to be introduced into the magnetic sector for the same nominal resolving power. Due to the convex curvature of the entry-face of the magnet and the concave curvature of its exit-face, as shown in Figure 2.15, the plane of focus of the ion optics is almost-linear (Loss 1986).

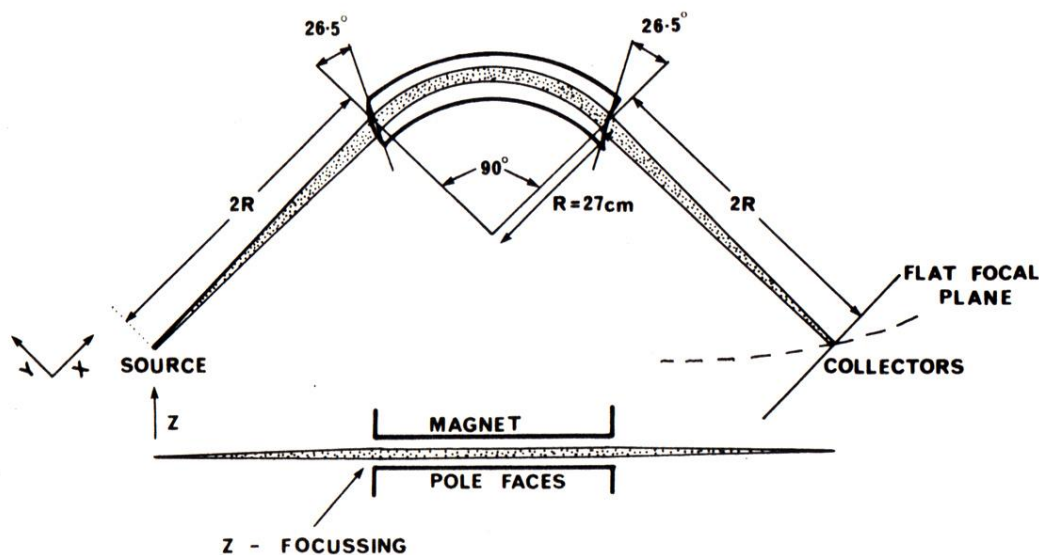


Figure 2.15. Radial (top) and axial (bottom) focusing of a magnetic sector mass spectrometer with oblique beam entrance and exit, as in the VG 354, from Loss (1986).

Mass separation

The mass spectrometer separates ions by passing them through a magnetic sector field, within which they undergo deflection along circular paths. The positively charged ions are deflected in the magnetic field following a circular path whose radius of curvature is determined by their mass-to-charge ratio. As thermal ionisation produces only singly-charged ions, the ions are deflected by the magnetic field according to the following formula:

$$Bev = m \frac{v^2}{R}$$

Where B is the magnetic flux density, e is the electron charge (C), v is the velocity of ion (ms^{-1}), m is the mass of ion (kg) and R is the radius of curvature of ion path (m).

A particular magnetic field setting is chosen such that the radius of curvature of the Pb ions is equal to the curvature of the flight path, so the Pb ions continue down the centre of the flight path and are collected by the ion detector. Rearranging the above equation gives the radius of curvature in the flight tube as:

$$R = \frac{1}{B} \left(\frac{2mV}{e} \right)^{1/2}$$

Heavier and lighter ions are retarded by collision with the walls of the flight tube.

Ion collection

Although the VG 354 features an array of nine Faraday cup collectors, the single high-sensitivity Daly detector system was used to measure the ion beams produced from the Law Dome samples. The Daly collector featured a lower baseline current compared to the Faraday system, and with the photomultiplier, allowed small ($\sim 10^{-15}$ A) ion currents to be measured accurately. The Daly detector system consists of a Daly knob and

scintillator screen arranged perpendicular to the path of the ions, as shown in Figure 2.16. A high negative potential was applied to the Daly knob, to attract Pb ions toward the knob. Ions impacting on the knob produced secondary electrons that were accelerated away from the knob toward a scintillator screen, which produced a photon for every secondary electron impact. The photons emitted from the scintillator screen were amplified by a photomultiplier, from which the signal current was determined as a potential across a $10^{11} \Omega$ resistor measured by a DVM. As the Daly system could only measure one ion beam at a time, the magnetic field was sequentially switched from one isotope to the next, to enable the measurement of two Ba isotopes (200, 201), five Pb isotopes (204 – 208), the one Bi isotope (209) and three backgrounds (corresponding to masses 203, 203.5 and 204.5) to be measured for each sample.

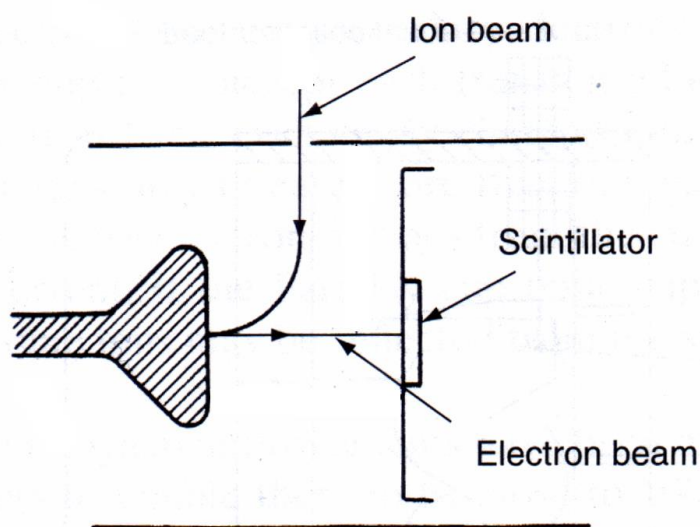


Figure 2.16. Schematic of a Daly collector, redrawn from de Laeter (2001).

Accuracy of isotopic ratio measurements

Instrumental mass fractionation can occur in the process of measuring isotope ratios by thermal ionisation mass spectrometry. The term is used to describe any process which may lead to a measured isotope ratio being different to that originally present in the sample. While different types of mass spectrometers introduce instrumental mass

fractionation from different processes, the process of thermal ionisation is the most important contributor to instrumental mass fractionation in TIMS instruments. In order to evaluate the accuracy of the data produced by the mass spectrometer, and correct the isotopic ratios measured, a reference standard, for which the isotopic composition is already known, is analyzed in the same way a normal sample would be measured. The difference between the measured result and certified value is then used to evaluate and correct for mass fractionation introduced by the instrument.

On each mass-spectrometer carousel loaded, one or two isotopic standards were loaded to verify the instrumental mass fractionation of Pb induced by the mass spectrometer. The National Institute for Standards and Technology (NIST) SRM 981 common lead isotopic standard was used to evaluate mass fractionation of the samples. Chisholm et al. (1995) have previously described the mass-fractionation bias of 0.24 ± 0.06 ‰ applied to Pb isotope ratios measured using the Curtin University VG-354 TIMS. As can be seen in Figure 2.17, the instrumental mass fractionation of the VG 354 observed during the course of measurements of the Law Dome samples has not changed significantly from that determined by Chisholm et al. (1995). Shown in Figure 2.17 are the results of 66 measurements of a 160 pg sample of NIST 981, with average Pb isotope ratios of $^{206}\text{Pb}/^{207}\text{Pb} = 1.0935 \pm 0.0026$, $^{208}\text{Pb}/^{207}\text{Pb} = 2.367 \pm 0.006$ and $^{206}\text{Pb}/^{204}\text{Pb} = 16.92 \pm 0.10$ (2σ uncertainties) determined after correction for instrumental mass fractionation by 0.24 ‰. For comparison, the certified values provided for NIST SRM 981 are $^{206}\text{Pb}/^{207}\text{Pb} = 1.0933$, $^{208}\text{Pb}/^{207}\text{Pb} = 2.370$ and $^{206}\text{Pb}/^{204}\text{Pb} = 16.94$. In the figure, it can be seen that there is no significant bias observed in the $^{206}\text{Pb}/^{207}\text{Pb}$ ratio after fractionation correction, while the corrected $^{208}\text{Pb}/^{207}\text{Pb}$ and $^{206}\text{Pb}/^{204}\text{Pb}$ ratios were observed to be 0.16% and 0.13% lower, after correction, than the values certified by NIST. However, considering the precision associated with these measurements (usually $>0.10\%$) and the 0.04% uncertainty associated with the isotopic compositions certified by NIST (Rosman 2001), there are not sufficient grounds to use a different mass fractionation correction to that evaluated by Chisholm et al. (1995).

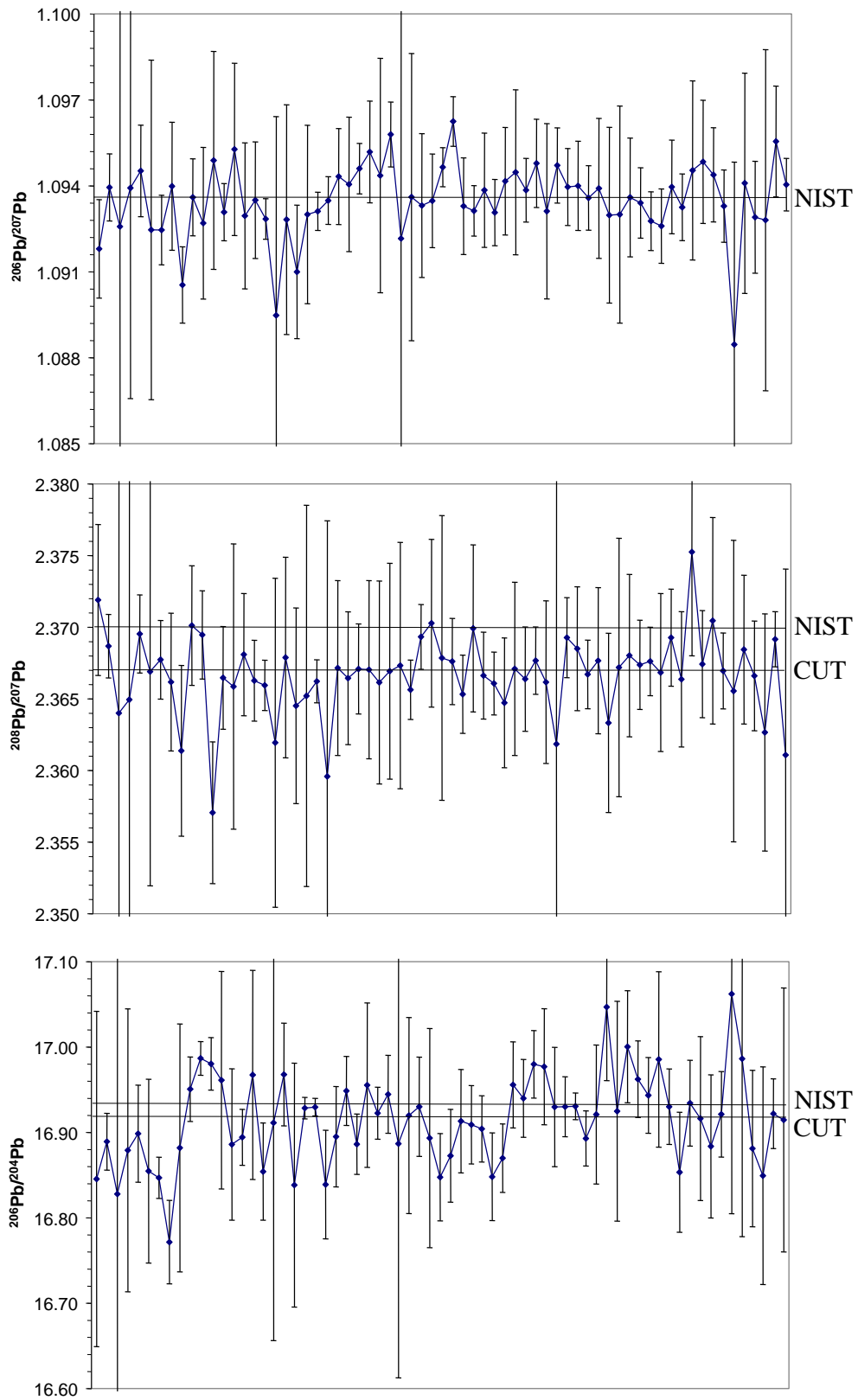


Figure 2.17. Results of measurements of the NIST SRM 981 common lead isotopic standard over twenty months.

Isotope dilution

Isotope dilution is a sensitive technique for determining the quantity of an element by the addition of a tracer, a prepared sample with an isotopic composition different to that of the naturally occurring element (de Laeter 2001). Isotope dilution is of particular assistance to thermal ionisation mass spectrometry, because although the mass spectrometer calculates isotope ratios based on the ion currents of the ion beams, these ion currents do not accurately reflect the absolute quantity of each isotope present on the filament. By the addition of a known quantity of monoisotopic tracer, the ratios of the ion beams, relative to that of the tracer can be used to determine the amount of sample being analysed. IDMS is recognised to be a highly accurate analytical method, commonly employed in standards laboratories for certifications and by Earth scientists for high accuracy measurements, such as those required for the determination of rock ages.

The amount of an element in a sample (s) can be determined from the addition of a tracer (t) using the isotope dilution equation shown below, from Webster (1960):

$$W_s = W_t \cdot \frac{AW_s}{AW_t} \cdot \frac{Abs^i}{Abt^r} \left[\frac{(i/r)_m - (i/r)_t}{1 - (r/i)_s \cdot (i/r)_m} \right]$$

where W_s is the weight of the element in the sample analyzed, W_t is the weight of the element in the tracer added, AW_s is the Atomic weight of the sample, AW_t is the Atomic weight of the tracer, Abs^i is the isotopic abundance of isotope i in the sample, Abt^r is the isotopic abundance of the reference isotope in the tracer, $(i/r)_m$ is the isotope ratio of any isotope i relative to isotope r in the tracer-sample mixture, $(r/i)_s$ is the isotope ratio of isotope r relative to any isotope i in the sample and $(i/r)_t$ is the isotope ratio of any isotope i relative to isotope r in the tracer. For isotope dilution to be accurate, it is necessary for the tracer to be completely mixed with the sample, so the tracer is usually added as a liquid to a solution containing the sample.

IDMS was used to measure amounts of Pb and Ba in the samples, by the addition of a $^{205}\text{Pb}/^{137}\text{Ba}$ spike solution prior to the evaporation of the sample. As the isotope ^{205}Pb is not naturally present on Earth, both Pb concentrations and Pb isotopic compositions could be determined from the analysis of one sample, as shown in Figure 2.18. The precision associated with the IDMS procedure is determined by the precision to which isotope ratios can be determined, and the precision to which the spike solution can be transferred to the sample. A calibration of the mixed spike solution, described further in Appendix 2, established the concentrations of ^{205}Pb and ^{137}Ba to be 0.383 ± 0.005 ng Pb/g and 10.56 ± 0.14 ng Ba/g. However, the overall precision of the concentrations determined by IDMS was limited by the precision to which the spike could be dispensed into the sample, with the overall precision of the Pb and Ba concentrations evaluated at $\pm 15\%$.

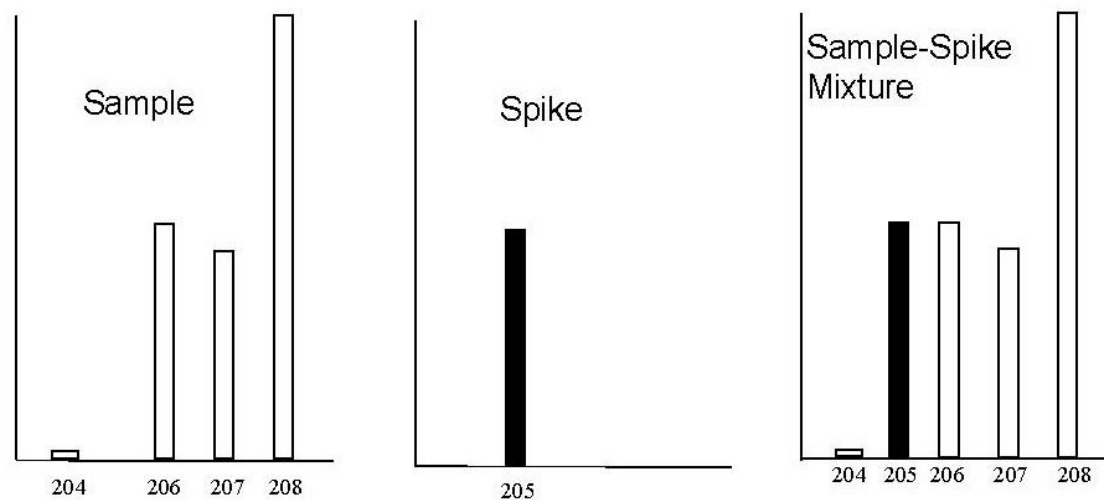


Figure 2.18. Mass spectra of a ^{205}Pb tracer, a common Pb sample and a tracer-sample mixture such as would be prepared for isotope dilution analysis.

2.5 RESEARCH ARTICLE: Recent advances in measurement of Pb isotopes in polar ice and snow at sub-picogram per gram concentrations using thermal ionisation mass spectrometry.

Submitted to *Analytica Chimica Acta* 3rd July 2001

Accepted for publication 25th October 2001

Published in 2002, vol. 453, pp. 1-12.

Chapter 3: Literature Review

The progress of analyses of heavy metals in snow and ice has essentially been driven by investigators' abilities to identify and control contamination of samples during collection, storage and analysis. The earliest measurements of polar ice and snow were invalidated by contamination of the samples, but as this was not recognized at the time, these studies concluded that urban areas were as *unpolluted* as the Earth's most distant and isolated regions: the polar ice sheets. Following demonstrations that reliable results could only be obtained by strict observation and control of sample contamination, studies of heavy metals in polar ice and other natural archives have been able to provide valuable information on the present and past state of the Earth's atmosphere, hydrosphere and biosphere. The importance of contamination control was first realised in the 1960's by Clair C. Patterson and co-workers at the Division of Geological and Planetary Sciences at the California Institute of Technology (Flegal 1998). Patterson's efforts were distinguished not only in regards to the foresight and dedication shown to tackling the many challenges of trace-metal analysis, but also in the effort required to convince an establishment of scientists, governments and corporations that global heavy metal pollution was a real and imminent threat to society and the environment. The work undertaken by Patterson and co-workers as well as a successive generation of Earth scientists has established the present knowledge of heavy metal fluxes to, and concentrations in, the various environmental compartments over time.

Although Patterson and co-workers were pioneers in the accurate measurement of Pb concentrations in ice and snow, they were not the first to attempt to measure heavy metals in natural archives. Interest in the fluxes and amounts of anthropogenic Pb distributed throughout the atmosphere, lithosphere and biosphere was stimulated from the 1920's by the potential threat of widespread Pb poisoning due to the consumption of leaded petrol in urban areas. These fears generally arose from the cases of extreme Pb poisoning observed at the tetraethyllead (TEL) manufacturing plant soon after production of TEL commenced (Nriagu 1990). The toxic effects of occupational exposure to Pb were first realized in the 19th century, however attempts to limit occupational Pb poisoning only emerged late in the 19th century (Tong et al. 2000). In 1925, the Surgeon General of the United States Public Health Service

chaired a meeting of public health experts and industry representatives intended to consider the possible health hazards of the addition of Pb to automobile gasoline. From this meeting, however, the nature of assessments of Pb levels in the atmosphere and in people were such that it was incumbent on the scientific community, and public health researchers, to prove that tetraethyl-lead additives had a significant detrimental effect on public health and/or environment (Nriagu 1998). Producers of TEL were essentially free to engage in the global production and distribution of a product that had not been proven safe, and there were few serious challenges to the position of the industry until the 1960's. In his history of the discovery, implementation and eventual reduction of alkyllead gasoline additives, Nriagu (1990) noted that social and industrial pressures counteracted and undermined the efforts of scientists and public health researchers to independently evaluate the health and environmental effects of the rapidly expanding TEL industry:

Dr Robert A. Kehoe, former director of the Medical Department of Ethyl Corporation and of the Kettering laboratory in the Department of Preventative Medicine, University of Cincinnati, was generally regarded for many decades as the foremost authority on lead poisoning. His authoritative work on the human toxicology of lead was mostly responsible for rescinding the order banning the production and sale of leaded gasoline and he thus deserves much of the credit for saving the TEL industry.

Objections to the widespread use of leaded gasoline on the basis of environmental and health risks that could not be documented by the science of the time were dismissed, more so because such suggestions were antipathetic to the economic and social conditions of the 1920's, which were tuned to the firm belief in industrial progress geared to the automobile.

The challenge of demonstrating the threat to environment and health posed by widespread Pb emissions required the distinction of natural Pb levels from typical Pb levels in the environment and in people, which was not recognized at that time. The invention of the atomic absorption spectrophotometer (AAS) in 1954 by Alan Walsh enabled concentrations of Pb and other heavy metals to be determined with relative ease, resulting in many determinations of Pb concentrations in various matrices.

However, since no one was conscious of contamination issues at the time, the samples collected were entirely contaminated by anthropogenic Pb and therefore served to maintain the position of the TEL industry, that Pb levels in urban areas were similar to those in remote areas, thus emissions of TEL were not significant in respect to normal (or, by implication, natural) Pb emissions.

Clair C. Patterson was the first investigator to recognize that anthropogenic Pb emissions were pervasive in the 20th century and that any attempt to establish the natural level of Pb in the atmosphere would require evaluation of archives completely isolated from the modern atmosphere, biosphere and hydrosphere (Flegal 1998). The development of TIMS and isotope dilution for analyses of smaller and smaller quantities of Pb in the field of geochemistry provided the opportunity for the pervasive levels of anthropogenic Pb emissions to be recognized. Patterson's work analysing microgram amounts of Pb in meteoritic zircons brought him to deal with the problem of Pb contamination encountered in general analytical laboratories. Through evaluations of Pb content in laboratory air and in water and other reagents, Patterson developed a comprehension of the levels of Pb in natural and urban environments. These findings were summarized in a paper entitled 'Contaminated and natural lead environments of man' (Patterson 1965).

From TIMS analyses of Pb in various natural archives, collected and measured with extreme precautions regarding contamination, Patterson and co-workers developed a body of evidence describing the various natural and anthropogenic sources of Pb emission to the atmosphere and their relative quantities of emission. They also provided the best available determinations of Pb concentrations and Pb isotopic compositions in various compartments of the atmosphere, biosphere and hydrosphere. Some of the matrices they sampled included urban and remote aerosols, coastal and open ocean waters, pelagic sediments, manganese nodules, coal and petrol (Flegal 1998 and references therein). The data confirmed the significant levels of anthropogenic Pb emission, but did not enable an evaluation of how Pb levels had changed over time nor prove conclusively that anthropogenic Pb emissions overwhelmed natural Pb emissions. To answer these questions, Patterson and co-workers turned their efforts from the distribution of Pb in contemporary times to the determination of 'natural' baselines of atmospheric Pb levels. Greenland ice was

selected as a candidate material for the evaluation of past Pb concentrations on account of its pristine nature – continental glacier strata were often subject to percolation from liquid precipitation, while relatively high snow accumulation rates meant it was difficult to practically access centuries-old ice. Additionally, there were concerns of mixing of glacier ice with underlying bedrock. For these reasons, Greenland provided a site where there were pre-existing tunnels to access centuries-old ice, free from percolation with a low snow accumulation rate and relatively (but not entirely) pristine atmospheric conditions.

3.1 The first reliable evaluation of Pb concentrations in polar snow and ice.

While Patterson and co-workers had earlier demonstrated the majority of Pb in urban air and coastal and open ocean waters to be due to anthropogenic sources, they were yet to establish how Pb levels had changed over time. To do this, they measured a suite of elements – Pb, Na, Cl, Mg, Ca, K, Ti and Si – in snow and ice they had sampled from Greenland and Antarctica using extreme precaution to minimize sample contamination (Murozumi et al. 1969). The samples were obtained in 1964 and 1965 and were comprised of surface snow samples, firn/ice blocks up to 300 years old obtained from pre-dug tunnels, and a block of Greenland ice dated to 2800 years before present. One important aspect of the paper was its description of the technical requirements involved in sampling and transporting polar snow and ice free from contamination. They argued that drill core samples were easily contaminated, and that the volume of sample available from a drill core was too small to allow Pb concentrations to be measured accurately. As a result, they described their techniques for obtaining 19 kg and 50 kg samples of snow and ice without contamination, and presented results which were not repeatable until 20 years later. Their results evaluated inputs from sea salt and crustal material in the samples, and correlated increasing Pb concentrations in the ice with increases in the production and emission of Pb in the Northern Hemisphere.

Murozumi et al. (1969) obtained samples from high-altitude locations in Greenland and Antarctica, whereas earlier investigations had usually analyzed continental glacier samples. The regular annual accumulation of polar ice caps contributed to a

more accurate dating of the samples, while the high altitude of the sites assisted in minimising the influence of continental and coastal Pb sources such as rock and soil dust and sea salt spray. Other investigators had obtained samples from continental glaciers, but these were recognised by Murozumi et al. (1969) to be vulnerable to mixing and percolation processes, and incorporated large quantities of dust which could diminish the anthropogenic Pb signal. Annual layers of snow deposited on continental glaciers were too thick to readily enable the collection of samples thousands of years old, and were subject to mixing by percolation (due to the melting of ice) and mechanical mixing due to the underlying rock. These mixing processes disturb the regular layering of annually-deposited ice, and led to a 'smoothing' of the annual signal, potentially corrupting the results. They recognised the perennially-frozen, remote high-altitude polar regions to be ideal locations for obtaining samples which would contain a minimum of both dust- and sea-derived Pb and also allow reliably- dated samples to be obtained.

They conducted a field sampling expedition in Greenland in 1965, where they collected samples of surface snow as well as samples of firn and ice accessed via tunnels dug by the US military in the 1950's. Snow samples from 0.3 m to 13 m (dated from 1965 to the 1930's) were obtained from a virgin trench site located 80 km from the Camp Century base. Firn and ice blocks were obtained from an inclined tunnel shaft at the Camp Century base, between depths of 13 m and 100 m, dated from the mid-18th century to the 1900's. One other block of ice, dated to 800 BC, was obtained from an ice tunnel at Camp Tuto, near the US military base at Thule. In Antarctica, surface snow samples were obtained from virgin trench sites between 35 and 215 km Northeast of Byrd station. These provided data for the period between from the 1940's to 1966s. Older samples were obtained from an inclined shaft at Byrd station, between depths of 6 m and 43.5 m, these dated from the late 17th century to the 1940's. Two other samples were obtained from the Meserve and Erebus glaciers, however these were observed to contain large concentrations of silt and salts, and volcanic dusts and sea salts, respectively.

Samples were obtained using techniques developed by Patterson and co-workers specifically to minimise the transfer of Pb to the samples. Over their warm clothing, personnel involved in the sampling wore polyethylene trousers and hooded coats

with elastic wrist, ankle and waist bands. They also wore disposable polyethylene gloves and sleeve guards over the joint between their gloves and coat sleeves. This equipment was replaced daily, except for the gloves, which were changed as often as necessary. All sampling equipment was made from plastic or stainless steel, which had been thoroughly cleaned in acid before use. Large (120 L) polyethylene drums with lids, used for melting firn and ice blocks, were immersed in a 200 L bath of concentrated reagent-grade nitric acid for a few minutes and then rinsed thoroughly with distilled water. They were then rotated a hundred times through a second bath of reagent-grade concentrated HNO₃ and rinsed four times with purified water before being sealed individually in acid-cleaned polyethylene bags filled with filtered Argon gas and then closed and knotted airtight. Polyethylene bottles used to contain melted water samples were cleaned in a similar manner. Sampling equipment used in the tunnels and snow pits were also acid-cleaned and sealed in polyethylene to minimise contamination. Such laborious procedures were undertaken to combat the high Pb levels in the urban environment in which the apparatus were prepared. Although they worked in a laboratory supplied with filtered air, Patterson and co-workers realised that the apparatus needed to be well cleaned in order to remove the Pb transferred to them during manufacturing and delivery to the laboratory. The apparatus was stored airtight in multiple acid-cleaned bags prior to sampling the snow and ice in order to ensure they free from contamination by polluted air during transport to the sampling site.

Virgin sites, located far from the locations of bases and known traverses and overflights, were selected for the collection of surface snow. It was recognized that the tunnels, which had been excavated by army engineers, were highly contaminated by cigarette smoke, beverages contained in cans sealed with Pb solder, and by the engineers' bodily excreta. Wall sections to be sampled were cut back by 40 to 80 cm, to remove any surface contamination, before the block was cut. A stainless steel auger was used to drill holes 50 cm deep at each corner of the block. From these guide holes, the sides were then cut out using an all-teflon hand saw, and each block was broken away from the back wall by inserting a stainless steel wedge into one of the side saw cuts. The blocks were gripped in a large pair of metal tongs operated by two men, removed from the wall, and transferred into a 120 L plastic drum. Two blocks were obtained for each drum, with four drums filled at each level. Blocks

measured ~75 cm (vertical) by 150 cm (horizontal width) by 45 cm (horizontal depth). Surface snow samples were collected with shovels and scooped into drums. The collection of suitably thin layers of snow required that an area 10 m long and $\frac{2}{3}$ m wide to be sampled. Blocks were melted in their polyethylene collection drums in polyethylene-lined Jamesways (transportable laboratories) on site in Greenland, and transferred to polyethylene storage bottles using a polyethylene siphon. Of the ~ 200 L collected for each sample, these were distributed between two 50 L bottles, four 19 L bottles and one 8 L bottle. To the two 50 L bottles and two 19 L bottles, 100 mL of 8M HCl and 15 μg of ^{208}Pb were added to enable the concentration of Pb to be determined by isotope dilution analysis. Also, 100 mL of 8M HCl was added to another 19 L bottle.

A suite of Pb and other elements (Na, Cl, Mg, Ca, K, Ti, Si) were measured to discriminate between inputs of sea salt and dust in the samples. In most cases, these elements were each measured by two different techniques, isotope dilution (Pb, Ca, K, Ti, Mg), neutron activation (Cl, Na), atomic absorption spectrophotometry (Na, Mg, K, Ca), emission spectrography (Si) and colorimetric spectrophotometry (Cl). Observed concentrations of elements in each sample were referenced to Na. Based on analyses of typical concentrations of the elements in seawater, the sea salt component in each sample was determined by calculating the amount of each element from the element/seawater ratio and the Na concentration in the sample. This sea salt-derived component was then subtracted from the total, with the remainder attributed to rock and soil dust. Averaged inputs from sea salt and wind-blown dust were determined for each location - Byrd station, in Antarctica, and Coastal Glacier (near Camp Tuto) and Camp Century, in Greenland. As shown in Table 3.1, it was found that virtually all of the alkali elements measured in Greenland were derived from sea salts, with concentrations in the coastal glacier approximately ten times higher than those at Camp Century, 100 miles inland from Thule and 1886 m in altitude. Concentrations of Na at Byrd station, Antarctica, were similar to those at Camp Century, but high concentrations of Ca, K, Ti and Si indicated the natural inputs were derived overwhelmingly from rock and soil dust.

Table 3.1. Averaged concentrations of sea salt- and dust-related elements in ice samples from Greenland and Antarctica (in ng/g), from Murozumi et al. (1969).

		Na	Cl	Mg	Ca	K	Ti	Si
Average of 1942, 1857, 1775 and 1694 from Byrd Station	Observed	32	59	4	1.3	1.6	0.01	0.4
	Calc. Sea Salts on Na basis	32	57	4	1.2	1.2	0.00	0.0
	Dusty Remainder					0.4	0.01	0.4
800 B.C. Coastal Glacier From Tuto	Observed	350	570	45	17	16	0.06	2.1
	Calc. Sea Salts on Na basis	350	630	42	13	13	0.00	0
	Dusty Remainder				4	3	0.06	2.1
Average of ten composites: 1753, 1815, '35, '59, '81, '92, 1900, '33, '46, and '65	Observed	20	39	5	6.4	2.7	0.1	6.8
	Calc. Sea Salts on Na basis	20	36	2	0.8	0.8	0.0	0
From Camp Century	Dusty Remainder			3	5.6	1.9	0.1	6.8

Lead was separated from the polar ice and snow samples using a two-stage CHCl_3 and dithizone extraction, followed by purification of the Pb by anion exchange chemistry. The Pb was then separated from the eluate by precipitation to PbS , and centrifuged. The sample was then ready for transfer to a Tantalum mass spectrometer filament by means of a micropipette. Lead amounts were determined by isotope dilution by measurement of the $^{207}\text{Pb}/^{208}\text{Pb}$ ratio in the samples. The Pb blank was determined to be 70 ng, with the analytical reagents containing Pb concentrations of 300 pg/g for NH_4OH , 400 pg/g for undistilled HCl, 50 pg/g for distilled HCl and distilled CHCl_3 . A second Pb isotopic tracer, ^{206}Pb , was added to each sample after the first dithizone extraction in order to determine the Pb yield from the dithizone extraction. This varied from 95% to 45%, with an average of 80%. The potential concern 'whether polyethylene cleaned with HNO_3 would absorb the more labile lead tracer before it could mix with the less labile pollutant lead' was also tackled by the addition of a ^{206}Pb tracer. Solutions of purified water mixed with HCl and NH_4Cl and spiked with ^{208}Pb were stored in several cleaned polyethylene carboys. The solutions were then sampled and analysed almost immediately from one set of carboys, and several months later from a second set of carboys – in each case using a ^{206}Pb spike. Ratios of $^{206}\text{Pb}/^{208}\text{Pb}$ were observed to be identical in all cases, and it

was determined that ‘no lead was absorbed by the polyethylene under these conditions’.

Murozumi et al. (1969) determined that Pb concentrations in Greenland had increased significantly since 800 BC and correlated these increases with important changes in the industrial processing and societal uses of Pb, as shown in Figure 3.1. In the sample dated to 800 BC, the measured Pb concentration was $<0.001 \mu\text{g/g}$, compared to the next-oldest sample, $\sim 1750 \text{ AD}$, which had a Pb concentration of $0.010 \mu\text{g/g}$. The following samples, between ~ 1810 and ~ 1940 , indicated slowly increasing Pb concentrations from $\sim 0.03 \mu\text{g/g}$ to $\sim 0.07 \mu\text{g/g}$. The most rapid increase was observed after 1940, with concentrations usually over $0.12 \mu\text{g Pb/g}$. The highest Pb concentration measured was in the most recent snow of Spring 1965, at $\sim 0.23 \mu\text{g/g}$. Lead concentrations in Antarctic samples were systematically lower, $0.05 \mu\text{g/g}$ in 1961 and less than $0.01 \mu\text{g/g}$ prior to $\sim 1940 \text{ AD}$. Measured Pb concentrations in Antarctic samples dated prior to 1840 AD were often $<0.005 \mu\text{g/g}$, too low to be accurately measured by the analytical techniques available at the time.

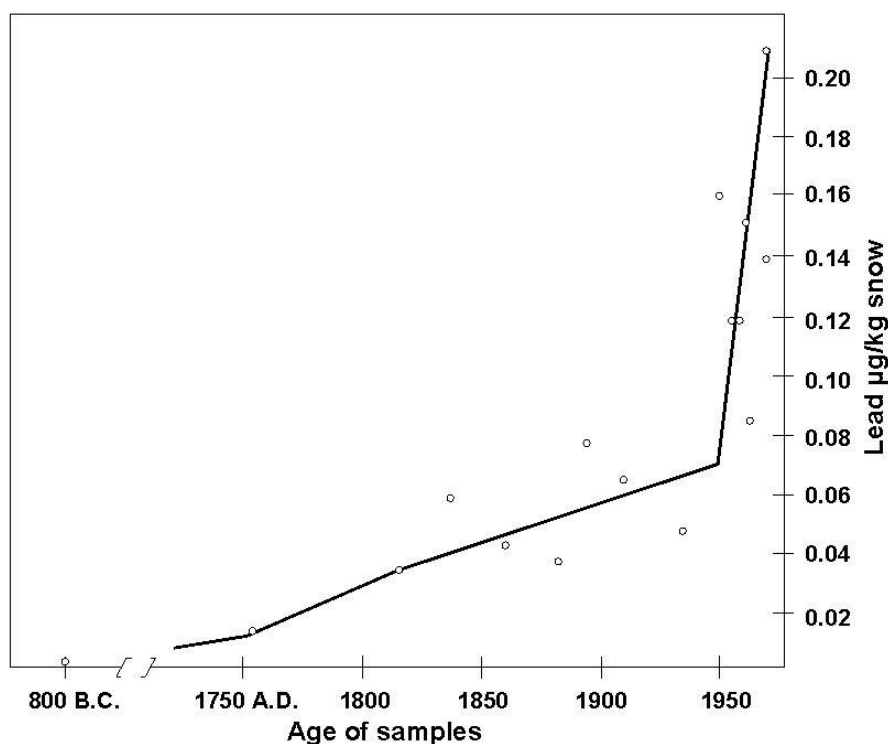


Figure 3.1. Increase of industrial Pb pollution in Camp Century snow with time since 800 BC. Units on vertical scale are $\mu\text{g Pb/kg}$, equivalent to ng Pb/g , redrawn from Murozumi et al. (1969).

The Greenland sample from ~1750 AD corresponded to the beginning of the industrial revolution in Europe, and indicated that even then Pb concentrations in Greenland were elevated above natural levels by about 25 times. While the amount of Pb smelted in the Northern Hemisphere increased steeply after 1860, Murozumi et al. (1969) suggested the much more gradual increase observed in Greenland Pb concentrations was likely to be due to improvements to furnace designs and smelting procedures. These enabled the loss of Pb fume (Pb oxide-rich aerosols) to be gradually minimised, partially as interest turned to the recovery of Pb and Ag from sulphide ores and as ore became more scarce in Europe toward the end of the 19th and beginning of the 20th centuries. The addition of Pb-alkyls to automobile gasoline, beginning in 1923, was cited as the source of the prodigious increase of Greenland Pb concentrations after 1940. During the 1940's, 36×10^3 tons of Pb was burned as Pb-alkyls compared to 110×10^3 tons in the 1950's, 180×10^3 tons from 1950 to 1958 and 310×10^3 tons from 1960 to 1966. This compared to 2400×10^3 tons of primary Pb smelted at the time in the Northern Hemisphere, of which losses as aerosol fume may be approximately 0.06%. It was recognised that about a half to a third of Pb-alkyls in gasoline were introduced into the atmosphere as fine aerosols, and were in such a form as to enable them to be transported long distances through the atmosphere.

In their paper, Murozumi et al. (1969) also identified other aspects involved with the deposition of heavy metals in polar ice sheets, which would later be studied in detail. Firstly, they observed that Pb concentrations were positively correlated to sea salt concentrations, and negatively correlated to dusts, and that higher Pb concentrations occurred in winter. Fluctuations of dust and sea salt did not coincide with the seasons, however. These observations would be later studied in more detail as the depositional characteristics of weather and mechanisms of atmospheric transportation and wet/dry deposition of Pb-bearing aerosols to Greenland. They observed Pb concentrations in Antarctica to be consistently lower than those in Greenland, and identified that the atmospheres of the Northern and Southern Hemispheres were relatively well-separated by the upwelling of air forced by a convergence of tropospheric meridional circulating cells at the equator. They also considered the anthropological potential of research into heavy metals in polar ice strata, as a tool to determine the intensity of human industrial activity in the past,

particularly during the Roman civilisation and during the middle ages. Finally, their measurement of Antarctic Pb concentrations led them to recognise that the snow and ice of Antarctica could not be accurately evaluated until sufficient improvements had been achieved in terms of analytical blanks and measurement sensitivity. In 1981, a second reliable measurement of ancient Greenland ice was published, again by Patterson and co-workers (Ng and Patterson 1981). However it was not until the 1990's that accurate evaluations of concentrations of heavy metals in recent and ancient polar snow and ice were being regularly reported.

3.2 Studies of heavy metals in ice and snow: 1969 to 1981

Following the results published by Murozumi et al. (1969), more attention was turned to evaluating natural fluxes of heavy metals (this was, in part, an attempt to discredit their findings) and determining suitable techniques for processing samples containing ng/g-levels of Pb concentrations. The majority of work published by Duce, Herron and co-workers involved the evaluation of various potential sources of natural Pb emission, such as from plants, volcanoes and the volatilization of Pb in rocks. These various potential sources were investigated with an interest in providing a natural source to account for the overwhelming increase in Pb concentrations in Greenland snow and ice Murozumi et al. (1969) observed and attributed to anthropogenic Pb emissions. In the 1970's, some researchers investigated concentrations of aerosols collected on filters in remote locations, while others attempted to analyse heavy metals in snow samples and/or ice cores obtained from Polar Regions. For the most part, these samples were contaminated during collection, storage and measurement, leading to inaccurate evaluations of atmospheric Pb fluxes and serious discrepancies between the published findings and those reported by Murozumi et al. (1969). A definitive explanation of these discrepancies was not to be published until 1981, however.

Duce et al. (1975) attempted to explain excessive concentrations of Pb and other heavy metals in terms of natural fluxes, based on evaluations of crustal enrichment factors. They compared element concentrations in aerosols collected from a number of open ocean locations in the North Atlantic Ocean to those sampled earlier at the South Pole. For most of the elements, crustal enrichment factors for elements were

identical for both locations. Crustal enrichment factors of heavy metals, such as Se, Pb, Sb, Cd, Cu and Zn, varied from 10^2 to 10^4 and were found to be similar in both hemispheres. While they acknowledged particulate pollutants emitted from the Northern Hemisphere were likely to be the cause of enrichment of Pb and other metals in the North Atlantic samples, they did not consider anthropogenic sources to be responsible for enrichment at the South Pole. They mentioned the possibility that the lesser size of Southern Hemisphere land masses may result in a decrease in Southern hemisphere dust emissions proportional to the lesser quantity of anthropogenic aerosols emitted from those continents, but did not consider it likely. They considered the extreme magnitude of the enrichments of the elements to be most likely attributed to unaccounted natural sources, such as a vaporization-type geological process, volcanism, biological mobilisation or elemental concentration in the ocean surface. Realistic estimates of the quantity of heavy metals emitted from natural and anthropogenic sources were slow to appear however, with the earliest compilation of this research published toward the end of the 1970's (Nriagu 1979).

Other studies attempted to duplicate the results of Murozumi et al. (1969) from samples of snow and ice obtained from Greenland and Antarctica. These all failed to duplicate steadily-increasing Pb concentrations in the ice since the 18th century, but did confirm the high Pb concentrations observed in recent snow from the 1970's. These studies generally lacked suitable precautions against sample contamination and were undertaken with instruments for which the measurement sensitivity was inferior to that of TIMS. For example, Herron et al. (1977) measured Na, SO_4^{2-} , Si, Al, Fe, Pb, Cd, Zn, V and Mn in ice and snow from Station Milcent in Greenland. They did not mention any attempts to minimise contamination during drilling or storage of the core sections, and described the cleaning of sample melting bottles as 'an acid leach in 7% HNO_3 for 3-4 days followed by an extensive rinsing with distilled deionized water and double-distilled deionized water'. They did not specify the grade of HNO_3 acid used for the cleaning and that this acid was more dilute than those used by Murozumi et al. (1969). The ice cores were decontaminated by pouring high-purity water over the surface of the ice, thereby melting and removing the contaminated outer layers. This technique was used to remove ~20% of the core, the remainder of which was then melted and analysed by atomic absorption spectrophotometry and instrumental neutron activation analysis. They observed

significant crustal enrichment of Zn, Pb, Cd and S, and determined early 1970's Pb concentrations in Greenland snow to be $\sim 0.144 \mu\text{g}/\text{kg}$. The earlier samples, dated between 1885/6 AD and ~ 1170 AD, did not display a trend in Pb concentrations, which were randomly distributed about an average of $0.045 \mu\text{g}/\text{kg}$. They took this value to be the natural background level of Pb in the atmosphere as it corresponded to the average of Pb concentrations determined by Murozumi et al. (1969) between ~ 1750 and ~ 1930 AD. Variations in Pb concentrations observed by Murozumi et al. (1969) over this period were not considered significant. On this basis, Herron et al. (1977) did not consider their data to be contaminated and, indeed, asserted the 800 BC Greenland ice sample measured by Murozumi et al. at $<0.001 \mu\text{g Pb}/\text{kg}$, was spurious. Herron et al. (1977) acknowledged their results did 'lend support to the concept of selective mobilization of certain elements involved in fossil fuel combustion', however they considered the 2 to 3 times increase in concentrations of Pb, Zn and S during the 1970's – compared to their natural level of $0.045 \mu\text{g}/\text{kg}$ – to be more likely due to inaccurate estimates of natural emissions. This interpretation suggested that emissions of Pb from anthropogenic sources were comparable to those from natural sources, and that the resulting Pb concentration increase was at most 2 to 3 times natural levels.

Boutron and Lorius (1979) studied a range of trace metals, also by atomic absorption spectrophotometry, in snow and firn obtained from Dome C, Antarctica. These samples covered most of the 20th century, from 1914 to 1974, and concentrations of Na, Mg, K, Ca, Fe, Al, Mn, Pb, Cd, Cu, Zn and Ag were reported. For the heavy metals, significant crustal enrichment was observed in all samples, however no overall concentration trend was observed. Lead concentrations were $\sim 25 \text{ pg}/\text{g}$ and K $\sim 1 \text{ ng}/\text{g}$. The authors interpreted the data as showing that concentrations of these metals 'are not strongly influenced by global pollution, but are related to natural phenomena, possibly volcanism'. They did not attempt to explain why they observed Pb concentrations significantly higher than those measured at Byrd Station ($\leq 0.01 \text{ ng}/\text{g}$) by Murozumi et al. (1969). Boutron and Lorius observed fluxes of Pb, Cd, Cu, Zn and Ag to correspond approximately to emission fluxes from volcanoes, and believed that volcanoes could account for the enrichment of heavy metals observed in the ice. These findings were challenged by results published by Ng and Patterson (1981), however.

While studies were being undertaken with an understanding that sample contamination was an issue, few researchers understood the theoretical approach required to minimising this contamination. Patterson and Settle (1976) published a report on 'The reduction of orders of magnitude errors in lead analysis of biological materials and natural waters by controlling the extent and sources of industrial lead contamination introduced during sample collecting, handling and analysis'. These findings provided a detailed specification of the techniques necessary to account for and minimise laboratory-based analytical blanks, however these techniques took some time to be successfully implemented in other laboratories, leading to the reporting of unreliable data through much of the 1970's and 1980's. In addition to the laboratory techniques, some quantification or assessment of quality control was also required for the collection of snow and ice samples obtained from ice sheets. An approach to solving this problem of verifying ice and snow samples to be pristine (uncontaminated) prior to measurement was outlined with the publication of Pb data from Greenland and Antarctic ice cores by Ng and Patterson in *Geochimica et Cosmochimica Acta* in 1981.

Ng and Patterson (1981) outlined a new technique for sampling ice cores for heavy metals and presented new data of Pb and K (a proxy of rock and soil dust) concentrations in ancient ice core sections from Camp Century, Greenland, and Byrd Station, Antarctica. They described the importance of identifying the real background of natural Pb concentrations in polar ices, to accurately apportion contributions from various natural sources as well as to evaluate the extent of anthropogenic Pb contamination. The sampling and analytical techniques described in the paper represented a significant improvement over those employed by Murozumi et al. (1969). A mechanical chiselling technique was used to remove contaminated external layers from the core, sample treatment was minimised and a lower Pb blank was established and mass-spectrometry techniques had improved in absolute accuracy and sensitivity. These improvements enabled Ng and Patterson (1981) to publish new results from ice cores which confirmed the natural fluxes of Pb and dust in Greenland and Antarctica.

While Pb concentrations in ice core sections had previously been published, previous researchers had not made any attempt to establish that these sections had not been contaminated during drilling or storage. Ng and Patterson (1981) identified a means of verifying that ice cores were free from contamination, by demonstrating a plateau of concentrations from the exterior of the core through to the interior. This technique was ideal in that it emphasized a technique of removing successive veneers from the ice core, attempting to minimise the entrainment of Pb from one layer to the next. They realised that this purpose would be best served by the mechanical removal of each veneer, instead of the technique adopted by Herron et al (1977), which involved the washing and melting of the exterior of each core section using chilled acetone and distilled water. Ng and Patterson (1981) found that cleaning of the core with liquids 'caused visible cracks to form in core sections (even though chilled to the same temperature as the ice) which undoubtedly transferred contamination inward' and believed these could be re-opened fractures originally caused during the drilling process. The liquid-rinsing technique was initially employed on cores drilled from the fluid-filled hole at Camp Century, as an attempt to remove traces of drilling fluid (diesel fuel and trichloroethylene). These samples displayed more contamination, penetrating deeper into the core profile, than the thermally-drilled dry hole core sections obtained from Byrd Station. Ng and Patterson (1981) removed four to eight veneers ~4 mm thick from each of the 5 core sections analysed. The core was laid flat on a bench covered by acid-cleaned polyethylene while the veneers were removed. Collected veneers were then collected into a polyethylene bottle and weighed. The final core section was usually 2 to 3 cm in radius, this being rinsed with CHCl_3 and 1% HNO_3 before also being stored in a polyethylene bottle. This final rinse was maintained as it was considered that 'there probably were fewer partially annealed fractures within the inner region of the core section'. Despite these precautions, no plateaus of Pb concentrations were established, however plateaus for K were clearly demonstrated in all but one sample. This technique of analysing the veneers sequentially removed from the core enabled Ng and Patterson (1981) to demonstrate the validity of the core sections they sampled, and enabled them to identify their results as upper limits of the real Pb concentration in ice.

Ng and Patterson (1981) analysed five ancient ice sections, three from Camp Century (dated 2700, 4500 and 5500 years before present) and two from Byrd Station (dated

1490 and 2010 years before present), in an attempt to establish the ancient pre-industrial background of Pb concentrations in the Northern and Southern Hemispheres. Although they could not establish Pb concentration plateaus in the samples, they did show results which supported the $<0.001 \mu\text{g/kg}$ Pb concentration measured at 800 BC in Greenland ice by Murozumi et al. (1969). Their lowest concentrations were 1.6 ng Pb/kg and $1.7 \mu\text{g K/kg}$ in Greenland and 1.4 ng Pb/kg and $0.9 \mu\text{g K/kg}$ in Antarctica.

Their results showed the measurements presented by Murozumi et al. (1969) to be correct and valid, that the concentrations of Pb in ancient Greenland and Antarctic ice were indeed $\leq 1 \text{ pg/g}$, similar to that expected from natural emissions of silicate dusts and over a hundred times less than Pb concentrations in 1970's snow. Ng and Patterson (1981) showed ice cores to be susceptible to extensive contamination during drilling, but that this contamination could be removed. Electromechanical cores drilled in fluid-filled holes appeared to produce exterior Pb concentrations $\sim 10^6 \text{ ng/kg}$, this being 100 times greater than Pb levels measured on thermally-drilled cores obtained from dry holes (those not filled with drilling fluid). They also observed that this contamination extended deep into the core, so that large-diameter cores ($\sim 10 \text{ cm}$ diameter) are more likely to furnish uncontaminated inner sections suitable for heavy metals analysis. They believed this contamination to be transferred into the core by cracks formed during drilling by thermal or mechanical shock, which were then annealed shut and thus may not be detectable by visual inspection. Their results demonstrated that the technique used by Herron et al. (1977), of using liquids to remove the external, contaminated, section of the core, was insufficient and unreliable. Additionally, Herron et al. (1977) removed 20% of the core volume, while Ng and Patterson (1981) found that contamination still remained after removing 75 – 85% of the core volumes. Ng and Patterson (1981) emphasized the objective in removing the external layers was primarily to minimise the entrainment of surface contamination to the inner layers.

Ng and Patterson (1981) also provided an evaluation of the natural fluxes of Pb through the various media in which Pb could be sequestered and then analysed to evaluate changing Pb levels over time. They recognised that the Pb emitted by industrial processes were in the form of fine particulate, while rock and soil dust

particles were likely to have different sizes and different chemical properties. They evaluated the differences between Pb in air and Pb in precipitation at a number of remote locations and compared these results to a typical urban location, to show that the nature of Pb/Silicate-dust ratios in air and precipitation were significantly different at these locations. They demonstrated that the majority of Pb transferred to remote locations occurred in precipitation (with Pb/Silicate-dust ratios in Greenland snow about 10 times greater than the air above the snow) while the Pb/Silicate-dust ratio in urban air was a thousand times greater than that observed in rain. They recognised that magnitudes of increases in Pb concentrations varied between different natural archives, such as ponds, lakes, pelagic ocean sediments and ice strata, and also noted the differing inputs of natural Pb to these media. They wrote:

It is not generally understood that increases of industrial lead concentrations in sediments are caused by much larger increases of lead concentrations in the atmosphere with time, because atmospheric inputs of industrial lead to watersheds of ponds and lakes must increase by large factors before they can overtake and effectively exceed natural fluvial inputs of lead to ponds and lakes.

They went on to explain that Pb/silicate-dust ratios observed in 1980's air should lie between the '300-fold excess of industrial lead in precipitation and a 4-fold excess of industrial lead in sediments' and that the study of polar ice was the most sensitive means of determining past atmospheric Pb fluxes.

After defining the nature of variations of Pb/Silicate-dust ratios in remote air and precipitation, Ng and Patterson (1981) concluded by evaluating the various natural sources of Pb. They showed that these could not possibly explain the 10^3 times crustal enrichment factors observed for Pb in remote locations. They reviewed the then published literature and estimated global fluxes of Pb from silicate dusts to be about 2000 tons Pb/year. Lead emissions from volcanoes were based on preliminary studies of volcanoes, and were calculated to contribute ≤ 1500 tons Pb/year. Studies of Pb emission from ocean salts, combined with measurements of Pb concentrations in seawater and considering the sea-surface to be contaminated about 10-fold by industrial Pb, suggested that sea salt-spray could contribute no more than 500 tons

Pb/year. Two other natural sources of Pb emission that had been proposed in the literature, rock volatilization and emission from plant leaves, were considered 'unworthy of quantitative consideration at this time because of their vagueness' and 'seriously compromised by positive errors due to improperly controlled lead contamination', respectively. In total, Ng and Patterson (1981) estimated natural sources of Pb to be no greater than 4000 tons/year, while 1970's levels of industrial Pb emission were 360,000 tons/yr in the Northern Hemisphere and 40,000 tons/year in the Southern Hemisphere. These estimates supported the findings of Patterson and co-workers, that modern polar snows (~200 ng Pb/kg) contain Pb levels hundreds of times in excess of those found in ancient ice (≤ 1 ng Pb/kg) and that natural atmospheric dust levels of ≤ 1 ng Pb/kg could be well-accounted for in terms of emission of Pb in silicate dusts. Their finding of ~ 35 μg dust/kg in ice, when combined with an estimate of 12 ng Pb/kg in dust, indicated that Pb concentrations in polar ice due to dust should be ~ 0.4 ng/kg. Based on their calculations that dust sources probably account for $\sim 50\%$ of natural Pb emissions to the atmosphere, this would suggest a natural Pb concentration in polar ice of 0.8 $\mu\text{g}/\text{kg}$, which corresponded well to the values reported by Murozumi et al. (1969) and Ng and Patterson (1981).

3.3 Studies of Pb concentrations in Antarctica: 1983 – 1993

During the 1980's and early 1990's a number of important studies were undertaken to resolve the discrepancies between results of Antarctic studies published in the 1970's, largely due to contamination of samples during collection and/or analysis. Boutron, Patterson and co-workers, collaborating between California Institute of Technology and the Laboratoire de Glaciologie et Geophysique de l'Environnement in Grenoble, published a series of analyses of Pb in snow and ice cores from several locations in Antarctica, confirming the initial results obtained by Patterson and coworkers in 1969 and 1981, and extending the record of Pb concentrations in Antarctic ice back to 155,000 years before present. A group at the British Antarctic Survey (including A.L. Dick, M.P. Landy, D.A. Peel, E.D. Suttie and E.W. Wolff) also presented a number of important findings concerning the influence of Pb emission from localised sources (such as bases) in Antarctica, spatial and seasonal variations in concentrations of Pb and other heavy metals in Antarctica, and

concentrations of heavy metals in Antarctic air. They also reported experimental techniques for the minimisation of contamination during separation and analysis of heavy metals as well as review papers covering developments in the analysis and distribution of pollutants in polar snow and ice. These studies by Patterson, Boutron, Wolff and co-workers were important to discovering the true values of natural Pb fluxes to Antarctica, estimates of its variability and dominant emission sources. This complemented studies of Greenland snow and ice, which primarily addressed the sources and influence of anthropogenic Pb pollution then observed in Greenland snow strata.

Boutron, Patterson and co-workers published a series of data of analyses of Pb in snow and ice cores from several locations in Antarctica, extending and confirming the initial results obtained by Patterson and coworkers since 1969. They studied ice core sections obtained from deep ice cores drilled at Dome C and Vostok, to establish natural levels and sources of Pb in Antarctica and investigate the extent of variability during glacial/interglacial transitions. Dome C and Vostok are both thermally drilled deep ice cores located on ice domes in East Antarctica. The Dome C core was obtained from a dry hole using no drilling fluid, while the Vostok core hole was filled with a hydrocarbon fluid. Boutron and Patterson (1986) obtained samples dating back to ~27,000 years before present from the 905 m deep Dome C ice core, which revealed changes in Antarctic Pb concentrations from the last glacial maximum (LGM) into the present Holocene interglacial. They measured Pb concentrations in 14 core sections, which varied from ~1 pg/g in the last (Wisconsin) ice age, up to 10 - 29 pg/g through the LGM and ~ 0.4 pg/g in the Holocene, as shown in Figure 3.2. Aluminium, Na and SO₄ concentrations were interpolated from data available from other Dome C core sections, and used to calculate Pb inputs from rock and soil dust, volcanism and sea salt, respectively. The data showed conclusively that rock and soil dust, which increased ~30 times during the transition, accounted well for the increased Pb concentrations also observed during the transition. While volcanism accounted for ~ 50% of the Pb deposited during the Holocene, it was shown to account for only ~1% of Pb in Antarctic ice during the transition. Sea salts were shown to be a negligible contributor of Pb to Dome C at all times, on the order of 0.1% during the Holocene and 0.01% during the LGM. In addition to proving conclusively that Pb concentrations in Antarctic ice could be

accounted for completely by known natural Pb emission sources, Boutron and Patterson (1986) showed that Pb concentrations in ice responded sensitively to variations in the proportion of emission from these sources. They also established a reliable value for Holocene background Pb concentrations at ~ 0.4 pg/g, substantially less than the best previous value of ≤ 1 pg/g (Ng and Patterson 1981).

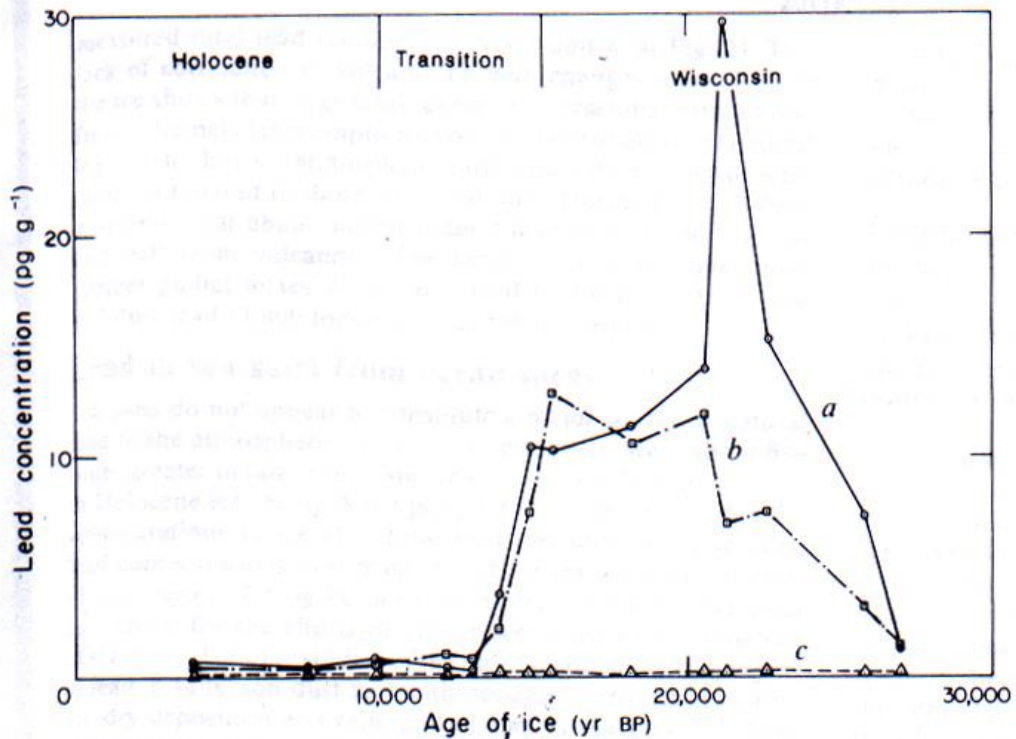


Figure 3.2. Variations of Pb concentration across the Wisconsin/Holocene boundary in the Dome C ice core, from Boutron and Patterson (1986). Shown are measured Pb concentrations in the centre of the analysed core sections (a), estimated Pb contribution from dust calculated from interpolated Al concentrations in the ice (b) and estimated Pb contribution from interpolated non-sea-salt sulphate concentrations in the ice (c).

These results were extended with the analysis of six samples from the Vostok ice core dated between 26,200 years before present and 155,000 years before present (Boutron et al. 1988). Of the six samples, only three could be considered to indicate true concentrations in the ice – for the other three, a plateau of concentrations across the innermost chiselled layers was not established. This was due to the use of drilling fluid in the drillhole, which significantly contaminated the majority of the core

profile. For the ~10 cm diameter Vostok core sections, inner cores 2 to 4 cm in diameter were recovered. Despite the sparseness of the data, Boutron et al. (1988) showed that Pb concentrations were relatively low (~2.5 pg/g) during the last ice age but increased in the next-to-last glacial maximum, these changes again corresponding with variations in Al inputs. The two samples corresponding to the last interglacial ~120,000 to 140,000 years BP were both contaminated, so it could not be established that Pb concentrations in the last interglacial matched those observed for the early Holocene. These publications provided a thorough description of the relationships between changes in the concentrations of natural Pb in Antarctic precipitation and various sources of this Pb – wind-blown rock and soil dust, volcanic emissions and sea salts. They also finally established the view that industrial Pb emissions overwhelmed natural Pb emissions, and that current levels of Pb in the polar ice caps were significantly greater than in pre-industrial times.

Boutron and Patterson also studied snow and firn deposited during the 20th century in an attempt to understand the history and extent of anthropogenic Pb contamination of Antarctica, with these samples obtained from locations on a transect inland from coastal Adelie Land and at the South Pole. Boutron and Patterson (1983) measured Pb concentrations in a snow and firn core collected at stake D55 (180 km inland from Dumont d'Urville station) and in several 10,000 year old ice blocks from Cap Prudhomme, both in Adelie Land, East Antarctica. A 10 m snow core was hand-drilled, providing samples dating back to 1797 AD. When decontamination profiles for these core sections were investigated, however, few of them produced plateaus. Some of the cores appeared to have been subject to partial melting during storage and transport, which transferred contamination to the centre of some cores. While these plateaus were not checked for every core section, most of the inner core results were considered to be close to real Pb concentrations in the snow. The data showed that Pb concentrations were ~1.6 pg/g in 1800 AD snow, corresponding well to the concentration observed in coastal blue ice: 1.7 pg Pb/g. From 1800, the Pb concentration increased slowly to ~4 pg/g by 1900, however between ~1915 AD and 1945 AD, Pb concentrations were significantly lower, at 0.9 pg/g and 1.2 pg/g, respectively. Lead concentrations from 1956 to 1966 were again about 4.5 pg/g. The results were ambiguous in that there was no definitive explanation for the low Pb concentrations observed early in the 20th century.

Ng and Patterson (1981) had calculated that volcanic activity could change Pb concentrations in Antarctic snow by at most ~ 3.5 pg/g, which was within the range of the observed variations, however it was equally possible that the values ~ 1 pg Pb/g were accurate while the others were contaminated. The extent of anthropogenic Pb contamination of 20th century Antarctic snow had not been resolved, however Boutron and Patterson (1983) had demonstrated that concentrations were in the 1 to 4 pg Pb/g range and so the majority of data reporting Pb concentrations in Antarctic snow were invalidated by sample contamination.

These results were re-examined following the investigation of ancient ice from the Dome C core (Boutron and Patterson 1986), with the study of Pb concentrations in blocks of surface snow collected from Adelie Land and at the South Pole (Boutron and Patterson, 1987). Snow blocks measuring 37 cm x 37 cm x 37 cm were collected at stakes D40, D47 and D80 and at the South Pole (located 33 km, 103 km, 433 km and 1274 km from the Dumont d'Urville coastal base, respectively) were collected using ultra-clean procedures and transported to Caltech. There they were decontaminated mechanically using stainless steel chisels and shovels to sample the contamination-free snow from the centres of each core. Decontamination plateaus were achieved, indicating that the results were representative of actual Pb concentrations in Antarctic surface snow. The results showed that Pb concentrations were high ~ 7 pg/g at Stakes D40 and D47 (near Dumont d'Urville station) and also at the South Pole (6.3 pg Pb/g). The Pb concentration at Stake D80, 433 km from Dumont d'Urville, was 2.3 pg/g. The interpretation of the results was that snow blocks from stakes D40 and D47 were contaminated by Pb emitted from Dumont d'Urville station while the South Pole snow block was contaminated by Pb emitted from Amundsen-Scott station, 7.3 km from the sampling site. This was found to be in accordance with several previous studies (including Murozumi et al. 1969) which observed excessively high Pb concentrations in surface snow within ~ 100 km of active stations and bases in Greenland and Antarctica. On this basis, the only reliable sample for evaluation of the Pb concentration in 1983 Antarctic snow was 2.3 pg/g, from stake D80, 433 km from Dumont d'Urville station. This result, combined with the ~ 1 pg Pb/g concentrations obtained in early-20th century snow from stake D55 (Boutron and Patterson 1983) and concentrations ~ 0.4 pg Pb/g from Dome C ice

from ~14,000 BP to ~4000 BP (Boutron and Patterson 1986), constituted the most reliable Pb concentration data collected from Antarctic snow and ice between 1969 and 1987. It showed that Pb concentrations had remained steady ~ 0.5 pg/g for most of the Holocene, but had increased to ~ 0.9 pg/g by 1915 AD. Lead concentrations continued to increase through to the 1940s (~1.3 pg/g) and had doubled again to 2.3 pg/g by 1983. On this basis, it was shown that about 80% of Pb in Antarctic snow originated from anthropogenic sources. There remained a significant gap in the data – from ~7600 BP to ~1915 AD – which would require investigation. This period would establish when anthropogenic Pb inputs to Antarctica first became significant, and would enable an evaluation of technological activity in the Southern Hemisphere, from the Incan civilization and the Spanish conquest of South America, to the colonization of Africa and Oceania and subsequent rise of industrial activity from the mid-19th century to the present.

While Patterson and co-workers established reliable values for natural Pb levels in ancient Antarctic ice, a group at the British Antarctic Survey were providing valuable data regarding the deposition and influences of Pb in Antarctic surface snow. The BAS scientists used a different analytical technique, differential pulse anodic stripping voltammetry (DPASV), to evaluate Pb, Cd and Zn concentrations. This technique had been established as a viable technique for measuring heavy metals in solution at pg/g concentrations with minimal contamination and high sensitivity (Landy 1980). Only small volumes were required for analysis, thus enabling snow strata to be analysed at reasonable depth resolution to observed seasonal variations in heavy metals concentrations. Landy and Peel (1981) analysed Cd, Na, Pb, Zn and microparticle concentrations in replicated series' of ~3 m of surface snow from a remote site on the Antarctic Peninsula. Heavy metals were analysed by DPASV, Na was measured by flame emission spectrometry and microparticles analysed by Coulter counter. Lead concentrations varied from 4 to 15 pg/g. Microparticle concentrations were analysed to deduce the input of wind-blown silicate particles from exposed rock local to the Antarctic Peninsula, and so determine the input of heavy metals at the site due to crustal material. This was found to average only 2% of Cd but 29% of Pb and 25% of Zn. The sampling was undertaken at high resolution (~5 cm depth intervals), enabling seasonal variations in heavy metals deposition to be evaluated for the first time. These variations were observed to be too large to be

accounted for by changes in emissions of heavy metals from anthropogenic or natural sources, and so were attributed to meteorological processes. A correlation factor of 0.45 was found between Na and Cd, the greatest correlation between any of the heavy metals and source indicators (Na and microparticles). This research demonstrated that the meteorological and depositional processes contributed significantly to the concentrations of heavy metals observed in Antarctic snow and ice.

Through the 1980's, Eric Wolff and co-workers at the BAS group also published reviews and descriptions of experimental techniques. In 1981, Wolff, Landy and Peel described, in *Analytical Chemistry*, a new technique for preconcentration of Cd, Cu, Pb and Zn in water samples by adsorption onto Tungsten wire and analysed by Flameless Atomic Absorption Spectrometry (AAS). This was a novel technique that proved to be simple and reliable and was ultimately intended for field use. A W wire loop was cleaned and activated by heating it in the spectrometer. The loop was then suspended from a platinum hook and immersed in the sample solution for less than an hour. Following immersion, the loop was then analysed in the AAS graphite rod. Negligible blanks for all metals were observed from the W wire. The technique was shown to be sensitive, requiring only 5 minutes plating time for Zn and between 30 and 60 minutes for Cd, Cu and Pb. Solution pH was found to play an important role in determining the W absorbance, with a pH of 3 proving optimal for collection of all metals. The addition of Al ions improved sensitivity of Pb measurements but lowered sensitivity of Cd and Zn analyses. Tungsten wires, preconditioned for up to a year before use, were found to function with no decrease in adsorption efficiency. The W wire technique, which was evaluated to have a precision of ~10%, was compared with DPASV and found to agree within ~20% at ppb concentrations.

Analytical blanks associated with this measurement technique were expanded upon by Wolff and Peel (1985), with analyses of Antarctic surface snow from Spaatz Island and southern Palmer plateau, on the Antarctic Peninsula. In this paper, the authors describe in detail their procedures for sampling and transporting snow cores, and their sub-sampling and measurement techniques. At Spaatz Island, a core several metres deep was drilled using a 10 cm diameter Aluminium hand-drill. From the southern Palmer plateau, 20 cm of surface snow was cleared away and three 60 cm

cores were obtained by driving cleaned acrylic tubes into the snow. All sampling was undertaken wearing cleanroom garb at pristine sites away upwind from equipment and vehicles. For each stage of sample handling, procedural blanks were evaluated, and an overall sensitivity and detection limit was defined for the analysis of each metal: Al, Cd, Cu, Pb and Zn. The W-wire preconcentration technique was employed for Cd, Cu and Pb analyses, while Al and Zn were analysed by direct injection into the AAS furnace. Snow cores were sub-sampled by splitting the core, so as to expose a fresh cross-section surface. The Spaatz Island cores were split using a PTFE slicer designed so as to not contact the innermost 37 mm of the core, which was to be sampled for analysis. Later, fresh core surfaces were prepared without the use of a slicer, by snapping them as they straddled two acrylic tubes. This technique was used for the southern Palmer plateau samples. The inner section of the core was then sampled using a pre-conditioned PTFE cylinder, which was forced into the centre of the core with a clean polyethylene mallet. The PTFE cylinder was then removed and used as the melting and preconditioning vessel for each sample. Concentration profiles were evaluated to determine the influence of contamination to core samples during collection. As a chiselling technique (such as that used by Ng and Patterson, 1981) was not employed, profiles were obtained using a small sub-sampler to extract several samples across the core. For the Spaatz Island core, decontamination profile plateaus were established for all elements except for Zn, which displayed inner core concentrations ~2% of those found on the exterior of the core. On the assumption that the other elements exhibited a similar concentration profile (2% of surface contamination penetrating to the centre of the core), Al and Pb contamination levels were calculated, respectively, to be ~0.2 pg/g and ~1 pg/g (below the detectable limits of the AAS technique used). For Cd and Cu, however, these contamination limits were ~1 pg/g and ~10 pg/g, respectively, approximately equal to observed inner core concentrations. On this basis, Pb and Al concentrations reported for the Spaatz Island core samples were considered correct, while Cd, Cu and Zn concentrations were, at best, upper limits. For the Palmer plateau cores, significantly lower surface concentrations were observed, and for all elements decontamination plateaus were established. It was determined that the contamination observed in the Spaatz Island core was predominantly due to the Aluminium corer used, in addition to the PTFE cutter, which assisted in transferring surface contamination toward the centre of the core. Another possible cause of contamination was the temperature of

the cores – air temperatures were lower (-10 to -15°C) during the collection and storage of the Palmer plateau cores, while the Spatz Island cores had been collected and stored nearer to -5°C. Increased temperatures could have assisted diffusion of contamination across the liquid-like layer on the surface of ice crystals. Wolff and Peel (1985) reported concentrations of 0.7 ± 0.3 ng Al/g, 0.26 ± 0.09 pg Cd/g, 1.9 ± 0.5 pg Cu/g, 6.3 ± 3.3 pg Pb/g and 3.3 ± 1.7 pg Zn/g in Palmer plateau surface snow. These samples represented mean crustal enrichment factors of 182 ± 94 , 4.5 ± 2.1 , 68 ± 35 and 6.3 ± 3.2 for Cd, Cu, Pb and Zn, respectively. Their reported concentrations were lower than all previously reported analyses for Antarctic surface snow, and although the possibility of sample contamination existed, constituted the best data available at the time, along with that of Murozumi et al. (1969).

Eric W. Wolff published reviews of global pollution as evidenced by polar snow and ice analyses in *Nature* (Wolff and Peel 1985) and *Antarctic Science* (Wolff 1990). These reviews provided a broad description of pollutants observed in polar regions, including gaseous species, radioactive and organic particulates, acids and heavy metals. A 1986 news article published in *Nature* by David Peel (Peel 1986) elucidated the significant findings of then-newly published data by Boutron and Patterson, who reported Pb concentrations in Dome C ice covering the LGM – Holocene transition. These articles and reviews evaluated the data available from the Arctic and Antarctica, and provided an impartial view of the extent to which anthropogenic activities have altered the natural fluxes of elements and molecules, particulate or gaseous, to the Earth's polar regions.

Dick (1991) sampled aerosols at the Antarctic Peninsula for heavy metals and marine and crustal source indicators such as Al, Na, K, sulphate and Ca. Average concentrations of Cd, Cu, Pb and Zn were reported to be 0.06 pg/m³, 1.0 pg/m³, 4.7 pg/m³ and 6.1 pg/m³, respectively. These concentrations were the lowest reported for aerosol samples anywhere in the world, and were lower than most previously reported data by an order of magnitude. While heavy metals were measured by AAS, these were verified in part by duplicate analyses of Pb, Ca and K by AAS and IDMS, and Al by AAS and INAA. Based on Na, K, Ca, Al and sulphate concentrations, anthropogenic sources were identified to be the dominant source of Pb and were considered likely to account for Zn concentrations in excess of calculated natural

inputs. Observed Cd and Cu concentrations could be accounted for by estimated natural inputs.

Suttie and Wolff (1992) reported heavy metals concentrations in a high-resolution series of snow samples also from the Antarctic Peninsula, demonstrating significant variations in concentration for all elements, but only a clear seasonal signal for Pb. A 1.7 m profile of surface snow was collected from a pit dug in a remote region on Dolleman Island, to the East of the Antarctic Peninsula. The profile contained approximately two years of snow accumulation (1984 and 1985 AD), with $\delta^{18}\text{O}$ isotopes and Cd, Cu, Pb, Zn, Na, Al, Cl^- and sulphate concentrations measured. Average concentrations observed were 0.08 pg Cd/g, 4 pg Cu/g, 4 pg Pb/g and 0.4 pg Zn/g. These were similar to previously reported Cu and Pb concentrations, but lower than previously reported Cd and Zn concentrations (Wolff 1990). It was found that Pb showed a strong seasonal signal and, like Na and Al, was elevated in concentration in the Austral autumn and perhaps also in spring. As with previous studies, Pb concentrations were too high to be accounted for by marine or crustal inputs. No seasonal trend was observed for Cd, Cu or Zn, for which concentrations were closer to the detection limit. It was concluded that ‘most of the Pb deposition to modern Antarctic snow originates in pollution from other continents, and this may be associated in transport with natural aerosol that is also transported over long distances. Since the accumulation rate and meteorology of this site are much different from that of most of Antarctica, these conclusions are tentative until confirmed by analysis of seasonal variations at other sites.’

Suttie and Wolff (1993) evaluated the extent of heavy metals contamination from point sources of emission in Antarctica and found Pb contamination was relatively limited. A petrol-driven generator (Lead content in petrol: 0.13 g/L) was operated for approximately 2 hours at a remote Antarctic site, after which surface snow was sampled about the generator. While surface Pb concentrations near the generator were very high, ~800,000 times higher than background levels, Pb concentrations were found to be indistinguishable from background levels over 40 m from the generator. Upwind from the generator, Pb concentrations were at normal levels only 5 m away. Of the Pb emitted, ~40% was calculated to be deposited in the surrounding snow, while ~60% was retained in the atmosphere and transported from

the immediate area. The contamination of surface snow about an Antarctic base (Halley 4 and 5, on the Brunt ice shelf) was also investigated, with surface samples up to ~300 km from Halley 4 and between the two bases (situated 12 km apart). It was found that for Cu, Pb and Zn, background concentrations were achieved within 10 km from the base. For Cd, concentrations did not vary significantly with distance, and there was only minimal evidence of decreasing concentrations as the distance from Halley increased. From Halley 4 base, the sampling traverse was approximately flat until the hinge zone (where floating ice meets continental ice) 30 km inland from the base. Altitudes increased with sampling sites further inland at 100 km (1189 m above sea level), 200 km (1676 m a.s.l.) and 300 km (1920 m a.s.l.) from the base. The predominant movement of katabatic winds, travelling radially from the elevated polar region out to the Antarctic coast, were considered to minimize the inland transport of pollutant aerosols. Along the traverse between the two stations, the data was more difficult to interpret. No significant variation in heavy metals concentrations was observed along the traverse, however one of the snow samples collected closest to Halley 5 did show a high Zn concentration, attributed to local waste burning. Unlike the other heavy metals, Pb concentrations were consistently close to background levels along the traverse. These results did not contribute to a clear picture of the pollution emissions from the two bases, and suggested that wind conditions are an important factor in the movement of pollutant aerosols emitted from the bases. Suttie and Wolff (1993) evaluated pollution of snow and ice by heavy metals, considering it unlikely to be significant >10 km from stations and >50 m from snowmobiles and other land-based transport. It was recognized that aircraft using leaded petrol could still have a discernible effect on heavy metals concentrations in remote locations, however. On this basis, the authors considered it unlikely that the elevated Pb concentrations observed in snow from Adelie Land by Boutron and Patterson (1987) was contaminated by emissions from the Dumont d'Urville base, located up to 100 km from sampling sites. Suttie and Wolff (1993) expected heavy metal emissions from Dumont d'Urville to be of a similar order as those from Halley 4, additionally because the samples analysed by Boutron and Patterson (1987) were also obtained on an inland traverse heading into katabatic winds and consistently increasing in altitude.

3.4 Evaluations of heavy metals emissions: 1980 to the present

Estimates of natural emissions of trace metals

Patterson and co-workers' collection and analysis of uncontaminated snow and ice samples was essential for the establishment of actual levels of natural Pb in the polar ice caps, from which natural emission sources could be accurately evaluated. However, natural background levels of Pb in polar ice required explanation in terms of calculated emissions of Pb from natural sources. Murozumi et al. (1969) were the first to determine natural Pb levels in Greenland ice, attributing approximately half of the Pb in ice to 'natural silicate dusts, and probably less than an equal amount [originating] from natural volcanic emanations or other natural exotic sources'. These approximations were based on evaluations of rock and soil dust inputs to the samples calculated from observed concentrations of indicators of dust input such as Si, Mg, Ca, K and Ti. With preliminary evaluations of volcanic Pb emissions, and measurements of proxies of dust, volcanism and sea-salt inputs, Boutron and Patterson (1986) produced better estimates of natural inputs of heavy metals to the atmosphere. They calculated global natural Pb emissions of ~1400 tonnes/y from rock and soil dust and ~1200 tonnes/y from volcanism. Natural Pb emissions from the oceans were calculated to be negligibly small. From the analyses of Pb in polar ice, research was undertaken to further develop preliminary estimates of natural emissions of trace metals, with the findings of these studies collected and assessed by Nriagu (1979, 1989) and Settle and Patterson (1980).

Estimates of the quantity of rock and soil dust emitted to the atmosphere have not varied greatly since its first calculation of 500×10^9 kg/y by Peterson and Junge (1971). Nriagu (1979) published the first global inventory of natural and anthropogenic emissions of Cd, Cu, Ni, Pb and Zn however, for Pb fluxes, this inventory was soon questioned by Settle and Patterson (1980). Nriagu (1979) estimated emissions of crustal rock and soil to be $6-1100 \times 10^9$ kg dust/y (average 500×10^9 kg/y) which combined with an average crustal Pb content of 32 ppm to produce emissions of 16×10^6 kg Pb/y. Patterson and Settle (1980) considered this estimate to be excessive:

Nriagu's estimates of natural lead emissions from silicate dusts are excessive because his estimate of natural lead concentrations in the dust is too high by a factor of 3 and he uses the highest estimate for dust in the air. The latter estimate is excessive; it is biased by measurements of dusts in rain and snow that are erroneously high due to dust contamination during sample collection.

Compared to Nriagu's estimate, Settle and Patterson (1980) evaluated dust emissions of 200×10^9 kg/y and crustal Pb concentrations of 10 ppm to calculate total Pb emissions of 2×10^6 kg/y due to rock and soil dust. The most recent evaluation of Pb emission due to rock and soil dust (Nriagu 1989) evaluated dust fluxes of $60\text{-}500 \times 10^9$ kg/y and average crustal Pb concentrations of 5.0-15 ppm, arriving at a total Pb flux of $0.3\text{-}7.5 \times 10^6$ kg Pb/y, with a median value of 3.9×10^6 kg Pb/y. From Nriagu's (1989) calculations, soil-derived dusts were found to account for over 50% of total natural emissions of Cr, Mn and V and probably 20-30% of natural emissions of Cu, Mo, Ni, Pb, Sb and Zn. Nriagu's earlier (1979) evaluation of natural sources of metal emissions did not consider biogenic sources, which were shown to significantly influence the atmospheric emission budgets of Cd and Hg as well as As, Cr, Cu, Ni, Pb and Sb.

Prior to the establishment of reliable natural crustal enrichment factors for Pb, volcanism was considered the most likely source for the apparent excess of atmospheric Pb emissions. Nriagu (1979) evaluated the global production of volcanogenic particles to be $6.5\text{-}150 \times 10^9$ kg/y (median 10×10^9 kg/y), of which Pb emissions were calculated to be $4.2\text{-}96 \times 10^6$ kg (median 6.4×10^6 kg/y). Nriagu (1979) evaluated average crustal Pb abundances of 16 $\mu\text{g/g}$ and a 40-fold enrichment of Pb in volcanoes. Patterson and Settle (1987) also estimated the global Pb flux from volcanoes, by measuring Pb/S ratios in volcanic plumes of a few volcanoes, and extrapolating this ratio to the estimated amount of S emitted from volcanoes globally. Lead, Bi, Tl and S were measured in Kilauea (Hawaii), Mt Etna and Vulcano Island (Italy) and White Island (New Zealand), with global S emissions chosen from a range of values published in several earlier studies. From earlier studies, it was also understood that Pb, attached to S particles, was emitted in significant quantities from volcanoes to the atmosphere. It was later shown by Hinkley (1991) that >99% of Pb emitted from volcanic plumes was in particulate form, as determined by the

collection of aerosols on a 0.4 μm pore-size Millipore filter. Patterson and Settle (1987) collected Pb from plumes using a cleaned 47 mm diameter, 0.4 μm pore-size, Millipore filter attached to a pump. Sulphur, Cl and F were collected using a sampling apparatus employing two cold-traps, another millipore filter and a pump, connected in series with clean Teflon FEP tubing. Water condensated in the cold traps was analysed for S, F and Cl content, with most of the Pb collected in the first trap. Observed Pb/S ratios varied from 0.16×10^{-5} in a Vulcano plume, $\sim 1 \times 10^{-5}$ in White island plumes, $\sim 5 \times 10^{-5}$ in a Kilauea plume, and $\sim 18 \times 10^{-5}$ in Mt Etna plumes. Thallium/Bi ratios were also variable, from 0.089 in Kilauea to 0.5-1.0 in White Island plumes. Bismuth/Pb ratios in plumes were more regular, ~ 6 at White Island and 7 in Kilauea. From these measurements, and using a global S flux of $\sim 17 \times 10^6$ tons/y, Patterson and Settle (1987) estimated a global volcanic flux of 1200 tonnes Pb/y, 600 tonnes Tl/y and 4000 tonnes Bi/y. This proved to be comparable to estimates of rock and soil-based Pb emissions (~ 2000 tonnes Pb/y), but far less than modern anthropogenic Pb emissions of $\sim 10^5$ tonnes/y.

Lambert et al. (1988) employed a different technique for the evaluation of volcanic outputs of sulphate and trace metals using ^{210}Po fluxes, but arrived at similar results. This research followed observations that ^{210}Po was highly enriched (by $\sim 10^5$ times) in volcanic plumes relative to atmospheric concentrations and calculations that volcanoes contributed over 50% of the atmosphere's ^{210}Po content, suggesting that ^{210}Po could be a more sensitive and accurate guide to estimating global volcanic fluxes. In earlier work, Lambert and co-workers (1982) had established the global volcanic ^{210}Po output to be 5×10^4 Ci per year. $^{210}\text{Po}/\text{SO}_2$ ratios were measured in three volcanoes, Mt St Helens, Momotombo and Mt Etna, and found to vary from ~ 0.1 to 2.4 mCi/ton. The ratio at Mt Etna was observed to vary from ~ 0.2 to ~ 0.6 mCi/ton from September 1983 to April 1985. From these measurements, an average $^{210}\text{Po}/\text{SO}_2$ ratio of 1 mCi/ton was used to calculate the global flux of SO_2 as 50×10^6 tonnes per year. Such a value was approximately threefold higher than those calculated directly from SO_2 flux measurements, but are within reasonable agreement. Fluxes of ^{210}Po and Pb were measured in lavas from Mt Cameroun, Mt St Helens, Piton de la Fournaise, Merapi and Mt Etna, with $^{210}\text{Po}/\text{Pb}$ ratios found to be within the range of 0.09 to 0.59 disintegrations per minute per μg of Pb (dpm/ μg Pb). Using an average $^{210}\text{Po}/\text{Pb}$ ratio of 0.4 dpm/ μg Pb, the global volcanic Pb flux to the

atmosphere was found to be ~2500 tonnes per year, in good agreement with the value calculated by Patterson and Settle (1987).

Other Pb emission processes considered as potential sources of the excess of natural Pb observed in polar snow were the concentration and re-emission of Pb at the sea surface, volatilization of Pb from rocks and emissions from vegetation. These processes were only seriously considered during the 1970's and 1980's, prior to the definitive establishment of natural atmospheric Pb levels by Boutron and Patterson (1986). The quantity of Pb emitted from the oceans was primarily determined by the Pb concentration estimated for ocean water and the calculated enrichment factor for Pb at the ocean surface. Such calculations were based on the hypothesis that Pb-bearing particles were concentrated in suspensions at the ocean surface, and re-emitted in sea spray. Lead enrichment factors of up to 5000 have been suggested (Nriagu 1979), however Nriagu (1989) used a value of 200. However, the concentration of Pb in seawater is sufficiently low (Chow 1978, p.201) that even with these concentration factors, sea-salt spray is at best a minor contributor of Pb to polar snow. Also, estimates of natural Pb emission from sea-salts are artificially increased by anthropogenically-enriched Pb concentrations at the ocean surface (Tatsumoto and Patterson 1963). As for Pb emissions based on rock volatility or vegetation, calculations of these emissions were shown to be physically unrealistic (Brimblecombe and Hunter 1977) and invalidated by contamination-based errors (Ng and Patterson 1981, Settle and Patterson 1980), respectively.

Jerome O. Nriagu's (1989) evaluation of global natural emissions of heavy metals concisely compiled and assessed the state of knowledge of natural emissions of As, Cd, Co, Cr, Cu, Hg, Mn, Mo, Ni, Pb, Sb, Se, V and Zn. This compilation defined two categories of emission: principle sources (wind-borne soil particles, seasalt spray, volcanoes and wild forest fires) and biogenic sources (continental particulates, continental volatiles and marine). For Pb, Nriagu (1989) calculated median emissions of 3.9×10^9 g/y (range 0.3-7.5) for wind-borne soil particles, 1.4×10^9 g/y (range 0.02-2.8) for seasalt spray, 3.3×10^9 g/y (range 0.54-6.0) for volcanoes, 1.9×10^9 g/y (range 0.06-3.8) for wild forest fires, 1.3×10^9 g/y (range 0.02-2.5) for biogenic continental particulates, 0.20×10^9 g/y (range 0.01-0.38) for biogenic continental volatiles and 0.24×10^9 g/y (range 0.02-0.45) for biogenic marine sources. Total natural Pb

emissions calculated by Nriagu were 12×10^9 g/y (range 0.97-23), with 87.5% of this Pb derived from non-biogenic sources. Additionally, Nriagu recognized that:

The data...pertain to emissions in recent years and therefore include some recycled anthropogenic materials. For some metals, the emission rates in prehistoric times were conceivably lower than those calculated today. Biological processing of trace metals dispersed in the environment by human activities is well documented. It is impossible, however, to use the available information to quantify the contribution of recycled material to the total flux of any of the trace metals and metalloids.

For this reason, the minima of the ranges of Pb emission from seasalt spray, wild forest fires and biogenic material are small ($\leq 0.02 \times 10^9$ g/y) compared to those from wind-borne soil or volcanoes. In comparison to estimates of anthropogenic sources of metal emission, Nriagu (1989) found that natural Pb accounted for only 4% of Pb emitted in 1983. Other metals most significantly affected by anthropogenic emissions included Cd (15% emitted naturally), Ni (35% emitted naturally), V (25% emitted naturally) and Zn (34% emitted naturally). For As, Hg and Sb, anthropogenic emissions were observed to exceed natural sources by 100 to 200%.

Since the most recent compilation by Nriagu (1989), there have been some alterations to estimates of natural Pb emissions. Hinkley et al. (1999) suggested a re-evaluation of the global flux of sulphur due to volcanoes and a revision of proportions of metals emitted from volcanoes. This re-evaluation was based on measurements of metal/S ratios (Pb, Ag, Cd, Cu, In, Tl, Zn, As, Se, Sn, Sb, Te, Bi) in the plumes of Kilauea volcano in Hawaii and plumes of Merapi and Papandayan volcanoes in Indonesia. Hinkley et al. (1999) also made use of a newer global S flux estimate (Bluth et al. 1993) of 4.5×10^{12} g S/y, instead of Nriagu's range of $(15-50) \times 10^{12}$ g S/y. Hinkley et al. (1999) observed different proportions of metals emissions to those calculated by Nriagu et al. (1989), however the proportions of metals vary greatly in volcanoes, with average ratios of Pb:Cu:Zn observed in the Kilauea plume (1:2.9:4:33) differing from those in Indonesian volcanoes (1:0.1:1.2:10) and Mt Etna (1:0.08:2.7:8.3). These proportions could at best only be roughly approximated by Nriagu (1989) (1:0.25:3:3) and Hinkley et al. (1999)

(1:0.3:1.2:7.9). Overall, the metals fluxes calculated by Hinkley et al. (1999) were significantly lower than those calculated previously, with Hinkley et al. (1999) calculating annual global Pb emissions of 855 tons Pb/y, compared to the value of 3300 tons Pb/y reported by Nriagu (1989).

It would be difficult to verify these fluxes to better than an order-of-magnitude estimate, as volcanism can be active or quiescent, and is subject to significant variability both spatially and temporally. Further, these fluxes cannot be readily verified in polar ice core records, as fluxes of natural Pb to Greenland are dominated by crustal dust, and fluxes of natural Pb to Antarctica are likely to be affected by the Antarctic circumpolar vortex and regional volcanism (around, for example, Ross Island, Deception Island and the South Sandwich Islands). It is likely that a more precise estimate of Pb fluxes from volcanism can be accomplished with more extensive sampling of metal/S ratios from volcanoes, and satellite-based monitoring of global volcanic S fluxes, however the usefulness of a more precise determination is questionable in consideration of the precision at which ice core or snow blocks can be sampled and dated.

Estimates of anthropogenic emissions of trace metals

The first evaluation of past and present emissions of heavy metals from anthropogenic sources was published by Murozumi et al. (1969) for comparison with the increasing trend of Pb concentrations observed in Greenland ice. Since then, more information has become available concerning mining and production statistics prior to the 20th century, particularly in the Southern Hemisphere. Evaluations of the output of heavy metals from various anthropogenic sources have improved, with changes in technology and use acting to increase or decrease the quantity of heavy metals emitted from each of these sources in different locations over time.

Murozumi et al. (1969) reported a history of anthropogenic Pb emissions based primarily on estimates and statistics of Pb production and Pb alkyl consumption, from 1750 AD to 1966 AD, for both the Northern and Southern Hemispheres. Lead production from 1890 to 1966 was based upon US Bureau of Mines yearbooks and similar publications, while Pb alkyl production data for 1924-1958 was based on US

Public Health Service publications. Estimates of earlier Pb production figures were based on a 1929 mining economics paper (1860 and 1880) and from silver production data (1800 and 1750). These data are shown in Table 3.2 and Figure 3.3.

Table 3.2. Amount of Pb (in 10³ tonnes) smelted or burned each year since 1750 AD, from Murozumi et al. (1969).

Date	Northern Hemisphere		Southern Hemisphere	Northern Hemisphere
	Primary smelting	Secondary smelting	Primary smelting	Burned alkyls
1966	2400	700	350	310
1960	1900	600	360	180 (1958 data)
1950	1300	550	240	110
1940	1300	400	230	36
1930	1200	400	170	4
1920	880	200	110	0
1910	940	60	100	
1900	750	0	80	
1890	520		40	
1880	400		2+	
1860	220		+	
1800	90		50	
1750	60		40	

The figure shows the majority (~90%) of Pb production and alkyllead-burning has occurred in the Northern Hemisphere. These activities were relatively constant prior to ~1890 AD, when the second industrial revolution took place. Increased mechanisation led to greater demand for Pb in the Northern Hemisphere, and Pb production figures steadily increase until early in the 20th century. At this time, demand increases even further with the implementation of alkyllead gasoline additives. In comparison, Pb production in the Southern Hemisphere remained relatively low and steady through to the 20th century.

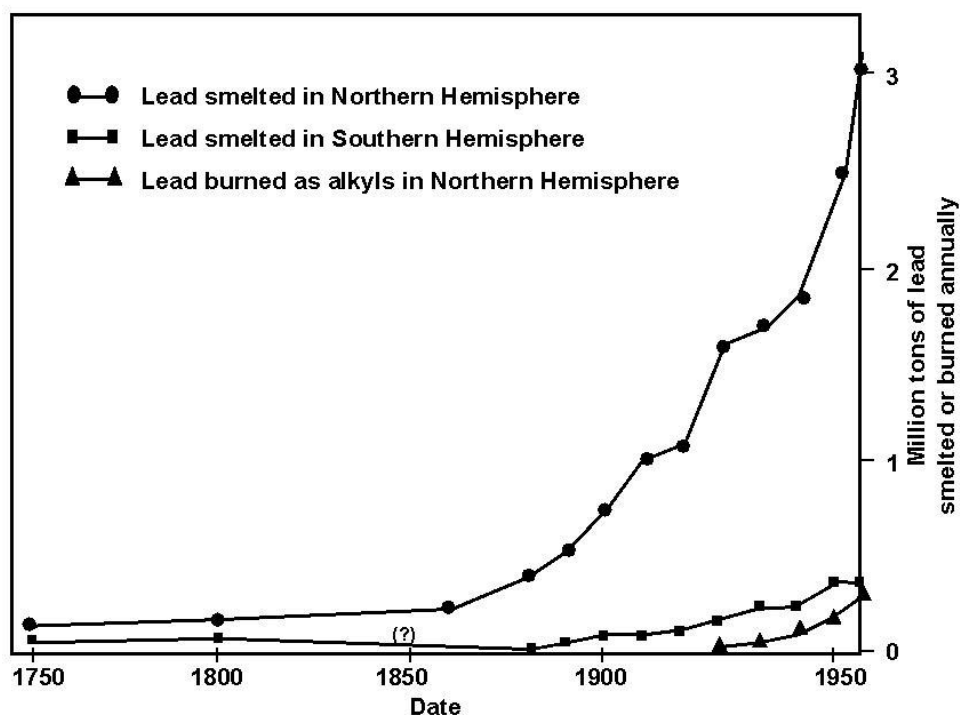


Figure 3.3. World Pb smelter production and alkyllead production since 1750 AD, redrawn from Murozumi et al. (1969).

Murozumi et al. (1969) noted that Pb smelting practices were much less efficient prior to 1880 AD, when recovery of Pb smelter fume became commonplace. This was estimated to have reduced Pb emissions as aerosol fume from ~2% of total Pb produced to ~0.5%, with later improvements further reducing this figure to ~0.06% by the middle of the 20th century. The data produced by Patterson and co-workers were limited but adequate for the time. No previous study of environmental heavy metals pollution had attempted to link metals production directly to concentrations observed in polar ice and no previous study had attempted to quantify emissions from anthropogenic sources. This work established a method for evaluating anthropogenic emissions of heavy metals and demonstrated that such evaluations were of use in understanding the origins of fluxes of heavy metals to the atmosphere.

Nriagu (1979) published the first dedicated evaluation of anthropogenic emissions of Cd, Cu, Pb, Ni and Zn. Included were emission efficiencies for various industrial

activities and a calculation of global consumption and emission of those metals from 1850 AD to 1979 AD. Whereas Patterson and co-workers had only studied Pb emissions, Nriagu (1979) extended this evaluation to other trace metals produced in great quantity, and considered the diverse methods of consumption of these metals. He calculated emission factors for each metal from each major industrial process, and used 1975 industrial statistics to calculate the quantity of each metal emitted from each industry. This enabled the total amount of each metal emitted from these sources to be calculated for 1975. This calculation was then applied to past years, taking into account variations in the size of industries, and changes in technology that may affect emissions. For most of the metals, primary non-ferrous metal production was observed to be a significant contributor to emissions, however, for some metals, particular emission sources were also found to be significant. It was calculated that 19% of Cd emissions originated from waste incineration, compared to 67% originating from non-ferrous metal production. 21% of Cu and 24% of Zn emissions originated from wood combustion, compared to 38% for Cu and 43% for Zn emitted from non-ferrous metal production. Finally, ~60% of Pb and Ni emissions, respectively, were due to combustion of leaded gasoline and nickeliferous diesel oil. These calculations demonstrated that anthropogenic sources contributed significantly to (for Cu and Ni), or overwhelmed (for Cd, Pb and Zn), natural metal emissions. Further, he calculated that emissions of these metals had increased by ~10x during the 20th century, and estimated the total quantity of each of these metals released into the atmosphere from anthropogenic sources. Estimated quantities of metals released globally due to all human activity were 0.32×10^9 kg Cd, 2.18×10^9 kg Cu, 19.58×10^9 kg Pb, 1.00×10^9 kg Ni and 14.00×10^9 kg Zn. This synthesis represented the best knowledge of metal emissions at the time, but for only a limited number of metals. As evaluations of metals emissions improved, and investigators turned their efforts to understanding the distributions of other metals in the environment, the need arose to extend and update the estimates of Nriagu (1979).

This reappraisal of the level of understanding of anthropogenic emissions of heavy metals was provided by Nriagu and Pacyna (1988). This synthesis extended the range of elements considered to 16 (As, Cd, Cr, Cu, Hg, In, Mn, Mo, Ni, Pb, Sb, Se, Sn, Tl, V and Zn) and provided an assessment of the fluxes of these metals to the air, waters and soils. Quantities of emissions were based upon consumption and production

figures available for 1983, with evaluations of water and soil discharges based on industrial and commercial users of water and producers of solid waste. Soil and water discharge calculations also took into account the lifetimes of major metal-containing products as well as principle applications of these metal products. For atmospheric emissions, non-ferrous metal production was found or confirmed as a significant anthropogenic source of emissions of As, Cd, Cu, In, Pb, Sb, Se and Zn. Coal or oil combustion was found as a significant source of emission for Cr, Mn, Mo, Ni, Se, Sn and V. Additionally, refuse incineration was found to emit significant quantities of Cd, Hg and Mn, Cr emissions were principally derived from steel and iron manufacturing and Tl was found to be principally emitted during cement production. Elements released into aquatic ecosystems in significant quantities included As, Cu, Mn and Ni (domestic wastewater), Cd and Mo (metal and chemical manufacturing), Cr (metals manufacturing and domestic wastewater), Hg and Se (steam electricity) and Sb and Zn (metals manufacturing). Of the processes responsible for mobilization of heavy metals into soils, fly ash deriving from coal production was found to contain significant quantities of all of the metals considered. Other processes which contributed to contamination of soils included wastage of commercial products (As, Cr, Cu, Pb and Zn), urban refuse (Cd) and animal wastes (Zn). This extensive collection of data offered a useful summary of emissions of heavy metals into various environmental compartments, and evaluated the principle sources of pollution for each metal. This work extended beyond previous considerations of atmospheric emissions of heavy metals as it not only considered several other metals but also considered the fate of metals released into the atmosphere, of which the majority would ultimately reside in soils or aquatic reservoirs. The work of Nriagu and Pacyna (1988) was primarily intended for use by administrators of pollution control programmes, researchers of public health, environmental toxicology and environmental pollution, particularly for previously-unstudied heavy metals such as As, Hg, In, Sb and Se.

3.5 Analyses of Pb in Greenland ice and snow: 1991 to the present

Between 1969 and the 1980's, Patterson and co-workers produced a summary of Pb concentrations in Antarctic and Greenland ice extending from contemporary times to the past interglacial. The techniques they had developed culminated in the analyses of Antarctic and Greenland ice reported by Ng and Patterson (1981). During the 1980's, further work took place at Caltech however this work was further refined at the LGGE in Grenoble, France. Few studies of Antarctic Pb concentrations undertaken during the 1980's actually produced reliable data, with many researchers failing to recognize or overcome the contamination of samples or sampling sites (Wolff 1990). The expertise accumulated at the LGGE in Grenoble, France, saw this group lead the field in the analysis of heavy metals and ionic species as well as the construction of past climate information based on ice core records. Collaborations with the heavy metals group at LGGE also sped the development of highly sensitive techniques in Australia for the analysis of Pb isotopes, and facilities in Belgium for organolead analyses, in Moscow for Bismuth analyses, and later in Venice the measurement of a wide range of elements including U, Pt, Pd and Rh. International collaborations between these groups saw widespread analyses undertaken on the same samples, giving a thorough evaluation of the deposition of heavy metals in Greenland. In addition to completing the long-term history of anthropogenic pollution in the Northern Hemisphere, research undertaken in Greenland in the 1990's saw allied programs of analyses of heavy metals, seasonal indicators (major ions, H₂O₂ and δ¹⁸O) and air mass back-trajectory calculations produce an integrated interpretation of seasonal inputs from various regional sources of heavy metals emissions within the Northern Hemisphere.

The heavy metals research undertaken at LGGE, led by Professor Claude F. Boutron, commenced with a description of the cleanroom facilities and analytical capabilities of the laboratory and its Graphite Furnace Atomic Absorption spectrometer (GFAAS), published in *Fresenius' Journal of Analytical chemistry* (Boutron 1990). In the paper, the layout of the laboratory was described, with evaluations of the air quality in the laboratories and water purification facilities. From measurements of Pb content in various volumes of laboratory water – between 1 L and ~3.5 L – the Pb content of their laboratory water was calculated to be 0.15 pg/g. The selection and

cleaning of plastic labware was also discussed as an extension of experience obtained in other trace-metal laboratories such as Caltech (Patterson and Settle 1976) and the U.S. National Bureau of Standards, later National Institute of Standards and Technology (Moody and Lindstrom 1977, Moody 1982). Conventional polyethylene (CPE) and polypropylene were used almost exclusively because of their low metals content, while labware was cleaned by immersion in a series of progressively more-dilute acid baths. Initially, plasticware was cleaned in 25% nitric acid, however later cleaning stages involved 0.1% nitric acid and 0.1% nitric acid solutions prepared with NIST ultrapure nitric acid. Boutron (1990) also provided an evaluation of the blank associated with the processing and measurement of a typical ice core by IDMS. Such a procedure involved mechanical decontamination of the core (estimated blank contribution: 10 pg Pb), melting of the inner core in a CPE beaker (17 pg Pb), chloroform-dithizone Pb extraction (29.4 pg Pb) and preparation for mass spectrometry (10 pg Pb). This procedure involved an overall blank of ~66 pg Pb, which was found to be 30% of the total Pb in a typical Antarctic ice core sample. These descriptions of the technical abilities of the Grenoble laboratory demonstrated the extent to which the ability to determine heavy metals concentrations had improved since 1969. Predominantly, advances had been achieved in the production of high-purity water and reagents, which ultimately meant that determinations were made more accurate and analytical blanks could be lowered. As sample storage containers could also be made cleaner, smaller sample aliquots could be made available to more collaborating laboratories and research groups.

The first of several significant publications by Boutron and co-workers regarding heavy metals concentrations in Greenland snow and ice reported decreasing concentrations of anthropogenic Pb, Cd and Zn in Greenland snows since 1967 (Boutron et al. 1991). These measurements were undertaken on a 10.7 m deep snow core drilled in 1989 near Summit, central Greenland, using an acid-cleaned polycarbonate drill. The core was collected in 50 cm long sections of 10.5 cm diameter and dedicated to heavy metals analyses. Decontamination of core samples was undertaken at the LGGE laboratory, where the majority of analyses were also carried out. Rather than using a stainless-steel chiselling technique like that adopted by Ng and Patterson (1981) at Caltech for Antarctic ice cores, these cores were subsampled using acid-cleaned polyethylene tubes and beakers. The cores were split

into two 20cm cylinders using an acid-cleaned polyethylene wedge and hammer, exposing the central, inner core surface. The inner core was then collected by hammering a CPE beaker into the centre of the core. A decontamination profile was established by inserting narrower beakers into the core around the central beaker, to the edge of the core's circumference. These samples were then melted and analysed for Al, Cd, Cu, Na, Pb and Zn by GFAAS (with an evaporative pre-concentration step for Pb, Cd and Cu).

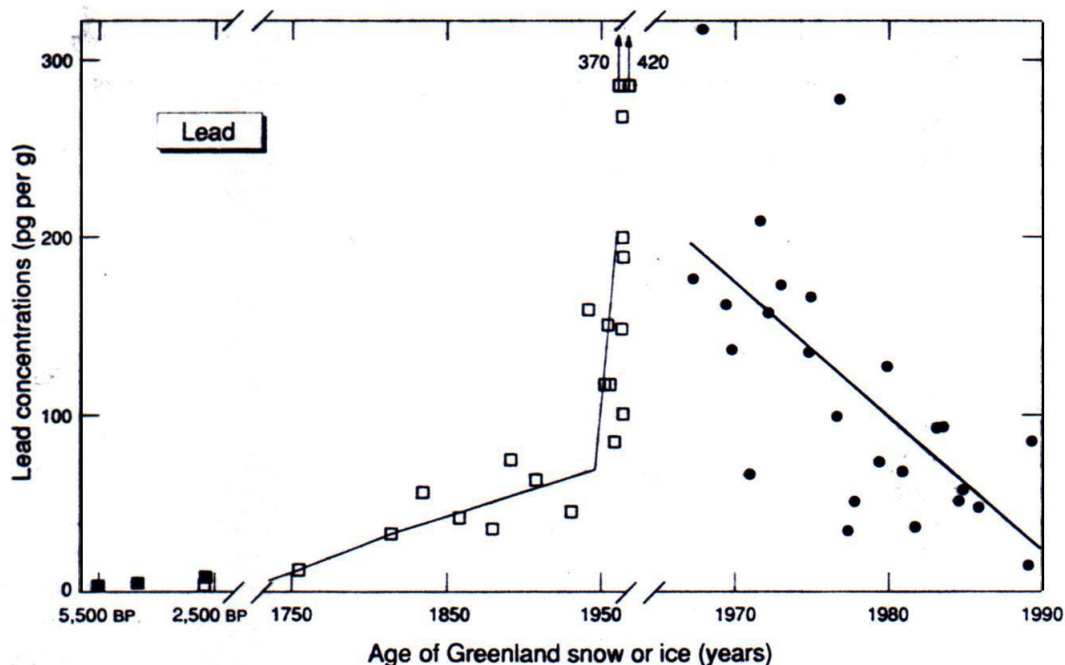


Figure 3.4. Changes in lead concentrations in Greenland ice and snow, from Boutron et al. (1991). Circles were new data by Boutron et al. (1991), while hollow squares were from Murozumi et al. (1969) and filled squares were from Ng and Patterson (1981).

Aluminium and Na were measured to account for inputs of metals from rock and soil dust and sea salts, respectively, however it was shown that sea salt inputs were negligible for all metals. Rock and soil dust contributions were observed to account for <2% of Pb and Cd and <20% of Zn. For Cu, however, rock and soil dust was found to regularly account for over 50% of the total quantity determined. Some Cd samples were also analyzed by direct ultrasensitive laser-excited atomic fluorescence spectrometry (LEAFS), showing good agreement in Cd concentrations between 1.3 pg/g and 3.9 pg/g. Analytical blanks from the subsampling stage on were said to represent less than 10% of the metals in the samples analyzed, and it was claimed

that 'concentrations always reached a good plateau in the centre parts of these core sections'.

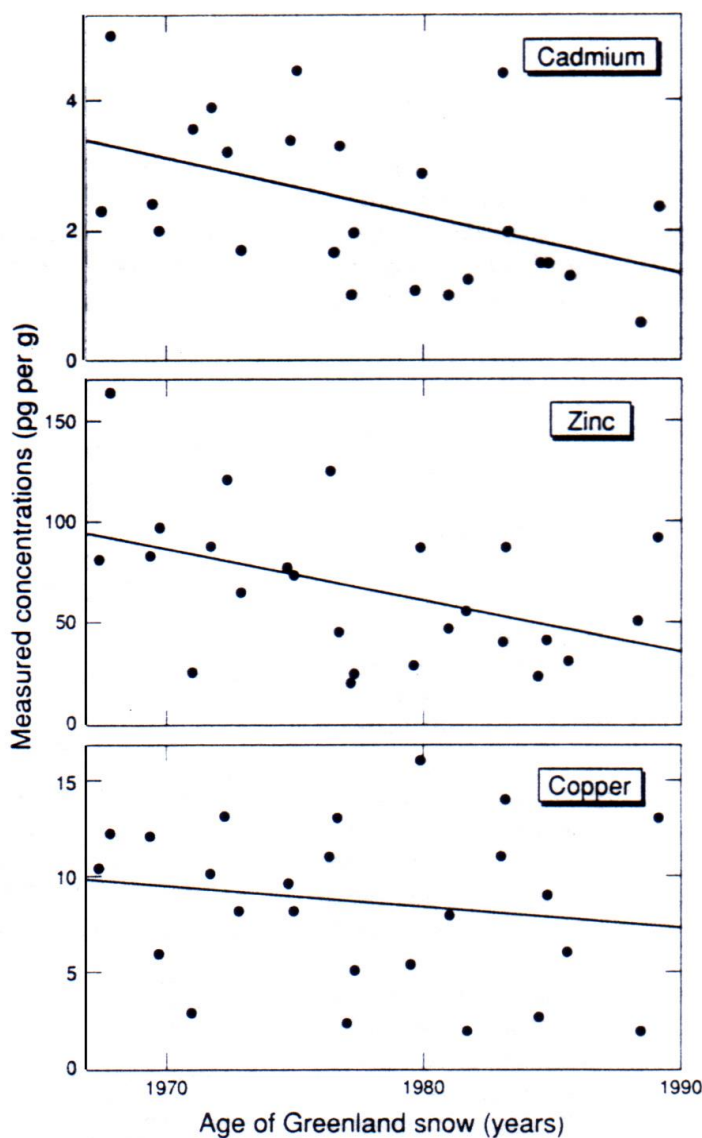


Figure 3.5. Changes in Cd, Zn and Cu concentrations in Summit snow from 1967 to present, from Boutron et al. (1991).

In the 25 samples analyzed by Boutron et al. (1991), dated from 1967 to 1989, anthropogenic inputs of Pb, Cd and Zn were observed to decrease consistently, as shown in Figures 3.4 and 3.5. Crustal enrichment factors for these metals were calculated by referencing the metal/Al ratio observed in snow to that observed in mean crustal material. These enrichment factors showed clear decreases from 1967 to 1989 for Pb (from 230 to 32), Cd (from 186 to 58) and Zn (from 19 to 6.3) and less so for Cu (from 3.0 to 1.2). Linear least-squares regression analyses (0.80

confidence levels) displayed gradients of -7.95 ± 1.86 pg Pb/g per year, -0.090 ± 0.035 pg Cd/g per year, -2.58 ± 1.08 pg Zn/g per year and -0.23 ± 0.16 pg Cu/g per year. These variations were seen to be consistent with the relative size of anthropogenic metal inputs relative to those from rock and soil dust. Those metals (Pb, Cd and, to a lesser extent, Zn) which were most influenced by anthropogenic inputs displayed the most significant concentration decreases. For Pb, this decrease was attributed to the rapidly diminishing use of leaded petrol products in the Northern Hemisphere, particularly in the United States and Western Europe. Unlike Pb, however, most Cd and Zn emissions originate from industrial processes such as nonferrous metal production, steel and iron manufacturing and refuse incineration in addition to fossil fuel combustion. Decreasing concentrations of these metals were attributed to efforts undertaken in various countries of the Northern Hemisphere, to reduce industrial emissions of metals and pollutants. These results provided a continuation of those published by Patterson and co-workers in 1969 and 1981, establishing a detailed history of Pb pollution in Greenland for the previous 250 years. The work presented by Boutron et al. (1991) indicated that Pb concentrations in Greenland were closely linked to atmospheric Pb emissions and responded relatively quickly to changes in those emissions. They also demonstrated that the Greenland ice sheet was also sensitive to changes in the emissions of other metals for which anthropogenic emissions were dominant over or comparable with natural emissions, such as Cd and Zn.

Following this relatively high-resolution analysis of Greenland snow was a confirmation of the anthropogenic origins of the Pb, based on Pb isotope systematics. Aliquots of the samples analyzed by Boutron and co-workers had been sent to the Curtin University isotope science laboratory in Perth, Western Australia for analysis by Isotope Dilution - Thermal Ionization Mass Spectrometry. These analyses, reported by Rosman et al. (1993), showed that while Pb concentrations had consistently decreased, $^{206}\text{Pb}/^{207}\text{Pb}$ ratios began at ~ 1.16 in 1968, increased to ~ 1.18 by 1978 and then had returned to ~ 1.16 by 1988. Mass spectrometric research had been conducted at Curtin University for many years, however until then it had had a limited history in the analysis of Pb for environmental applications. Under the guidance of Professor K.J.R. Rosman, the laboratory has pioneered many significant

advances in the preparation of contamination-free samples and the accurate analysis of Pb isotopes in small quantities of snow and ice since 1993.

The first of these significant contributions to the understanding of Pb fluxes to the polar ice caps was a letter to Nature in 1993 (Rosman et al. 1993). This reported $^{206}\text{Pb}/^{207}\text{Pb}$ ratios in Greenland snow and used Pb isotope systematics to confirm the interpretations of Pb concentration data presented by Boutron et al. (1991). Details of experimental procedures were kept to a minimum in the letter however these would be published the following year, with a more extensive data set. Samples were measured by isotope dilution using a ^{205}Pb tracer, and prepared in PFA beakers with HNO_3 , H_3PO_4 and ^{205}Pb added prior loading into the mass spectrometer on Re filaments. The accuracy of the mass spectrometer was monitored by regular measurement of NIST common lead isotopic standard SRM981, with the procedural blank amounting to ~3% of the sample analyzed. This was said to change the measured $^{206}\text{Pb}/^{207}\text{Pb}$ ratios by less than 0.3%. On account of the natural variation in Pb isotopic compositions in different ore bodies (due primarily to different rates of radiogenic production of ^{206}Pb , ^{207}Pb and ^{208}Pb), Pb isotopes could be used to identify Pb emission sources. The natural variations in Pb isotopic compositions found in Pb ores means that there is the potential to identify Pb emitted from various industries if they consume Pb from different ores. This firstly requires the emitted Pb to be isotopically distinguishable, and secondly requires the Pb isotopic compositions of emissions from each source to be adequately documented over time. In producing a summary of the Pb isotopic compositions and quantities of Pb emissions from the US, Europe and Canada for the period 1968 – 1988, Rosman et al. (1993) were able to apportion the anthropogenic Pb observed in Greenland between these sources.

Rosman et al. (1993) indicated that US Pb emissions had a relatively consistent $^{206}\text{Pb}/^{207}\text{Pb}$ ratio, ~1.18 about 1968 and remaining within the range 1.21 ± 0.01 from 1972 to 1988, as shown in Figure 3.6. Canadian aerosols had a lower $^{206}\text{Pb}/^{207}\text{Pb}$ ratio, approximately 1.15 ± 0.01 from 1968 to 1988, however there was some evidence to suggest that Canadian aerosol compositions had increased to ~1.20 by late 1988. Conversely, European $^{206}\text{Pb}/^{207}\text{Pb}$ ratios were quite variable, between 1.06 and 1.18, so an average of 1.14 was taken to represent the region from 1968 to 1988. Given the consistency and similarity of $^{206}\text{Pb}/^{207}\text{Pb}$ ratios in Eurasian and Canadian

emissions, these two sources were considered as one and attributed with a $^{206}\text{Pb}/^{207}\text{Pb}$ signature of 1.14. This enabled anthropogenic Pb deposited in Greenland to be accounted for as a binary combination of Pb from the two source regions - 1) the United States and 2) Eurasia and Canada.

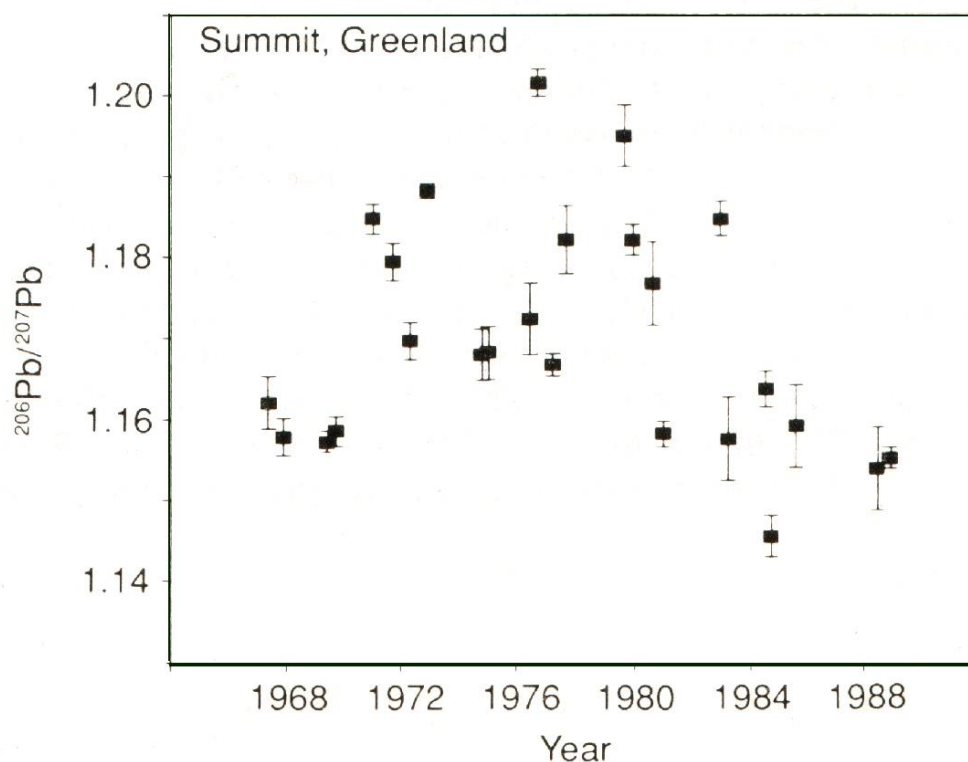


Figure 3.6. Changes in the $^{206}\text{Pb}/^{207}\text{Pb}$ ratio in Greenland snow between 1967 and 1988, from Rosman et al. (1993).

From such an evaluation of $^{206}\text{Pb}/^{207}\text{Pb}$ ratios in Greenland snow, Rosman et al. (1993) found that the Greenland Pb signature was consistent with decreasing emissions of Pb from the US from 1972 to 1989 and approximately constant Pb emissions from Eurasia and Canada. The partitioning of Pb emissions to the US or Eurasia and Canada was not significantly altered by small changes in the $^{206}\text{Pb}/^{207}\text{Pb}$ value used to represent Eurasian/Canadian emissions. Rosman et al. (1993) also found that contributions of Pb in Greenland snow from the United States, calculated from $^{206}\text{Pb}/^{207}\text{Pb}$ ratio systematics, matched the pattern of US alkyllead consumption almost perfectly, as shown in Figure 3.7. Consumption of alkyllead in the US was ~200,000 tonnes Pb/yr in 1968, peaking at ~250,000 tonnes Pb/yr in 1972 and then decreasing steadily to less than 50,000 tonnes Pb/yr by 1986. Such a strong correlation between the trends in $^{206}\text{Pb}/^{207}\text{Pb}$ ratios and Pb concentrations between

Greenland snow and emission statistics for the Northern Hemisphere assisted greatly in the acceptance of Pb isotopes as a powerful and sensitive tool for investigating long-range transport of Pb aerosols.

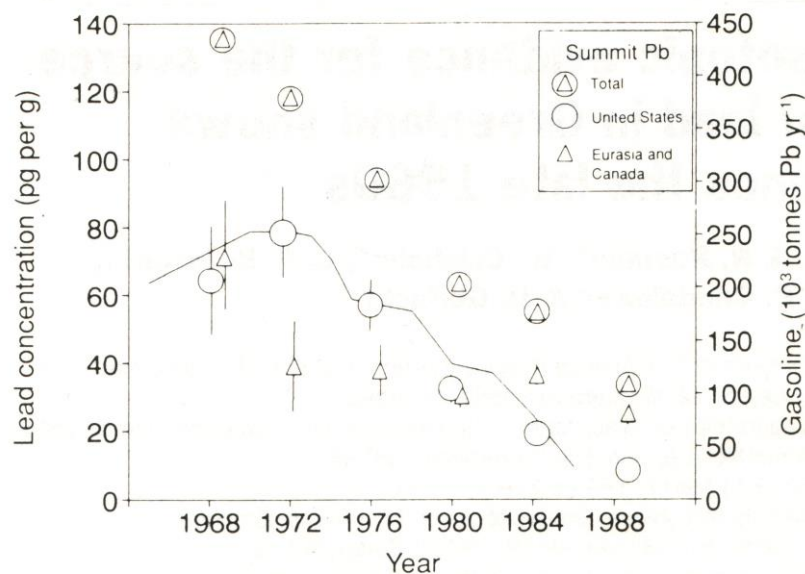


Figure 3.7. Concentrations of the lead in Greenland snow (left-hand scale) from the principal source regions and US lead consumption in gasoline (right-hand scale) as a function of time, from Rosman et al. (1993).

Another important finding of the research was that there were inter-annual and possibly inter-seasonal variations in the sources of Pb deposited in Greenland. Each of the core sections integrated 3-8 months of snowfall, with significant Pb isotopic variations observed in adjacent samples. Rosman et al. (1993) observed changes in the $^{206}\text{Pb}/^{207}\text{Pb}$ ratio from 1.172 to 1.201 in 1976 and from 1.185 to 1.158 in 1979. In considering that the more radiogenic (greater $^{206}\text{Pb}/^{207}\text{Pb}$ ratios) values indicated a dominant contribution of US Pb, it was then apparent that air masses from Europe or the US could travel more-or-less directly to Greenland. Rosman et al. (1993) noted ‘that there are occasions when air masses from different source regions have fairly direct access to Summit’, further confirming Summit (and Greenland) as a suitable location for investigating atmospheric emissions from North America and Eurasia.

The following year Rosman and co-workers published another paper, presenting full Pb isotopic compositions for the data in their letter to Nature and provided

supplementary data over the period 1960 – 1974 (Rosman et al. 1994a). The supplementary data was obtained from another Summit, Greenland, ice core this time drilled to 70 m depth. Only the depths from 8 to 13 m were analysed for Pb isotopes, however. For all samples, Pb concentrations and $^{206}\text{Pb}/^{207}\text{Pb}$, $^{208}\text{Pb}/^{207}\text{Pb}$ and $^{206}\text{Pb}/^{204}\text{Pb}$ ratios were given. The provision of ratios for all of the stable Pb isotopes enabled a more sensitive analysis of the sources of Pb to Greenland to be undertaken, as more isotopic data was being used to discriminate between pollution sources. Figure 3.8, included below, shows $^{208}\text{Pb}/^{207}\text{Pb}$ ratios versus $^{206}\text{Pb}/^{207}\text{Pb}$ ratios for the Greenland snow samples, including the then-available data for aerosol emissions from two cities (Paris and Helsinki) and various regions in the Northern Hemisphere.

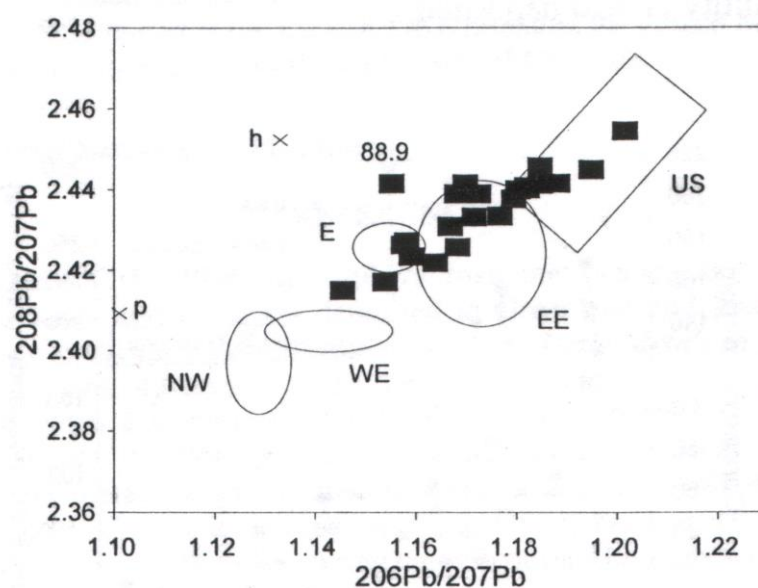


Figure 3.8. The isotopic composition of lead in Summit snow, and USA and Eurasian aerosols for the years 1971-1989. The regions enclosed by lines are characteristic of aerosols emitted from Eurasia: EE-Eastern Europe, E-East (former USSR, Finland), WE-Western Europe, NW-Northwest (Sweden, Norway), p-Paris, h-Helsinki and from the USA, from Rosman et al. (1994a).

Figure 3.8 shows that the Pb isotopic compositions in Greenland snow are between the signatures representative of US Pb aerosols and European Pb aerosols, indicating that Pb deposited at Greenland is a mixture of emissions from the two sources. Aside from this, the paper did not contribute more information than that which had been presented in the letter to Nature – the new results confirmed those data which had

been previously published by Rosman et al. (1993) and Boutron et al. (1991). Lead emissions from the US, characterised by radiogenic $^{206}\text{Pb}/^{207}\text{Pb}$ values >1.20 , steadily decreased from ~1970 to 1989 while Pb emissions from Eurasia and Canada were more constant over the same time period and were characterised by less radiogenic $^{206}\text{Pb}/^{207}\text{Pb}$ ratios. The trend of Northern Hemisphere alkyllead consumption had been confirmed in the Greenland ice record and the isotopic evidence presented by Rosman and co-workers confirmed the hypothesis of Boutron et al. (1991), that variations in Greenland Pb concentrations were directly attributable to Pb emissions from North America and Europe.

These studies were important as a final proof of the efforts of Patterson and co-workers, to establish that anthropogenic emissions of some heavy metals overwhelmed natural emissions, that this pollution was a global problem, and that direct and immediate action to decrease anthropogenic emissions produced a significant and rapid improvement. From a scientific viewpoint, however, the studies were essential for demonstrating that Greenland was a suitable site for evaluating atmospheric emissions from North America and Eurasia, and that air masses from each continent could access Greenland in a fairly direct manner. Also, Summit was an excellent site for other investigations of continental emissions as it received relatively large amounts of rock and soil dust (originating from the continents) and very little sea-salt, so emissions from the continents could be evaluated without having to make significant corrections for potential sea-salt contributions. With these important features of Greenland precipitation established, new research took advantage of ancient ice recovered by the deep-ice core drilling GRIP and GISPII programs to extend the Greenland heavy metals record back to thousands of years before the present.

While the previous studies had made use of snow cores which had been obtained using an acid-cleaned auger and sampled by plunging acid-cleaned tubes into the cores, the drilling and sampling of deep ice cores required a different approach. The deep ice cores penetrated more than three kilometers into the ice sheet, requiring the use of drilling heads, wires and core barrels made of metal and drilling fluid, used to equalize the pressure in the drillhole to that of the surrounding ice. These logistic requirements meant that the exteriors of the cores would be significantly

contaminated with metals, requiring extensive decontamination measures to be taken if pristine samples were to be obtained. Additionally, techniques had to be developed for cores for which only part of the cross section was available. Such a situation would occur when the cores were obtained through an international program and so various sections of each core would be cut to accommodate different types of measurements (Candelone et al. 1994). Finally, the dense single-crystal structure of ice meant that tubes could not be easily plunged into the core, so a means had to be developed to accommodate the different texture and structure of ice, compared to snow.

Candelone et al. (1994) described a technique for decontaminating ice cores, using a special lathe and stainless steel chisels, which provided the solution to these requirements. The technique made use of the approaches adopted by Ng and Patterson (1981) and Boutron and Patterson (1986) for the decontamination of Greenland and Antarctic ice cores but minimized contamination by supporting the core in a custom-built lathe (see Figure 3.9). Whereas Patterson and co-workers chiselled each ice core while it rested on a polyethylene surface, the lathe enabled the core to be suspended in clean air while it was chiselled, thereby minimizing the transfer of contamination from the surface to the core. The lathe could also be adjusted to support cores of various lengths and cross-sections, with original diameters between ~4 cm and ~12 cm. Using stainless steel chisels, ice, firn and snow cores could all be decontaminated using the same technique and the same equipment. The technique required two operators – one would chisel the ice core, and the other would catch the chiselled ice in an acid-cleaned scoop. The chiselled ice would then be transferred to a bottle in which it would be melted and aliquotted. With each layer of ice, new chisels, scoops and bottles would be used, to ensure that external contamination was not entrained toward the inner core layers. When three to four layers of ice had been removed from the core, the inner core was collected by breaking one end of the core and removing its supporting lathe stand. While the core was supported with acid-cleaned tongs, a wide-mouthed polyethylene bottle was placed around the exposed core, and the other end of the core was broken from its support. The length of the bottle (~18 cm) was such that the inner core could be collected in one piece and melted within that same bottle, thus minimizing contact with the inner core. For longer core sections, the inner core would be split into two or

more sections, each section being collected within its own bottle. The duplication of sets of chisels, scoops and melting bottles meant that the decontamination of ice cores could be carried out more often, as one set of equipment could be used for a decontamination while other sets were being cleaned.

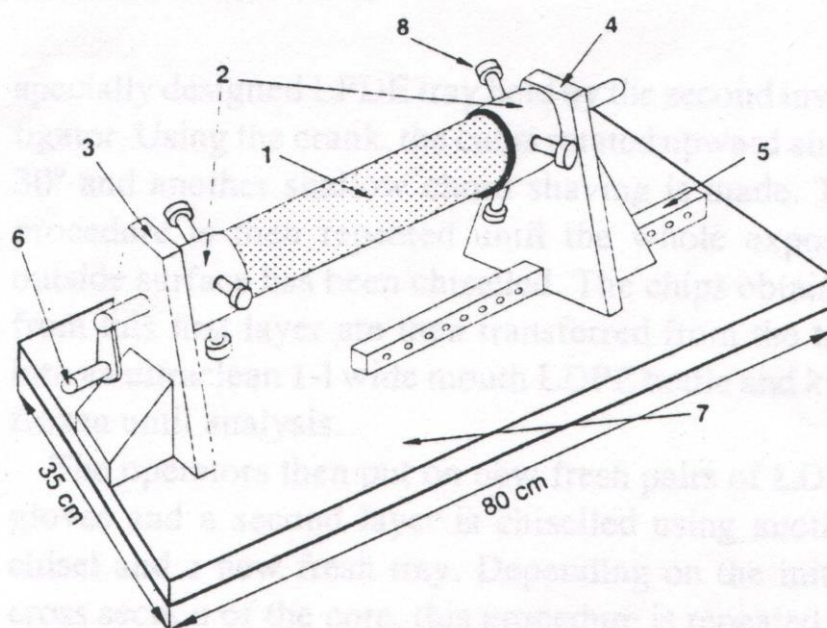


Figure 3.9. The LDPE lathe described by Candelone et al. (1994) for decontamination of snow and ice cores.

Candelone et al. (1994) also evaluated the decontamination technique using a number of ice cores drilled from different locations and by different methods. Decontamination profiles of electromechanically drilled core sections of shallow snow/firn (to 70.3 m) and deep ice (1286 m depth) from Greenland were compared to core sections of ice obtained from the thermally drilled Antarctic Dome C ice core (515 m depth). For all of these core sections, decontamination plateaus were observed in most cases and the contamination was restricted to the first few centimetres of the core surface. In some cases, decontamination plateau were not observed, for unknown reasons, however it was suggested that this could be due to difficulties encountered in the field during drilling operations and/or core handling. High concentrations of Cd, Cu, Pb and Zn were observed in all external layers for the ice cores, irrespective of whether or not drilling fluid had been used in the drill hole, or whether the corer was thermal or electromechanical. The Greenland deep ice sample (dated to 7760 years BP) featured a Pb concentration of 0.55 pg/g, which was

representative of natural Pb inputs to Greenland as it was dated prior to Greco-Roman times, when anthropogenic Pb emissions became significant. The natural Pb observed in the sample was noted to mainly originate from rock and soil dust. Concentrations of Pb (7.8 pg/g) and Cd (0.5 pg/g) observed in the Dome C sample (dated to 14,500 years BP) were described as typical for Antarctic ice from the Last Glacial Maximum, a period 'when the climatic conditions led to increased aridity, stronger winds and enhanced meridional circulations'.

An additional benefit of the decontamination technique presented by Candelone et al. (1994), which has been further developed in this thesis, was that a procedural blank associated with the decontamination technique could be determined. Candelone et al. (1994) froze their cleanest laboratory water in an acid-cleaned 2 L PTFE bottle, then removed the ice from the bottle to produce a cylindrical length of clean ice – an artificial ice core. By initially analyzing the levels of Cd, Cu, Pb and Zn in the water, the quantity of these metals contributed to the ice core during the decontamination procedure could be determined and so the blank associated with the technique could be quantified. From an initial water content of 0.25 pg Pb/g, 0.01 pg Cd/g, 0.2 pg Cu/g and 0.3 pg Zn/g, the procedural blank was found to be ~0.1 pg Pb/g, ~0.02 pg Cd/g, ~0.4 pg Cu/g and ~0.5 pg Zn/g. For the processing of recent Greenland snow, which is significantly affected by anthropogenic Pb emissions, this blank was found to be negligible, however it does become significant for the processing of ancient ice from Greenland or Antarctica which contain much lower levels of heavy metals. Candelone et al. (1994) calculated the blank contribution of the decontamination procedure to the processing of such ancient ice samples might be up to 30% for Cu, 25% for Pb and 10% for Cd and Zn. A re-evaluation of the decontamination blank, described within this thesis, has established a much lower blank value. This is most likely due to the higher-purity laboratory water currently available (Pb~0.005 pg/g, Ba~0.087 pg/g), which enables the decontamination apparatus to be better cleaned and allows cleaner artificial ice cores to be produced. Lowering the Pb content in the artificial ice core enables the decontamination blank to be determined with higher sensitivity, and hence enables a more accurate evaluation of the blank to be established.

The essential aspect of the decontamination technique described by Candelone et al. (1994) was that physical contact with an ice core should be minimized, particularly the inner core. This was accomplished by suspending the core in clean air, thus avoiding any physical transfer of contaminants to the ice core or from one chiselled layer to the next, while it was being decontaminated. This technique enabled ice and snow cores of various sizes and cross-sections to be decontaminated in a relatively straightforward method, which assisted in making the decontamination process more repeatable. The cleanliness of the technique could be quantified by decontaminating an artificial ice core and enabled decontaminations to be carried out in a relatively repeatable, or standardized, manner, giving some measure of confidence that the procedural blank for the decontamination of an artificial ice core was generally representative of that for a polar ice core.

The decontamination procedure described by Candelone et al. (1994) was first employed on the GRIP ice core drilled at Summit, Greenland, to a depth of 3028 m (Hong et al. 1994). Hong et al. (1994) analyzed GRIP core sections covering the period from 470 BP to 7760 BP – including the birth of lead and silver metallurgy, the Greek and Roman civilizations and the medieval and enlightenment periods. This research was anticipated 27 years earlier, in a book chapter written by C.C. Patterson regarding the potential for analyses of heavy metals deposited in Greenland ice strata as a means of investigating Roman metals production. This sentiment was repeated in the concluding statement of the paper written by Murozumi et al. (1969), however the technical and analytical demands of the work could not be met until the 1990s. As shown in Figure 3.10, Hong et al. (1994) found that Pb concentrations increased from ~2500 BP and remained high until the decline of the Roman civilization ~1500 BP. Lead concentrations remained low until ~1100 BP, after which they began to increase in accordance with increasing industrialization following the Middle Ages. They analyzed Pb by GF-AAS, also measuring Al, Na and SO₄ to calculate Pb inputs from dust, sea salt and volcanic sources. As with previous studies of Summit snow and ice, dust sources were found to overwhelmingly dominate natural Pb fluxes. Using Al to infer natural Pb inputs from dust, Hong et al. (1994) presented Pb crustal Enrichment Factors (EFs) in addition to Pb concentrations, with good agreement between the two. It was noted that at 7760 BP, the EF was ~0.8, indicating that virtually all Pb deposited in Greenland ice at that time originated from natural

sources. Following inputs of anthropogenic Pb after ~2500 BP, EFs were consistently greater than unity and increased to ~2.5 at the peak of the Roman civilization (~2000 BP). The lowest anthropogenic Pb levels observed since 2500 BP occur at 1500 BP with an EF~1.1.

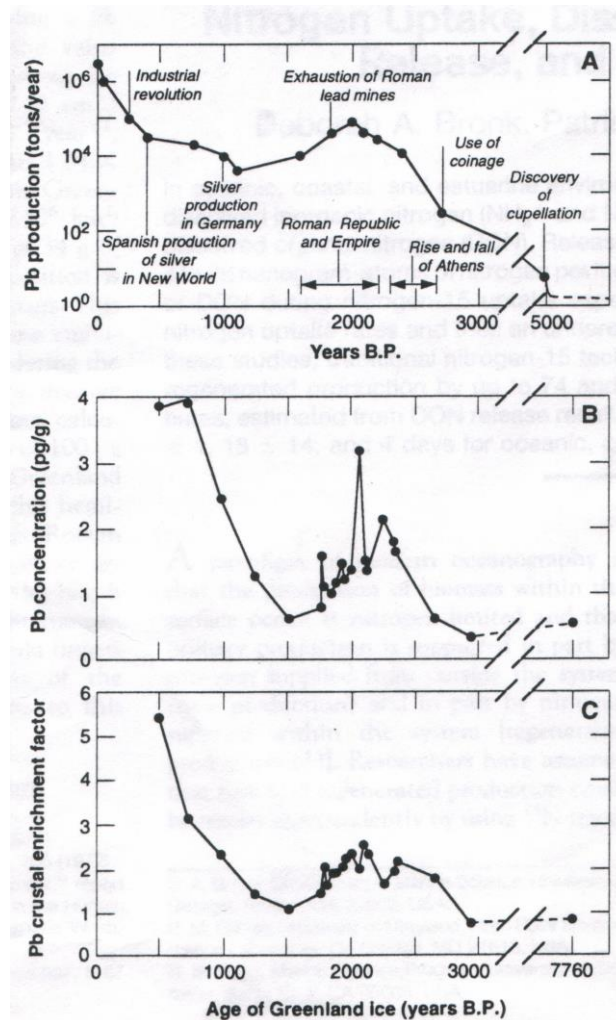


Figure 3.10. Changes in worldwide Pb production over the past 5500 years (A) and Pb concentration (B) and Pb crustal enrichment factor (C) in central Greenland ice from 2960 to 470 years ago, from Hong et al. (1994).

Hong et al. (1994) observed the earliest known case of hemispheric Pb pollution and attributed this to emissions of Pb due to the mining and smelting activities of the Greek and Roman civilisations. Shirahata et al. (1980) estimated world Pb production to be approximately 10,000 tonnes per year at the introduction of silver coinage ~2700 BP and approximately 80,000 tonnes per year at the height of the

Roman Empire ~2000 BP. Hong et al. (1994) observed that, based on estimated atmospheric emissions of ~5% from mining and smelting at the time, these activities would have produced atmospheric Pb emissions of ~500 tonnes per year at ~2700 BP and ~4000 tonnes per year at ~2000 BP. This estimate of Pb emissions compared well to estimates of Pb emitted to the atmosphere by rock and soil dust (~4000 tonnes per year globally) and supported the EF values ~2.5 observed in Greenland ice about 2000 BP. During Greco-Roman times, Spain was the main location of lead-silver mining and smelting and represented ~40% of total Pb production. Other locations of Pb mining and smelting included Central Europe, Britain, the Balkans, Greece and Asia Minor. Hong et al. (1994) noted that due to the high elevation of Summit (3238 m), the Pb pollution observed at ~2000 BP had reached the middle troposphere and was hemispheric in its influence. Based on an average Pb excess in Greenland from ~2500 BP to 1700 BP, they calculated that Greco-Roman industry had emitted approximately 400 tons of Pb to the Greenland ice sheet over 800 years. This quantity was shown to be approximately 15% of the total Pb deposited in Greenland from 1936 to 1996, the approximate period during which Pb alkyl additives were added to gasoline in the US and Western Europe. Hong et al. (1994) concluded by noting that studies of other natural archives, such as sea sediments, might be able to confirm the hemisphere-scale of Greco-Roman Pb pollution. They also noted that analyses of Pb isotopes might be able to identify the relative contributions from different sources of the pollution.

The results presented by Hong et al. (1994) were an impressive demonstration of the potential of ice cores for trace-level analysis of Pb. It also proved a legacy to the intentions expressed by Murozumi et al. (1969), who anticipated the broad scientific knowledge that could be gained from investigations of the past as revealed by natural archives. The research undertaken up to 1995 had established that Pb concentrations in Greenland were low, ~0.5 pg/g, until ~2700 BP, when the introduction of silver coinage prompted the large-scale processing of lead-bearing silver ores. Since then, Pb concentrations peaked about 2000 BP at the height of the Roman Empire, decreased during the middle ages and increased consistently from ~500 AD until ~1970 AD, after which alkyl Pb additives were banned in the US. This history was composed of results reported by Hong et al. (1994) for the period 7760 BP – 500BP, Murozumi et al. (1969) for the period 1773 – 1960 and Boutron et al. (1991) for the

period 1960 – 1989. While the most recent and most ancient periods had been determined from several sections of recently-collected and well-dated ice core samples, that reported by Murozumi et al. (1969) consisted of relatively few data points obtained from large firn/ice blocks. While decontamination profiles could be established in ice core samples, the data obtained from the firn/ice blocks could not be evaluated for contamination. Also, some variability in the data of Murozumi et al. (1969) may have been due to their collection technique, as they did not collect full-years of accumulation. In such a case, seasonal variations of Pb deposition in snow could have enhanced the variability of their results. The availability of new ice core samples, combined with analytical techniques for measuring Pb, Cd, Cu and Zn at low concentrations, meant that the results reported by Murozumi et al. (1969) could finally be repeated.

This was accomplished by Candelone et al. (1995), who measured Pb, Cd, Cu and Zn in samples dating from 1773 AD to 1974.5 obtained from a 70.3 m snow core drilled in July 1989 at Summit, Greenland. Snow and firn samples (dated 1946 - 1974) were processed using the technique described by Boutron et al. (1991), wherein the cores were split and acid-cleaned polyethylene beakers were hammered into the central section, while dense firn and ice samples (1773 – 1940 AD) were decontaminated using the chiselling technique described by Candelone et al. (1994). Ten samples were collected to cover the period 1773 AD – 1940 AD, with approximately twenty years between each sample. After 1946, the sampling was more frequent, with 16 samples collected from 1946 - 1974 at an approximate resolution of one sample every two years. Dating of the samples was based on continuous measurement of $\delta^{18}\text{O}$ values in a parallel core, with an uncertainty of ± 2 years at the bottom of the core (1772 AD). The provision of $\delta^{18}\text{O}$ data ensured that Candelone et al. (1995) could produce samples that integrated complete years of snow deposition and so avoid the potential variability introduced by the sampling technique used by Murozumi et al. (1969).

As shown in Figure 3.11, the Pb results obtained by Candelone et al. (1995) for the period 1773 – 1933 were consistently lower than those reported by Murozumi et al. (1969), however both observed similar values from 1940 to 1974. From 1773 to 1870, Candelone et al. (1995) observed a slight increase in Pb concentrations from ~

8 pg/g to ~18 pg/g, while Murozumi et al. (1969) observed higher Pb values, from ~10 pg/g at 1750 to ~45 pg/g by 1870. The lower concentrations observed by Candelone et al. (1995) may have been due to the sampling location, as Murozumi et al. (1969) sampled snow from North Greenland, which is more significantly affected by Arctic Haze than Summit. Also, the location of Summit at >3000 m altitude may have resulted in less pollution being deposited there, or finally, the results of Murozumi et al. (1969) may have been subject to contamination. Higher Pb concentrations ~65 pg/g were observed by both Candelone et al. (1995) and Murozumi et al. (1969) about 1900 AD, and somewhat lower values ~40 pg/g from 1915 to ~1940. These increases were attributed to increased Pb emissions from non-ferrous metal production (Pb, Cu-Ni and Zn-Cd), iron and steel manufacturing and combustion of coal and wood. Candelone et al. (1995) noted only a slight decrease in Pb concentrations from 1900 to 1930, which may have been due to the great depression, as was the case for other pollutants such as SO₂. After 1940, with the introduction of alkyl Pb gasoline, Pb concentrations were observed to increase dramatically to ~80 pg/g during the 1950's and 1960's. This was in agreement with the results of Murozumi et al. (1969) and Boutron et al. (1991) as well as statistics of alkyl Pb production in North America and Europe.

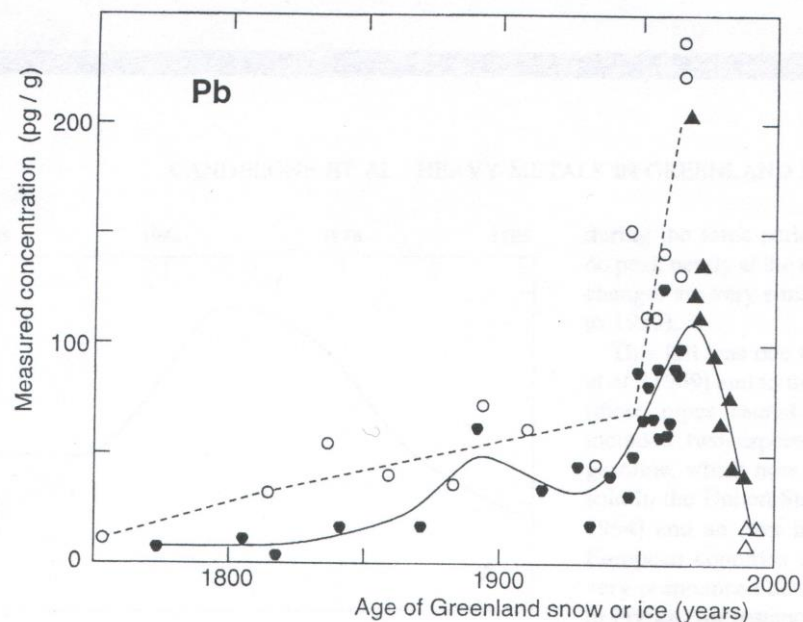


Figure 3.11. Changes in Pb concentrations in snow/ice deposited at Summit, central Greenland, from 1773 to 1992, from Candelone et al. (1995). Solid circles and open triangles from Candelone et al. (1995), solid triangles from Boutron et al. (1991) and open circles from Murozumi et al. (1969).

For Cd, Cu and Zn, Candelone et al. (1995) observed similar trends, with concentrations increasing abruptly from ~1850 AD (Cd, Cu) and ~1920 (Zn) to peak concentrations ~ 1980, after which concentrations decreased gradually. Concentrations of Cd, Cu and Zn at 1773 were approximately equal to those in Summit ice dated to 7760 BP, indicating no significant level of anthropogenic emissions at 1773. Zinc concentrations were observed to increase steadily from 1773 to 1920, however. Finally, Candelone et al. (1995) evaluated fluxes of Pb, Zn, Cd and Cu to the Greenland ice cap at pre-industrial (7760 BP) times and at 1773, 1850, 1992 and during the 1950's and 1960's, as shown in Table 3.3. These calculations demonstrated the significant quantity of Pb deposited in the Greenland ice cap due to human activities, as well as indicating the maximum levels of pollution of Cd, Cu and Zn in the Northern Hemisphere. These data for Cd, Cu and Zn confirmed that pollution abatement strategies introduced in the Northern Hemisphere in the 1970's and 1980's had led to decreasing atmospheric concentrations of those elements. This trend was first suggested by Boutron et al. (1991).

Table 3.3. Past and present-day deposition fluxes of heavy metals to the Greenland ice cap, redrawn from Candelone et al. (1995).

Year	Flux, t yr ⁻¹			
	Pb	Zn	Cd	Cu
7760 B.P.	0.24	9.8	0.11	0.72
1773	3.3	6.8	0.11	≤1.2
1850	6.5	13	0.11	1.0
1992	7.2	22	0.33	3.1
1960s and 1970s (maximum)	46	37	0.75	4.1

The following year the Greenland heavy metal record was further extended by research published by Hong et al. (1996a,b) that reported investigations of natural sources to the ice sheet. While much of the work undertaken by Boutron and co-workers had sought to evaluate the period and extent of anthropogenic Pb inputs to Greenland, their research following after this further defined the variations of Pb, Cd, Cu and Zn observed in Greenland due to natural processes. Particularly, Hong et al. (1996a) reported the changing source strengths of Pb, Cd, Cu and Zn over the last glacial cycle, from 8,250 to 149,100 years BP while Hong et al. (1996b) reported variations in fluxes of Pb, Cd, Cu and Zn resulting from the 1783/4 AD eruption of Laki volcano in Iceland. While the work of Hong et al. (1996a) to investigate metal deposition during the past climate cycle was comparable to those studies undertaken earlier by Boutron and co-workers on Antarctic ice (Boutron and Patterson 1986, Boutron et al. 1988), their investigation of volcanic debris deposited in ice cores proved an innovative means of evaluating statistical estimates of heavy metals' contributions from volcanic sources.

Hong et al. (1996a) produced a record of Pb, Cd, Cu and Zn from 8,250 to 149,100 years BP in Greenland ice, extending back to the past glacial cycle. This research recorded heavy metals deposition from the present Holocene back through the Last Glacial Maximum (LGM) cold event ~14,000 to 20,000 years BP and the last ice age, featuring a number of stadial (cold) and interstadial (milder) glacial stages,

through the second-to-last interglacial (the Eemian, ~128,000 years BP) and into the next-to-last ice age (the Saale, ~150,000 years BP). Their data set was composed of 24 sections of the GRIP ice core, drilled at Summit, Greenland, and decontaminated by the ice-chiselling procedures described by Candelone et al. (1994). The majority of the samples were obtained between 8,250 and 64,100 years BP, with four additional samples obtained at 91,900 years BP, 95,800 years BP, 127,800 years BP and 149,100 years BP. Lead, Cd, Cu, Zn and Al concentrations were measured by GFAAS, while Ca, Na, SO₄ and NH₄ concentrations were measured by ion chromatography. Calcium, Na, Al, SO₄ and NH₄ were determined to evaluate heavy metal inputs due to rock and soil dust (Ca, Al), sea-salt (Na), volcanism (SO₄) and biomass burning (NH₄). The results they obtained indicated that inputs of all heavy metals had varied considerably over the past climate cycles, as can be seen in Figure 3.12, with ratios of highest-to-lowest concentrations of ~320 for Pb, ~150 for Cu ~36 for Zn and ~13 for Cd. For Pb, concentrations varied from <8 pg/g during warmer periods to ~120 pg/g during the colder periods. Despite the low resolution of sampling for the earliest data (pre-50 ky BP), it could be seen that metal concentrations during the Saale ice age were comparable to those observed during the last ice age and that metal concentrations observed during the Eemian interglacial were also comparable to those observed during the Holocene and interstadial warm-climate events. Approximately similar trends were observed for Pb/Al and Cu/Al (higher values during colder periods, and lower values during warm periods), but a different trend was observed for Cd/Al and Zn/Al (low values during cold periods, but higher values during warm periods especially the Holocene).

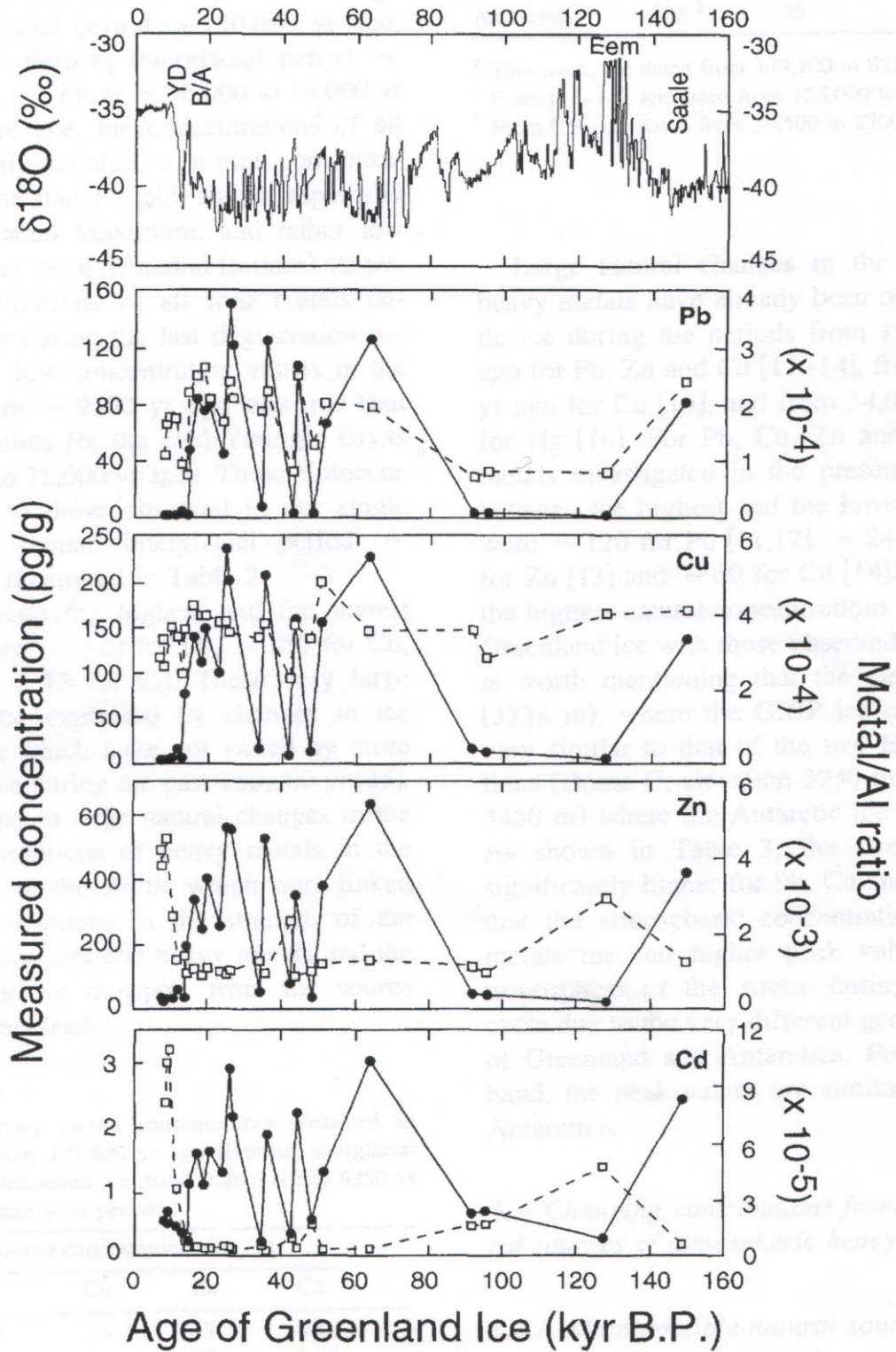


Figure 3.12. Observed changes in $\delta^{18}\text{O}$ isotopes, Pb, Cu, Zn and Cd concentrations (dots, continuous lines) and Pb/Al, Cu/Al, Zn/Al and Cd/Al ratios (squares, broken lines) in Summit, Greenland, ice from 149,100 to 8,250 years ago, from Hong et al. (1996a).

Hong et al. (1996a) determined that contributions of heavy metals from sea-salt, volcanic and biomass burning sources were all negligible, while linear relationships between concentrations of Pb, Cd, Cu and Zn and those of Al was a reliable indication that the enhancements in heavy metals concentrations were due to elevated inputs of rock and soil dust. They also noticed that there were essentially two populations of crustal inputs, those with Al concentrations greater than 200 ng/g, and those with concentrations less than 45 ng/g. As shown in Figure 3.13, it can be seen that trends are different for Pb and Cu to those observed for Cd and Zn. Particularly, in the populations with Al concentrations <45 ng/g, Pb/Al and Cu/Al ratios decrease below levels observed for samples with higher Al concentrations, despite the likelihood that Pb and Cu were almost completely derived from rock and soil dust inputs at all times. This indicated that the composition of rock and soil dust deposited in Greenland changed from colder periods (high Al concentrations) to warmer periods (low Al concentrations). In contrast, Zn/Al and Cd/Al ratios were higher in the low-Al concentration sample population compared to those with high Al concentrations. So, during warmer periods, another emission source appeared to be present for Zn and Cd. Since Hong et al. (1996a) had determined the natural inputs of Zn and Cd from rock and soil dust, volcanism, sea-salts and biomass burning, they attributed the additional inputs of Zn and Cd observed during warm periods to emissions of biogenic particulates and volatiles from continental vegetation.

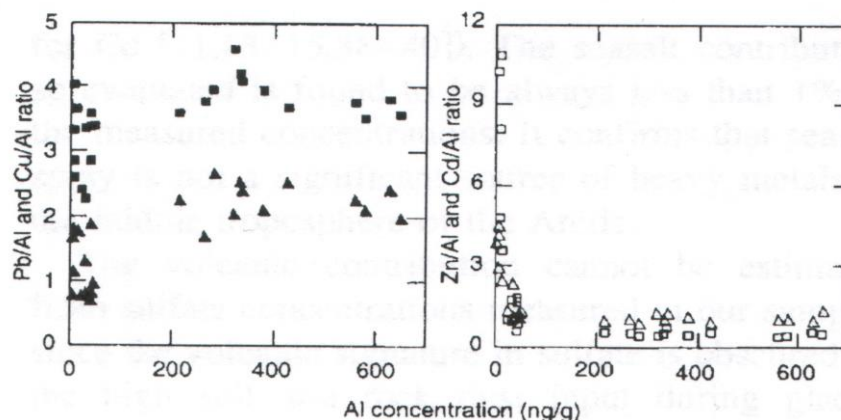


Figure 3.13. Lead/Al, Cu/Al, Cd/Al and Zn/Al ratios measured in 24 ice core sections dated from 149,100 to 8,250 years ago vs Al concentrations in the sections, from Hong et al. (1996a).

In their investigation of changes in heavy metal fluxes during the last deglaciation, Hong et al. (1996a) observed particular changes during the Younger Dryas (colder) and Bolling-Allerod (warmer) events. These variations in heavy metal fallout flux (heavy metal concentration referenced to snow accumulation rate) and metal/Al ratio are shown in Figure 3.14. In the figure, it can be seen that the Pb/Al and Cu/Al ratios decrease significantly after ~16,000 years BP, with the transition to warmer temperatures, however the Pb and Cd fallout fluxes respond to variations in temperature, locations of dust production and climate occurring during the transition. In contrast, Zn/Al and Cd/Al ratios also decline after ~16,000 years BP, but Cd/Al ratios are higher again from ~12 ky BP to ~8 ky BP while those of Zn/Al remain constant after ~16 ky BP. Fluxes of Zn and Cd increase after ~13 ky BP to a maximum ~ 9 ky BP, then decrease to Holocene levels. Hong et al. (1996a) interpreted these changes in the light of known and calculated changes in the Earth's climate and geography during the last deglaciation. Decreasing fallout fluxes of all heavy metals after ~17 ky BP were attributed to the climate becoming milder and less stormy and so reducing the strength of rock and soil dust sources and the intensity of atmospheric transport. Variations in Pb/Al and Cu/Al ratios during the variations from LGM (colder) to Bolling-Allerod (warmer) to Younger Dryas (colder) to Pre-Boreal (warmer) and then Holocene (current) conditions were associated with the changing inputs from different sources of rock and soil dust between warmer and colder periods with less rock and soil dust contributions from the North African and central Asian deserts during the Pre-Boreal period.

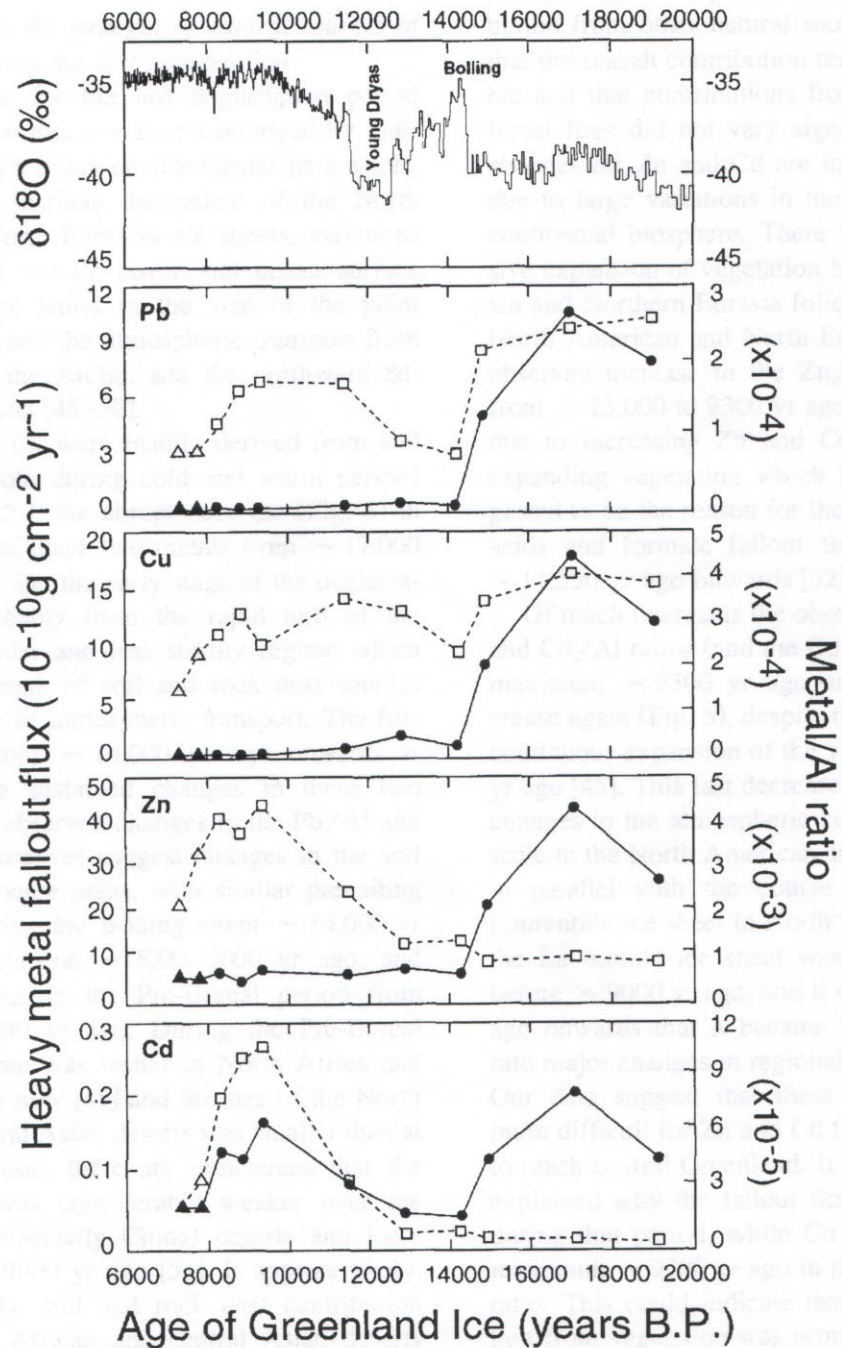


Figure 3.14. Changes in heavy metal fallout fluxes (full symbols, continuous lines) and heavy metals/Al concentration ratios (open symbol, broken lines) in Greenland ice from 18,910 to 7,260 years ago, from Hong et al. (1996a).

Increases of Zn/Al and Cd/Al ratios, observed from ~13 ky BP, were associated with the spread of vegetation northward after the retreating Northern Eurasian and North American (Laurentide) ice sheets. Decreasing Zn/Al and Cd/Al ratios after 9 ky BP

were attributed to the deglaciation of the Laurentide ice sheet, which essentially began ~ 9ky BP and was complete by 6 ky BP, when concentrations and metal/Al ratios for all heavy metals are similar to those observed in the late-Holocene. Hong et al. (1996a) suggested that the climate changes associated with deglaciation of the Laurentide ice sheet acted to diminish the transport of biogenic emissions of Cd and Zn to Greenland, but noted that this failed to explain the discrepancy between Zn and Cd fallout fluxes observed from ~13 ky BP to ~ 8 ky BP. They indicated that the increasing emissions of Zn following the retreat of the Northern Eurasian and North American ice sheets may have been balanced by decreases in the levels of Zn from rock and soil dust inputs, whereas for Cd the increase in biogenic emissions was sufficiently great to temporarily overcome the overall decrease due to rock and soil dust inputs.

The results of Hong et al. (1996a) impressively demonstrated the level of coherence available from studies of various signals in ice cores, such as stable isotopes, major ions and heavy metals. They evaluated and confirmed the estimates of natural sources of heavy metals undertaken earlier by Nriagu (1989) and illustrated variations in the levels in the deposition of those heavy metals to the Greenland ice sheet in response to alterations in geography and meteorology associated with long-term climate change. Particularly, the significantly greater levels of heavy metals deposited in Greenland enabled the implications of climate change for heavy metals fluxes to be more clearly realized than similar studies of Antarctic ice undertaken by Boutron and Patterson (1986) and Boutron et al. (1988).

The final effort undertaken by Boutron and co-workers in their exploration of the variations in natural inputs of heavy metals to Greenland was to evaluate heavy metals concentrations in Greenland ice during the deposition of debris from a volcanic eruption. Hong et al. (1996b) investigated an ice core section corresponding to the deposition of debris from the 1783/4 AD eruption of Laki, in Iceland. The core section was obtained from the 70.3 m firn/ice core drilled at Summit in July 1989 as part of the Eurocore program, from which Candelone et al. (1995) had evaluated the Pb pollution history of Greenland for the period 1773 – 1974. The core had been obtained particularly for measurement of heavy metals, with special procedures developed for handling the core during drilling and transport. Hong et al. (1996b)

had identified the presence of Laki debris in the core by measurements of Electrical Conductivity on the core surface, indicating that the volcanic debris occurred within the 67.52 – 67.72 m depth interval. The core section covering depths 67.1 m to 68.025 m was then sampled for heavy metals analysis, with 9 inner core samples (varying from 7 cm to 10 cm in length) collected from 67.155 m – 67.625 m and from 67.645 m – 67.945 m (see figure 3.15). At ~67 m depth, one year of snow deposition equalled ~27 cm of firn/ice, with the core integrating snow deposition from 1782 to 1785.

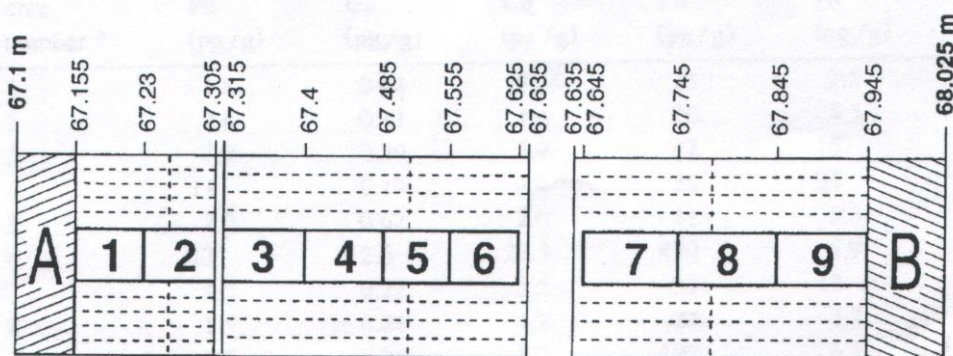


Figure 3.15. Representation of the inner core samples collected by Hong et al. (1996b) from a section of a Summit snow/ice core from 67.1-68.025 m depth, from Hong et al. (1996b).

In addition to Pb, Cd, Cu and Zn concentrations, Hong et al. (1996b) determined Al, Na, and SO₄ concentrations in the inner core samples in order to determine heavy metal inputs from crustal (Al) and marine (Na) sources. Evaluations of SO₄ concentrations were of use for confirming the location of the Laki debris in the core as well as for referencing metal enrichments to S concentrations, a standard practice in calculating metal emissions from volcanoes. After compensating for inputs of heavy metals from crustal and marine sources, Hong et al (1996b) observed significantly enhanced concentrations of all metals and SO₄ in the 67.555 m - 67.625 m inner core section – that which corresponded to the Electrical Conductivity peak. In the core section they observed enhancement factors of ~3 for Pb, 40 for Cd, 7 for Cu and 25 for Zn, calculated relative to mean values measured in nearby samples. For Cd, Cu and Zn, a significant enhancement occurred only in one core section, however significant enhancements of Pb were also observed in the three core

sections following that containing the SO₄ peak. As they noted, it was ‘the first direct evidence ever reported of the impact of a well identified volcanic eruption on the heavy metal content of Greenland (and Antarctic) ice’.

In addition to illustrating the deposition of heavy metals in Greenland ice due to volcanism, Hong et al. (1996b) also evaluated aspects of the emission and transport of debris from Laki to the ice sheet. Particularly, they noted the eruption of Laki began on 8th June 1783 and continued with decreasing intensity until February 1874 and that the plume of ash, dust and aerosol-forming gases primarily affected the troposphere, with minimal penetration into the stratosphere. This was supported by the observation of a volcanic debris signal of relatively short duration, essentially confined to one ice core section 7 cm thick. This core section could have corresponded to no more than three months’ deposition, which was in agreement with tropospheric transport of the debris, whereas the volcanic signal would have been more likely to persist for several months or at least one year if stratospheric transport of debris had been involved. For Pb, however, the presence of an extended signal of enhancement suggested that an additional emission source, such as anthropogenic Pb emissions from Europe, might have been present at the time. The analyses of Candelone et al. (1995) supported this explanation, as they had observed Pb concentrations in Greenland ice at ~1770 AD were approximately ten times greater than those observed in samples corresponding to natural levels of emissions ~7700 years BP. Hong et al. (1996b) also evaluated heavy metal/S ratios for Pb, Cd, Cu and Zn of 0.30×10^{-4} , 0.33×10^{-4} , 0.52×10^{-4} and 13×10^{-4} , respectively. They also calculated the quantity of each metal deposited in the Greenland ice due to the Laki eruption, evaluating these to be approximately equal to the quantity of Cu, Cd and Zn deposited in Greenland annually during the 1960’s and 1970’s, but the quantity of Pb deposited was somewhat less significant at about four times the annual natural Pb flux.

The work of Hong et al. (1996a,b) demonstrated the extent to which measurements of heavy metals in polar snow and ice had advanced from those accomplished by Murozumi and others in 1969. By 1996, it was possible to sample ice more than 150,000 years old and reliably measure Pb concentrations of <1 pg/g. Also, the natural and anthropogenic sources of emissions of heavy metals were relatively well-

known with good estimates available for their current and past emission rates, while in 1969 argument still centered on what the natural and anthropogenic sources of Pb emissions actually were. The last element of one of the legacies of Patterson and co-workers, to determine the variations of atmospheric Pb fluxes during the technological development of the human civilization from Greenland ice strata, was provided by Rosman et al. (1997), who investigated the origins of Pb emissions during the Greco-Roman epoch. This was achieved by their measurement of Pb isotopic compositions in the GRIP samples reported by Hong et al. (1994) to contain Pb pollution from Greek and Roman mining and smelting activities and their assessment of changing sources of Pb emission based on the available historical and Pb isotope data pertaining to locations of Greco-Roman metallurgical activity. This research provided a confirmation of the earliest known period of hemispheric Pb pollution and established firmly the utility and sensitivity of Pb isotope analysis as an investigative tool not only for scientists but also for other fields of research such as archaeology and economic history.

Rosman et al. (1997) analyzed Pb isotopic compositions and concentrations in 26 sections of the GRIP ice core drilled at Summit. Most of these sections were dated from 962 BC to 1523 AD, within the period of significant anthropogenic Pb emissions as evaluated by Hong et al. (1994), however five samples were obtained from deeper ice strata, prior to the influence of anthropogenic Pb emissions. These five samples, dated from 7313 BC to 5295 BC, were obtained to define background Pb concentrations and Pb isotopic compositions for Greenland ice during the Holocene. Fourteen samples were collected for the period 366 BC – 220 AD, while 5 samples were collected pertaining to more recent times (473 AD, 746 AD, 1009 AD, 1271 AD and 1523 AD). From an evaluation of the available research into Greco-Roman mining and metallurgy, Rosman et al. (1997) described the importance of the Iberian Peninsula as a source of silver during ancient times:

This region was successively controlled by the Phoenicians (750-580 B.C.), the Carthaginians (535-205 B.C.) and the Romans (205 B.C.-410 A.D.). Spain became Rome's greatest silver-producing region. Mines near Cartagena and Mazarron alone were estimated, from the slag heaps and workings, to have produced 2-3 times more silver than the Greek Laurion

mine. The vast scale of mining was also in evidence further west at Rio Tinto where an estimated 6.6 million tons of Roman slag remained. The period 237-218 B.C., between the first and second Punic wars, was probably a period of intense mining activity by the Carthaginians in Spain.

They also noted the relative importances of other mining regions exploited in ancient times, such as Laurion in Greece (worked from ~600 B.C. - ~100 A.D.) and the Mendips region in England (worked after 49 A.D.). Rosman et al. (1997) indicated that the Laurion mine was nearly exhausted by ~150 B.C., while English Ag production was only ~10% of that in Spain. Silver production in other European regions such as Gaul, Italy and Sardinia, the Carpathians and the Balkans, was also evaluated to be small in comparison to that produced in Spain. Rosman et al. (1997) compiled Pb isotopic signatures for various Ag/Pb mines in various European regions [Including the Aegean, Britain (Mendips, Shropshire, Derbyshire, Cornwall, Devon), Europe (Germany, Austria), Greece (Laurion) and Spain (Cabo de Garta, Mazarron, Cartagena, Rio Tinto)] for comparison with the Pb isotopic compositions they observed in Ancient Greenland ice.

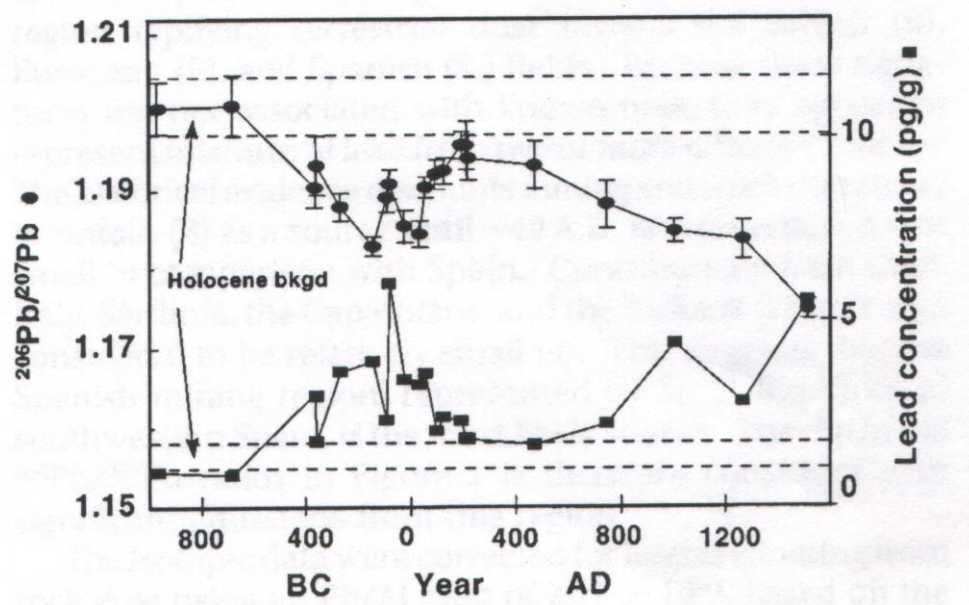


Figure 3.16. $^{206}\text{Pb}/^{207}\text{Pb}$ isotopic ratio (upper curve) and concentration (lower curve) of lead in Greenland ice from 962 B.C. to 1523 A.D., from Rosman et al. (1997).

In Figure 3.16, it can be seen that Pb concentrations were approximately equal to Holocene background levels ~ 1.5 pg/g until after 680 BC, when they increased to 2 – 4 pg/g from 366 BC to 58 AD. From 100 AD to 193 AD, Pb concentrations were ~ 2.2 pg/g, after which they decreased to near-background levels after 211 AD. From 1009 AD, Pb concentrations increased again, with 5.5 pg Pb/g observed by 1523 AD. These variations in Pb concentrations corresponded with variations in $^{206}\text{Pb}/^{207}\text{Pb}$ ratios from ~ 1.202 (during the Holocene background) to 1.183 – 1.191 (between 366 BC to 58 AD) and then ~ 1.194 (from 100 AD to 473 AD). After 473 AD, $^{206}\text{Pb}/^{207}\text{Pb}$ ratios consistently decreased to 1.1748 ± 0.0012 by 1523 AD. The trends in Pb concentrations and $^{206}\text{Pb}/^{207}\text{Pb}$ ratios observed by Rosman et al. (1997) were consistent with those previously reported by Hong et al. (1994), while the significant decreases in $^{206}\text{Pb}/^{207}\text{Pb}$ ratios they observed were unequivocal proof of the anthropogenic source of Pb enhancements occurring between ~ 500 BC and ~ 200 AD.

The Holocene background determined by Rosman et al. (1997) of $^{206}\text{Pb}/^{207}\text{Pb} = 1.201 \pm 0.003$, $^{208}\text{Pb}/^{207}\text{Pb} = 2.482 \pm 0.004$ and Pb concentration = 1.4 ± 0.3 pg/g was consistent with background Pb concentrations in Greenland ice determined by other investigators. While Hong et al. (1994) had observed lower values ~ 0.6 pg Pb/g from ~ 3000 BP and 7760 BP, Hong et al. (1996a) had observed higher concentrations ~ 0.9 pg Pb/g in samples dated to 8250 – 9310 BP. Lead isotopic compositions measured by Rosman et al. (1997) in ancient ice dated from 3.3 – 5.3 ky BP matched those observed in samples dated to 962 BC and 680 BC as well as those published for Atlantic ocean sediments obtained near the western Sahara (see Figure 3.17). This indicated that the isotopic composition of natural Pb in Greenland ice did not vary greatly during the Holocene, and that Saharan dust may be a source of this natural Pb component. Several other investigators had observed the predominance of rock and soil dust over other natural sources of Pb deposited in Summit ice, and Rosman et al. (1997) noted that reddish dust detected on filters located at Dye 3, in southern Greenland, had been attributed to dust transported from the Sahara.

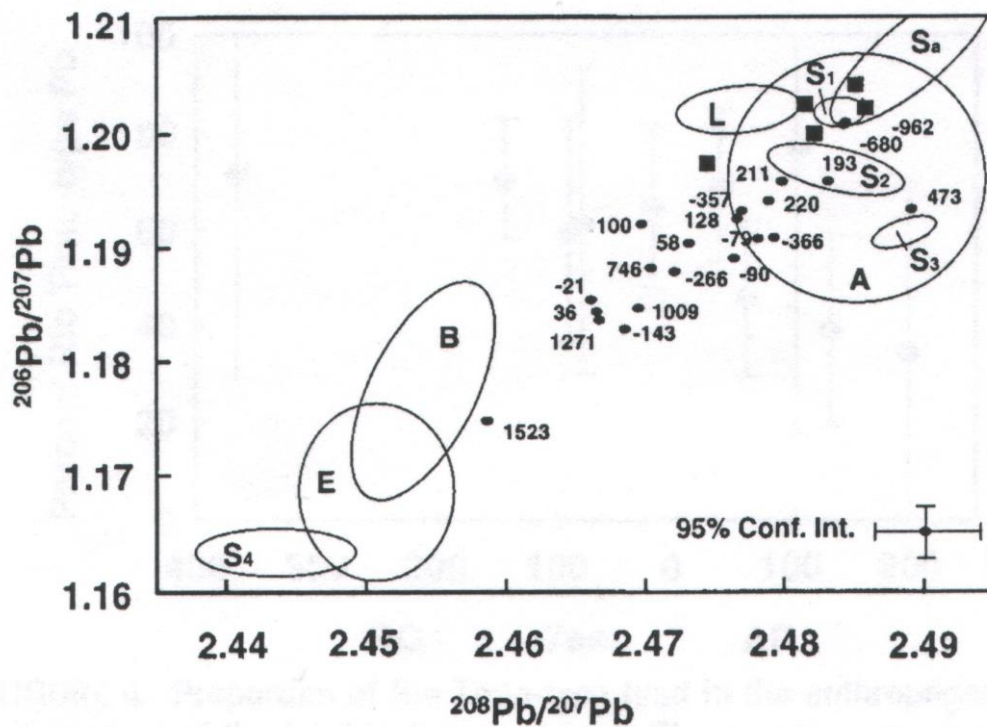


Figure 3.17. Isotopic composition of lead in Greenland ice between 7313 BC and 1523 AD, from Rosman et al. (1997). Sample dates are shown, with BC dates given a negative prefix. Lead ores are shown as elliptical fields: A, Aegean; B, British (Mendips, Shropshire, Derbyshire, Cornwall, Devon); E, Europe (Germany, Austria); L, Greek (Laurion); S, Spanish, S₁ (Cabo de Garta region), S₂ (Cabo de Garta and Mazarron regions), S₃ (Cartagena region), S₄ (includes Rio Tinto region); S_A, Atlantic Ocean sediments near the western Sahara. Samples used to represent the Holocene background are shown as solid squares.

After 680 BC, Rosman et al. (1997) observed variations in the sample Pb isotopic compositions consistent with significant inputs of anthropogenic Pb. None of the samples indicated a substantial input of Pb with the signature similar to that of the Laurion mine ($^{206}\text{Pb}/^{207}\text{Pb} \sim 1.205$, $^{208}\text{Pb}/^{207}\text{Pb} \sim 2.477$), however. This was most likely due to the absence of samples between 680 BC and 366 BC, corresponding to the height of the Greek civilization, with historical studies suggesting that $\sim 75\%$ of Laurion Ag production probably occurred during the 5th century BC. From 366 BC to 36 AD, during the height of the Carthaginian civilization and the rise of the Roman empire, the Greenland Pb isotopic composition changed consistently from background signatures to $^{206}\text{Pb}/^{207}\text{Pb} \sim 1.183$ and $^{208}\text{Pb}/^{207}\text{Pb} \sim 2.467$, indicating Pb

inputs with isotopic signatures consistent with those of mines in Britain, central Europe or Rio Tinto (in Spain). Historical evidence indicated that Pb emissions from Britain did not begin until ~49 AD, and that throughout the Greco-Roman period silver production in central Europe and Britain was relatively small compared to that conducted in Spain. On this basis, Rosman et al. (1997) attributed the Pb concentration increases observed to Pb emissions from mining and smelting of Ag/Pb ores in the Rio Tinto region of Spain. They noted that the Pb isotopic composition in Greenland ice was still somewhat removed from the signature of Rio Tinto ores, however, and attributed this discrepancy to inputs of Pb from other regions in Spain, such as Cartagena, Mazarron and Cabo de Gata, which all featured more radiogenic signatures. Rosman et al. (1997) evaluated the $^{206}\text{Pb}/^{207}\text{Pb}$ ratios observed in Greenland ice from 366 BC to 220 AD as a mixture of Pb from Rio Tinto and from other Spanish mining regions. Based on Pb isotopic systematics, they calculated that Pb with a Rio Tinto-type composition accounted for ~70% of Pb emissions to Greenland from ~150 BC to ~50 AD. No influence of Pb emissions from mines in Britain, Germany or Austria was apparent during the Roman period, however after 473 AD (well into the decline of the Roman empire), $^{206}\text{Pb}/^{207}\text{Pb}$ ratios are observed to decrease again. Such a trend was consistent with the exploitation of lead and silver mines in central Europe from ~1000 AD, as noted by Hong et al. (1994).

By identifying Pb isotopic signatures corresponding to potential Pb emission sources in ancient times and with the assistance of historical evaluations of locations and statistics of Pb production in ancient times, Rosman et al. (1997) were able to interpret the changes in Pb isotopic compositions observed in Greenland ice corresponding to the Greco-Roman period. In turn, the Pb isotopic compositions observed in the ice confirmed the existing historical data, and offered some evaluation of the relative levels of silver production from different Spanish mining regions. The study had illustrated how evaluations of heavy metals and particularly Pb and Pb isotopes could offer a sensitive technique to confirm and complement other forms of quantitative historical research.

During the 1990's, parallel to the efforts of Boutron and co-workers to complete and extend the Pb pollution history of Greenland, investigations were undertaken to

evaluate the seasonal, or interannual, variations of deposition of heavy metals on the Greenland ice sheet. These variations were first observed by Murozumi et al. (1969), who measured Pb in snow deposited in North-West Greenland in 1964 and 1965 and identified higher Pb concentrations in winter snow compared to those in spring – autumn snow. Seasonal inputs of heavy metals were also investigated to provide a more thorough understanding of the atmospheric transport of pollutants to Greenland. The data could also be used to identify short-term changes in the relative contributions of heavy metals contributions from North America and Eurasia and further evaluate mechanisms by which heavy metals were deposited in the Greenland ice cap. Ultimately, however, the evaluation of seasonal variations of heavy metals deposition in Greenland served to illustrate the level of caution required in interpreting and evaluating changes in natural systems, such as the changing levels of anthropogenic Pb emissions to the atmosphere during the twentieth century.

Savarino et al. (1994) presented one of the first dedicated attempts to identify seasonal variations in Pb concentrations in Greenland snow. One sample of snow was obtained from the ATM site, located approximately 25 km south of the GISP2 drilling camp in central Greenland, on 20th August 1990. They sampled approximately 80 cm of snow deposited between winter 1989 and summer 1990, by plunging a single acid-cleaned polyethylene tube into surface snow and later sampling the snow in the central part of the tube at 4 cm intervals. Dating of the samples was primarily established by comparison of $\delta^{18}\text{O}$ data with other snow pit data obtained at Summit and Dye 3. In the samples, pronounced increases of Na, Al and SO_4 were all observed in April/May, compared to relatively low and stable concentrations throughout the rest of the year. As shown in Figure 3.18, concentrations of Pb, Cd, Cu and Zn were all observed to increase from low values in the winter (~15 pg/g for Pb) to high values in April/May. For Pb, Cd and Zn, these higher concentrations were maintained throughout summer 1990, however Cu concentrations returned to low levels soon after May 1990. For Pb, high concentrations ~50 pg/g were observed in April/May 1990, with somewhat lower concentrations ~30 pg/g observed in summer 1990. Lead concentrations observed in the samples were in agreement with previous evaluations of snow deposited in Greenland during 1980's (approximately 30 – 50 pg Pb/g), with insignificant levels of natural Pb contributions (<2%).

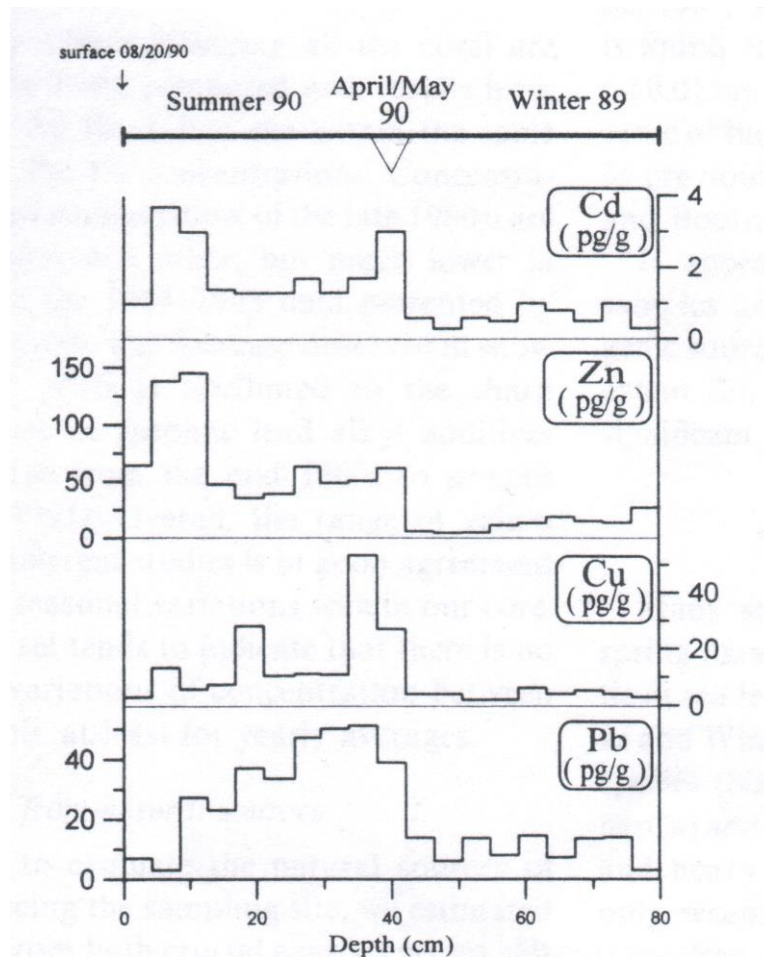


Figure 3.18. Depth profiles of Cd, Zn, Cu and Pb concentrations in Greenland snow from winter 1989 to summer 1990, from Savarino et al. (1994).

The spring peak of heavy metals concentrations observed by Savarino et al. (1994) confirmed earlier expectations based upon Arctic aerosol concentrations and measurements of major ions in Greenland snow. Evaluations of the Arctic climate suggested that the location of the polar front in winter, at low latitudes, resulted in many anthropogenic emission sources (located at mid-latitudes) polluting the polar basin at that time. Relatively low levels of precipitation during the winter led to increased levels of pollutants in the polar basin – the Arctic Haze. While the Greenland ice sheet is relatively isolated from the Arctic haze in winter (primarily due to its elevation), the poleward movement of the polar front during spring leads to greater vertical and latitudinal movement of air masses, consistent with inputs from polluted air masses over Summit during spring. Savarino et al. (1994) noted that it should be possible to distinguish between “engine exhaust” (denoted primarily by Pb) and “combustion” (denoted primarily by Zn and Cd) signals in the air masses

arriving at Summit, as a means of determining source regions of pollution. “Exhaust” signals were derived mostly from alkyl Pb additives in automobile gasoline, while “combustion” signals, associated with non-ferrous metal smelting, had been previously identified in air masses arriving over Greenland and Finland from the former USSR and Kola Peninsula. Savarino et al. (1994) finally noted that future seasonal studies required a longer time-series and should preferably be combined with other studies including air mass back-trajectories, climatology data and Pb isotopes and speciation analyses.

Later that year, Boyle et al. (1994) presented a more extensive evaluation of Pb deposition in Greenland based on measurements of samples obtained from a snow pit located 1 km from the Summit ATM site. The snow pit was approximately 6 m deep, and a continuous record of Pb concentrations was obtained from 1981 to 1990. Within the data, significant interannual variations were observed for Pb concentrations, varying from ~5 pg/g to ~160 pg/g, with an average increase of 35 times from trough-to-peak. While Pb peaks were observed to occur approximately during the spring seasons, the determination of the exact timing and sources of seasonal variations in Greenland snow were not the principle aim of their research. Instead, they intended to sample recently deposited Greenland snow during the 1980’s to compare the interannual variations of Pb concentrations with the inter-decadal variations observed by Boutron et al. (1991), who evaluated a 7.5-times decrease in Greenland Pb concentrations during the 1980’s. This decrease was observed to be similar to the recorded ~7-times decrease in US alkyl Pb consumption from 1970 to 1988. Boutron et al. (1991) sampled Summit firn cores at relatively low resolution (9 data points for the period 1980 – 1989), and evaluated the Pb concentration decrease of 7.5-times from simple least-squares regression of the data collected from 1968 to 1989. It was the aim of Boyle et al. (1994) to demonstrate that the sampling undertaken by Boutron et al. (1991) was insufficient to support such an interpretation of the data, which was not supported by evaluations of Pb concentrations in North Atlantic Ocean surface waters.

The attempts of Boyle and co-workers to determine changes in North Atlantic Ocean Pb concentrations as a result of the phase-out of alkyl Pb in gasoline in the USA in the 1970’s led to their evaluation of ^{210}Pb as a normalizing isotope. The weekly-

monthly variations in average oceanic Pb concentrations, driven by atmospheric patterns, oceanic eddies and biological removal, were significantly greater than overall changes in Pb levels which would occur over time scales on the order of years. ^{210}Pb , however, was recognized as a potential normalizing agent for Pb concentrations, as ^{210}Pb was produced by decay of ^{226}Ra in soils and was being continuously and constantly emitted to the atmosphere. The continental sources of both anthropogenic Pb and natural ^{210}Pb enabled Boyle and co-workers to normalize their seawater Pb concentrations to ^{210}Pb concentrations, and so resolve decadal changes in oceanic Pb levels from higher-frequency variations observed in stable Pb concentrations. After normalization, they observed Pb in surface waters of the North Atlantic Ocean, near Bermuda, decrease by a factor of ~4 from 1979 to 1987.

In the light of the decrease in Pb concentrations observed in the North Atlantic Ocean, and the inter-comparison of their snow pit data and that collected by Boutron et al. (1991) from firn core samples (shown in Figure 3.19), Boyle et al. (1994) evaluated Pb concentrations in Greenland snow from 1970 to 1990 to have decreased, however they attributed to the magnitude of this decrease an uncertainty of approximately a factor of two. They noted that the data collected by Boutron et al. (1991) may have been subject to aliasing, a phenomenon of data sampling wherein a high-frequency signal is sampled at intervals greater than half of the period of that signal, which ultimately results in the identification of an artificial signal of lower frequency. Boyle et al. (1994) noted that firstly, the high-frequency seasonal signal observed at Greenland was much greater in amplitude than the expected decadal change of at most 7-times (the decrease in US alkyl Pb consumption) and secondly, that the sampling resolution of Boutron et al. (1991) was insufficient to adequately overcome the problems associated with aliasing of the seasonal Pb signal.

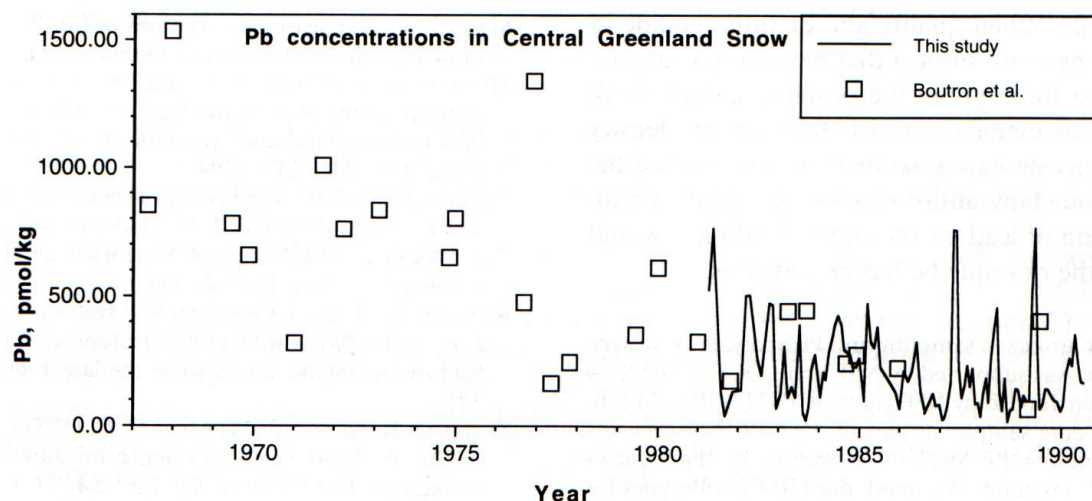


Figure 3.19. Lead in Greenland from 1955 to 1990, comparison of data sets of Boutron et al. (1991) and Boyle et al. (1994), from Boyle et al. (1994).

Boyle et al. (1991) noted that the presence of changing Pb isotope ratios during the 1970's and 1980's and the observed decrease in Pb concentrations in North Atlantic Ocean surface waters supported the presence of a definite trend in the Greenland snow deposition record, but questioned the validity of evaluating the magnitude of that trend as a 7-times decrease. They suggested that the best solution to the problem was to evaluate trends over a longer period, such as from ~1970 to 1980, but noted the huge technical effort required in continuously-sampling the required 10-12 m snow pit. A compromise would be to attempt to sample and correlate Pb records obtained from a number of snow/firn cores, so as to overcome the discontinuous nature of analyses of core sections but maintain the continuity of the pollution record. Boyle et al. (1994) also stated their belief that, following the decrease in US Pb emissions during the 1970's, European Pb emissions became a more important source of anthropogenic Pb to Greenland in the 1980's, as supported by the Pb isotope data of Rosman et al. (1993). Their conclusion included the emphasis that discontinuous time-series' of Greenland Pb concentrations were 'likely to be affected by aliasing and should be regarded with reservation until confirmed by independent samplings'. The work of Boyle et al. (1994) demonstrated that the seasonal variations in Pb concentrations at Summit were significant in the light of overall changes in Pb levels, but they did not attempt to evaluate the cause(s) of this signal. Although they presented the longest evaluation of seasonal variations in Pb

concentrations observed at Greenland, the next advance in the understanding of the causes and influences of seasonality in the Greenland Pb signal was that of Candelone et al. (1996).

Candelone et al. (1996) produced a two-year record of seasonal Pb, Cd, Cu and Zn deposition by sampling a snow pit in central Greenland (elevation 3270 m) at high-resolution. The snow pit was located only a few kilometers from the sampling sites of Savarino et al. (1994) and Boyle et al. (1994). Candelone et al. (1996) obtained a continuous sequence of 36 samples, each integrating 4.5cm of snow, dating from spring 1990 to summer 1992. In addition to heavy metals, Na, Al, SO₄, H₂O₂ and MSA were analyzed to identify inputs of heavy metals from marine (Na), crustal (Al) and volcanic (SO₄) sources and to verify the season during which the sample was deposited (H₂O₂ and MSA). They observed that significant seasonal variations occurred for Pb, Cd, Cu and Zn, with concentrations of these metals varying by a factor of 22 (Zn) to 75 (Pb). Higher concentrations of all metals were observed in spring and summer strata than in autumn and winter strata. A good correlation was observed between concentrations of Pb and Cd, with the influence of natural Pb inputs from rock and soil dust indicated by a good correlation between Pb and Al concentrations. In contrast, poor correlation was observed between Pb and Na, indicating no significant marine source of Pb.

As might have been expected, the data presented by Candelone et al. (1996) was in excellent agreement with those of Boyle et al. (1994) and Savarino et al. (1994), which covered the periods 1980-1990 and spring 1989 – summer 1990, respectively. The observation of low levels of heavy metals in winter snow by Candelone et al. (1996) indicated that the high-altitude central Greenland ice sheet was well separated from the polluted air masses that commonly affect coastal Greenland sites. In spring, high concentrations of heavy metals and Al, indicating inputs from anthropogenic as well as crustal sources, were associated with ‘changes in synoptic conditions induced by the Northward retreat of the polar front at the end of winter’. A different pattern was also observed in summer, with lesser inputs from crustal sources, but similarly high inputs from anthropogenic sources. Differences in the proportions of Pb, Cd, Cu and Zn in each of the samples corresponding to summer were potentially attributed to changing emission sources. Isobaric air mass back-trajectory data for the site

indicated that summer trajectories were generally shorter than winter trajectories, and that winter trajectories from North America were twice as likely during the winter. Candelone et al. (1996) noted that although less than 10% of back-trajectories originated from Europe or Western Asia, these regions were good candidates for heavy metals emissions. Firstly, Rosman et al. (1993) had shown isotopically that, by 1990, Pb emissions from North America were only a small part of the total Pb input to Greenland. Secondly, some Pb and Zn smelters within the former USSR, located in or near the Arctic Circle, were well located to emit heavy metals which could be transported directly to Greenland, as was observed in spring snow strata.

As with other investigations in Greenland snow and ice, the identification of likely Pb emission sources by Pb isotope fingerprinting also clarified the earlier concentration-based results that had been found regarding seasonal Pb deposition in Greenland prior to 1998. Rosman et al. (1998a) reported Pb concentrations and Pb isotopic compositions in snow from Dye 3, southern Greenland, deposited between August 1988 and August 1989. The Dye 3 sampling site was located approximately 800 km south of Summit, at an altitude of 2479 m (~700 m lower than Summit). As much as possible, individual snow falls were collected, with usually 0 – 4 days delay between the end of the snowfall and the date of collection. Samples were obtained from 13th August 1988 (early summer) to 17th October 1988 (early autumn) and from 7th January 1989 (early winter) to 6th August 1989 (mid-summer). Lead concentrations and $^{206}\text{Pb}/^{207}\text{Pb}$ ratios observed in the samples are shown in figure 3.20.

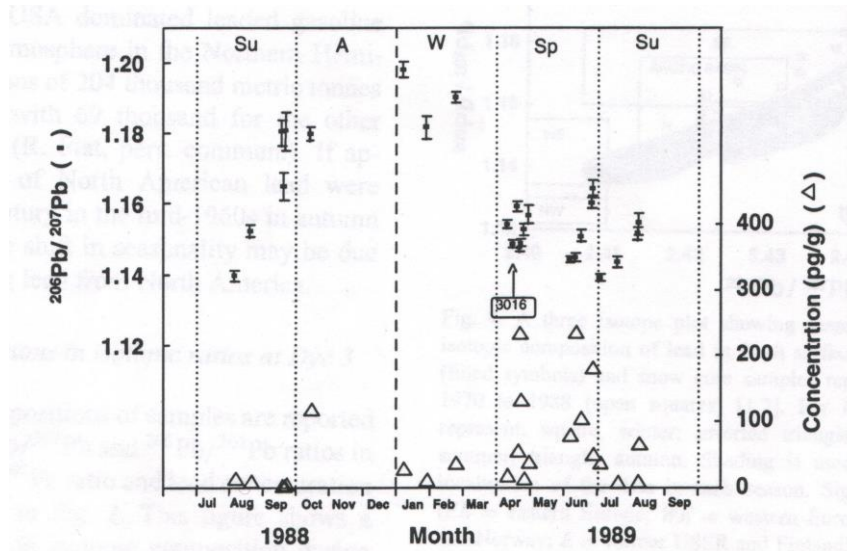


Figure 3.20. The isotopic composition and concentration of lead in fresh surface snow collected at Dye 3 during 1988 and 1989, from Rosman et al. (1998a). Seasons are abbreviated Su (summer), A (autumn), W (winter) and Sp (spring).

It was observed that Pb concentrations were low in winter (13 - 37 pg/g) compared to the higher and more variable values observed in spring (14 - 3016 pg/g). Concentrations in summer 1988 were very low (3 - 14 pg/g), while those in early summer 1989 were higher (9 - 67 pg/g). Only one data point was collected during autumn, with a high Pb concentration of 119 pg/g. The concentration data presented by Rosman et al. (1998a) was in agreement with studies of Summit snow by Candelone et al. (1996) and Boyle et al. (1994), who observed maximum Pb concentrations in spring. These results were in contradiction to those of Murozumi et al. (1969) however, who observed higher Pb concentrations in autumn and winter snow deposited near Camp Century, northern Greenland in 1964/5. Rosman et al. (1998a) suggested two possible explanations for this difference. Firstly, they noted that Camp Century was further North than Dye 3, and thus was more susceptible to pollution of the Arctic Basin from Eurasia in the winter and early spring, which arrived from over the North pole. Secondly, Pb emissions from the US had decreased since 1970, which may have resulted in lower Pb concentrations observed in autumn and winter if appreciable amounts of Pb arrived from North America during that time of the year.

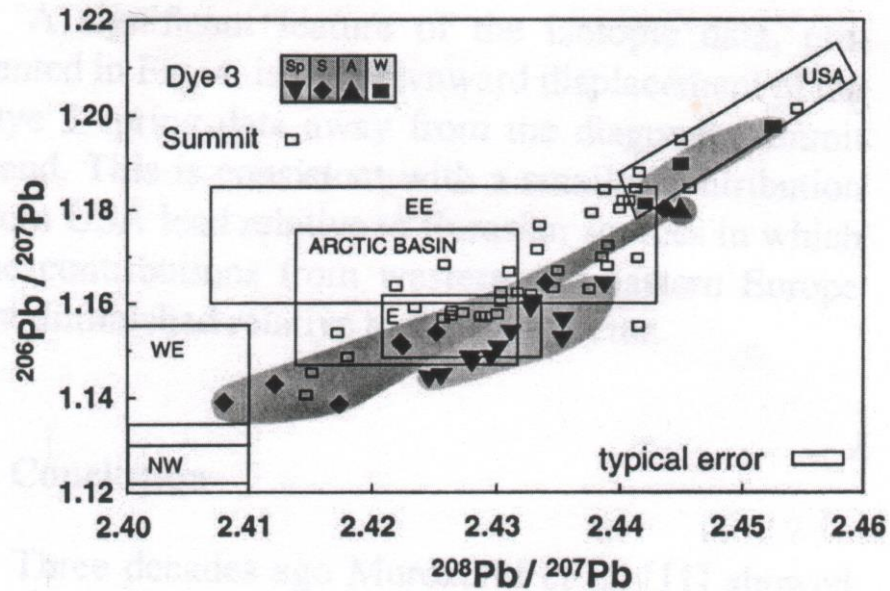


Figure 3.21. Seasonal changes in the isotopic composition of lead in fresh surface snow from Dye 3 (filled symbols) and snow core samples representing the years 1970 to 1988 (open squares), from Rosman et al. (1998a). Eurasian signatures are abbreviated EE (Eastern Europe), WE (Western Europe), NW (Sweden and Norway) and E (Former USSR and Finland).

Significant variations in $^{206}\text{Pb}/^{207}\text{Pb}$ ratios were also observed in the Dye 3 samples over the 13 month period, with values between ~ 1.14 and ~ 1.18 in summer, higher values from ~ 1.18 to ~ 1.20 in autumn and winter and lower values from 1.144 to 1.639 in spring, as shown in Figure 3.21. These isotopic variations were compared to available Pb isotopic compositions of aerosol signatures from Eastern Europe, Western Europe, Sweden and Norway, the former USSR and Finland, the USA and from the Antarctic Basin. The Pb isotopic signatures of emissions from the USA and the Eurasian regions were distinct and could be used to differentiate between different source regions, while air mass back-trajectory data was also available for evaluation of the data. Rosman et al. (1998a) clearly observed higher $^{206}\text{Pb}/^{207}\text{Pb}$ ratios in snow deposited from late summer to winter, attributing most, if not all, of this Pb to emissions from the USA. This conclusion was supported by the back-trajectory data. In spring, Rosman et al. (1998a) observed Pb isotopic compositions in Greenland snow to become more like signatures of Eastern (former USSR and Finland) and, to some extent, Eastern European emissions. This also correlated with

back-trajectory data, which indicated sources mainly located in the North Atlantic, Northern and Western Europe and in the Arctic Basin, rather than North America. They also observed more scattered Pb isotopic signatures in summer snow, with isotopic compositions similar to emissions from Western and Eastern Europe, the former USSR and Finland and, at the end of summer, the USA. This was supported by back-trajectory data that indicated short-range transport of aerosols from all directions to Greenland during the summer. Finally, Rosman et al. (1998a) noted that the variations in Pb isotopic composition observed in Dye 3 snow agreed with significant variations in $^{206}\text{Pb}/^{207}\text{Pb}$ ratio observed in adjacent Summit snow core samples by Rosman et al. (1994a). They also noted that ‘even the lowest $^{206}\text{Pb}/^{207}\text{Pb}$ ratios at Summit were significantly elevated during the period 1970-1980 indicating that a substantial proportion of USA lead (~50%) was present even during spring’. This data supported the second explanation offered by Rosman et al. (1998a), that of changing US Pb contributions, for the different seasonal Pb deposition patterns observed by Murozumi et al. (1969) in 1960’s Greenland snow.

Following the investigation of seasonal changes to Pb isotopic compositions in Pb fluxes to Greenland by Rosman et al. (1998a), showing the dominance of Eurasian emissions to Greenland, the emphasis of studies of heavy metals in snow and ice archives turned to more detailed investigations of Eurasian emissions. Such studies included evaluations of heavy metal concentrations and Pb isotopes in snow and firn samples from the French Alps (Veysseyre et al. 2001) and Mont Blanc (Rosman et al. 2000). Other investigations included evaluations of emissions of Pd, Pt and Rh, increasing after the introduction of catalytic converters (Barbante et al. 2001), and more detailed studies of Pb isotopes in aerosols throughout the Northern Hemisphere (Bollhöfer and Rosman 2001, 2002). Complementary research has also been recently undertaken in establishing by geochemical means the source(s) of rock and soil dust deposited in Greenland, so as to provide an insight into the atmospheric transport of aerosols to Greenland (Bory et al. 2002). The most recent evaluation of Pb concentrations and Pb isotopes in Greenland was that by Sherrell et al. (2000), which re-evaluated seasonal variations in Pb and Cd concentrations and Pb isotopes and questioned the interpretation of the Pb pollution histories of Greenland as presented by Boutron and co-workers from 1991 to 1995.

Sherrell et al. (2000) primarily presented Pb and Cd concentrations and Pb isotopes for the period 1981-1990, from a 10 m Summit snow pit previously analyzed by Boyle et al. (1994) for Pb concentrations only. They also presented seasonal variations in Pb and Cd concentrations obtained from ice cores covering the periods 1780-1788 (from a solar-powered electromechanical core drilled ~30 km from the GISP2 drilling site) and 1698-1700 (from the GISP2 core). Air mass back-trajectories calculated for the Summit indicated a similar pattern of atmospheric transportation to those calculated for Dye 3, with dominance of air masses from Eurasia in wintertime (67%) at the 500-hPa pressure altitude, but dominant North American sources of air during all seasons at the 700-hPa pressure altitude. The primary advantages of the 1981 – 1990 seasonal data set presented by Sherrell et al. (2000) over previous evaluations of seasonal Pb inputs to Greenland were the chemical species evaluated (Pb, Cd, Pb isotopes, SO₄) and the length of time sampled (10 seasonal cycles). Throughout the ten-year record, good correlations were observed between concentrations of Pb, Cd and SO₄, all primarily emitted by anthropogenic processes, thus confirming the dominance of anthropogenic aerosols in Greenland snow. The lengthy time period sampled ensured a representative evaluation of seasonal variations was produced, with a modern “anthropogenic baseline” of Pb concentrations determined by averaging the lowest concentrations observed over the period.

The data set obtained by Sherrell et al. (2000) essentially confirmed those results reported earlier by Candelone et al. (1996), with large variations in Pb concentrations (~5 pg/g – 160 pg/g) occurring as spring maxima and autumn/winter minima. As with previous studies, natural sources of Pb and Cd were found to be insignificant in even the lowest concentration samples, observed in autumn/winter, with Pb concentrations of ~5 – 25 pg/g. Evaluations of Pb isotopes in the samples confirmed the anthropogenic nature of Pb emissions to Greenland and further illustrated the different seasonal sources of Pb deposited in Greenland.

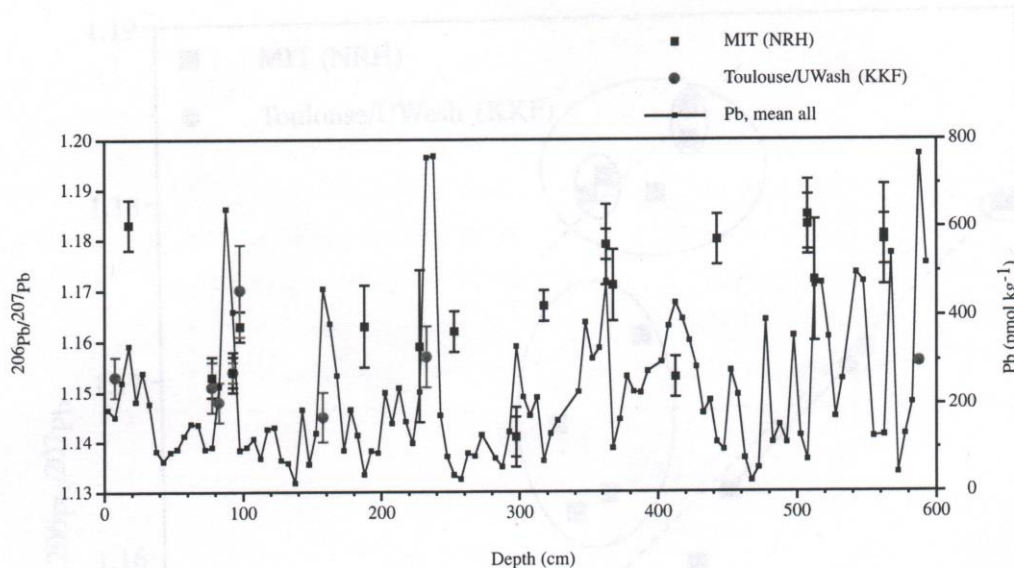


Figure 3.22. $^{206}\text{Pb}/^{207}\text{Pb}$ isotope ratios (circles and large squares) and lead concentrations (small squares, continuous line) in a Summit snow pit, from Sherrell et al. (2000).

While $^{206}\text{Pb}/^{207}\text{Pb}$ ratios in the 10 m snow pit clearly decrease from ~ 1.18 in 1981 to ~ 1.15 in 1989 (Figure 3.22), in accordance with changing proportions of emissions from different sources, evaluation of a $^{206}\text{Pb}/^{207}\text{Pb}$ versus $^{208}\text{Pb}/^{207}\text{Pb}$ plot (Figure 3.23) indicates a more complex variation in Pb deposition sources. Lead isotopic compositions in the snow pit data were observed to vary between signatures of US Pb, USSR and Eastern European Pb ores, and Western European aerosols. Particularly, it was observed that the earliest data (1981/2) were most isotopically-similar to US Pb, while later samples (1983 – 1989) exhibited Pb isotopic signatures more like those of European and Asian emissions. Sherrell et al. (2000) noted that low-concentration autumn/winter periods were associated with US-type Pb, while short-term spikes of high Pb concentration observed in the spring were consistent with Pb from Eurasian sources. They offered the suggestion that these short-term events may be produced by atmospheric injections of pollution-rich air from the low-latitude Arctic haze up to the high-altitude Summit site. They also noted that ‘only a few short-term events may provide inputs that are then smoothed by surface snow mixing, producing consistent annual spring peaks in the snow pit’. However, between 1987 and 1990, influences of US-type Pb could still be observed in the samples, albeit to a lesser extent than in 1981/2. Sherrell et al. (2000) noted that whereas emissions of Pb in the US had probably decreased 3-fold during the 1980’s,

emissions from European sources had at most decreased by ~14% in the same period. These changes in emissions were likely to produce a decrease in the total Pb flux of 25 – 33% during the 1980's, which was small in comparison to the large seasonal variations in Pb concentration observed in Greenland snow, and may not be resolvable over a relatively short period such as one decade. They noted their data 'suggests that attempts to quantify the precise magnitude of any intradecadal trend in concentration or source mixture will be severely limited by high-frequency noise and uncertainties in isotopic source signatures'.

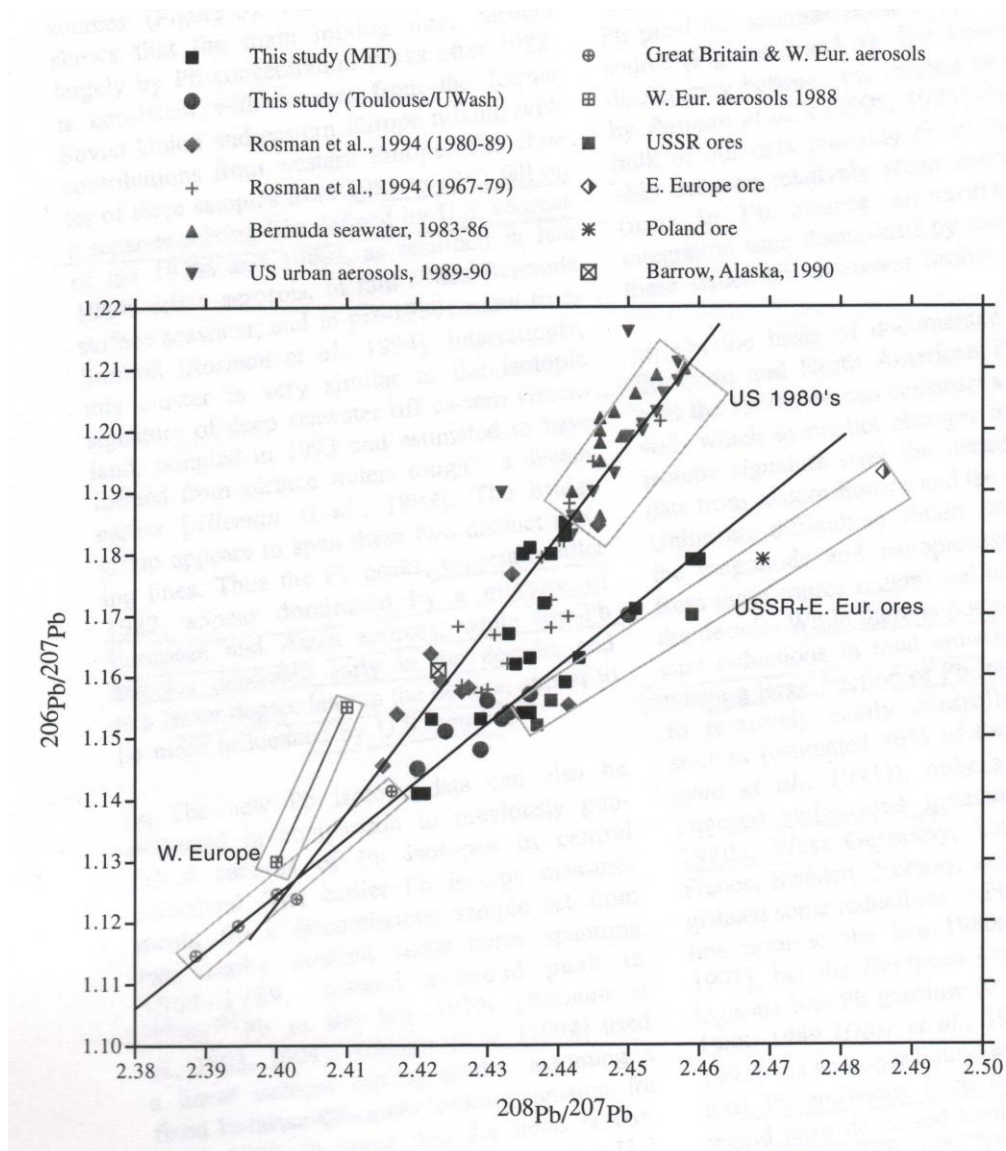


Figure 3.23. Lead isotopic compositions from a Greenland snow pit (1981-1990), from Sherrell et al. (2000).

Sherrell et al. (2000) also investigated two ice core sections for early-industrial variations in seasonal Pb and Cd deposition (see Figure 3.24). In an electromechanical drill core section covering the period 1780-1788, they observed regular changes in Pb concentration from ~4 pg/g to ~30 pg/g. While these samples included deposition from the 1783 AD Laki eruption, variations were observed throughout the core section, confirming the presence of seasonal variations in Pb deposition. It was noted that Pb concentrations observed in the samples were about twice those observed by Hong et al. (1996), which may have indicated the presence of minor levels of contamination in the samples. In the GISP2 core samples, dated to 1698-1700, Pb concentrations varied again from ~7 pg/g to ~14 pg/g. Although the Pb concentrations presented in the samples were very close to detection limits, concentration maxima appeared to occur roughly in spring-summer, providing a preliminary confirmation of the seasonal variations observed in 1980's Greenland snow. Sherrell et al. (2000) concluded by noting that Pb levels in Greenland had approximately doubled from ~1700 to ~1780 and had doubled again by the 1980's, with current Greenland Pb levels most likely to be further reduced by control of automotive and industrial emissions in Eurasia.

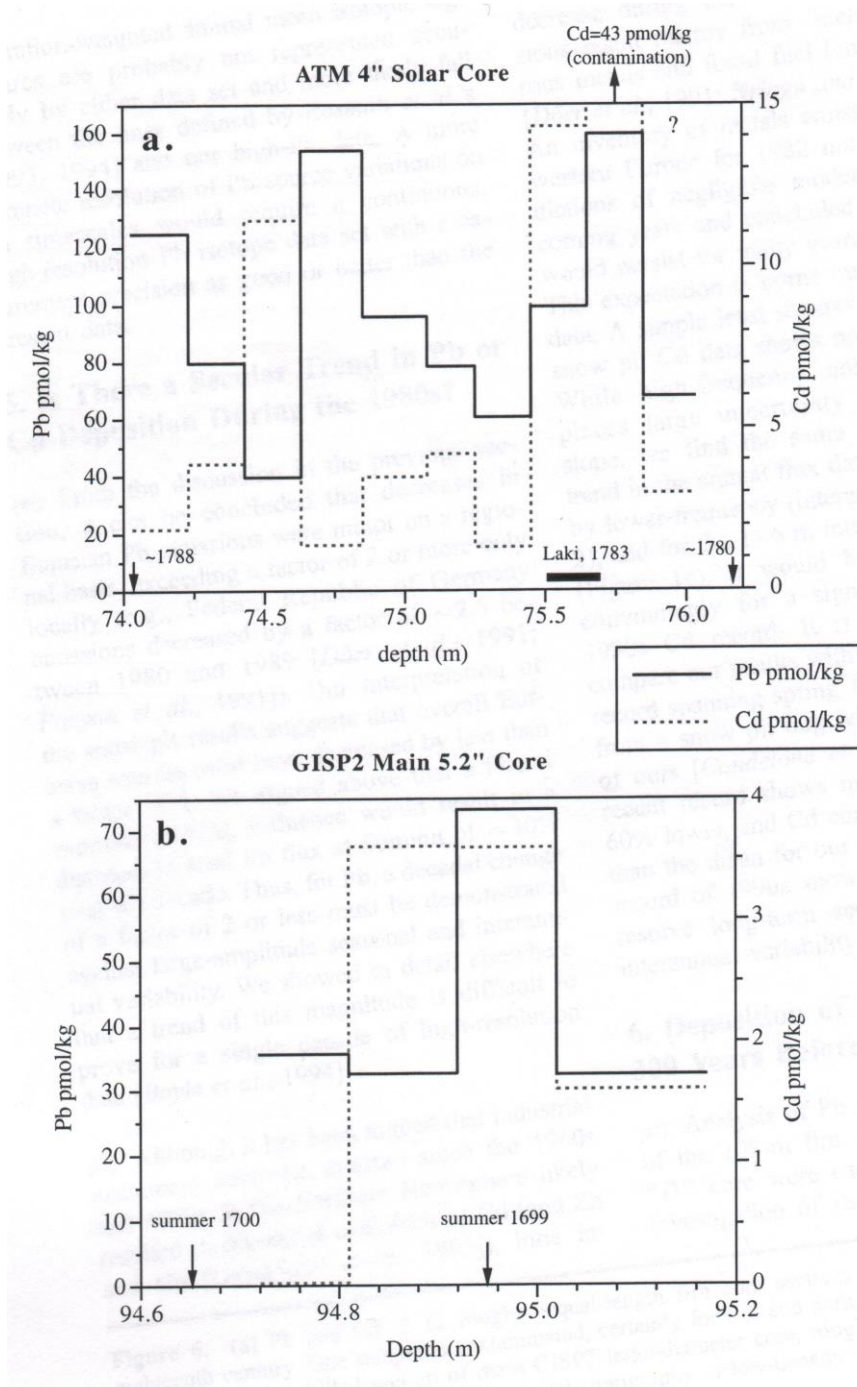


Figure 3.24. Intra-annual variations in Pb and Cd concentrations in Greenland firn core sections dated from ~1780 to ~1788, and from 1698-1700, from Sherrell et al. (2000).

The skills and techniques required to accurately sample the Earth's polar ice caps and determine reliable heavy metals concentrations from those samples developed over 30 years, from the 1960's to the 1990's. The evaluation of natural and anthropogenic fluxes of heavy metals to Greenland over the past climate cycle was made possible

by the development of laboratory and analytical procedures following the approach to scientific investigation established by C.C. Patterson, in which the reliability and the meaning of a measurement was of the utmost importance. This understanding of the level of attention required for trace-metal analyses was adopted by various investigators described earlier, including C.F. Boutron, K.J.R. Rosman, E.A. Boyle, E.W. Wolff and their co-workers, who essentially established the current body of knowledge regarding Pb fluxes to Greenland. With the skills developed during these studies of Greenland ice and snow, investigators were at last adequately prepared to determine the fluxes of Pb and other heavy metals to Antarctica, where natural Pb concentrations were at least an order of magnitude lower than at Greenland. The ultra-low levels of Pb observed in Antarctic ice also led to a shift in the emphasis of analyses, particularly concerning Pb isotopic analyses. While many analyses of heavy metals in Greenland snow and ice were made by GFAAS during the 1990's, concentrations of metals in Antarctic samples were regularly below the detection limits of the GFAAS technique. More sensitive techniques requiring smaller sample sizes, such as TIMS, DPASV and ICP-MS proved essential for analyses of Antarctic snow and ice. Also, the technique of Pb isotope fingerprinting for determining sources of Pb to Antarctic snow and ice proved essential for Pb fluxes to Antarctic snow and ice to be interpreted meaningfully. The demands placed upon researchers to develop techniques for accurately evaluating Pb levels in Antarctica led to a change in the manner in which such research was conducted, with emphasis once again on the importance of producing reliable results and accurately interpreting the data collected. Whereas for Greenland research, the evaluation of Pb isotopes was complementary to the interpretations applied to Pb concentration data, for Antarctic research the availability of Pb isotope data has been fundamental to the interpretation of the Pb concentration data. This has primarily been due to the extremely low levels of natural and anthropogenic Pb deposited in some Antarctic sites, and also due to the relatively limited data available regarding past and present emissions of heavy metals from natural and anthropogenic sources in the Southern Hemisphere.

3.6 Analyses of Pb in Antarctica: 1993 to the present

Rosman (2001) recently reviewed the extent of natural variations that have been reported for Pb isotopic compositions in Antarctic snow and ice, however the first evaluation of the sources of Pb transported to Antarctica did not require the sampling of Antarctic ice or snow. Instead, Flegal et al. (1993) reported Pb concentrations and isotopic compositions in seawater collected off the Antarctic Peninsula in 1987 and 1988, evaluated the likely sources of Pb to the seawater and extrapolated those findings to the Antarctic ice sheet. In March and June 1987 and June-August 1988, 19 samples of seawater were collected from 14 locations using rigorous trace-metal techniques. Lead was separated from the seawater by dithizone extraction, with concentrations and isotopic compositions determined by TIMS and Pb and Fe concentrations determined by GFAAS. Iron was also measured in the samples as they were obtained during periods of intense biological productivity.

Flegal et al. (1993) observed a wide range of Pb concentrations from 2 to ~21 pg/g, however most samples displayed concentrations below 7.7 pg/g. They observed that although some samples contained relatively large amounts of particulate Pb, Antarctic sea waters generally contained low levels of dissolved-Pb. Their results were in agreement with other measurements of dissolved-Pb concentrations in Antarctic surface waters (0.8 – 6.2 pg/g) and Antarctic rainwater (2.2 pg/g). They observed a positive correlation between Pb and Fe concentrations, and associated the high Pb concentrations observed in some samples with the presence of particulates. The lowest total-Pb concentrations measured by Flegal et al. (1993) were lower than the lowest dissolved-Pb concentrations reported for any other oceanic surface waters, attesting to the cleanliness of the Antarctic environment in comparison to other regions on Earth. The low concentration of Pb in Antarctic sea waters was expected in part from comparisons of aeolian Pb fluxes to the Antarctic polar cell (100 femtomol/cm²/yr) and the Arctic polar cell (14 picomol/cm²/yr) and the ratio of atmospheric Pb inputs to surface-water Pb concentrations observed in other oceanic surface waters.

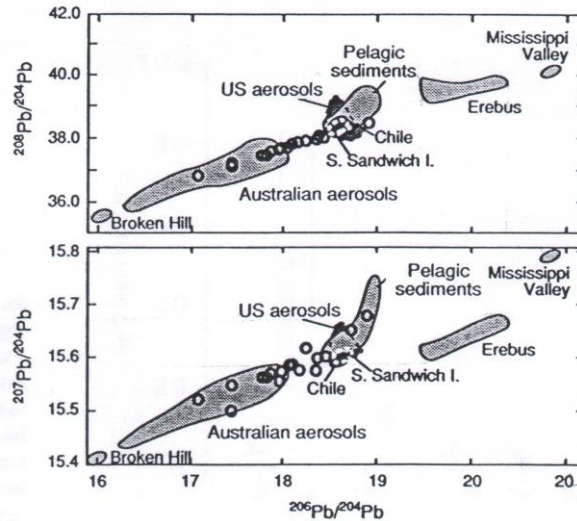


Figure 3.25. Lead isotopic compositions of Antarctic surface waters (circles) collected in 1987 and 1988, from Flegal et al. (1993).

Flegal et al. (1993) observed Pb isotopic compositions in Antarctic seawater samples fit a simple regression line, suggesting two primary sources of Pb (see figure 3.25). Their data varied from Pb isotopic compositions of $^{206}\text{Pb}/^{207}\text{Pb} \sim 1.10$ and $^{208}\text{Pb}/^{207}\text{Pb} \sim 2.37$ (similar to Australian aerosols) to $^{206}\text{Pb}/^{207}\text{Pb} \sim 1.19$ and $^{208}\text{Pb}/^{207}\text{Pb} \sim 2.45$ (similar to Southern Ocean pelagic sediments, lavas from Chile, sediments from the South Sandwich Islands and US urban aerosols). They attributed the Pb in Antarctic seawaters to two groups of sources, the more-radiogenic source being that of natural Pb sources, including volcanic emissions, aeolian dust and sediment transport by ice rafting, while the less-radiogenic source was due to anthropogenic emissions primarily originating from combustion of lead additives in automobile gasoline throughout the Southern Hemisphere. The signature of anthropogenic Pb emissions was primarily evaluated from Pb isotopic compositions of aerosols in Perth, Australia, collected from 1985 to 1988. These aerosols have $^{206}\text{Pb}/^{207}\text{Pb}$ ratios from 1.057 to 1.062, evaluated as a mixture of Australian Broken Hill and Mount Isa Pb ores ($^{206}\text{Pb}/^{207}\text{Pb} \sim 1.04$) and US Mississippi Valley Pb ores ($^{206}\text{Pb}/^{207}\text{Pb} \sim 1.35$). Flegal et al. (1993) noted that lead from Australian deposits had been observed as principal components in urban aerosols in Australia and South Africa and aerosols and surface waters in the South Pacific, and that these measurements were all consistent with anthropogenic Pb emissions significantly overwhelming natural Pb emissions. Although most of the world's anthropogenic Pb

emissions occur in the Northern Hemisphere, Flegal et al. (1993) discounted the possibility of anthropogenic Pb emissions from the Northern Hemisphere being present in the samples on the grounds of the minimal inter-hemispheric transport of Pb in the troposphere and ocean surface currents. Their evaluation of natural Pb emission sources included volcanism, such as that from Mount Erebus, aerolian dust emission from South America and sediment transport by ice rafting. Mount Erebus was noted to be the largest and most active volcano in Antarctica, for which emissions had been traced as far as 1000 km away. The Pb isotopic composition of Ross Island basalts was found to be more radiogenic than those observed in Antarctic seawater, however other potential natural Pb emission sources also displayed radiogenic signatures. Flegal et al. (1993) noted that it had been previously observed that the dust in Dome C ice was attributed to sources in South America by Grousset et al. (1992), and that the Pb isotopic signatures in various potential dust emissions sources such as Marie Byrd Land rocks, South Sandwich Island sediments and Chilean lavas were all relatively radiogenic. They also considered the possibility that particulate-Pb could be advected into the Antarctic seawaters by coastal polynyas, as has been observed to occur in the Arctic. It is unlikely however that the value they quoted for Arctic sediment-laden ice (30-600 mg/L) should be applicable to Antarctic ice, however. Of these various natural sources, Flegal et al. (1993) presumed that Southern Ocean pelagic sediments would represent a mixture for which the Pb isotopic composition could be considered representative. The Pb isotopic compositions in these pelagic sediments were also similar to the more-radiogenic end of the Antarctic seawater samples.

Based on the Pb isotopic compositions of anthropogenic and natural Pb sources, Flegal et al. (1993) calculated the possible contribution of anthropogenic Pb to Antarctic seawater. Estimating the dominant natural Pb input to be Mount Erebus or South American dust, they calculated anthropogenic Pb inputs to vary from 30 – 70% or 0-60%, respectively. These results emphasized that the proportions of anthropogenic to natural Pb in Antarctic seawater varied considerably, and that usually, comparable quantities of natural and anthropogenic Pb were deposited in the samples. They noted, however, that the variability observed in the proportions of natural and anthropogenic Pb present in the samples may be due to point sources of industrial Pb such as ships, aircraft and Antarctic research operations, and that the

low levels of Pb observed in Antarctic seawaters may be due to scavenging during periods of intense primary productivity. Flegal et al. (1993) determined that, despite the action of the circum-Antarctic polar cell to minimize transport of industrial Pb aerosols to Antarctica, Antarctic surface waters were clearly contaminated with anthropogenic Pb, however the proportions of anthropogenic Pb to natural Pb varied considerably but were generally comparable in size.

Flegal et al. (1993) presented the first conclusive evidence that significant levels of anthropogenic Pb were present in the Antarctic environment. Of particular note was the fact that even though Antarctic seawaters contained lower Pb concentrations than any other ocean surface waters on Earth, anthropogenic Pb was still present and in significant quantities. The limitations of their work, from the perspective of snow/ice studies, were that there was no means of evaluating past Pb fluxes, and that the inputs of Pb to seawater were more diverse than for snow, which only samples atmospheric Pb emissions.

From 1994, however, reliable Pb concentration and Pb isotope data were obtained from the Antarctic ice sheet. Wolff and Suttie (1994) provided the longest continuous record available for Antarctic Pb concentrations as well as an early compilation of anthropogenic Pb emissions in the Southern Hemisphere, in reporting their analyses of samples covering the period 1986 – 1925, obtained from a Coats Land snow pit. The 8.3 m deep snow pit was dated by evaluation of a parallel snow core for which beta-radioactivity measurements were made. Snow strata pertaining to the 1954 and 1964 bomb test peaks were identified, and the calculated snow accumulation rate of $56 \text{ kg/m}^2/\text{yr}$ was found to agree with snow stake measurements made in the 1960's and between 1986 and 1990. The uncertainty in the dating at the bottom of the core was estimated as ± 3 years. Blocks were subsampled in a Class 100 clean laboratory, with each sample corresponding to approximately $\frac{1}{2}$ to $\frac{1}{3}$ of a year of snow accumulation. The samples were analyzed in a clean laboratory by GFAAS, with a Pb detection limit of 0.2 pg/g. Concentrations of Al, Na and SO_4 were also determined to evaluate natural Pb inputs. It was estimated that the precisions of reported Pb concentrations were $\sim \pm 15\%$.

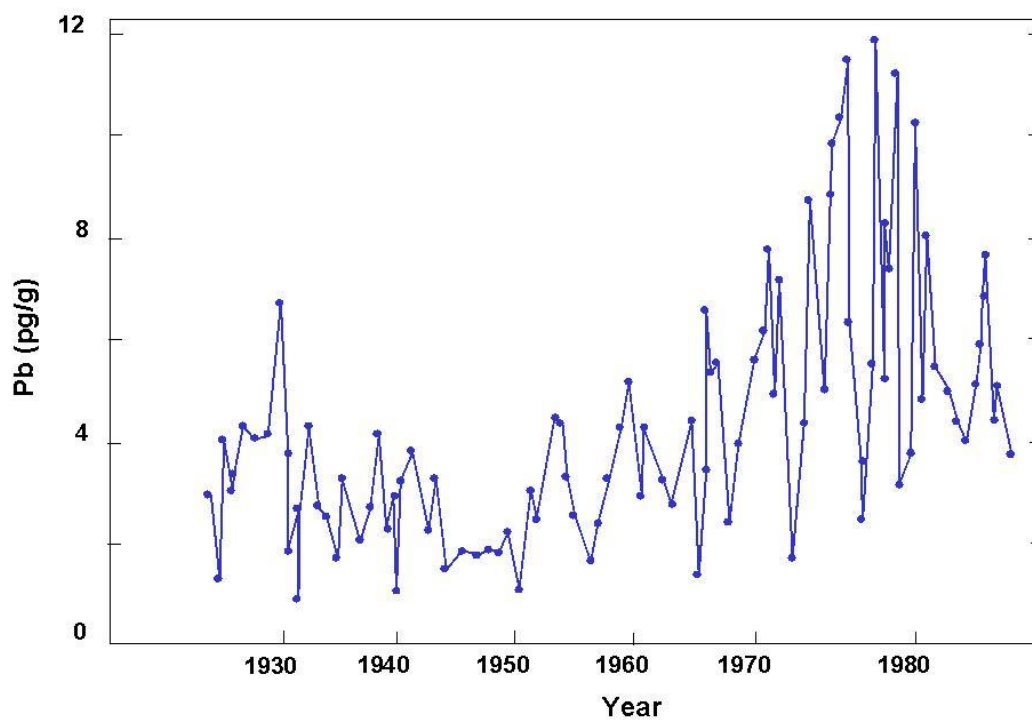


Figure 3.26. Lead concentrations in snow from a pit in Coats Land, Antarctica, redrawn from Wolff and Suttie (1994).

Wolff and Suttie (1994) observed Pb concentrations at Coats Land vary from ~1 pg/g to ~12 pg/g (see figure 3.26). Lead concentrations were ~2.5 pg/g from 1920 to 1950, with somewhat higher values in the late 1920's and lower values in the 1940's. From 1950, Pb concentrations rise steadily to ~8 pg/g in the late 1970's and then decrease to ~5.5 pg/g in the 1980's. Significant variability was observed from sample-to-sample, most likely due to seasonal variations in snow deposition, however Wolff and Suttie (1994) noted that a few high Pb concentrations >10 pg/g observed in the late 1970's may have been due to overflights by Russian aircraft using leaded petrol.

Table 3.4. Annual Pb emissions from major Southern Hemisphere sources, 1925-1986, from Wolff and Suttie (1994).

Source	Emission factor ^b g t ⁻¹ metal	Production / kt yr ⁻¹			Pb emitted / t yr ⁻¹		
		1925	1950	1986	1925	1950	1986
OCEANIA							
Aus Pb mining	500-1000	185	219	448	130	155	320
Aus Pb prodn	3000-8000	149	199	357	730	975	1750
Aus Zn prodn	1200-2500	46	84	308	80	145	530
AFRICA south of equator							
Zaire/Zambia Cu pm	1300-2600	88	432	990	160	790	1820
S Africa Cu prodn	1300-2600	0	32	184	0	60	340
S. AMERICA south of equator							
Peru/Brazil Pb pm	3000-8000	0	31	153	0	150	750
Chile/Peru Cu pm	3000-8000	211	363	1438	387	670	2650
PASSENGER CARS							
		/Millions of cars			c		
Oceania		0.5	1	8.4	0	700	5600
Africa south of eq		0.1	0.6	4.1	0	420	2700
Brazil		0.1	0.3	9.9	0	210	<<6000
Rest of S. Am south of eq		0.1	0.4	5.6	0	280	3700

After their evaluation of the possibility of local contamination of the samples, Wolff and Suttie (1994) then evaluated trends of Pb emissions in the Southern Hemisphere over the period 1925 – 1986, based on various UN and UK statistical summaries, as shown in Figure 3.27 and Table 3.4. Their estimates of Southern Hemisphere Pb emissions were based upon evaluations of the primary producers of non-ferrous metals (Pb, Cu-Ni, Zn-Cd) and consumers of leaded gasoline in each Southern Hemisphere continent, with gasoline consumption represented approximately by the most representative statistics then published: numbers of passenger cars. In Oceania, Wolff and Suttie (1994) noted that Australian production of Pb and Zn and consumption of leaded gasoline were all significant emission sources. They discounted the contribution from Indonesia due to its low-latitude location and the minor level of vehicle usage. In Southern Africa, production of Cu in Zaire, Zambia and South Africa were considered significant, as was vehicle usage in South Africa. In South America, Pb production in Peru and Brazil and Cu production in Chile and Peru were considered the main Pb emission sources from non-ferrous metals production. Although Brazil dominated vehicle usage, it was noted that other countries further south, such as Argentina, Chile and Uruguay, also featured great numbers of passenger cars. In summarizing their emissions estimates, Wolff and Suttie (1994) noted that with all of the metal production facilities and most of the major cities of the Southern Hemisphere located north of 40°S, in addition to the

strong zonal winds circling Antarctica, industrial lead deposited in Antarctica was likely to arrive from all continents and was probably mixed to some extent *en route*. While non-ferrous metal production probably dominated Southern Hemisphere Pb emissions until ~1950, the emission factors associated with these production processes were very uncertain and were complicated by the likely introduction of pollution-abatement measures, which have effectively gone undocumented. For estimates of consumption of leaded gasoline, it was realized that these statistics did not take into account increases in annual mileage and fuel efficiency nor did they reflect decreases in automobile use such as in times of economic recession and also it became necessary to estimate the Pb content of gasoline. However, by 1986, few countries in the Southern Hemisphere had introduced unleaded petrol and Brazil was the only Southern Hemisphere country that had completely stopped consuming leaded gasoline by 1990.

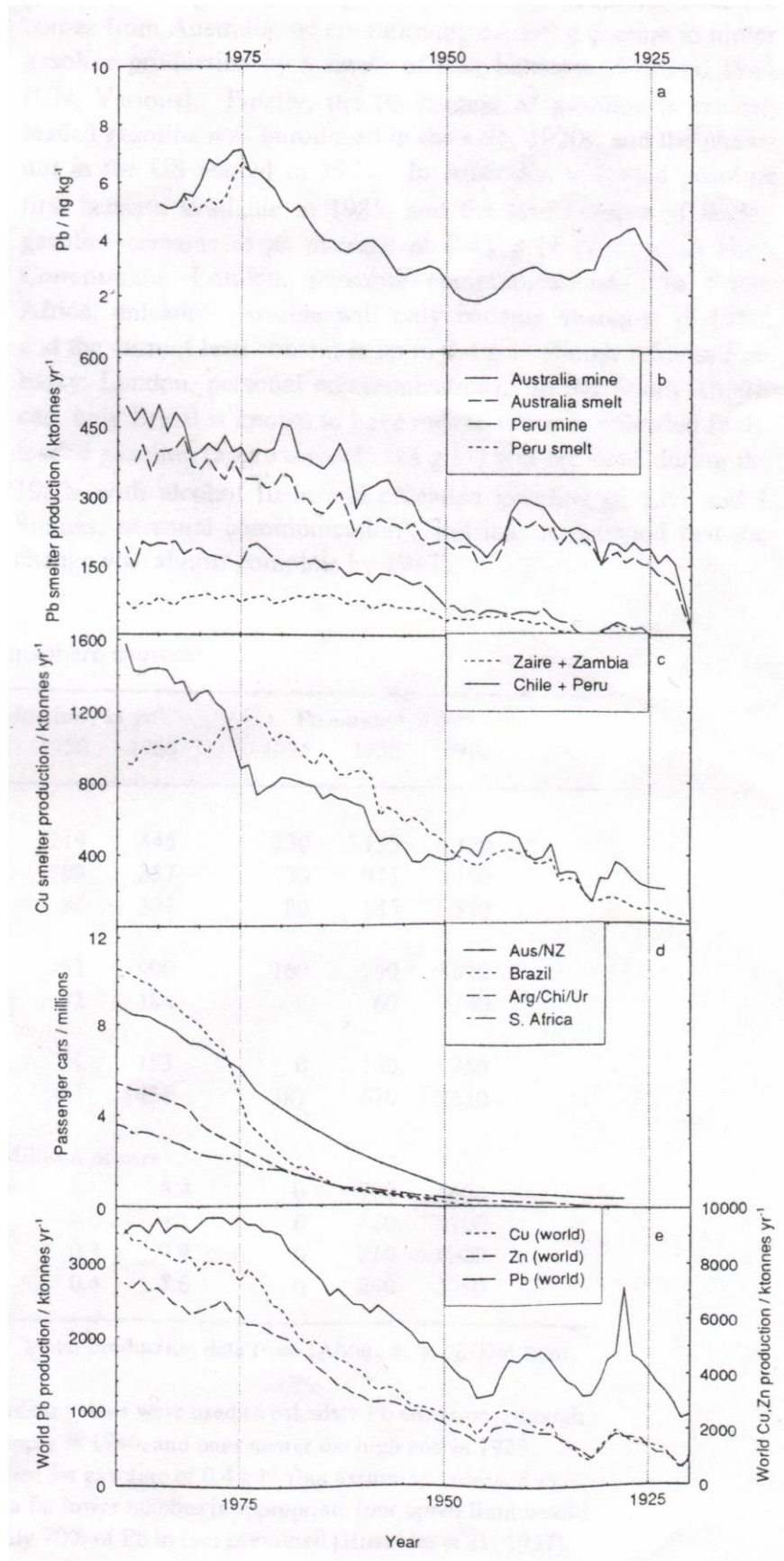


Figure 3.27. Statistics for Pb-emitting processes, 1920-1990, from Wolff and Suttie (1994).

Wolff and Suttie (1994) observed that anthropogenic Pb inputs of Coats Land snow from 1925 to 1986 significantly dominated natural Pb inputs, and that changes in Pb concentrations over that time generally reflected global trends in Pb emission. They determined Pb contributions from crustal (0.4 pg/g), marine (<0.3 pg/g) and volcanic (0.15 pg/g) sources, calculating a total natural Pb input of ~0.8 pg Pb/g. While this value was comparable to Pb concentrations determined in ancient Dome C ice by Boutron and Patterson (1986), it was still approximately 2 – 4 times less than the Pb concentration observed in the earliest Coats Land samples, indicating that anthropogenic Pb contributions to Antarctica were significant before 1925. It was noted that the peak in Coats Land Pb concentrations ~1975 was only about twice as great as that of ~1925, suggesting that emission factors of non-ferrous metal production had gradually decreased during the 20th century. Wolff and Suttie (1994) observed the Coats Land data to show ‘a very strong relationship with the global Pb production trends (share of total production, (1920-1950: NH (89-82%), Australia (10-12%), rest of SH (1-6%))’ during the first half of the 20th century and a doubling of Pb concentrations from 1950 to 1980 as a result of automobile Pb emissions. Finally, the lowered Pb concentrations they observed during the 1980’s they attributed to the introduction of unleaded fuels both in the Northern Hemisphere and in Brazil. On the basis of the consistency they observed between the Coats Land data and global Pb emission trends, Wolff and Suttie (1994) felt they could not rule out the possibility that Northern Hemisphere emissions play a role, even though they recognized that Patterson and Settle (1987) had shown that there was little inter-hemispheric transport of Pb aerosols. Wolff and Suttie (1994) were the first to determine a long-term continuous record of accurate Pb concentrations in Antarctica and link the observed variations in concentration to expected variations in continental Pb emissions. They established that Pb concentrations in the 1920’s were approximately 2 to 4 times greater than natural Pb inputs, and that Coats Land Pb concentrations did not more than double during the 20th century. They recognized, however, that regional differences in Pb deposition to Antarctica may occur, and indicated that these different patterns may allow researchers to understand atmospheric transport patterns to Antarctica.

While Wolff and Suttie (1994) showed convincingly that the concentration of Pb in Antarctic snow did indeed follow variations in Pb production, they could not

adequately determine the sources of Pb emission and their results even suggested the possible involvement of Pb emissions from the Northern Hemisphere. For almost a decade, their results were the defining data regarding anthropogenic Pb fluxes to Antarctica, predominantly due to the high-resolution sampling undertaken and the length of the pollution record they produced. Most other evaluations of Antarctic Pb concentrations were either limited by the number of samples collected or by the period of time sampled. Questions regarding Pb fluxes to Antarctica, such as the possible influence of Pb emissions from the Northern Hemisphere, or when anthropogenic Pb emissions could be first detected in Antarctica, or the relative inputs from different natural Pb sources to Antarctic ice, were not easily answered and some are still being addressed. The first attempt to answer some of these questions through analysis of Pb isotopic compositions was undertaken by Rosman et al. (1994b), on samples of snow blocks from East Antarctica and the South Pole as well as an ancient ice core sample obtained from Dome C.

The techniques employed by Rosman and co-workers for the analysis of Pb isotopes and Pb concentrations in polar snow and ice were described by Chisholm et al. (1995). They also described the experimental techniques involved in sampling snow and ice cores, laboratory and analytical procedures involving Isotope Dilution and Thermal Ionization Mass Spectrometry (TIMS) and also presented decontamination profiles for various Greenland and Antarctic core sections. Chisholm et al. (1995) presented a decontamination profile for a snow core section (70 m depth) collected at Summit in Greenland and also for two ice core sections obtained from Vostok (500 m depth) and Dome C (515 m depth) in Antarctica. These core sections were decontaminated at LGGE, Grenoble, using the techniques described by Candelone et al. (1994) then aliquotted and transported frozen to Australia. The samples were all prepared in a clean laboratory (called the “femtolab”) over-pressured with HEPA-filtered air as described in section 2.3 (Loss and Rosman 1987). The laboratory was constructed with an emphasis on producing a dust-free working area, employing the principles described by Moody (1982), with equipment for producing “high-purity” water and a refrigerator and freezer for storing enriched isotopes (spikes) and samples, respectively. The quality of the air in the laboratory was regularly monitored by exposing a clean PFA beaker containing dilute nitric acid (HNO_3) to the airstream, with the contamination rate from air evaluated to be ~ 1 pg/day for a 7

cm² area. Chisholm et al. (1995) described the two grades of water used, Millipore Milli-Q (MQ) water (containing 0.16 pg Pb/g) and quartz sub-boiling distilled water (called 'high purity' water and containing <0.03 pg Pb/g). They also described the methods of preparing HNO₃ acid (sub-boiling quartz distillation, containing 0.4-2 pg Pb/g) and Aluminium (contributing <0.1 pg Pb per analysis) and silica gel/phosphoric acid (H₃PO₄) solutions (containing ~0.02 pg Pb/μL) added to samples prior to analysis. Evaluations of the Pb concentrations within these solutions, as determined by Chisholm et al. (1995), are shown in Figure 3.28.

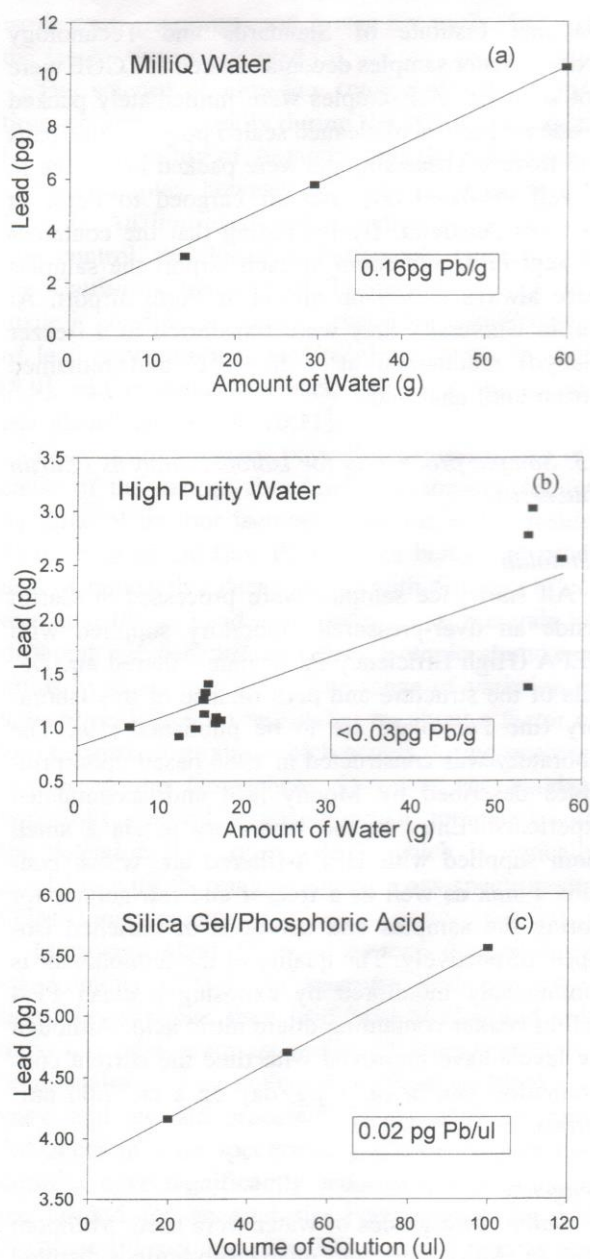


Figure 3.28. Measurement of Pb concentrations of Milli-Q water (a), high purity water (b) and the silica gel/phosphoric acid activator, from Chisholm et al. (1995).

Chisholm et al. (1995) also described the sequential bath sequence, a variation on the technique described by Boutron (1990), for cleaning PFA beakers and micropipette tips. They evaluated two blanks, the filament blank and the beaker blank, in evaluating the overall procedural blank. The filament blank was determined by measuring the quantity of Pb on a prepared Re filament containing the analytical reagents normally added to a sample: silica gel/H₃PO₄, Al and ²⁰⁵Pb spike solutions, and was found to be 0.5±0.1 pg Pb. The beaker blank was evaluated by evaporating high purity water in a preconditioned beaker, and determining the quantity of Pb in the sample. Beakers were preconditioned by adding ~15 mL of high purity water containing 50 µL conc. HNO₃ and 50 µL dilute H₃PO₄ to a beaker, which was then sealed and heated in an acid cleaned PTFE chamber for 2 hours. The beaker blank was then prepared by emptying the beaker, refilling it with high purity water and adding 10 µL conc. HNO₃, 3 µL silica gel/H₃PO₄ solution and 3 µL ²⁰⁵Pb spike solution (~5 pg Pb) by micropipette. This solution was then evaporated in the PTFE chamber and transferred by micropipette to an acid cleaned Re filament using 3 µL of a silica gel/H₃PO₄/Al solution. During the preparation of samples, 10 µL ²⁰⁵Pb spike solution (~20 pg Pb) was added, however the same quantities of other reagents were added. From evaluations of the beaker blank, determined from the data shown in Figure 3.28, the Pb contributed to each sample was found to be 0.4 pg from the water, 0.5 pg from the beaker, reagents and air deposition during evaporation and 0.5 pg from the filament, loading reagents and mass spectrometer. This total analytical blank of 1.4±0.9 pg Pb enabled isotopic compositions to be accurately reported on samples as small as 20 pg Pb with a precision of ~0.2% (95% confidence interval) on reported ²⁰⁶Pb/²⁰⁷Pb ratios. The technique for measurement of Pb isotopes by TIMS was described, with the accuracy of Pb isotope ratio measurements evaluated by repeated analyses of NIST common Pb SRM 981. It was shown that the measured isotope ratios could be adequately corrected by applying an instrumental mass fractionation bias of 0.24 (±0.06)%/u, however the ²⁰⁸Pb/²⁰⁷Pb ratio was still ~0.1% lower than the certified value after applying the correction (see Figure 3.29).

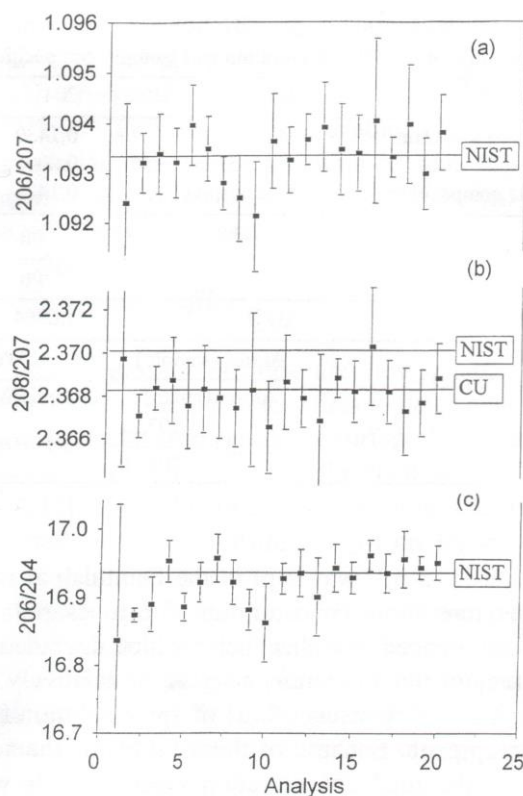


Figure 3.29. Results of analyses of 100 pg samples of the NIST SRM 981 isotopic standard after correction for isotopic fractionation by 0.24 ± 0.06 ‰, from Chisholm et al. (1995).

Chisholm et al. (1995) measured Pb amounts by Isotope Dilution Mass Spectrometry (IDMS), a sensitive technique for determining amounts of small Pb samples. They added ^{205}Pb ($T_{1/2} \sim 1.5 \times 10^7$ y), which is not present in terrestrial Pb, to each sample to determine Pb amounts and isotopic compositions from one measurement. The procedure used by Chisholm et al. (1995) to evaluate Pb concentrations by IDMS is shown in Table 3.5. The table shows the isotope spectra (isotopic ratios referenced to ^{205}Pb) of a spiked sample and the ^{205}Pb spike, and shows how the sample spectra is calculated by the subtraction of the spike spectrum from that of the spiked sample spectrum. In the bottom-most frame of the table, the IDMS equation is shown. The accuracy of the isotope dilution measurement was determined by the accuracy to which the concentration of the spike solution was known, and the accuracy at which the spike solution could be transferred to the sample solution. While Chisholm et al. (1995) found their spike solution concentration to be 2.4 ± 0.1 ng/g, the accuracy of the IDMS measurement was set conservatively to 20%, due to the gradual

evaporation of spike solution, the precision associated with micropipetting the spike and the difficulty of calibrating the tracer at that early stage in the use of the spike. The measurement capability of the techniques described by Chisholm et al. (1995) for samples as low as 1.7 pg/g were evaluated at ~0.2% and 0.4% (95% confidence intervals) on measurements of $^{206}\text{Pb}/^{207}\text{Pb}$ and $^{208}\text{Pb}/^{207}\text{Pb}$ ratios, respectively. This is also shown in Table 3.6.

Table 3.5. Measurement of the Pb concentration and isotopic composition of a sample using a ^{205}Pb spike, redrawn from Chisholm et al. (1995).

Pb isotope	(i)	204	205	206	207	208
Measured spectrum	(i/205)	0.1430	1.0000	2.4668	2.2025	5.2108
^{205}Pb spike	(i/205)	0.0005	1.0000	0.0607	0.0079	0.0186
Sample composition	(meas-spike)	0.1425		2.4061	2.1945	5.1922
		$\frac{^{206}\text{Pb}}{^{207}\text{Pb}}$	$\frac{^{208}\text{Pb}}{^{207}\text{Pb}}$	$\frac{^{206}\text{Pb}}{^{204}\text{Pb}}$		
Sample	(i/j)	1.0964	2.3660	16.8869		

$$\begin{aligned} \text{Sample Pb (pg)} &= \frac{\text{Atoms (sample)}}{\text{Atoms (spike)}} \times \frac{\text{Atomic Weight (sample)}}{\text{Atomic Weight (spike)}} \times \text{Added Spike (pg)} \\ &= 9.133 \times \frac{207.21}{205.10} \times 9.89 = 91.3 \text{ pg} \end{aligned}$$

Chisholm et al. (1995) also evaluated Pb concentrations and $^{206}\text{Pb}/^{207}\text{Pb}$ ratios in decontamination profiles from sections of a Greenland snow core and two Antarctic ice cores. For the Greenland snow core section, obtained at 70 m depth using an electromechanical drill, a plateau of Pb concentrations ~11 pg Pb/g and $^{206}\text{Pb}/^{207}\text{Pb}$ ratios ~1.186 was observed from the second snow layer to the inner core. The external layer displayed a higher Pb concentration ~70 pg/g and a lower $^{206}\text{Pb}/^{207}\text{Pb}$ ratio ~1.16, indicative of contamination. The Antarctic Vostok ice core section, obtained at 500 m depth from a fluid-filled drill hole using a thermal drill, did not show a plateau of Pb concentrations or $^{206}\text{Pb}/^{207}\text{Pb}$ ratios however. Lead concentrations were observed to decrease from the outer layer (>200 pg/g) to the inner core (~20 pg/g), while $^{206}\text{Pb}/^{207}\text{Pb}$ ratios decreased from the external layer (~1.158) to the next-to-external layer (~1.14) and then increased to the inner core

section (~1.16). This was interpreted as indicating two sources of Pb contamination in the core, with drilling fluid ($^{206}\text{Pb}/^{207}\text{Pb} < 1.158$) contaminating the inner core sections prior to the core surface being contaminated by a Pb source characterized by $^{206}\text{Pb}/^{207}\text{Pb} \sim 1.16$. The Dome C core section, obtained from a dry hole at 515 m depth by a thermal drill, displayed a plateau of Pb concentrations ~ 7 pg/g and $^{206}\text{Pb}/^{207}\text{Pb}$ ratios ~ 1.20 . The external and next-to-external layers displayed lower $^{206}\text{Pb}/^{207}\text{Pb}$ ratios (~ 1.165) indicating surface contamination of the core. Varying Pb concentrations observed in duplicate measurements of the 3rd layer and inner core sections exceeded the precision of the IDMS measurement, suggesting that the Pb content in the solution may have been heterogeneous. An explanation offered was that the changing Pb concentrations may be due to particles settling out of the solution, with this problem being minimized by agitating the bottle immediately prior to sampling.

Table 3.6. Measurements on selected samples reflecting the measurement precision achieved by Chisholm et al. (1995), redrawn from Chisholm et al. (1995).

Sample	$\frac{^{206}\text{Pb}}{^{207}\text{Pb}}$	$\frac{^{208}\text{Pb}}{^{207}\text{Pb}}$	$\frac{^{206}\text{Pb}}{^{204}\text{Pb}}$	Sample size (pg)	Concentration (pg/g)
<i>Blanks:</i>					
Filament	1.10(2)	2.37(2)	17.0(3)	0.5	
Beaker	1.08(1)	2.34(1)	16.46(4)	0.9	
<i>Sample:</i>					
Roman period	1.196(2)	2.473(4)	18.51(7)	25	1.7
<i>Processing effects:</i>					
(surface snow):					
Dye3 (regular)	1.159(2)	2.427(4)	17.7(2)	158	183
Dye3 (purified)	1.159(4)	2.428(7)	17.9(5)	105	
NIST SRM 981	1.0933(7)	2.370(2)	16.94(2)	91	

The techniques described by Chisholm et al. (1995) represented a significant advance in the ability to measure Pb isotopic compositions in small samples, as well as a contribution to the progressing field of clean laboratory techniques. The ongoing evaluation of heavy metals content in plastics and metals, labware and analytical reagents, in addition to techniques for the preparation of clean reagents, especially

water, have been described by Patterson and Settle (1976), Moody (1982), Boutron (1990) and Chisholm et al. (1995). These works described the state of the art, at the time, to determine and control sources of Pb contamination in the laboratory environment and were paralleled by the decreasing levels of Pb concentrations in polar snow and ice samples that could be accurately determined.

Using the techniques just described, Rosman et al. (1994b) analyzed Pb isotopic compositions in snow blocks collected and previously analyzed for Pb concentrations by Boutron and Patterson (1987). These snow blocks were collected in 1983 on an inland transect at distances of 33 km, 103 km and 433 km from Dumont d'Urville station in East Antarctica, shown in Figure 3.30. Another snow block was also collected at the South Pole, ~1274 km from Dumont d'Urville. At the sites 33 km, 103 km, 433 km and 1274 km (South Pole) from the station, Boutron and Patterson (1987) found Pb concentrations within the snow blocks to be 6.6, 7.4, 2.3 and 6.3 pg/g, respectively. They interpreted the higher Pb concentrations in the 33 km and 103 km blocks as contamination from Dumont d'Urville station, while the higher concentration at the South Pole was attributed to Pb contamination from the South Pole station. They also observed that the lowest observed Pb concentration in surface snow (2.3 pg/g) was still much higher than the ~0.4 pg/g observed in ancient Dome C ice, and so indicated significant levels of pollution. Rosman et al. (1994b) measured Pb isotopes in these snow block samples to identify variations in anthropogenic Pb contributions to the different Antarctic locations these blocks represented, as well as ancient ice from a Dome C ice core. The ice core sample was from 308 m depth, corresponding to snow deposited ~7,500 years BP, well before anthropogenic Pb emissions. The location of Dome C, approximately in line with the transect, provided a baseline of concentrations and isotopic compositions for comparison with the snow block data. Rosman et al. (1994b) found lower $^{206}\text{Pb}/^{207}\text{Pb}$ ratios on the exteriors of the snow blocks compared to the interiors, consistent with higher Pb concentrations on the exteriors signifying anthropogenic contamination. In the central snow block sections, they found $^{206}\text{Pb}/^{207}\text{Pb}$ ratios of 1.1092, 1.1662, 1.1614 and 1.1498 for the locations 33 km, 103 km, 433 km and 1274 km from Dumont d'Urville station, respectively. For the ice core section, they measured a Pb concentration of 2.1 pg/g and a $^{206}\text{Pb}/^{207}\text{Pb}$ ratio of 1.2521 in the inner core. Although the Pb concentration in the ice core was higher than those observed in

other Dome C sections by Boutron and Patterson (1986), a decontamination plateau verified that the result was accurate.

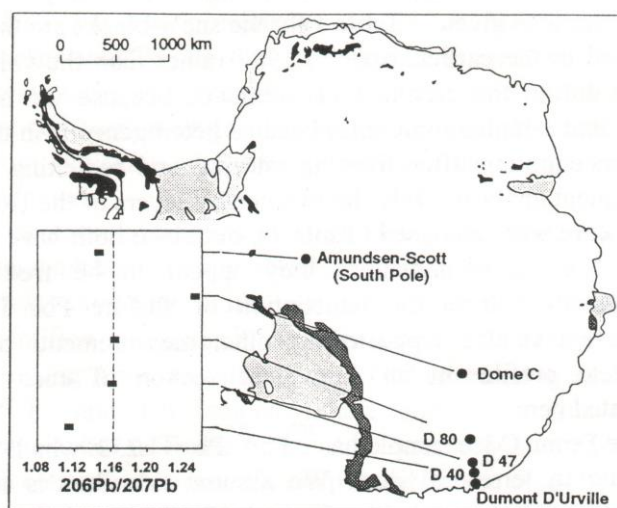


Figure 3.30. Sampling sites and $^{206}\text{Pb}/^{207}\text{Pb}$ ratios in Antarctic snow blocks collected in 1983 and a Dome C ice core section dated to ~7500 years BP, from Rosman et al. (1994b).

Rosman et al. (1994b) attributed the higher $^{206}\text{Pb}/^{207}\text{Pb}$ ratio ~1.252 observed in the Dome C section to inputs from terrestrial dust, as Boutron and Patterson (1986) had observed that aeolian dust inputs accounted for >95% of the natural Pb deposited at Dome C during the Holocene. They also noted the work of Grousset et al. (1992), who had determined that South America was a dominant source of Antarctic dust, from analyses of Sr and Nd isotope ratios and rare earth element concentrations. They attributed the Dome C dust signature, $^{206}\text{Pb}/^{207}\text{Pb}$ ~1.252, as one of the three principal isotopic signatures of Pb inputs to Antarctica. The second signature they observed was Australian Pb used in gasoline additives. This signature was associated with the lower $^{206}\text{Pb}/^{207}\text{Pb}$ ratios observed in the snow blocks located at 33 km (near Dumont d'Urville) and at 1274 km (near the South Pole) on the transect. While Suttie and Wolff (1993) considered it unlikely for significant levels of pollution to be transferred upwind 33 km from Dumont d'Urville, Rosman et al. (1994b) noted that Dumont d'Urville station had been using Australian leaded gasoline (with a $^{206}\text{Pb}/^{207}\text{Pb}$ ratio from 1.062 to 1.083 in 1982/1983) since 1970. The Pb isotopic signature of Australian leaded petrol emitted from Dumont d'Urville was consistent

with the lower $^{206}\text{Pb}/^{207}\text{Pb}$ ratio observed in surface snow 33 km inland, however Rosman et al. (1994b) acknowledged that the lower $^{206}\text{Pb}/^{207}\text{Pb}$ ratio observed in the snow may have been due to Australian Pb emissions transported directly to Antarctica. They noted the results of atmospheric general circulation models operated by Joussaume (1993), suggesting an Australian source for dust inputs to Antarctica. About 1983, Australian Pb emissions reflected a combination of alkylleads imported from the UK ($^{206}\text{Pb}/^{207}\text{Pb} \sim 1.07$) and the US ($^{206}\text{Pb}/^{207}\text{Pb} \sim 1.19$), with a representative $^{206}\text{Pb}/^{207}\text{Pb}$ ratio ~ 1.09 . Based on a combination of natural dust inputs ($^{206}\text{Pb}/^{207}\text{Pb} \sim 1.25$) and anthropogenic emissions from either Dumont d'Urville station ($^{206}\text{Pb}/^{207}\text{Pb} \sim 1.072$) or the Australian continent ($^{206}\text{Pb}/^{207}\text{Pb} \sim 1.09$), Rosman et al. (1994b) calculated the proportion of anthropogenic Pb contributed to the 33 km snow block to be 54% or 67%, respectively. At the South Pole, the $^{206}\text{Pb}/^{207}\text{Pb}$ ratio observed in the snow block (~ 1.15) was calculated to result from a combination of 30% natural dust ($^{206}\text{Pb}/^{207}\text{Pb} \sim 1.25$) and 70% anthropogenic Pb emitted from the South Pole station. The results of this calculation were more tentative, however, as the station had used Greek gasoline in 1984, but the source of gasoline in 1982 and 1983 was unrecorded, and the signature used to approximate Greek gasoline was $^{206}\text{Pb}/^{207}\text{Pb} \sim 1.14$, which was an average of all available European alkyllead values.

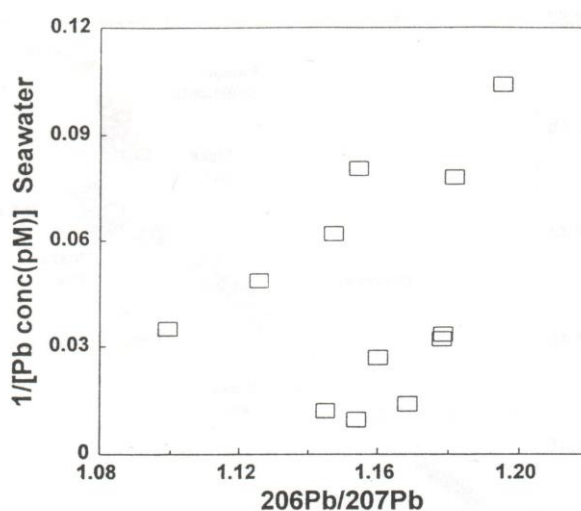


Figure 3.31. The inverse of the Pb concentration versus the $^{206}\text{Pb}/^{207}\text{Pb}$ ratio for Antarctic seawater measured by Flegel et al. (1993), from Rosman et al. (1994b).

Rosman et al. (1994b) then considered the third Pb input to be that reflected in the snow blocks 103 km and 433 km from Dumont d'Urville, with a $^{206}\text{Pb}/^{207}\text{Pb}$ ratio ~ 1.163 . In re-evaluating the Pb isotope data from Antarctic seawater obtained by Flegal et al. (1993), they observed a third Pb component with a $^{206}\text{Pb}/^{207}\text{Pb}$ ratio ~ 1.16 , in addition to the two more-radiogenic (natural) and less-radiogenic (anthropogenic) Pb components Flegal et al. (1993) had observed (see Figure 3.31). Rosman et al. (1994b) considered this third component, with a $^{206}\text{Pb}/^{207}\text{Pb}$ ratio ~ 1.16 , to be some type of "background" Pb observed throughout Antarctica. They could not establish an origin of this background Pb, but evaluated it as some combination of natural and anthropogenic sources. Using a $^{206}\text{Pb}/^{207}\text{Pb}$ ratio ~ 1.25 for the natural Pb component, and a minimum anthropogenic $^{206}\text{Pb}/^{207}\text{Pb}$ ratio of ~ 1.07 , Rosman et al. (1994b) evaluated that this background Pb must consist of at least 49% anthropogenic Pb. When they considered the geochemical arguments of Boutron and Patterson (1987), who determined anthropogenic Pb inputs of $\sim 80\%$ in Antarctica, the $^{206}\text{Pb}/^{207}\text{Pb}$ ratio for the anthropogenic component of background Pb was ~ 1.14 , similar to that seen in European gasoline Pb. They noted that due to 'the paucity of Pb isotope data for the Southern Hemisphere it is not possible to identify the origin of the *background* Pb with certainty'. They presented their data on a plot of $^{208}\text{Pb}/^{207}\text{Pb}$ ratios versus $^{206}\text{Pb}/^{207}\text{Pb}$ ratios (shown in Figure 3.32), with the Pb isotopic compositions of Antarctic seawater (Flegal et al. 1993), South Atlantic pelagic sediments (Chow and Patterson 1962) and aerosols from Perth, Australia from 1982-83 (K. Rosman, unpublished data) and the US from 1971-74 (Rabinowitz and Wetherill 1972, Chow et al. 1975). In the plot, the Pb isotopic compositions of all of the snow block samples were similar to those observed in Antarctic sea water, and lay within in the field bounded by Australian aerosols, US aerosols and ancient Dome C ice. Pelagic sediments were somewhat displaced from the mixing line representing the Antarctic snow and seawater data, however.

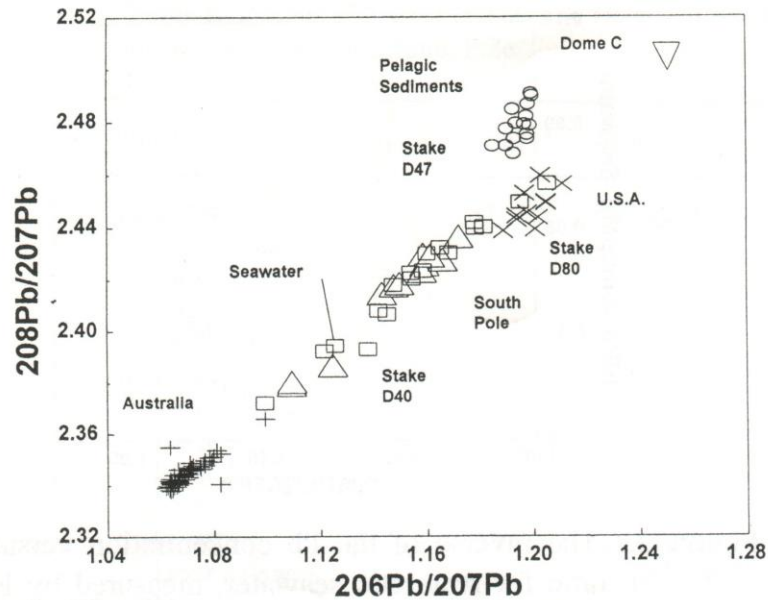


Figure 3.32. Lead isotope ratios in recent Antarctic snow (triangles) and Dome C ice (inverted triangle) compared to Antarctic seawater (squares), South Atlantic Ocean pelagic sediments (circles) and gasoline (x: USA, +:Australia), from Rosman et al. (1994b).

Rosman et al. (1994b) presented the first Pb isotopic data for Antarctic snow and ice, determining the extent of Pb pollution to different locations in Antarctica from various anthropogenic sources. As with the earlier research by Patterson, Boutron, Wolff and Flegal and their co-workers, it was apparent that significant levels of anthropogenic Pb were present in Antarctic surface snow and seawaters, however the compositions of Pb inputs, and their actual emission sources, were still quite uncertain. While Flegal et al. (1993) had identified a natural Pb source represented by a radiogenic Pb signature and an anthropogenic Pb source represented by the Pb isotopic signature of Australian aerosols, Rosman et al. (1994b) had identified a second type of Pb input to Antarctica, called “background” Pb, which was also comprised of an anthropogenic Pb component. Rosman et al. (1994b) had defined the $^{206}\text{Pb}/^{207}\text{Pb}$ ratio of natural Pb deposited in Antarctica as ~ 1.25 , calculated from Dome C ice, but did not evaluate how representative this figure was to other Antarctic locations where the influence from other sources such as volcanic and marine Pb emissions may have been more prevalent. For example, Flegal et al. (1993) had evaluated two potential signatures of natural Pb, one representing volcanic inputs ($^{206}\text{Pb}/^{207}\text{Pb} \sim 1.25$) and the other representing crustal inputs

($^{206}\text{Pb}/^{207}\text{Pb} \sim 1.20$), in Antarctic seawater, and from measurements of Al, Na and SO_4 , Wolff and Suttie had determined that marine and volcanic sources accounted for approximately 50% of natural Pb inputs to Coats Land. So, while Rosman et al. (1994b) had established the extent of variations of Pb isotopic composition over a large area of the Antarctic continent and in ancient Dome C ice, there still remained much speculation regarding the sources of anthropogenic and natural Pb fluxes to Antarctic snow, and their variations over time.

Barbante et al. (1997) provided a confirmation of some of the more recent trends observed by Wolff and Suttie (1994) from their evaluation of Pb concentrations in snow obtained from Victoria Land, in East Antarctica. In January 1991, they collected snow samples from two sites, with 4 samples obtained between 5 cm and 348 cm depth at McCarthy Ridge and 25 samples obtained between 5 cm and 1030 cm depth on the Styx Glacier plateau. Samples were obtained from a 2.5 m deep snow pit, below which they were collected from snow cores drilled from the snow pit base. Sample dating was determined from a parallel snow core by observation of seasonal variations in H_2O_2 and $\delta^{18}\text{O}$ values. The McCarthy ridge site was at elevation 700 m a.s.l., 40 km from the sea with a mean snow accumulation rate of 27 $\text{g}/\text{cm}^2/\text{yr}$, while the Styx Glacier site featured an elevation of 1700 m a.s.l., 50 km from the sea and a mean snow accumulation rate of 16 $\text{g}/\text{cm}^2/\text{yr}$. The collected samples were used to produce a record of natural and anthropogenic Pb inputs to Victoria Land from 1965 AD to 1991 AD. Snow core sections were decontaminated at the LGGE in Grenoble and measured by DPASV in Italy. Ultra-clean procedures were adopted for the preparation and analysis of samples, with no procedural blank applied. Triplicate measurements were made of each snow pit sample and duplicates of snow core samples, with the final results taken as the average of the collected data. For the snow cores, plateaus were observed for most of the analyzed core sections, with inner core Pb concentrations varying from 2.3 to 12.8 pg/g . NASS-3 and NASS-4 seawater reference materials were analyzed to verify the accuracy and precision of the DPASV procedure with mean Pb concentrations of 39 pg/g and 13 pg/g respectively determined. Aluminium concentrations were also determined in the samples by GFAAS, while Na and SO_4 were determined in a parallel series of samples.

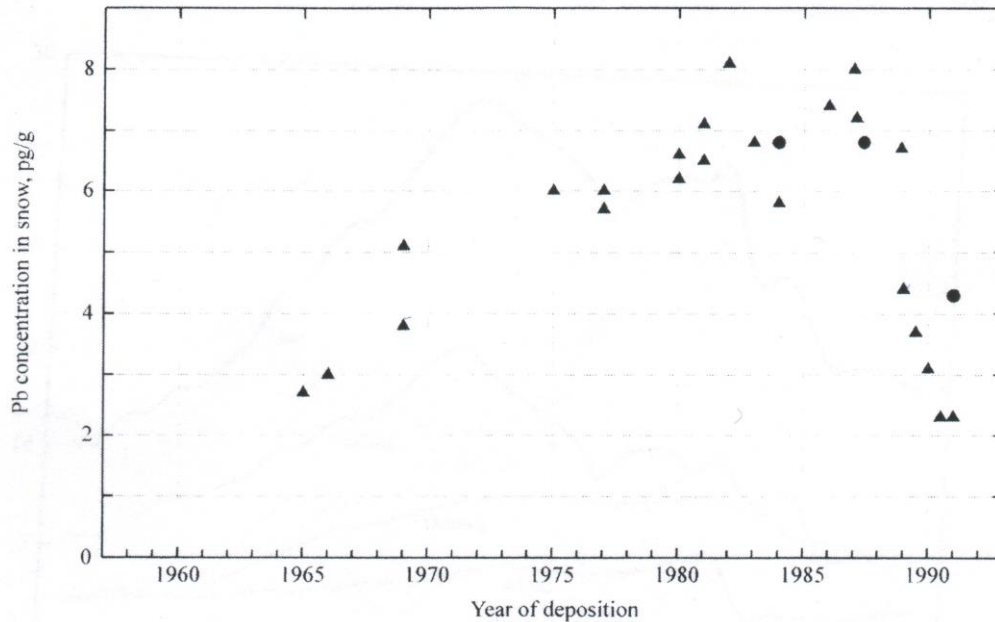


Figure 3.33. Lead concentrations in Antarctic (Victoria Land) snow from 1965 AD to 1991 AD, from Barbante et al. (1997).

As shown in Figure 3.33, Barbante et al. (1997) observed average Pb concentrations in Victoria Land snow increase consistently from ~3 pg/g in the mid-1960's to ~7 pg/g in the 1980's, with Pb concentrations then lowering to ~3 pg/g by 1991. With the exception of one sample, dated to Summer 1990-91, excellent agreement was observed between Pb concentrations in the McCarthy Ridge and Styx Glacier samples. The Pb concentrations they reported for recent Antarctic snow were within the ranges published by Boutron and Patterson (1987), Suttie and Wolff (1992) and Wolff and Suttie (1994). The trend of Pb concentrations from 1965 – 1991 observed by Barbante et al. (1997) approximately matched that which Wolff and Suttie (1994) had observed in Coats Land snow, however the Coats Land record showed a peak in Pb somewhat earlier, in the late 1970's. With the accuracy of their results justified, Barbante et al. (1997) then evaluated the natural and anthropogenic inputs of Pb to Victoria Land snow. Of the natural inputs, they determined ~0.065 pg Pb/g from crustal sources, ~0.15 pg Pb/g from volcanic sources and ~0.03 pg Pb/g from marine aerosols, with the total evaluated natural Pb inputs of 0.2-0.3 pg Pb/g contributing <10% of total Pb in the samples. The quantity of natural Pb inputs calculated for Victoria Land was also found to be in general agreement with those of Boutron and Patterson (1987), 0.25-0.47 pg Pb/g, and Wolff and Suttie (1994), <0.8 pg Pb/g.

Of the anthropogenic Pb inputs to Victoria Land snow, Barbante et al. (1997) attributed Pb concentrations in excess above natural levels to inputs from local and/or remote emission sources. They noted that while Pb contamination from Antarctic research stations contaminated only the immediate vicinity around the station, the only research station in Victoria Land region was the Italian base only operated on a small scale since 1985. They therefore considered the pollution observed at Victoria Land to be predominantly due to anthropogenic Pb emissions from continental locations in the Southern Hemisphere. Of these anthropogenic emissions, they noted the two most prominent emission sources in recent times were non-ferrous metal production and consumption of leaded gasoline, and provided statistics of production and consumption as well as estimates of emissions from these sources. Over the period studied, 1965 – 1991, they noted that the Pb concentrations in Victoria Land snow followed changes in consumption of leaded gasoline, while there was no correlation between Pb concentrations in snow and Southern Hemisphere non-ferrous metal production.

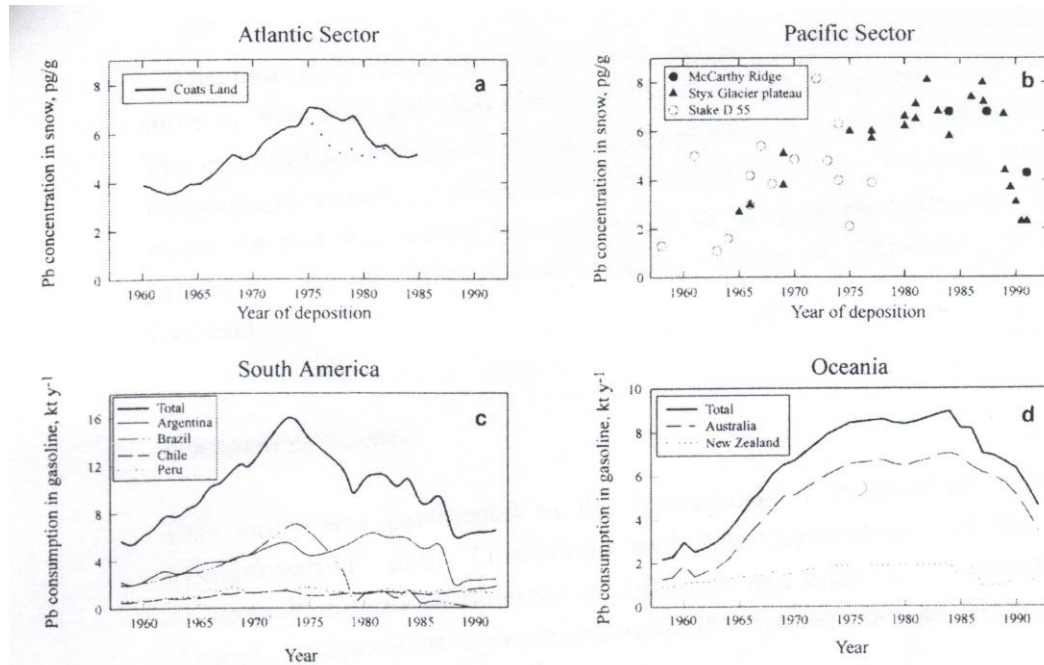


Figure 3.34. Comparison of the temporal trends of Pb concentrations in the Atlantic sector (Coats Land, a) and the Pacific sector (Victoria Land and Adelie Land, b) of Antarctica with gasoline Pb consumption in South America (c) and Oceania (d), from Barbante et al. (1997).

Barbante et al. (1997) compared trends of Pb concentrations in snow from Victoria Land and Coats Land with consumption of leaded gasoline in various continents of the Southern Hemisphere, and observed that the Coats Land record, with an earlier Pb peak ~1975, was consistent with alkyllead consumption in South America (they quoted a correlation of 0.47, $p=0.01$), while the Victoria Land record was more consistent with alkyllead consumption in Oceania (correlation of 0.80, $p=0.0002$), as shown in Figure 3.34. From this data, they evaluated South America and Oceania to be the predominant source areas for anthropogenic aerosols arriving at Coats Land and Victoria Land, respectively. With this data, Barbante et al. (1997) also confirmed the findings of Wolff and Suttie (1994), who had observed Pb concentrations in recent Antarctic snow increasing from the 1960's to the late-1970's and then decreasing through the 1980's. In both cases, the Pb concentration trend was observed to match changes in consumption of leaded gasoline in the continents of the Southern Hemisphere. These trends were also of a similar shape to that observed in Greenland, but with Greenland Pb concentrations over an order of magnitude greater than those observed in Antarctica.

The data presented by Barbante et al. (1997) indicated that inputs of natural Pb to Victoria Land were different to those for Coats Land and that this may also be the case for anthropogenic Pb inputs, based on statistics of Pb consumption in South America and Oceania and the different Pb pollution trends observed in Victoria Land and Coats Land. They also noted that conclusive data to support these hypotheses could potentially be provided by isotopic analyses and/or determinations of rare earth elements or other applicable tracers. Their hypothesis regarding sources of anthropogenic Pb in Antarctica was not readily solved, however, with the following research reporting evaluations of past levels of anthropogenic and natural Pb deposited in Antarctica. From 1998, results were published for research conducted on ice cores from Law Dome, another site in East Antarctica, while in 2001 data became available regarding ancient fluxes of metals to Taylor Dome.

The most extensive research regarding the evaluation of sources of aerosols to Antarctica was that presented by Basile et al. (1997), who extended the work of Grousset et al. (1992). Grousset et al. (1992) measured $^{87}\text{Sr}/^{86}\text{Sr}$ and $^{143}\text{Nd}/^{144}\text{Nd}$ ratios and REE's in a Dome C sample dated to the LGM, approximately 16 ky BP,

and observed that the sample was isotopically similar to loess from the Patagonian plain in South America, indicating that dust emitted from Patagonia was a significant Antarctic dust source. The technique required large samples, however, with 5.5 m of ice collected to produce just one sample. They also observed that while Patagonia was the main emission source, Antarctica, Southern Africa and Australia were all considered potential minor dust sources, with the possibility of enhanced dust emissions from the Argentine continental shelf that was exposed as a result of the 120 m decrease in sea levels during the LGM.

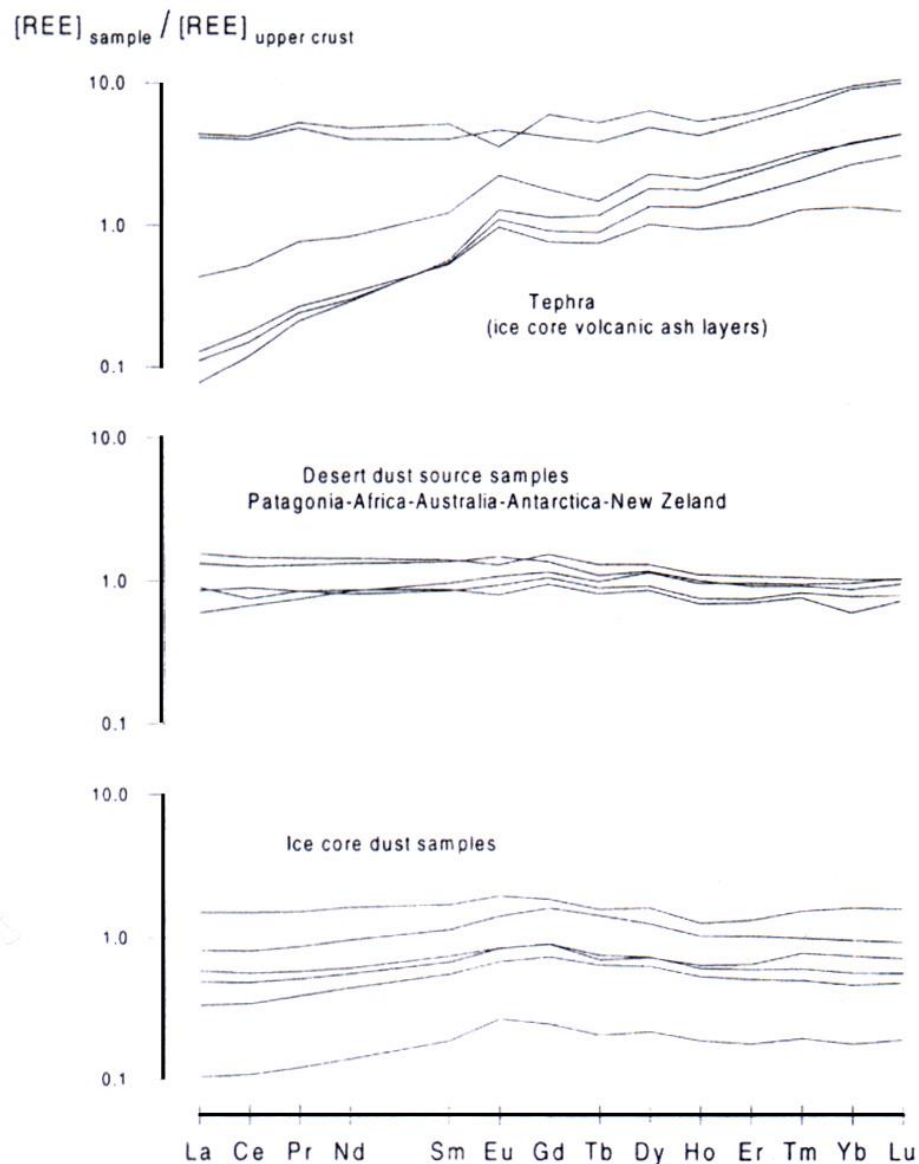


Figure 3.35. REE patterns for volcanic ash layers, continental desert dust and Antarctic ice core dust, from Basile et al. (1997).

Basile et al. (1997) extended this work by analyzing 5 more samples from three interglacial-glacial transition events and obtaining more loess and dust samples for better-characterizing the potential dust emission source areas. They evaluated $^{87}\text{Sr}/^{86}\text{Sr}$ and $^{143}\text{Nd}/^{144}\text{Nd}$ ratios and REE's in six samples, two obtained from Dome C dating to the LGM (16-18 ky BP and 18-20 ky BP) and four obtained from Vostok dating to glacial stage 4 (60.4-60.9 ky BP and 60.9-61.7 ky BP) and glacial stage 6 (158.8-162.6 ky BP and 162.7-166.8 ky BP). Each of the samples integrated ~7 kg of ice, and they all displayed similar $^{87}\text{Sr}/^{86}\text{Sr}$ and $^{143}\text{Nd}/^{144}\text{Nd}$ ratios and REE patterns, indicating that the source of this dust was similar in each glacial period. From their evaluations of particle size distributions and REE concentration patterns, they determined that dust inputs to the samples were not due to volcanic particles (see Figure 3.35), but were instead due to small particles that had been transported to Antarctica through the atmosphere from continental dust sources. From the Sr and Nd isotopic data, they calculated that the signature of glacial dust deposited in Antarctica could be evaluated as a combination of dust from the Patagonian plain in South America with component of either 10% Australian dust or 15% southern African dust, as shown in figure 3.36. This work confirmed the initial results of Grousset et al. (1992), but identified that dust emissions from the exposed Argentine continental shelf were insignificant, and that at least 85-90% of the dust deposited in Antarctica during glacial maxima originated from South America. These studies have been the most reliable evaluations of dust sources to Antarctic ice, and have been used to support interpretations of sources of trace metals observed in Antarctica. It is uncertain if the results are applicable to interglacial conditions, however, but the enormous quantity of ice required by the technique to measure Holocene-levels of Sr and Nd prohibits any attempt at such an evaluation.

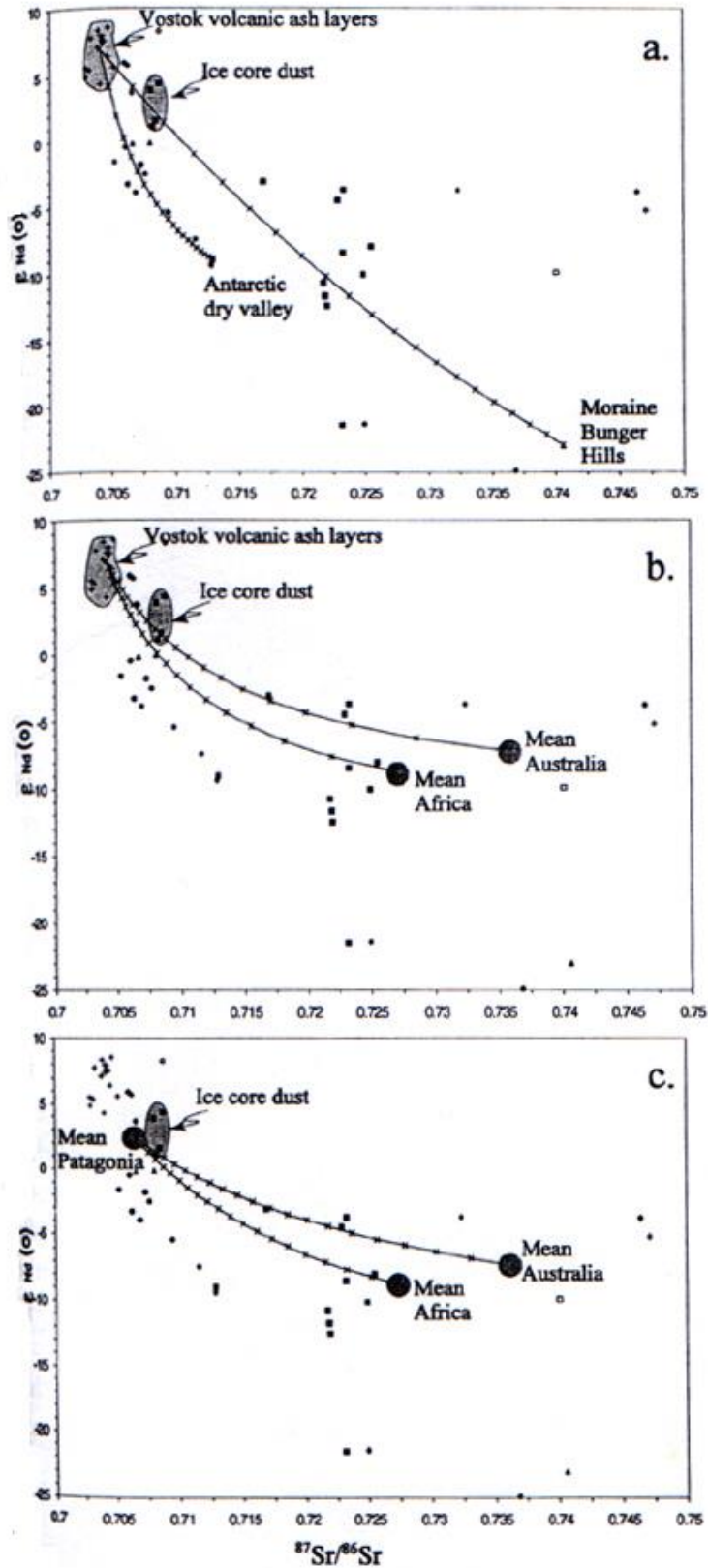


Figure 3.36. Theoretical mixing hyperbolae constructed for combinations of Antarctic dust sources (a), Antarctic and continental dust sources (b) and continental dust sources (c), from Basile et al. (1997).

Hong et al. (1998) evaluated Pb, Cd, Cu and Zn concentrations in Law Dome ice core sections dating from 2946 BP to 1940 AD. Eight core sections were obtained from two cores, DE08 and DSS, drilled at sites near the summit of the Law Dome ice cap and located at altitudes of 1250 and 1370 m a.s.l. and snow accumulation rates of 116 g H₂O/cm²/y and 64 g H₂O/cm²/y, respectively. Ice cores were dated by observation of annual cycles of $\delta^{18}\text{O}$ and electrical conductivity (DE08 and DSS) and H₂O₂ (DSS only), with dating precisions estimated to ~1% for the past few centuries and ~5% at 4000 years BP. Of the samples collected, eight sampled the period from 1843 AD to 1940 AD while one, dated to ~2950 years BP, was used to evaluate natural concentrations of heavy metals in Law Dome ice during the Holocene. The core sections sampled varied in length from 24 cm to 30 cm, which corresponded to significantly less than a year of deposition in all cases except for the ancient core section, which sampled approximately two years' deposition. All core sections were decontaminated using the chiselling technique described by Candelone et al. (1994), however for two core sections (dated to 1887 AD and 1929 AD), two inner core samples were collected to allow an evaluation of seasonal variations in heavy metals deposition to be undertaken. Concentration plateaus were observed for all core sections except one, DSS 28A, however the upper limit attributed to the Pb concentration in this core section was 0.86 pg/g. Concentrations of Pb, Cd, Cu, Zn, Al and Na were determined by GFAAS, with precisions of $\pm 10\%$ for the highest concentrations and $\pm 30\%$ for the lowest. Samples were corrected for a total analytical blank, which represented ~15-20% of Pb, Cd and Zn in the lowest concentration sample (DE08 77A2, 0.58 pg Pb/g).

Lead concentrations were generally observed to be low, <2.8 pg/g, however no clear trend was observed from 1834 AD to 1940 AD, while the Pb concentration in the ancient sample was similar to that seen in the 1834 AD sample and the average of values observed over the 19th and 20th centuries. While Hong et al. (1998) could not deduce any clear trend in Pb concentrations from their limited data set, they acknowledged that this finding contradicted that of Wolff and Suttie (1994), who observed significant inputs of anthropogenic pollution (2-4 times above natural levels) in Coats Land snow by 1925 AD. Hong et al. (1998), however, did not discuss the variability of their results in terms of the short (sub-annual) period of deposition sampled by each core section (see figure 3.37), a significant omission,

particularly considering that within the same paper, they evaluated the seasonal variations in Pb deposition to Law Dome.

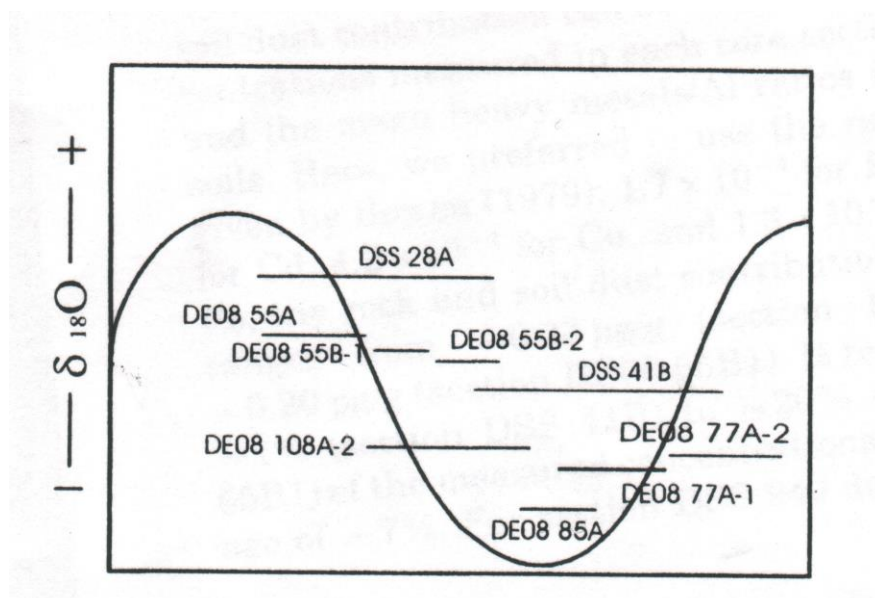


Figure 3.37. Seasonal position of the core sections analyzed by Hong et al. (1998) relative to an idealized $\delta^{18}\text{O}$ profile, from Hong et al. (1998).

From the data they presented, Hong et al. (1998) also provided evaluations of seasonal variations in, and natural sources of, heavy metals deposition to Law Dome. The evaluation was predominantly evaluated from the two DE08 core sections that were split into two adjacent inner core sections, with DE08 55B1 (96.40-96.55 m) and DE08 55B2 (96.55-96.70 m) covering the spring and winter/spring of 1929 AD, respectively, and DE08 77A1 (136.01-136.16 m) and DE08 77A2 (136.16-136.31 m) covering the winter/autumn and autumn of 1887 AD, respectively. From these data, Hong et al. (1998) evaluated Pb concentrations in winter snow at Law Dome to be 2-4 times greater than in spring-summer deposition, in agreement with those published by Suttie and Wolff (1992) for the Antarctic Peninsula. They also evaluated some natural inputs of Pb to Law Dome, from concentrations of Al and Na. From these data, it was shown that Pb inputs from crustal sources vary from ~ 0.03 pg/g to ~ 0.20 pg/g, representing $\sim 1\%$ to $\sim 20\%$ of total Pb in the samples, with an average contribution of $\sim 7\%$. The contribution of crustal dust to the ancient ~ 2950 BP sample was found to be 2% of the total Pb measured, much lower than that evaluated for Dome C by Boutron and Patterson (1986). From measurements of Na, the contribution of Pb from sea salt spray (marine aerosols) to Law Dome was found to

be ~10% to ~40% of total Pb in the samples. Hong et al. (1998) also noted that the 'large contribution from sea salt spray is further reflected by the fact that Pb, Cu, and mainly Cd are significantly correlated with Na, with correlation coefficients of 0.53, 0.42, and 0.76, respectively'. Lead inputs from other sources, such as volcanoes, wild forest fires and continental and marine biogenic sources, could not be established. Although SO₄ concentrations were measured in the samples, it was recognized that this molecule was emitted both from volcanoes and marine biogenic activity, and so could not be used to resolve these two sources. They indicated that the potential of marine biogenic sources, as a significant contributor of Pb to Law Dome, was likely based on the high Pb concentration observed in sample DSS 41B (4.5 pg/g, 1908 AD), which also contained large peaks of Na, SO₄ and MSA, indicators of inputs from marine and marine biogenic sources.

The work of Hong et al. (1998) described heavy metal deposition in another coastal Antarctic site, Law Dome. Their conclusions were critically limited, however, by the relatively small set of data measured and particularly the absence of any apparent trend in Pb concentrations from 1834 AD to 1940 AD, despite their observation of decontamination plateaus for all but one core section. These were resolved later that year with the presentation of Pb, Ba and Bi concentrations and Pb isotopic compositions in the same samples but measured by TIMS. Rosman et al. (1998b) analyzed aliquots of the samples prepared by Hong et al. (1998) and another DSS core sample, dated to the last interglacial, (>110,000 years old). Their combined results indicated firstly that some of the inner core samples were contaminated, and secondly that the Pb concentrations observed by Rosman et al. (1998b) were significantly lower than those reported by Hong et al. (1998). Rosman et al. (1998b) analyzed the samples by TIMS as described by Chisholm et al. (1995) with concentrations of Pb and Ba determined by isotope dilution and Bi concentrations determined from the relative sizes of the ²⁰⁸Pb and ²⁰⁹Bi ion beams as described by Chisholm et al. (1997). They applied a decontamination blank of 0.11 pg/g to the samples, which was determined by Candelone et al. (1994) in their evaluation of the amount of Pb transferred to an ice core sample during the ice core decontamination procedure, but has recently been evaluated as an overestimate (Vallelonga et al. 2002a). The discrepancy between the results observed by Rosman et al. (1998b) and

those of Hong et al. (1998) indicated that the Pb concentrations in the samples were too low for reliable determinations to be made by GFAAS.

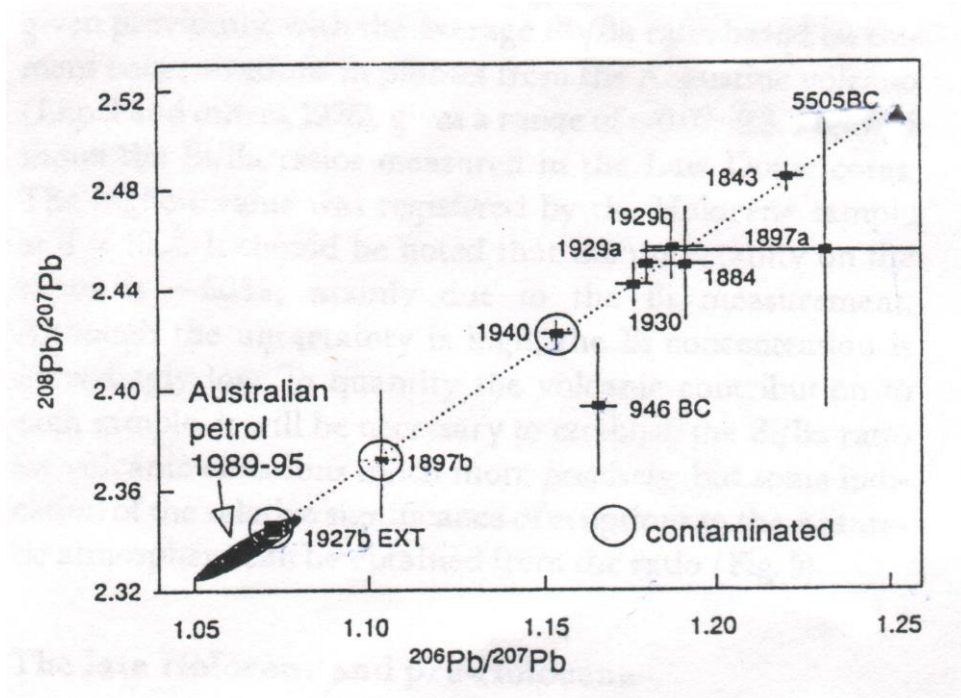


Figure 3.38. A three-isotope plot for ice from Law Dome and Dome C and Australian petrol, from Rosman et al. (1998b).

Rosman et al. (1998b) noted that the Pb concentrations in the Law Dome samples were very low, and that on account of the observed concentrations and Pb isotopic compositions, it was difficult to determine which samples were contamination-free. The low concentrations of Pb and Ba were attributed to the high snow accumulation rate at the sampling sites, while the reported Pb isotopic compositions were sensitive to the analytical blank correction because of the low concentrations of Pb observed. For example, evaluations of Pb isotopic compositions in a decontamination profile revealed that the $^{206}\text{Pb}/^{207}\text{Pb}$ ratio of contamination on the external core layers was ~ 1.06 , consistent with the Pb signature of urban aerosols in the southern cities of Australia. When the Pb isotopic compositions of all of the samples were compared, as in Figure 3.38, it could be seen that most of the samples fell on a mixing line between that of Australian Pb (pollution) and that which Rosman et al. (1994b) had considered representative of natural Pb. Rosman et al. (1998) observed that the Pb isotopic composition in one of the DE08 77A (1897) inner core samples was similar to that of Australian Pb, consistent with the poor plateau observed in the decontamination profile, indicating that the sample was contaminated. For the

sample dated to 1940, DSS 28A, no decontamination plateau was observed. On account of the similarity of Pb isotopic signatures in the other samples, Rosman et al. (1998b) did not consider them to be contaminated. Similar to the findings of Hong et al. (1998), there was too little data to discern any significant trend, however they identified that Pb concentrations from 1884 to 1908 were lower ~0.2 pg/g and those at 1929/1930 were ~1.1 pg/g (see Figure 3.39). Rosman et al. (1998b) also compared the $^{206}\text{Pb}/^{207}\text{Pb}$ ratios observed at Law Dome with those observed in Greenland (K. Rosman unpublished data, see Figure 3.40), which were approximately similar, however once again there was too little data to evaluate any trend.

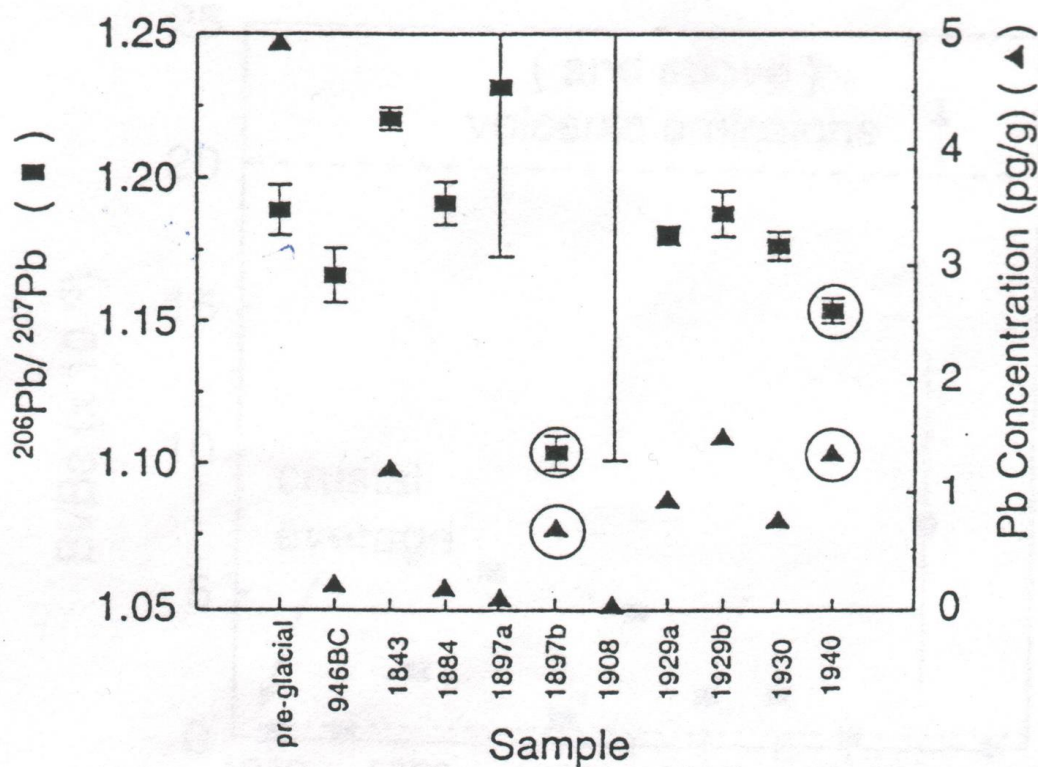


Figure 3.39. Lead isotopic compositions and concentrations in selected samples from Law Dome, from Rosman et al. (1998b).

Rosman et al. (1998b) also analyzed Bi and Ba, providing the first measurements of Bi concentrations in Antarctica. Concentrations of Bi were observed to vary from 0.4 to 17 fg/g, while Ba varied from 0.9 pg/g to 30.4 pg/g. Barium was evaluated as a proxy of crustal dust inputs, with comparison of Ba and Al concentrations showing excellent agreement. Bismuth was determined as an indicator of volcanic inputs, and was referenced to Ba concentrations in order to identify volcanic eruptions in the ice core record. From an average of reported crustal values, Rosman et al. (1998b)

evaluated the crustal Bi/Ba ratio to be $\sim 3.2 \times 10^{-4}$, while those indicating volcanic emissions should be $> 20 \times 10^{-4}$, however in the Law Dome samples they observed Bi/Ba ratios within the range $(0.09-8.18) \times 10^{-4}$. Of the two ancient samples, they both displayed anomalous $^{206}\text{Pb}/^{207}\text{Pb}$ ratios. The sample dated to 946 BC displayed a low Pb concentration ~ 0.21 pg/g, but with an unusual Pb isotopic composition of $^{206}\text{Pb}/^{207}\text{Pb} \sim 1.166$ and $^{208}\text{Pb}/^{207}\text{Pb} \sim 2.393$. Rosman et al. (1998b) considered it possible that the sample had been contaminated, on account of the low $^{206}\text{Pb}/^{207}\text{Pb}$ ratio and the lower Pb concentrations (0.03 and 0.09 pg/g) observed in other samples, however they also considered the possibility of a molecular interference in the ^{207}Pb ion beam during measurement, which may have resulted in the anomalously low $^{206}\text{Pb}/^{207}\text{Pb}$ ratio observed in the sample. The other ancient sample, dating to the last interglacial, also displayed anomalous results with a Pb concentration of 5 pg/g and a Pb isotopic composition of $^{206}\text{Pb}/^{207}\text{Pb} \sim 1.189$ and $^{208}\text{Pb}/^{207}\text{Pb} \sim 2.784$. The highly-radiogenic $^{208}\text{Pb}/^{207}\text{Pb}$ ratio observed in the sample suggested the presence of Thorium-rich source rock, as ^{232}Th is the radioactive decay parent of ^{208}Pb . This interpretation was complemented by the high Pb, Ba and Bi concentrations observed in the samples, and the reporting of visible impurities at the bottom of the ice core, located only 5 m below the sample. While the findings of Rosman et al. (1998b) did not resolve any of the existing questions regarding the inputs of anthropogenic or natural Pb to Antarctica, they were important for accurately identifying the concentrations of Pb, Ba and Bi in Antarctic snow and ice and for illustrating the extensive technical capabilities required to undertake such measurements. Their findings illustrated that Pb concentrations in the Law Dome samples could not be accurately evaluated by GFAAS, and that once again Pb isotopic analyses were an extremely sensitive technique for verifying the pristine nature of snow/ice core and snow block samples.

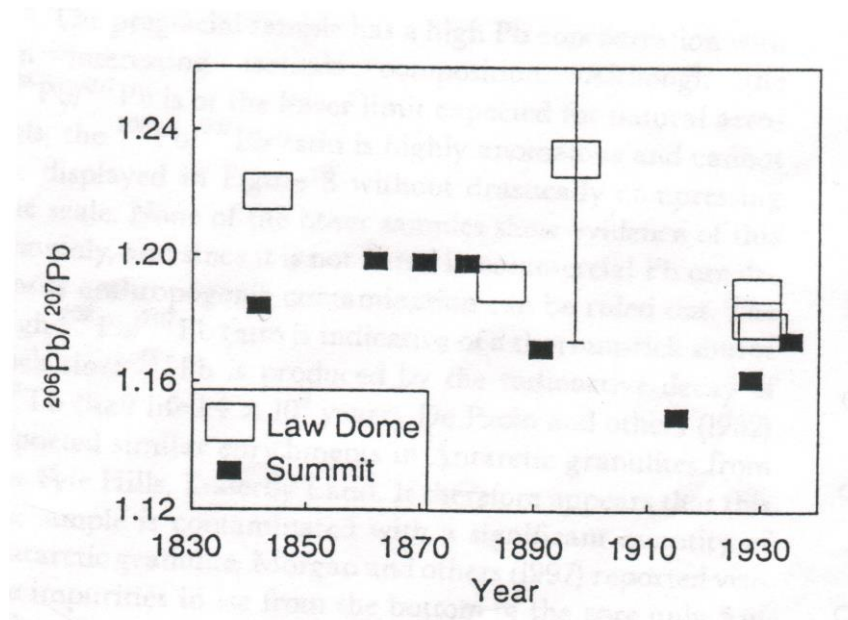


Figure 3.40. Comparison of the isotopic composition of ice at Summit, central Greenland, with Law Dome, Antarctica, from Rosman et al. (1998b).

Rosman et al. (1999) provided one more measurement of Pb isotopic compositions in Antarctic ice, in a paper published in the *Korean Journal of Polar Research*. They analyzed a sample of the Dome C ice core dating to 22.6 ky BP, prepared by Boutron and Patterson (1986) but analyzed only for concentrations of Pb, Al, Na and SO_4 . From analysis of a 2.3 g sample, Rosman et al. (1999) determined a Pb concentration of ~16 pg/g and a Pb isotopic composition of $^{206}\text{Pb}/^{207}\text{Pb}=1.196\pm 0.002$, $^{208}\text{Pb}/^{207}\text{Pb}=2.469\pm 0.004$ and $^{206}\text{Pb}/^{204}\text{Pb}=18.72\pm 0.07$. This Pb concentration was in agreement with Boutron and Patterson (1986), while the Pb isotopic composition yielded an interesting result in comparison to the other Antarctic Pb isotope data available (see Figure 3.41). The Pb isotopic composition was found to be similar to South Atlantic Ocean pelagic sediments, taken by Flegal et al. (1993) as representative of dust and volcanic Pb emissions principally from South America. Rosman et al. (1999) noted that although Pb isotope data was not available for 'Patagonian loess, however, the Andean volcanics in Chile from which the loess is believed to have derived has a similar composition to the pelagic sediments, and presumably the Pb in the latter originated from the former'. The research of Boutron and Patterson (1986) indicated that >95% of Pb in the sample was derived from crustal inputs, consistent with the Pb isotopic composition in the sample being similar to that associated with suspected dust sources in South America.

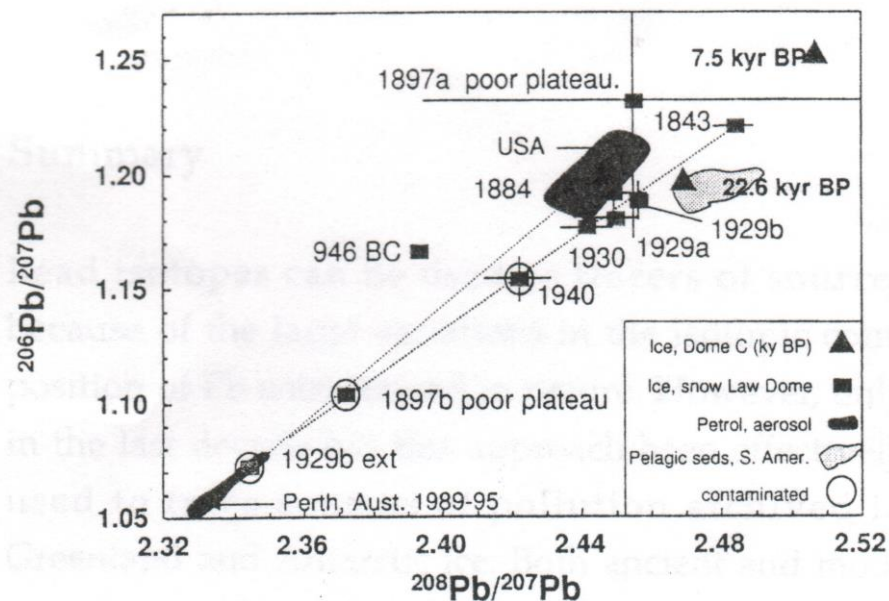


Figure 3.41. The isotopic ratios of Pb in Antarctic ice, from Rosman et al. (1999).

The most recent paper to report Pb isotopic compositions in Antarctic ice was that by Matsumoto and Hinkley (2001), who reported Pb isotopes and Pb, Cd, In and Tl concentrations by TIMS in ancient Taylor Dome ice. Their research was prompted by the manner in which dust inputs in Antarctic snow and ice samples had been evaluated in earlier studies:

Problems of contamination control and reliability of analysis for trace metals in ice cores and snow, important records of atmospheric deposition, have been largely solved. However, there has been inherent imprecisions in the widespread use of single-species proxies for dust and salt in ice (typically Ca or Al; and Na, respectively), and trace metals and dust-salt proxies have not always been measured in the same samples of ice. Despite these uncertainties, there have been claims and assumptions that in pre-industrial times dust was adequate to account for trace metal masses in ice.

Matsumoto and Hinkley (2001) analyzed 9 pieces of ice from Taylor Dome, located to the southwest of the Victoria Land sites sampled by Barbante et al. (1997). The samples, estimated at ages from 1.3 ky BP to 72.9 ky BP (87 m to 488 m depth), were sampled from pieces of ice approximately 13 cm long. Each sample was

considered likely to integrate a few years to a few tens of years of snow accumulation, however the accuracy of the dating for the samples was not described. They decontaminated their samples by trimming away the outermost layer using a bandsaw, and then layers of ice were chiselled from the remaining core following the methods described by Ng and Patterson (1981) and Candelone et al. (1994). The inner core samples were then melted, acidified and spiked and passed through ion exchange columns prior to mass spectrometry. All concentrations were determined by ID-TIMS and in addition to the measurement of Pb, Cd, In and Tl concentrations and Pb isotopic compositions, concentrations of six salt- and dust-forming metals were also determined: K, Rb, Cs, Ca, Sr and Ba. Only one decontamination profile was provided, as shown in Figure 3.42, indicating that inner core concentrations were much lower than those in the outer layers but not being of sufficient detail to illustrate that Pb contamination had not been entrained through to the inner core.

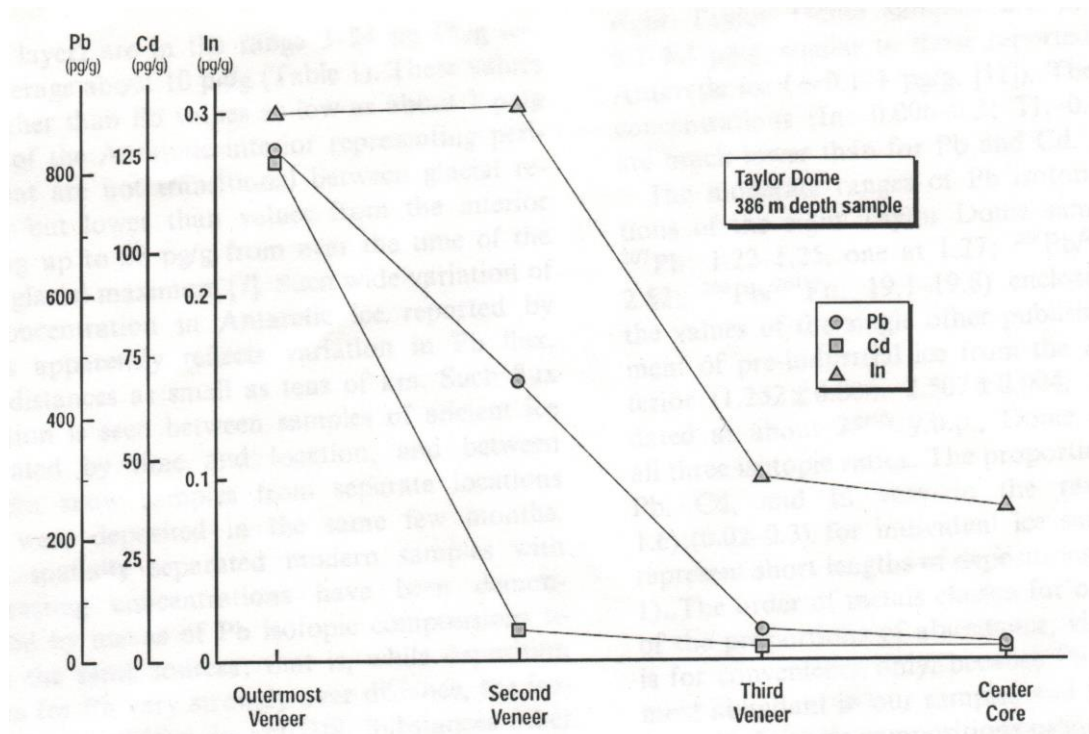


Figure 3.42. Differences in metal concentrations in the successive thick exterior concentric shells trimmed from cylindrical core segments and in the final axial samples, from Matsumoto and Hinkley (2001).

As shown in Table 3.7, Pb concentrations observed by Matsumoto and Hinkley (2001) varied from 3 – 24 pg/g, with averages ~5 pg/g in samples dated from ~2.2 ky

BP to ~10 ky BP and ~11 pg/g in samples dated from ~10.4 ky BP to ~27.2 ky BP. The most recent sample (~1.3 ky BP) and the most ancient sample (~72.9 ky BP) contained the highest concentrations of Pb, with 24 and 37 pg/g, respectively, however it was noted that within the 72.9 ky BP sample were visible quantities of tephra deposited from an explosive volcanic eruption. These Pb concentrations were significantly higher than any others measured for the pre-industrial Holocene period, and were only comparable to those measured by Boutron et al. (1988), 10-38 pg/g, corresponding to the past glacial-interglacial transition periods. As for the Pb concentrations they observed, they noted that 'such wide variation of Pb concentration in Antarctic ice reported by others apparently reflects variation in Pb flux, over distances as small as tens of km'. No explanation for the change in Pb concentrations ~5 pg/g during the late-Holocene to those ~11 pg/g observed during the early Holocene, however the changing proportions of Pb: Cd: In: Tl were attributed to possible changes '...in composition of atmospheric dusts at Taylor Dome, also about 7000–10000 y.b.p., from distinctly potassic (K/Ca: ~0.8) to more calcic (K/Ca: ~0.5), may have coincided with differences in the chemical and physical regime of the atmosphere at that time, leading to different fractionation of trace metals.'. Dust inputs to the samples, shown in Table 3.8, were found to vary from 6 – 32 ng/g in the samples from ~1.3 ky BP to ~13.4 ky BP, with 300 ng/g in the ~27.2 ky BP sample and 20000 ng/g in the ~72.9 ky BP sample. From these data, with the exception of the ~72.9 ky BP sample affected by tephra, Pb contributions from dust were calculated to vary from 0.83% to 38%, but were normally <5%. On this basis, Matsumoto and Hinkley (2001) evaluated that the calculated inputs of dust to Antarctica were insufficient to account for the Pb concentrations observed in snow and ice, and suggested that volcanic Pb inputs would be able to easily account for the difference they observed.

Table 3.7. Trace metal concentrations and Pb isotopic compositions in Taylor Dome ice samples, from Matsumoto and Hinkley (2001).

Sample	Concentrations (pg metals/g ice)				Proportion (Pb: Cd: In)	Pb isotopic compositions		
	Pb	Cd	In	Tl		²⁰⁶ Pb/ ²⁰⁴ Pb	²⁰⁷ Pb/ ²⁰⁴ Pb	²⁰⁸ Pb/ ²⁰⁴ Pb
1 87-m depth (~ 1300 y.b.p.)	24	0.56	0.041	< 0.2	10:0.2:0.02	19.09 (3)	15.50 (3)	38.27 (7)
2 131-m depth (~ 2200 y.b.p.)	3.3	0.18	0.0060	< 0.2	10:0.5:0.02	19.22 (7)	15.50 (5)	38.55 (14)
3 250-m depth (~ 5800 y.b.p.)	8.9	0.35	0.055	no data	10:0.4:0.06	19.13 (7)	15.67 (6)	38.99 (15)
4 280-m depth (~ 7000 y.b.p.)	4.2	0.58	0.023	< 0.2	10:1.4:0.05	19.46 (3)	15.76 (2)	38.93 (6)
5 335-m depth (~ 10000 y.b.p.)	2.6	0.41	0.050	0.24	10:1.6:0.19	19.56 (4)	15.66 (4)	39.26 (9)
6 340-m depth (~ 10400 y.b.p.)	11	0.94	0.30	0.35	10:0.9:0.27	19.82 (4)	15.62 (4)	39.35 (9)
7 368-m depth (~ 13400 y.b.p.)	10	1.3	0.24	0.10	10:1.2:0.23	19.52 (3)	15.64 (3)	39.10 (7)
8 386-m depth (~ 27200 y.b.p.)	11	0.44	0.083	0.37	10:0.4:0.08	19.42 (2)	15.79 (2)	39.23 (4)
9 ^a 488-m depth (~ 72900 y.b.p.)	37	2.8	0.34	2.8	10:0.8:0.09	19.47 (2)	15.57 (2)	39.07 (5)

Hinkley et al. (1999) had provided a re-evaluation of volcanic metal emissions predominantly based on their studies of Kilauea volcano in Hawaii and an earlier study of two volcanoes in the Indonesian Island arc. As described earlier, Hinkley et al. (1999) provided a new, higher, evaluation of the average Pb/S ratio for volcanic emissions but arrived at a lower estimate of the total quantity of Pb emitted from volcanoes worldwide. They noted that previous studies had placed too much emphasis on emissions from explosive eruptions, and failed to adequately consider metal emissions from quiescent degassing activity as a significant, or perhaps dominant, source of volcanic metal emissions. From this re-evaluation of the global Pb emissions from volcanoes, Matsumoto and Hinkley (2001) averaged these emissions over the surface of the earth and calculated the expected concentration of Pb at Taylor Dome due to global volcanism. They calculated a volcanic Pb input of 26 pg Pb/g, higher than the Pb concentrations normally observed in the samples, and considered ‘the difference in metal concentrations between what is measured in the ice, and calculated to be expected in the ice from the volcano emissions, may be due to inefficient atmospheric injection, and/or loss during transport’. They did not elaborate on the presence of the circum-Antarctic polar cell to remove particulates from the air, nor did they consider the physical locations of volcanoes that could or could not contribute to the volcanic Pb deposited in Antarctica. Specifically, the volcanic Pb input to Antarctica by quiescent degassing could only derive from volcanoes located in the Southern Hemisphere, so those volcanoes located in the

Northern Hemisphere could not possibly contribute to the Pb fluxes observed at Taylor Dome. Also, the location of Taylor Dome, in the vicinity of Mount Erebus, the largest and most active Antarctic volcano, was never mentioned as a possible source of the excess-Pb observed over dust inputs. A substantial incongruity in the work of Matsumoto and Hinkley (2001) was that they spent such effort on determining the dust inputs to Taylor Dome, but never actually attempted to measure the volcanic Pb inputs. Further, they did not acknowledge the work of Barbante et al. (1997), which indicated that volcanic inputs to their Victoria Land sampling sites represented a greater proportion (33% - 100%) of natural Pb inputs compared to those reported for other Antarctic sites: ~19% at Coats Land (Wolff and Suttie 1994) and ~50% at Dome C (Boutron and Patterson 1986). Irrespective of the sources of Pb deposited in the Taylor Dome samples, no satisfactory explanation has been found for the large discrepancy in Pb concentrations reported for that site compared to other Antarctic sampling sites such as Coats Land, Victoria Land, Dome C and Law Dome.

Table 3.8. Trace metal concentrations expected in ice, as contributions from rock and soil dusts present in Taylor Dome ice samples, from Matsumoto and Hinkley (2001).

Sample	Dust in ice		Expected (calculated) metals in ice, from amount of dust present			Expected (calculated) as percent of measured			
	Depth (m)	Age (y.b.p.)	(ng/g)	Pb (pg/g)	Cd	In	Pb (%)	Cd	In
1	87	~1 300	14	0.20	0.0015	0.00069	0.83	0.27	1.7
2	131	~2 200	6	0.08	0.0007	0.00029	2.4	0.39	4.8
3	250	~5 800	16	0.22	0.0018	0.00078	2.5	0.51	1.4
4	280	~7 000	14	0.20	0.0015	0.00069	4.8	0.26	3.0
5	335	~10 000	29	0.41	0.0032	0.0014	16	0.78	2.8
6	340	~10 400	32	0.45	0.0035	0.0016	4.1	0.37	0.53
7	368	~13 400	31	0.43	0.0034	0.0015	4.3	0.26	0.63
8	386	~27 200	300	4.2	0.033	0.015	38	7.5	18
9	488 ^a	~72 900	20000	280	2.2	0.98	760	79	290

Lead isotopic compositions observed by Matsumoto and Hinkley (2001) corresponded well to those associated with natural Pb inputs by Flegal et al. (1993) and Rosman et al. (1994b, 1998b). These data also supported the successful decontamination of the cores and the accurate reporting of inner core Pb concentrations. Relatively little use was made of the Pb isotopic data ($^{206}\text{Pb}/^{207}\text{Pb}$: 1.22 - 1.27, $^{208}\text{Pb}/^{207}\text{Pb}$: 2.47 - 2.52) presented by Hinkley et al. (2001), however, which were within the range of natural Pb isotopic compositions determined by Rosman et al. (1994, 1999) for Dome C ice. The Pb isotopic signature in the tephra-

containing sample (numbered “9” in Tables 3.7 and 3.8) was not found to be different from those in the other samples, which were all generally similar to Ross Island basanitoids, the Pb signature associated with emissions from Mount Erebus.

Overall the progress of understanding regarding fluxes of anthropogenic and natural Pb inputs to Antarctica since 1993 has been slow. Wolff and Suttie (1994) and Barbante et al. (1997) evaluated Pb concentrations for the periods 1926-1986 and 1964-1991, respectively, however these trends could only be compared generally to trends in continental Pb emission. The absence of Pb isotopic data limited the further interpretation of these results. Evaluations of snow blocks collected in 1983 essentially evaluated pollution from Antarctic bases, while the only evaluations of Pb isotopes in ancient Antarctic ice were those reported by Rosman et al. (1994b, 1998b) for Dome C ice dated to 7,500 and 22,600 years BP. Evaluations of Pb isotopes in Law Dome ice cores were troubled by contamination, and those data which were not considered to be contaminated were too few to observe any consistent trend, while the arguments of Matsumoto and Hinkley (2001) served to highlight the level of uncertainty regarding natural metal fluxes to Antarctica.

The difficulty of accurately measuring Pb concentrations or isotopic compositions in Antarctic samples, combined with the cost and logistical difficulties of providing for the collection, storage and dating of Antarctic snow and ice samples, ensured that only the most dedicated efforts could produce sufficient reliable data as to be meaningfully interpretable. These challenges have only been surmounted with the development of techniques for analyzing such samples and so producing reliable data. The research presented in this thesis is representative of the effort and time required to adequately explain some of the questions of Pb levels in Antarctica which the preceding research has uncovered and shaped: what are the current levels of Pb pollution in Antarctica, and how have these changed over time? do different regions of Antarctica sample emissions from different parts of the Southern Hemisphere? what are the natural sources of Pb to Antarctica, and what influence does volcanism have on natural Pb fluxes? do the predominant natural sources of Pb to Antarctica vary with location and what is the range of natural Pb isotopic compositions in Antarctica? do fluxes of Pb and Ba to Law Dome vary seasonally, does the Pb isotope signal at Law Dome display seasonal variability?

Chapter 4: Results & Discussion

What are the current levels of Pb pollution in Antarctica, and how have these changed over time?

4.1 Changes in Pb and Ba concentrations and Pb isotopes at Law Dome over the past 500 years

Investigating the variations in Pb and Ba concentrations and Pb isotopic compositions in Law Dome snow and ice has been the principal focus of this thesis. The only previous analyses of Pb, Ba and Bi fluxes to Law Dome are those by Hong et al. (1998) and Rosman et al. (1998), who independently analyzed aliquots of the same core samples. Samples were obtained from the DSS and DE08 cores obtained from high-accumulation sites near the Law Dome summit. These core samples were originally intended for investigations of seasonal variations of Fe, and were not usually decontaminated with the caution necessary to ensure contamination-free samples (Edwards et al. 1998). The isotopic analyses undertaken by Rosman et al. (1998) identified the extent to which contamination had affected most of the samples. Essentially, the uncontaminated samples enabled Pb isotopes and concentrations to be evaluated at 1843, 1884 and 1929/30. This sequence was insufficient in resolution or duration, however, to determine natural Pb levels at Law Dome, or the time at which anthropogenic Pb inputs became significant. In addition, Rosman et al. (1998) overcompensated for the blank associated with the ice-core decontamination procedure (see the comments in sections 2.5 and 2.6). This led to Pb concentrations and isotopic compositions being artificially distorted and gave the impression of additional variability in the results. Although these Pb and Ba data were the first available from Law Dome they were too few to produce a coherent understanding of the fluxes of anthropogenic or natural Pb. However, they indicated that Pb concentrations were lower than those observed further inland at Dome C and Vostok, but did not allow the extent of modern Antarctic Pb pollution to be confidently determined.

Data have been collected from various Law Dome firn/ice cores covering the period from 4500 years BP to 1989 AD, and are included in Appendix 1. The resolution of

sampling is such that data has been collected approximately every fifty years between 1530 AD and 1850 AD, every decade between 1850 AD and 1932 AD and every 5 years from 1932 AD to 1989 AD. The most recent data point discussed is that from 1989 AD, collected from the DSS-W2k snow/firn core. These analyses are limited by the absence of snow pit samples, which can be collected at high resolution (~10 samples per year), and would allow the Law Dome Pb and Ba record to be linked from 1989 to the present. To partially compensate for this, high-resolution sampling of the DSS-W2k snow/firn core was undertaken to collect data for the period 1981–1985. This data was not measured in time to be published with the other Law Dome data presented here. Instead the data are discussed in section 4.10 with emphasis on the interannual variations and recent trends in deposition of Pb and Ba at Law Dome.

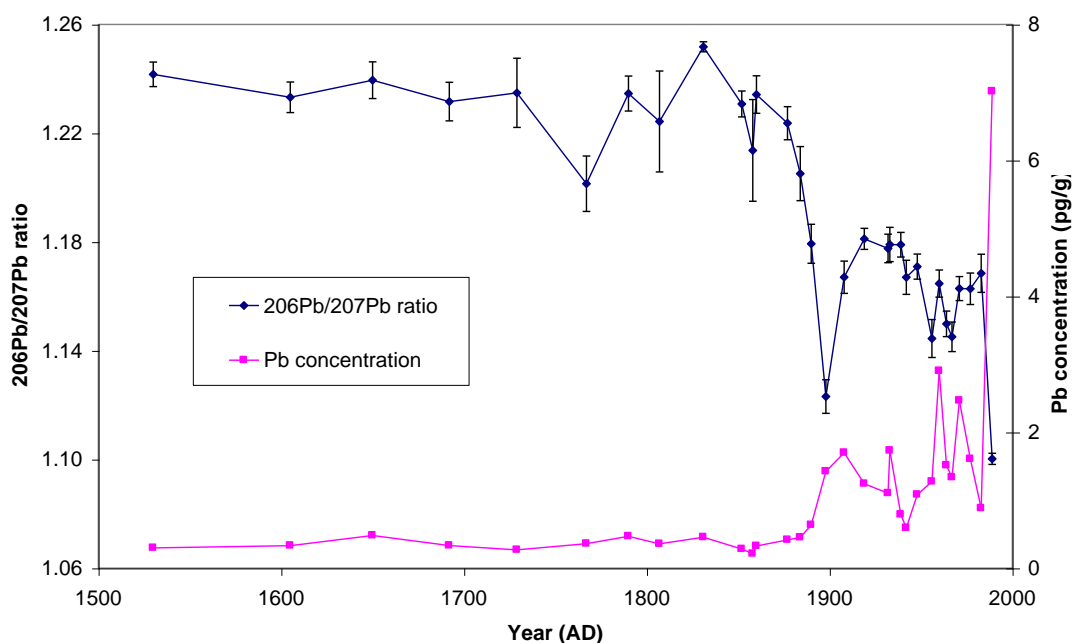


Figure 4.1. Lead concentrations and $^{206}\text{Pb}/^{207}\text{Pb}$ ratios at Law Dome, 1530 AD to 1989 AD.

At Law Dome, Pb concentrations remained at natural, pre-industrial, levels until approximately 1880 AD, after which concentrations increase and $^{206}\text{Pb}/^{207}\text{Pb}$ ratios decrease in a manner consistent with anthropogenic Pb inputs. This is shown in figure 4.1, which shows Pb concentrations and $^{206}\text{Pb}/^{207}\text{Pb}$ ratios at Law Dome from 1530 AD to 1989 AD. Natural Pb concentrations average 0.36 pg/g and vary between 0.21 and 0.48 pg/g from 1530 to 1880. Natural Pb isotopic compositions occur

within the range $^{206}\text{Pb}/^{207}\text{Pb} = 1.225 \pm 0.025$, $^{208}\text{Pb}/^{207}\text{Pb} = 2.48 \pm 0.02$, $^{206}\text{Pb}/^{204}\text{Pb} = 19.2 \pm 0.7$, which is distinct from Pb isotopic compositions observed after 1880 AD. After 1880 AD, Pb concentrations average 1.7 pg/g and display isotopic compositions within the range $^{206}\text{Pb}/^{207}\text{Pb} = 1.14 \pm 0.04$, $^{208}\text{Pb}/^{207}\text{Pb} = 2.41 \pm 0.04$, $^{206}\text{Pb}/^{204}\text{Pb} = 17.9 \pm 0.6$. These data are consistent with those reliable results reported by Hong et al. (1998) and Rosman et al. (1998) for 1843 AD, 1884 AD and ~1930 AD.

Law Dome Ba concentrations do not show any consistent increase following the commencement of anthropogenic Pb inputs, however anomalously high Ba concentrations are observed from 1956 to 1964 and in samples corresponding to the years 1932 and 1989. Barium concentrations and Pb/Ba ratios for Law Dome from 1530 AD to 1989 AD are shown in Figure 4.2. These increases in Ba concentration at Law Dome are consistent with increased dust deposition observed in Victoria Land snow during the 1930's and from 1950 to 1960 (Maggi and Petit 1998). The dust increases were correlated with rainfall anomalies in South America, suggesting these Antarctic dust fluctuations are most likely due to natural variations in aridity and dust production in South America – a source of Antarctic dust particles identified by the Sr-Rb and Nd-Sm geochemical studies of Basile et al. (1997).

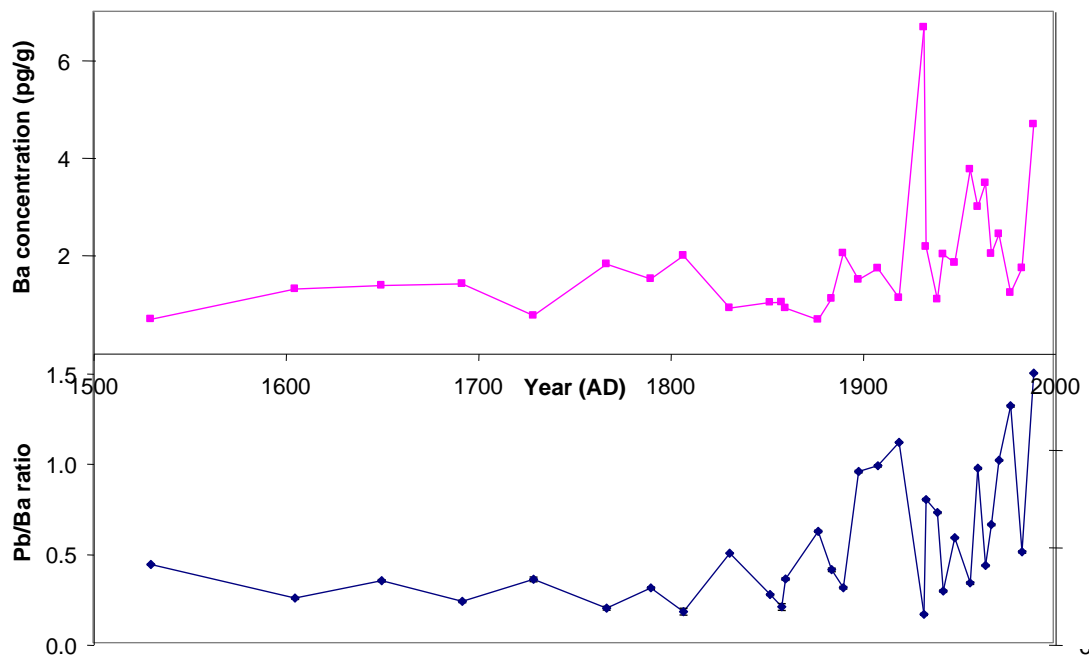


Figure 4.2. Barium concentrations and Pb/Ba ratios at Law Dome, 1530 AD to 1989 AD.

The results presented here indicate that anthropogenic Pb inputs have significantly affected Law Dome Pb levels since ~1880 AD. Average Pb concentrations increase by 4.8 times from natural levels to those observed in 1880 AD, with a corresponding decrease in the average $^{206}\text{Pb}/^{207}\text{Pb}$ ratio from ~ 1.225 to ~1.14. Lead concentrations increase to ~1.5 pg/g between 1898 and 1908 AD, then consistently decrease until the lowest modern Pb concentration of ~0.6 pg/g is observed at 1942 AD. Since then, Pb concentrations have generally increased consistently, with Pb concentrations ~1.5 pg/g from the mid-1950's to the mid-1970's. Some higher Pb concentrations are observed at 1960 (2.9 pg/g), 1971 (2.5 pg/g) and 1989 (7.0 pg/g). The 1983 data point displays a relatively low Pb concentration (~0.9 pg/g), which may be some confirmation of the findings of Wolff and Suttie (1994) and Barbante et al. (1997) whose high-resolution studies of recent Antarctic snows (at Coats Land and Victoria Land, respectively) indicated that Antarctic Pb concentrations have been generally decreasing since the 1980's. As will be shown in section 4.2, decreasing $^{206}\text{Pb}/^{207}\text{Pb}$ ratios and increasing Pb concentrations observed at Law Dome from ~1880 to ~1898 are consistent with mining and smelting of Ag/Pb ores at Broken Hill and Port Pirie, in Australia. From 1908 to 1939, Pb concentrations do not decrease significantly despite the $^{206}\text{Pb}/^{207}\text{Pb}$ ratio in Law Dome ice increasing to ~1.18, consistent with Pb isotope ratios observed in coal and South Atlantic Ocean pelagic sediments. However, during the period 1908 – 1939, production of non-ferrous metal and coal in the southern hemisphere increased rapidly (Wolff and Suttie 1994). A similar increase should be expected of coal-burning, however these statistics are not available for the southern hemisphere.

From 1942, $^{206}\text{Pb}/^{207}\text{Pb}$ ratios decrease to ~1.145 during the 1950's and 1960's while Pb concentrations increase steadily over this period. This trend is consistent with the introduction of leaded gasoline and domestic automobile use in the southern hemisphere following World War II (Wolff and Suttie 1994). Intermittent reports of Pb isotope data for southern hemisphere aerosols are available, for example from Chow et al. (1972), but often personal communication with K. Rosman has been cited in a number of papers since the mid-1980's, with the first extensive survey published in 2000 (Bollhöfer and Rosman 2000). These data suggest decreasing $^{206}\text{Pb}/^{207}\text{Pb}$ ratios in Law Dome ice during the 1950's and 1960's are consistent with the consumption of significant quantities of Australian and Canadian Pb

($^{206}\text{Pb}/^{207}\text{Pb}\sim 1.06$, $^{208}\text{Pb}/^{207}\text{Pb}\sim 2.33$) in alkyllead gasoline additives. From 1971 to 1983, $^{206}\text{Pb}/^{207}\text{Pb}$ ratios are higher, ~ 1.165 , indicating greater consumption of US Mississippi Valley-type Pb ($^{206}\text{Pb}/^{207}\text{Pb}\sim 1.23$, $^{208}\text{Pb}/^{207}\text{Pb}\sim 2.46$) in alkyllead additives. This is consistent with passenger car statistics for the southern hemisphere, which show the number of passenger cars in South America has increased rapidly since the 1970's (Wolff and Suttie 1994). Available aerosol data also indicate that aerosols in all but the southern-most South American cities feature a $^{206}\text{Pb}/^{207}\text{Pb}$ ratio > 1.10 and are comprised of a significant proportion of Mississippi Valley-type Pb (Bollhöfer and Rosman 2000).

Wolff and Suttie (1994) and Barbante et al. (1997) primarily attribute decreasing Pb concentrations in Antarctic snow to Brazil's total removal of gasoline alkyllead additives since the mid-1980's. As there is only one published Law Dome data point pertaining to this period, at 1989 AD, a trend cannot be determined. The 1989 data point is notable, however, because it displays a low $^{206}\text{Pb}/^{207}\text{Pb}$ ratio ~ 1.10 and high Pb concentration ~ 7 pg/g. This is consistent with a significant influx of Australian Pb, possibly due to anomalous meteorological conditions observed at Law Dome in 1989 (Pook 1994), or due to local contamination of the site (located 2 km to the West of the DSS main ice core drilling station).

In summary, anthropogenic Pb inputs have increased Law Dome Pb concentrations five-fold from natural Holocene concentrations of ~ 0.36 pg/g to average 20th century concentrations of ~ 1.7 pg/g. Anthropogenic Pb inputs to Law Dome commence ~ 1880 AD, consistent with the exploitation of Australian Ag/Pb/Zn deposits, particularly those at Broken Hill. During the 20th century, Pb concentrations are consistently high, except for the period from 1932 to 1942, which Wolff and Suttie (1994) associated with the economic turmoil of the great depression and World War II. High Pb concentrations and $^{206}\text{Pb}/^{207}\text{Pb}$ ratios ~ 1.18 observed from 1908 to 1932 are associated primarily with coal-burning, while lower $^{206}\text{Pb}/^{207}\text{Pb}$ ratios ~ 1.14 - 1.16 observed from 1956 to 1983 are associated with the burning of alkyllead gasoline additives throughout the southern hemisphere. After 1983, there is insufficient data available to comment on any recent trend in Law Dome Pb deposition.

4.2 RESEARCH ARTICLE: The lead pollution history of Law Dome, Antarctica, from isotopic measurements on ice cores: 1500 AD to 1989 AD

Submitted to *Earth and Planetary Science Letters* 4th January 2002

Accepted for publication 27th August 2002.

Published in 2002, vol. 204, pp. 291-306

4.3 Comparison of Law Dome and Coats Land pollution records

The record of Pb and Ba deposition at Coats Land reported in Planchon et al. (2002b) was principally produced from a series of snow blocks collected from the surface to a depth of 8.3 m (covering the period 1986 – 1920) and a hand-drilled snow core obtained from the bottom of the snow pit to a depth of 16.3 m (1914 – 1834) obtained in 1986. Additional samples were collected from a 2 m snow pit in 1991, incorporating snow deposition from 1989.4 to 1990.6. From 1835 to 1923, samples were usually collected every 2 – 3 years (except for >10 year gaps between 1856-1872 and 1872-1888 and ~7 year gaps between 1890-1897 and 1898-1905). For the periods 1942-1986 and 1989-1991, two to four samples per year of snow deposition were collected (except for gaps in the record between 1944-1950, 1979-1983 and 1986-1989). Members of the British Antarctic Survey collected the samples in 1986 and have published Pb, Cd, Cu and Zn concentrations for the period 1920 – 1986 (Wolff and Suttie 1994 and Wolff et al. 1999). Recently, Planchon et al. (2002b) have completed the Coats Land Pb record commenced by Wolff and Suttie (1994) and have also measured Pb isotopes and Ba concentrations in the samples. Figures 4.3, 4.4 and 4.5 respectively compare Pb concentrations, Ba concentrations and Pb/Ba ratios measured at Law Dome with those measured at Coats Land.

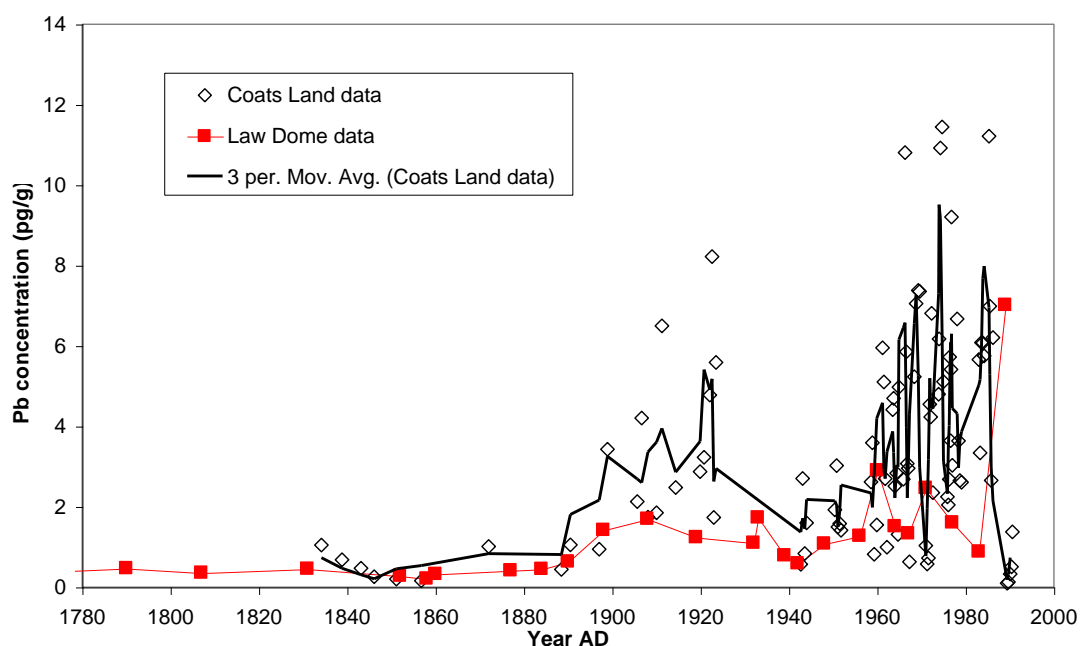


Figure 4.3. Comparison of Pb concentrations at Law Dome and Coats Land.

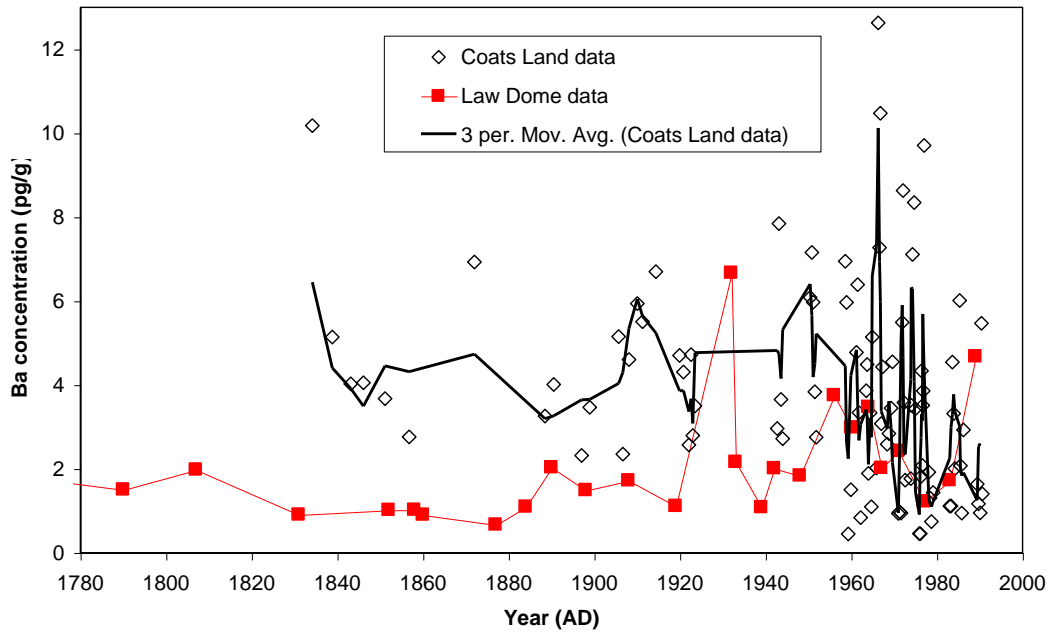


Figure 4.4. Comparison of Ba concentrations at Law Dome and Coats Land.

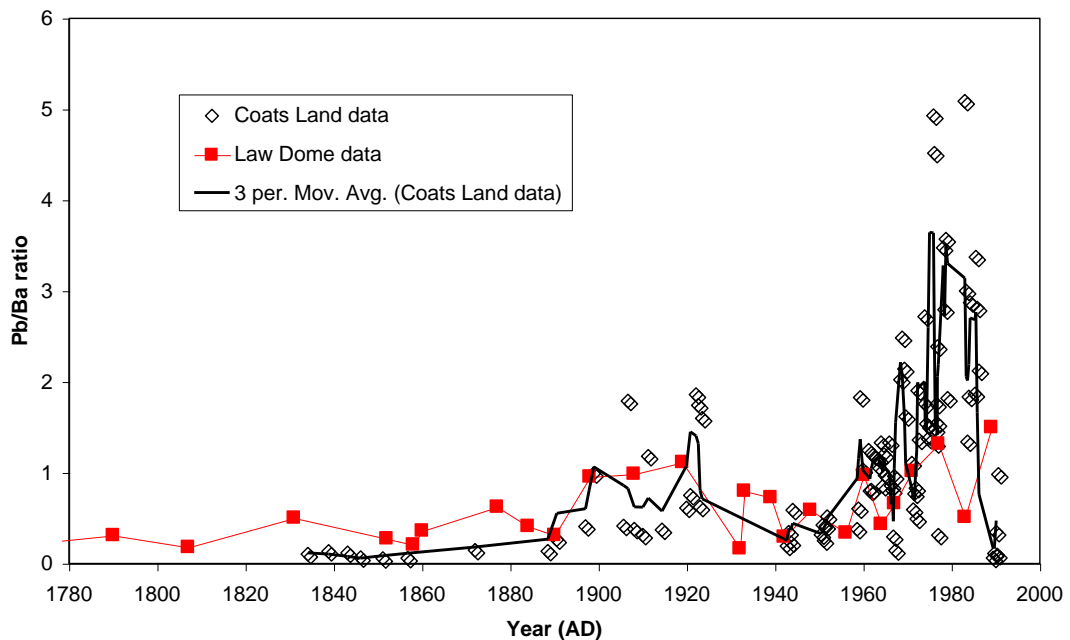


Figure 4.5. Comparison of Pb/Ba ratios at Law Dome and Coats Land.

From Figure 4.3, it can be seen that Pb concentrations at Coats Land are generally <1 pg/g prior to 1898, after which they fluctuate greatly but generally increase to ~ 5 pg/g during the 1920's. Samples dated from 1923 to 1942 were not analyzed for Pb isotopes, however Wolff and Suttie (1994) show Pb concentrations peak at ~ 4 pg/g by 1930, after which they decrease gradually to ~ 2 pg/g by the late 1940's. From

1960 on, Pb concentrations are high ~4-6 pg/g, with the only consistently low Pb concentrations (~0.5 pg/g) observed in samples dated to 1989/1990. No plateau in $^{206}\text{Pb}/^{207}\text{Pb}$ ratios is observed for the earliest Coats Land samples, with the highest $^{206}\text{Pb}/^{207}\text{Pb}$ ratio of 1.208 found in the earliest sample. From 1830 to 1851, $^{206}\text{Pb}/^{207}\text{Pb}$ ratios generally decrease from ~1.19 to ~1.17, remain constant at ~1.17 until 1888 and then decrease to a minimum of 1.096 by 1897. $^{206}\text{Pb}/^{207}\text{Pb}$ ratios then fluctuate, increasing to 1.166 by 1908, decreasing to 1.15 by 1914 and increasing again to 1.18 by 1923. From 1960 to 1990, the samples remain within the range $^{206}\text{Pb}/^{207}\text{Pb} = 1.14 \pm 0.02$, possibly increasing from ~1.14 during the 1960's to ~1.16 during the 1970's. For the period 1980 – 1990, there is insufficient data to discern any overall trend in $^{206}\text{Pb}/^{207}\text{Pb}$ ratios. In the Coats Land samples, Ba concentrations vary within the range 0.45 – 12.6 pg/g, with greater variability in concentrations observed after 1960. Between 1830 and 1944, Ba concentrations are generally stable and average 4.4 pg/g (range 2.3-10.2 pg/g). From 1950 to 1990, the average Ba concentration is lower at 3.6 pg/g, with a wider range from 0.45 pg/g to 12.6 pg/g. Highest Ba concentrations are observed in individual samples dated to 1966, 1972 and 1974, however no consistent variations in Ba concentration are observed.

Similarities and differences between the Law Dome and Coats Land records.

A comparison of the Law Dome and Coats Land records shows that while the overall trends observed for Pb and Ba in the two records are similar, various features occur in each of the records that are not observed in the other. The overall similarities in the two records are:

- Low Pb concentrations are observed prior to 1890.
- Lead concentrations observed in the late 20th century are only moderately greater than those observed in the early 20th century.
- With the exception of values prior to 1890, overall trends in $^{206}\text{Pb}/^{207}\text{Pb}$ ratios are similar. Firstly, the c.1900 (Broken Hill) pollution event features prominently as a significant decrease in $^{206}\text{Pb}/^{207}\text{Pb}$ ratio. Secondly, $^{206}\text{Pb}/^{207}\text{Pb}$ ratios in the first half of the 20th century are ~1.18, then lower (~1.11 - 1.15) during the 1950's and 1960's and marginally higher again (~1.13 - 1.17) during the 1970's and 1980's.

The overall differences between the two records are:

- The Law Dome record shows no indication of Pb pollution until ~1880, while the Coats Land record is clearly affected by anthropogenic Pb prior to 1830.
- Higher $^{206}\text{Pb}/^{207}\text{Pb}$ ratios are consistently observed in the Law Dome record.
- Perhaps due to the difference in sampling resolution, the Law Dome record appears to have less sensitivity to fluctuating Pb emissions during the 20th century.
- Lead concentrations observed in the two records are similar prior to 1890, however after 1890, Pb concentrations at Coats Land are consistently higher than at Law Dome.
- Prior to 1890, Pb/Ba ratios at Law Dome are consistently higher than at Coats Land. However, after 1890, Pb/Ba ratios in the Coats Land record are usually equal to, or higher than, those in the Law Dome record.
- Prior to 1950, Ba concentrations at Law Dome are consistently lower than at Coats Land, however from 1950 – 1983, average Ba concentrations at the two sites are approximately equal.
- The Law Dome record appears to be more sensitive to natural variations in dust levels – for example, the excess dust deposition observed by Maggi and Petit (1998) at Victoria Land in 1930 and 1950-1960 are observed at Law Dome, but not at Coats Land.

Can snow accumulation account for differences in Pb or Ba concentration?

These differences can be explained in a number of ways. Firstly, the two sites feature different snow accumulation rates (56 kg/m²/yr at Coats Land and 150 – 600 kg/m²/yr at Law Dome). This means that if Pb or Ba are deposited independently of snowfall, the concentration will be affected by the quantity of snow deposited. In such a case, the concentration of Pb or Ba would be lower at Law Dome, which features a higher snow accumulation rate. Such a phenomenon should not alter Pb or Ba concentrations if these elements are only deposited during snowfall, nor should it significantly affect Pb/Ba ratios in any case. It should be noted that the Law Dome record is composed of samples from various ice cores that have different

accumulation rates. No significant differences are observed in Pb or Ba concentrations between the samples, so we assume that snow accumulation rate does not significantly alter Pb or Ba concentrations in these samples.

This discussion of snow accumulation rates assumes that the two sampling sites receive equal quantities of Pb and Ba. While this assumption appears to hold for natural Pb fluxes, it is completely untenable when anthropogenic Pb fluxes are considered. Unfortunately, the Pb isotopic signature of natural Pb fluxes to Coats Land cannot be identified, as anthropogenic pollution is identified in the earliest samples collected. At the same time, ~1830, snow deposited in Law Dome did not contain any significant quantity of anthropogenic Pb and such a signal is not observed until 50 years later. From 1830 – 1880, similar Pb concentrations are observed at Coats Land and Law Dome, suggesting that both sites should have been similarly affected if they received similar amounts of anthropogenic Pb. This disparity in the appearance of anthropogenic Pb inputs indicates that fluxes of anthropogenic Pb to Law Dome and Coats Land are not equal, with a significantly greater proportion of anthropogenic Pb deposited at Coats Land. The simplest explanation for this difference in anthropogenic Pb deposition is that the emission source was closer to Coats Land than Law Dome. From an evaluation of the available statistics of coal and non-ferrous metal production in the southern hemisphere, it can be seen that South America was the only continent with significant levels of industrial activity prior to 1880 (Vallelonga et al. 2002b). During the 19th century, Chile was the only copper-producing country in South America, with ~ 10,000 tonnes of refined Cu produced annually prior to 1850. Assuming a maximum Pb emission factor of 8000 g/tonne of refined Cu produced, this would have resulted in maximum Pb emissions of 80 tonnes per year. Considering the proximity of Coats Land to South America, it is reasonable that such levels of Pb emissions would be observed at the Coats Land site, while they are not observed at Law Dome, approximately situated on the opposite side of the continent. The Pb isotopic composition of Coats Land samples during the period 1830 – 1872 are generally within the range $^{206}\text{Pb}/^{207}\text{Pb} = 1.18 \pm 0.02$ and $^{208}\text{Pb}/^{207}\text{Pb} = 2.45 \pm 0.02$. Such a composition is similar to South Atlantic Ocean pelagic sediments (Chow and Patterson 1962), rocks from Chile (Hildreth and Moorbath 1988) and the South Sandwich Islands (Barreiro 1983) and Pb ores from Argentina (Sangster et al. 2000).

These Pb isotope signatures are less radiogenic than those observed at Law Dome during periods of natural Pb deposition, and may support enhanced emissions of Pb from sources in South America.

Anthropogenic Pb inputs to Coats Land and Law Dome.

From the presence of anthropogenic Pb in the Coats Land record as early as 1830, it can be seen that the Coats Land site is more sensitive to Pb emissions from South America than is the Law Dome site. In comparison, the anthropogenic Pb pollution event that occurs c.1900 appears to affect both sites equally. At both sites, the anthropogenic Pb signal is observed at the same time (1890 at Law Dome, 1888 at Coats Land), the $^{206}\text{Pb}/^{207}\text{Pb}$ ratios decrease to similarly low values (~1.12 at Law Dome, ~1.09 at Coats Land) and then both quickly return to higher values (1.167 by 1908 at Law Dome, ~1.14 by 1906 at Coats Land). Based on Pb isotope systematics and statistical constraints, the origin of this influx of pollution has been attributed to the mining and smelting of Ag/Pb at Broken Hill and Port Pirie in Australia. Planchon et al. (2002b) also considered it likely that anthropogenic Pb emissions from Australia were the source of the pollution. Median Pb emissions from Australia are calculated to increase from ~300 tonnes Pb/y at 1890 to ~680 tonnes Pb/y by 1900 (Vallelonga et al. 2002b). At Law Dome and Coats Land, Pb concentrations both increase three-fold, from 0.36 to 1.0 pg/g and from 0.55 to 1.47 pg/g, respectively. However, Ba concentrations remain approximately similar at Law Dome (1.2 pg/g background and 1.8 pg/g from 1890-1898) while at Coats Land, Ba decreases from a background average of 5.3 pg Ba/g to 3.3 pg Ba/g. Consequently, Pb/Ba ratios at Coats Land increase approximately fourfold during the c.1900 event (from 0.1 to 0.45) while Pb/Ba ratios at Law Dome approximately double (from 0.34 to 0.63). While the quantity of Pb emitted from Australia during the period 1890-1910 was much greater than that emitted from Chile during the 1800's, it is clear that this event contributed approximately similar quantities of Pb to the Coats Land and Law Dome sites. While Law Dome is geographically closer to Australia than Coats Land, it is still much more distant from Australia than Coats Land is to Chile. As such, it seems likely that emissions from continents that are relatively far from Antarctica (such as Australia) affect Coats Land and Law Dome equally with their

emissions. Lead emissions from South America, which is closer to Antarctica, appear to have a more significant effect on the Coats Land record than that of Law Dome.

During the 20th century, Pb inputs from anthropogenic sources dominate over those occurring from natural Pb emissions. Within this time, anthropogenic Pb emissions were predominantly due to non-ferrous metal production and coal burning prior to ~1950 while from 1950 to the present, Pb emissions have been mostly due to consumption of alkyllead additives in gasoline (Wolff and Suttie 1994). For this reason, fluxes of anthropogenic Pb to Antarctica are treated separately over the periods 1910 – 1950 and 1950 – 1990. The Pb isotope signature of non-ferrous metal production can be evaluated from published Pb isotope compositions of various Pb/Ag/Zn/Cu ore bodies and what statistics of metals production or international trade in metals are generally available. The process of evaluating a representative Pb isotopic composition for Pb emitted from automobiles requires a more generalized approach, as international trade is prevalent in the alkyllead manufacturing industry, and statistics of production and consumption may not be available. Evaluating Pb emissions from automobiles requires some estimates to be made, such as estimates of petrol Pb content, quantity of gasoline consumed, percentage of alkyllead released into the atmosphere and so on, are required. Due to these various caveats, the study of alkyllead gasoline additive emissions using Pb isotopes is most reliable when applied to a particular region where approximations can be kept to a minimum. Only recently have widespread programs of Pb isotope monitoring in urban aerosols been carried out (Bollhofer and Rosman 2000) to characterize Pb isotopic signatures of aerosols predominantly in large cities. Such global studies are essential for evaluating the international or inter-regional transport of pollution from Pb isotope data. Considering that this is a study of hemispheric alkyllead emissions, the interpretation of Pb isotope data pertaining to emissions from individual countries is, at times, limited.

During the 20th century, sources of anthropogenic Pb emissions are more diverse and cannot be easily attributed to single dominant locations or areas. Reflecting this, the overall trends within the Coats Land and Law Dome records are generally similar. The Coats Land and Law Dome records both indicate that Pb concentrations during the 1920's and 1930's (~1.2 pg/g at Law Dome, ~4.4 pg/g at Coats Land) were not

significantly less than those observed during the 1970's and 1980's (1.7 pg/g at Law Dome, ~4.9 pg/g at Coats Land). They also both show higher $^{206}\text{Pb}/^{207}\text{Pb}$ ratios during the period 1910 – 1930 (1.18 at Law Dome, ~1.16 at Coats Land) than during the period 1958 – 1980 (~1.16 at Law Dome, 1.14 at Coats Land). During the second half of the 20th century (1950-1986), the two sites also feature approximately constant $^{206}\text{Pb}/^{207}\text{Pb}$ ratios, with average values from 1.15 to 1.16 at Law Dome and average values ~1.14 at Coats Land.

Anthropogenic Pb inputs in the first half of the 20th century.

From 1910 to 1950, the Coats Land and Law Dome pollution records are generally similar, indicating that Pb levels increase until ~1930, and then decrease to low levels during the 1940's. This trend is less apparent in the Coats Land data presented here, due to the absence of data between 1923 and 1942 and between 1944 and 1950, however it is confirmed by Wolff and Suttie (1994). Higher Pb concentrations are observed in the Coats Land record over this period (1910-1930 average ~ 4.1 pg Pb/g) as compared to Law Dome (1910-1930 average ~ 1.4 pg Pb/g), however Pb/Ba ratios are approximately similar (0.76 at Law Dome, 1.0 at Coats Land). Higher Pb concentrations at Coats Land, compared to Law Dome, may be due to the South America origin of Pb emissions during the period 1910 – 1930. Statistics of non-ferrous metal production indicate that Pb emissions from South America increased significantly after 1920, primarily due to increased Cu production in Chile (Mitchell 1998b). Copper smelter production in Africa (Zaire and Zambia) is also observed to increase from 1920 (Wolff and Suttie 1994). $^{206}\text{Pb}/^{207}\text{Pb}$ ratios in Law Dome and Coats Land are generally stable over the period 1910 – 1930, at ~1.18 and ~1.16, respectively. In the 1940's, however, Coats Land Pb concentrations and Pb/Ba ratios decrease to 1.5 pg/g and 0.3, lower than Pb concentrations and Pb/Ba ratios observed at Law Dome (~1 pg Pb/g, Pb/Ba ~ 0.6). This trend reflects decreases in the quantity of non-ferrous metal production in the southern hemisphere during the 1940's. Australian Pb production decreases, while production of Cu in Chile, Peru, Zaire and Zambia remains constant, as does Peruvian Pb production (Wolff and Suttie 1994). Despite these decreases in Pb emissions, and Antarctic Pb concentrations, $^{206}\text{Pb}/^{207}\text{Pb}$ ratios at Law Dome remain constant at ~1.17. Due to the absence of data from Coats Land between 1923 and 1944, it is difficult to comment on any trend in Pb isotopic

compositions. The absence of data also limits the interpretation of an anomalously high Ba concentration observed in the Law Dome record at 1932. This Ba increase does coincide with an increase in dust deposition at Victoria Land, which was linked with rainfall anomalies in South America (Maggi and Petit 1998). Although the dust anomaly is observed in the Victoria Land core from 1932 to 1944, it is not observed in other Law Dome samples (dated to 1933, 1939 and 1942).

Anthropogenic Pb inputs in the second half of the 20th century.

From 1950 to 1990, the Coats Land record displays significantly more variability in Pb concentration and $^{206}\text{Pb}/^{207}\text{Pb}$ ratio than does the Law Dome record, however this is partially due to the different sampling resolutions adopted for each site. The Coats Land record was obtained from snow pit samples obtained at high resolution, while the Law Dome record has been obtained from firn core sections sampled to minimize interannual variability in the data. Despite the different sampling regimes adopted, the Coats Land record features distinctly lower $^{206}\text{Pb}/^{207}\text{Pb}$ ratios and significantly higher Pb concentrations than the Law Dome record. Additionally, after 1950, Ba concentrations in the Coats Land and Law Dome records are observed to consistently decrease. At Coats Land, Ba decreases from ~ 4.5 pg/g in the 1950's to ~ 3 pg/g by the 1980's, while at Law Dome Ba concentrations decrease from ~ 3.4 pg/g to ~ 1.5 pg/g over the same period. Increasing Pb concentrations and decreasing Ba concentrations from the 1950's to the 1980's result in Pb/Ba ratios consistently increasing at both locations, and exceeding 1930's levels after 1970. Consistently increasing Pb concentrations observed at Coats Land and Law Dome are in agreement with other analyses of recent Antarctic snow (Wolff and Suttie 1994 and Barbante et al. 1997) and statistics of gasoline consumption and non-ferrous metal production.

There is no reason to associate decreasing Ba concentrations observed at Coats Land and Law Dome since 1960 with anthropogenic activities. Barium is primarily emitted into the atmosphere in rock and soil dust and has no anthropogenic emission source of comparable size. While Maggi and Petit (1998) did observe elevated dust levels in a Victoria Land snow core from 1932 to 1944 and from 1951 to 1965, they did not observe decreasing dust levels after 1965. The decreasing concentration of Ba in Law

Dome and Coats Land snow since 1960 may possibly be attributed to increasing snow accumulation. Along a 700 km segment of East Antarctica, snow accumulation rates have been observed to increase significantly over the past 30 years (Morgan et al. 1991). If this effect has occurred consistently across Antarctica, it may have resulted in the observed dilution of Ba, derived from rock and soil dust, in annually deposited snow at two independent locations such as Coats Land and Law Dome.

$^{206}\text{Pb}/^{207}\text{Pb}$ ratios in Law Dome and Coats Land ice generally increase from 1960 to the 1980's. At Law Dome, $^{206}\text{Pb}/^{207}\text{Pb}$ ratios increase from ~1.14 in the 1960's to 1.168 in 1983, while at Coats Land average $^{206}\text{Pb}/^{207}\text{Pb}$ ratios increase from ~1.13 in the early 1960's to ~1.15 to the early 1980's. This trend is not readily apparent in the Coats Land record, however, due to its high-resolution sampling leading to the incorporation of interannual variations in $^{206}\text{Pb}/^{207}\text{Pb}$ ratios. Increasing $^{206}\text{Pb}/^{207}\text{Pb}$ ratios observed in Antarctica from the 1960's to the 1980's correlates with increasing numbers of passenger cars (associated with consumption of alkyllead petrol) in South America since the 1950's (Wolff and Suttie 1994). There is some supporting evidence for this in $^{206}\text{Pb}/^{207}\text{Pb}$ ratios observed in urban aerosols collected in Southern hemisphere cities during the 1990's. $^{206}\text{Pb}/^{207}\text{Pb}$ ratios 1.06-1.10 have been observed in urban aerosols along the south coast of Australia, New Zealand, Southern Africa and the southern part of South America (predominantly Chile), while higher $^{206}\text{Pb}/^{207}\text{Pb}$ ratios 1.10-1.18 have been observed in more northern locations in South America (Argentina, northern Chile, Brazil) as well as central Africa and the north coast of Australia (Bollhofer and Rosman 2000). Increased $^{206}\text{Pb}/^{207}\text{Pb}$ ratios observed in Antarctica do provide some validation of increasing alkyllead emissions from South America, particularly Brazil, from the 1960's to the 1980's.

Recent Pb inputs to Law Dome and Coats Land: the 1980's and 1990's.

Lead concentrations in the Coats Land samples dated to 1989/1990 are lower than those dated to 1983-1986. This is in agreement with results presented by Wolff and Suttie (1994) and Barbante et al. (1997), however too few data are presented here to demonstrate a reliable trend. The samples representing the period 1983 – 1986 average ~6 pg Pb/g, while those corresponding to the period 1989-1990.6 feature an

average of ~ 0.5 pg Pb/g. This discrepancy may be due to local variations in deposition, as the samples dated to 1989-1990 were obtained from a site 150 km away from the main sampling location, however Planchon et al. (2002b) attributed these changes to variations in the use of leaded gasoline in the Southern Hemisphere. Additional uncertainty regarding the 1989/1990 samples arises when it is considered that the Pb concentrations observed in these samples are approximately equal to those observed in the earliest Coats Land samples, when anthropogenic Pb emission levels were much lower. The $^{206}\text{Pb}/^{207}\text{Pb}$ ratio in the 1989/1990 samples are also unusual, considering the low Pb concentrations observed. It would be expected that samples featuring such low Pb concentrations would feature a $^{206}\text{Pb}/^{207}\text{Pb}$ ratio >1.21 , approximate to those natural Pb values observed in the sample dated to 1834. Instead, these samples contain $^{206}\text{Pb}/^{207}\text{Pb}$ ratios averaging ~ 1.14 , generally similar to other values observed at Coats Land during the late-20th century. The data presented here do not indicate convincingly that Pb concentrations at Coats Land have decreased since the 1980's, or that anthropogenic Pb contributions to Coats Land have decreased in recent times. Unfortunately there is insufficient data available from the Law Dome record to support this finding. The only relevant data available are a sample dated to 1983 (~ 0.9 pg Pb/g) and one dated to 1989 (7 pg Pb/g). The sample dated to 1989 displays significantly elevated Pb and Ba concentrations and a low $^{206}\text{Pb}/^{207}\text{Pb}$ ratio ~ 1.10 . This sample has been clearly affected by Pb with a signature similar to that of Australian aerosols. This was attributed to either meteorological effects or contamination of surface snow at the time, as described in section 4.2. In summary, the data presented in the Law Dome and Coats Land records do not provide a clearer description of anthropogenic Pb levels in Antarctica since the 1980's than those data presented by Wolff and Suttie (1994) and Barbante et al. (1997). Lead isotope data observed in the most recent Antarctic samples are representative of aerosols in large southern hemisphere cities, confirming alkyllead additives as the dominant source of current anthropogenic Pb emissions. $^{206}\text{Pb}/^{207}\text{Pb}$ ratios at Coats Land (~ 1.15) are somewhat lower than those observed at Law Dome (~ 1.165), perhaps reflecting a greater proportion of anthropogenic Pb emissions from South America in the Coats Land record.

4.4 Evaluation of Pb and Ba concentrations and Pb isotopes at Victoria Land since 1891 AD

The pollution record for Victoria Land, as yet unpublished, covers the period 1891 to 1994. It was obtained from a 116 m snow/ice core (1891 – 1985) and a 2 m deep snow pit (1986-1994). The snow/ice core was sampled approximately every 3 years, while the snow pit was sampled at higher resolution (~3 samples per year) and 20 samples were obtained between Summer 1991/2 and Summer 1993/4. This record spans a time period comparable to those already discussed for Law Dome and Coats Land, but illustrates the fluxes of natural and anthropogenic Pb to Victoria Land, the Antarctic coastal region to the East of the Ross Sea. The collected data is included in Appendix 1.

The dating of the Victoria Land core, as described above, was calculated from an ice flow model (Udisti et al. 1999) coupled with major ion analysis. The snow pit, however, was dated using a multiparametric approach based on measurements of H_2O_2 , MSA and nssSO_4^{2-} (Udisti 1996). While there is no evidence to question the accuracy of the dating of the snow pit samples, there appears to be some discrepancy between the $^{206}\text{Pb}/^{207}\text{Pb}$ record observed at Victoria Land and those observed at Law Dome and Coats Land. Particularly, the pollution event observed during the period 1888-1898 at Coats Land and 1890-1898 at Law Dome, is observed during the period 1915-1921 in the Victoria Land record, as shown in Figure 4.6. Since the pollution event is observed at the same time in the Law Dome and Coats Land record, the hypothesis is offered that this event should also be observed at that same time in Victoria Land. On the basis of this hypothesis, it appears that the dating provided for the Victoria Land samples results in too-recent dates for the samples, and therefore requires correction.

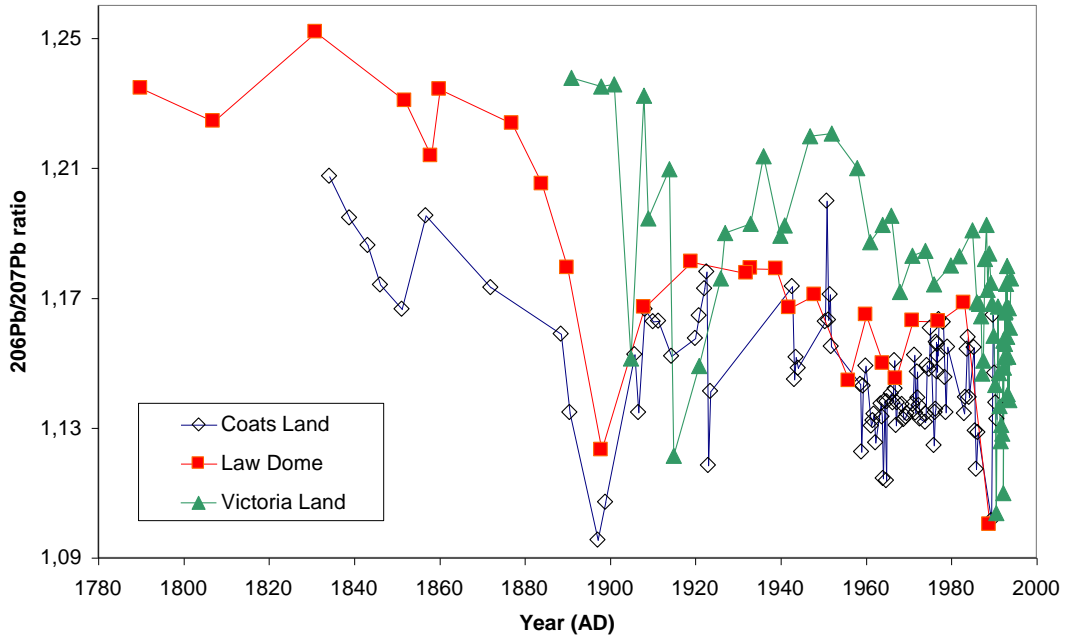


Figure 4.6. Comparison of $^{206}\text{Pb}/^{207}\text{Pb}$ ratios at Law Dome, Coats Land and Victoria Land (dated using the ice flow model of Udisti et al. 1999).

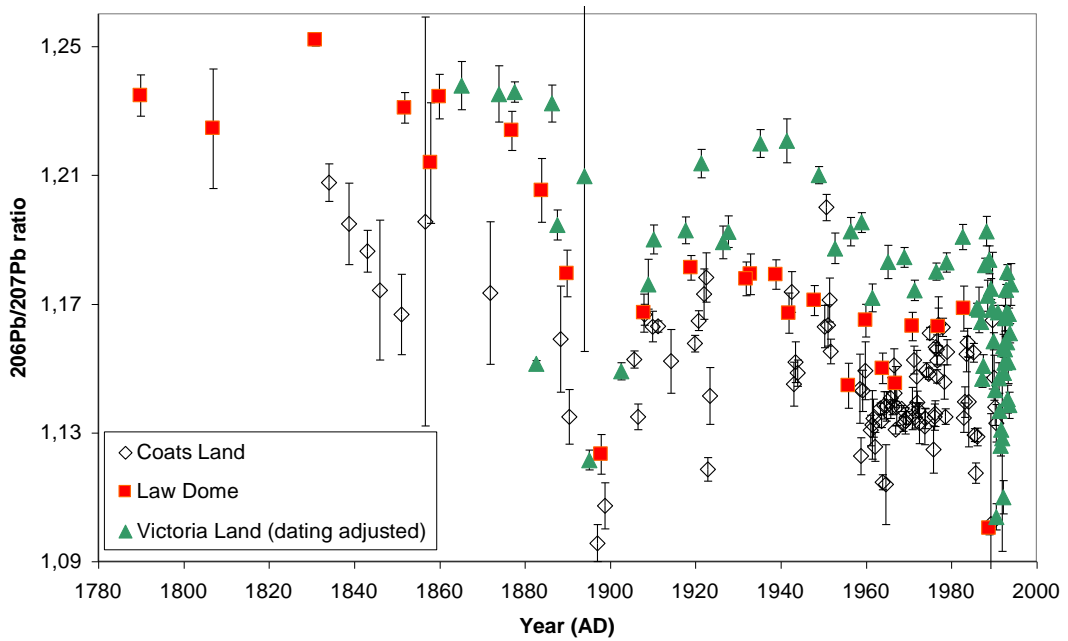


Figure 4.7. Comparison of $^{206}\text{Pb}/^{207}\text{Pb}$ ratios at Law Dome, Coats Land and Victoria Land (dating adjusted to match the c.1900 pollution event to those of Law Dome and Coats Land).

The discrepancy of the Victoria Land record, as compared to those at the other two locations, is most simply solved by altering the dating scheme applied to the Victoria Land core, so the pollution feature is brought into alignment with those of the other two pollution records. The adjusted dating scheme, applied to the Victoria Land data, is shown in Figure 4.7. In order to align the pollution events, the ages of each of the samples was increased by 25%. This shifted the earliest sample from a dating of 1891 AD to 1865 AD. The sample at which the $^{206}\text{Pb}/^{207}\text{Pb}$ ratio is lowest (~ 1.12) was previously dated to 1915 AD, but after adjustment was dated to 1895 AD. The dating adjustment had a relatively minor effect on the most recent samples, with the sample previously dated to 1985 now being dated to 1983. There is no reason to alter the dating of the snow pit samples, so the dating provided for these samples has been maintained. **For the remainder of this discussion, the adjusted dating of the Victoria Land ice/snow core, based on the coincidence of the c.1900 pollution event (sample ages increased by 25%), will be applied to the Victoria Land data.** The adjustment applied to the dating scheme is based on the assumption that the pollution event did indeed affect all of Antarctica. This assumption is not unreasonable, as the independent dating schemes of the Law Dome and Coats Land records both located the maxima of the pollution event at approximately the same time, 1890 – 1900 AD, and these two sites are located at approximately opposite ends of Antarctica. Dating of the Law Dome samples were directly linked to the DSS main core dating scheme (Palmer et al. 2001), which features a dating accuracy of $<\pm 1$ year at ~ 1900 AD, and so are considered to be more reliable than the dating provided for the Victoria Land samples. This application of the $^{206}\text{Pb}/^{207}\text{Pb}$ feature observed at ~ 1895 AD as a dating correction tool may be of use in future for verifying the dating of other ice core records for which Pb isotopes have been analysed. While Pb isotope analyses are slow and costly relative to $\delta^{18}\text{O}$ or major ion analyses, the identification of distinguishing features in the Antarctic Pb isotope record may be an added means of ensuring the quality of a particular ice core dating scheme.

The overall pattern of Pb and Ba deposition at Victoria Land displays a similar pollution history to those at Coats Land and Law Dome, with the earliest indication of pollution occurring ~ 1900 , high levels of anthropogenic Pb at the beginning of the 20th century, and increasing levels of anthropogenic Pb since the 1950's. Lead

concentrations, as shown in Figure 4.8, are significantly influenced by natural rock and soil dust inputs, as indicated by high Ba concentrations in the record. From 1891 to 1994, the average Ba concentration at Victoria Land is ~20 pg/g, compared to averages of ~2.5 pg/g at Law Dome and ~3.8 pg/g at Coats Land, over a similar period. This dust probably originates from local exposed rock outcrops and/or the nearby Trans-Antarctic mountain ranges and Ross Island, where Mount Erebus is located. The presence of a local crustal Pb source for the Hercules Neve area is supported by the findings of Maggi and Petit (1998), who observed a significant proportion of large-diameter (>12 μm) dust particles deposited in a Hercules Neve snow core. The presence of larger dust particles in the snow record was attributed to ‘short-range transport both from local dust sources, probably originating from the weathering of the rocks that outcrop in the Hercules Neve area, and from the sedimentary deposits at the glacier margins and in deglaciated areas’. Observed dust inputs to Victoria Land are also highly variable, ranging from ~7 to ~32 pg Ba/g between 1891 and 1927, and from ~1 to ~95 pg Ba/g between 1935 and 1994. Such variability inhibits the effectiveness of the Pb concentration record as an accurate indicator of pollution at Victoria Land. Instead, the Pb/Ba record is much more reliable at indicating levels of anthropogenic Pb deposited at the site, as it shows enhancements of Pb relative to dust levels. The Victoria Land Pb/Ba record indicates significant levels of pollution between 1895 and ~1920 and from 1969 to 1994.

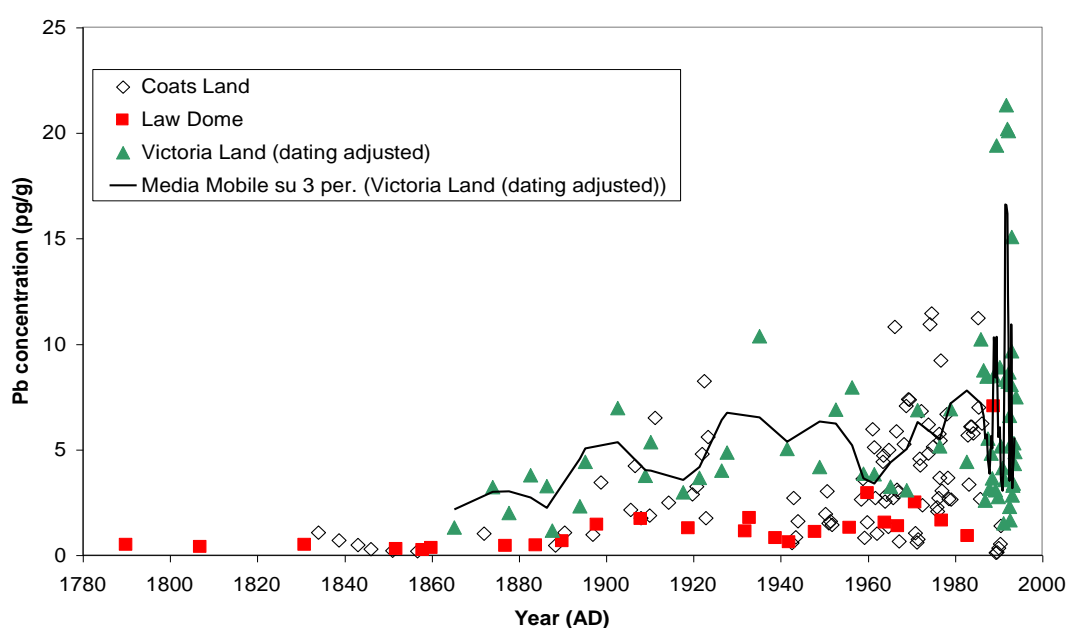


Figure 4.8. Comparison of Pb concentrations at Law Dome, Coats Land and Victoria Land.

$^{206}\text{Pb}/^{207}\text{Pb}$ ratios may be a more sensitive indicator of pollution at Victoria Land, in consideration of the significant levels of rock and soil dust observed at the site. The earliest samples (1865-1877) display constant $^{206}\text{Pb}/^{207}\text{Pb}$ ratios ~ 1.23 , which may be taken as representative of natural Pb inputs. From this natural value, the $^{206}\text{Pb}/^{207}\text{Pb}$ ratio in the record decreases significantly between 1894 and 1909. While $^{206}\text{Pb}/^{207}\text{Pb}$ ratios are ~ 1.19 from 1910 to 1927, they approach natural values (> 1.22) during the 1930's and 1940's. From an average value of ~ 1.19 during the 1950's, $^{206}\text{Pb}/^{207}\text{Pb}$ ratios decrease to ~ 1.17 during the 1960's and then gradually increase through the 1970's, returning to a value of ~ 1.19 by 1983. These trends correspond well to those observed for Victoria Land Pb/Ba ratios, with a significant peak at about 1900 AD, consistently high values until 1926, near-natural values from the mid-1920's to 1960, and increasing values from the 1960's to the 1990's. From the Victoria Land data, the isotopic signature of anthropogenic Pb inputs can be deconvoluted from natural Pb inputs (Rosman 2001). For this calculation, the Pb isotopic composition observed in the earliest Victoria Land samples ($^{206}\text{Pb}/^{207}\text{Pb} \sim 1.23$, $^{208}\text{Pb}/^{207}\text{Pb} \sim 2.50$) and the lowest Pb concentrations observed in the record (Pb concentrations ~ 1.5 pg/g) were taken to be representative of the natural Pb component deposited in Victoria Land snow. This natural component was then removed from the data observed in each sample, assuming the remainder to be anthropogenic Pb. From the calculation, it is estimated that the isotopic signature of anthropogenic Pb deposited during the 1895 pollution event is $^{206}\text{Pb}/^{207}\text{Pb} \sim 1.06$, $^{208}\text{Pb}/^{207}\text{Pb} \sim 2.37$, which is consistent with the Pb isotopic composition calculated from the Law Dome data ($^{206}\text{Pb}/^{207}\text{Pb} \sim 1.03 \pm 0.09$, $^{208}\text{Pb}/^{207}\text{Pb} \sim 2.24 \pm 0.20$). While calculated anthropogenic $^{206}\text{Pb}/^{207}\text{Pb}$ ratios vary from 1.15 to 1.20 during the period 1910 – 1927, they are more consistent after the 1940's. During the 1950's, anthropogenic $^{206}\text{Pb}/^{207}\text{Pb}$ ratios are ~ 1.175 , during the 1960's they are lower (~ 1.13) and then increase again during the 1970s to ~ 1.16 . Anthropogenic $^{206}\text{Pb}/^{207}\text{Pb}$ ratios during the 1980's are marginally higher at ~ 1.17 . Anthropogenic $^{206}\text{Pb}/^{207}\text{Pb}$ ratios calculated from the Victoria Land data for the 1960's match those measured in the Coats Land data, while the anthropogenic $^{206}\text{Pb}/^{207}\text{Pb}$ ratios calculated for the period 1972 – 1982 are in close agreement with those observed in the Law Dome record. This may be due to the location of Victoria Land core, as it is situated on the Antarctic coastline approximately equidistant from Coats Land and Law Dome. If the Law Dome and Coats Land pollution records are influenced differently by emissions from the continents of the southern hemisphere,

then the Victoria Land record may also be influenced by the varying levels of emissions from each continent. Changing continental sources of Pb emissions from the 1960's to the 1970's and 1980's may be the reason why the Victoria Land record is more similar to that from Coats Land during the 1960's but more similar to that from Law Dome during the 1970's and 1980's. In general, higher $^{206}\text{Pb}/^{207}\text{Pb}$ ratios are observed in the Victoria Land record compared to that of the Law Dome record, while higher $^{206}\text{Pb}/^{207}\text{Pb}$ ratios are observed in the Law Dome record compared to that of the Coats Land record. Such a shift is compatible with the variations seen in the Pb/Ba ratios in each record, for which the Coats Land Pb/Ba values are higher than those in the Law Dome record, which are higher than those in the Victoria Land record.

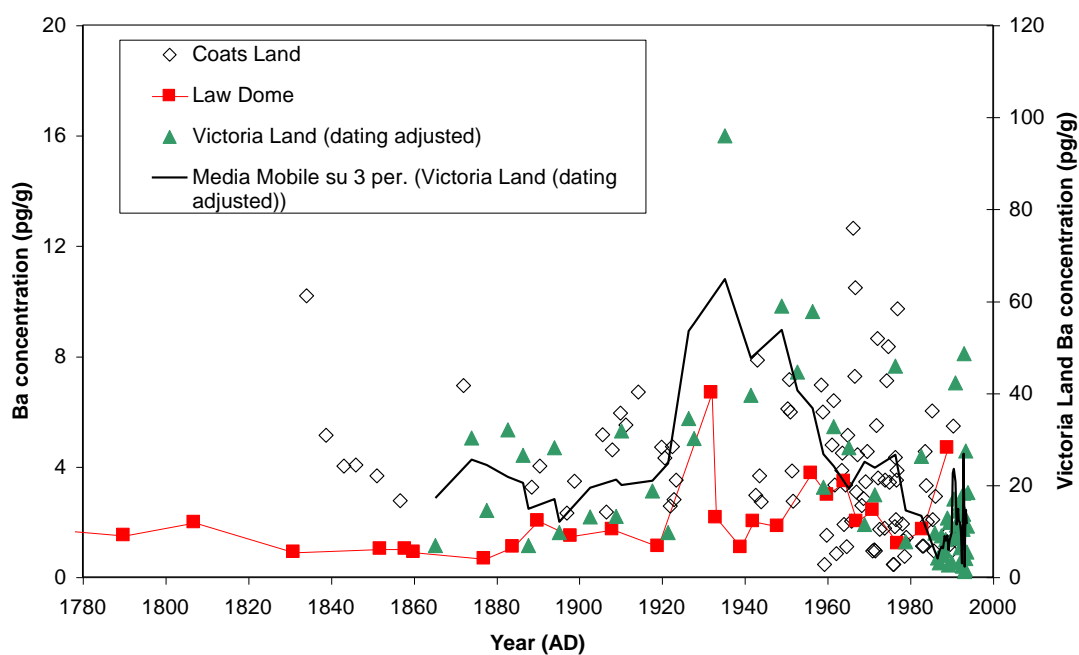


Figure 4.9. Comparison of Ba concentrations at Law Dome, Coats Land and Victoria Land.

The trend of decreasing Ba concentrations in Antarctic snow since the 1960's is observed in all three pollution records discussed here. Figure 4.9 shows Ba concentrations at Law Dome, Coats Land and Victoria Land for the period 1780 – 1994. The decrease is consistent in all three records despite the large scatter of Coats Land Ba concentrations and the much higher Ba concentrations generally observed in the Victoria Land record relative to those from Coats Land and Law Dome. Also, the relative magnitude of the Ba concentration decrease is approximately similar in each

record, as shown in Table 4.1. The observed percentage decrease in Ba concentrations is ~46% at Coats Land, ~39% at Law Dome and ~56% at Victoria Land. Table 4.1 also shows that the levels observed during the 1950's and 1960's at Coats Land and Victoria Land are generally representative of long-term values observed since the beginning of those records. This is not the case for the Law Dome record, however, where background Ba concentrations are approximately equal to, or lower than, those observed in the period 1971 – 1983. This may be associated with the observed increases in Ba concentrations at Law Dome associated with variations in dust levels observed by Maggi and Petit (1998) in Victoria Land. At Victoria Land, no corresponding increase in Ba concentration is observed, and at Coats Land, no data is available corresponding to the period at which dust-related Ba increases are observed at Law Dome. Consequently, it appears most likely that the Ba concentration decreases observed since the 1960's at Coats Land and Victoria Land are independent of dust inputs. In the Law Dome record, decreasing dust levels cannot be dismissed as a potential explanation for decreasing Ba levels. Although the decreasing Ba concentrations observed at these Antarctic locations are generally consistent with the ~20% increase in Antarctic snow accumulation reported by Morgan et al. (1991), a satisfactory explanation is yet to be found. The variability in Ba concentrations observed in Antarctic ice core records may lead to artificial errors when Pb pollution levels for the ice core records are calculated from crustal Enrichment Factors (EFs) based solely on Ba as an indicator of crustal Pb inputs. If Ba concentrations in ice core records are affected by accumulation rate changes, care must be taken to establish that Ba levels are a reliable indicator of crustal Pb inputs to the record.

Table 4.1 Average Ba concentrations in various Antarctic sites, 1530-1994.

AVERAGE BARIUM CONCENTRATIONS IN VARIOUS ANTARCTIC SITES, 1530 - 1994					
Coats Land year range	(pg/g)	Law Dome year range	(pg/g)	Victoria Land year range	(pg/g)
1989-1990	2.12	1989	4.68	1990-1994	12.97
1983-1986	2.67	1983	1.72	1980-1990	8.13
1970-1979	3.25	1971-1977	1.82	1971-1979	23.78
1960-1970	4.42	1960-1967	2.82	1961-1969	24.04
1950-1960	4.52	1948-1956	2.79	1952-1959	40.61
1834-1944	4.44	1530-1942	1.58	1865-1949	27.76
					average
% decrease*	45.80		38.95		56.11
					46.95

*Coats Land % decrease calculated from difference between 1960-1970 values and average of 1983-1990 values

Law Dome % decrease calculated from difference between 1960-1967 values and 1983 value

Victoria Land % decrease calculated from difference between 1961-1969 values and average of 1980-1994 values

What are the natural sources of Pb to Antarctica, and what influence does volcanism have on natural Pb fluxes?

4.5 Natural Pb and Ba inputs at Law Dome, Coats Land and Victoria Land.

Evaluations of the natural sources of Pb deposited in various Antarctic sites have arrived at different conclusions. Generally, the dominant sources of natural Pb deposited in Antarctica are rock and soil dust and volcanism, and, at coastal sites, marine aerosols. Boutron et al. (1988) determined that volcanic and rock and soil dust sources each account for approximately 50% of the Holocene Pb flux to Dome C and Vostok, in East Antarctica. The total natural Pb flux was ~0.4 pg Pb/g, with sea-salt, volcanic and crustal Pb sources calculated from Na, SO₄ and Al concentrations, respectively. Wolff and Suttie (1994) evaluated natural Pb fluxes to Coats Land from crustal, marine and volcanic sources. Hong et al (1996) evaluated natural sources of Pb to Law Dome, attributing Pb fluxes to sea salt-spray and crustal dust, but other natural sources could not be evaluated. Barbante et al. (1997) evaluated natural Pb sources at two locations in Victoria Land, attributing natural Pb fluxes to rock and soil dust, volcanic sources and marine aerosols/sea-salt spray. More recently, Matsumoto and Hinkley (2001) evaluated a suite of dust- and salt-forming metals in ice from Taylor Dome, near Victoria Land, to evaluate the contributions of Pb, Cd, In and Tl from crustal emission sources. They found that crustal sources usually accounted for <5%, <1% and <5% of Pb, Cd and In inputs and attributed the remainder of natural inputs to emissions from quiescently-degassing volcanoes. Natural Holocene levels of Pb at Taylor Dome are significantly higher than at any other known location in Antarctica, however, with Pb concentrations between 2.6 and 24 pg/g. Overall, these evaluations indicate that volcanic and rock and soil dust emission sources are significant natural sources of Pb observed in Antarctica. As to the proportions of these two sources and the importance of other sources such as marine aerosols, there appears to be significant variability within the sources, which potentially capture aerosols emitted from different source regions. At coastal locations such as Law Dome, Coats Land and Victoria Land, marine aerosols are more apparent with Pb contributions of 10-40%, <38% and 6-20%, respectively. At Dome C, an inland location, no significant marine

aerosol contribution was observed. In comparison, crustal Pb contributions appear to vary greatly in significance, from <5% at Taylor Dome and 1-20% at Law Dome, to 20-30% contributions at Victoria Land and ~50% contributions at Coats Land, Vostok and Dome C. At all locations, volcanic inputs are apparent, with ~19% contribution at Coats Land, ~50% contributions at Vostok and Dome C, 50% - 70% contributions to Victoria Land and >95% of Pb contributions attributed to volcanic sources at Taylor Dome.

Natural levels of Pb and Ba are observed at Law Dome prior to 1890 AD, with average concentrations of ~0.36 pg Pb/g and ~1.34 pg Ba/g. From 1890 onwards, increased concentrations of Pb and Ba are observed with changes in Pb isotopic compositions indicating the influence of anthropogenic Pb. Since only Pb and Ba concentrations are available for the Law Dome record, only the influence from rock and soil dust sources can be calculated. This calculation is based on reported values for the average ratio of Pb to Ba reported for crustal rock, ~0.03, from Mason and Moore (1982), Rudnick and Fountain (1995) and Taylor and McLennan (1985). The crustal Pb/Ba ratio of 0.03 is applied to the Ba concentration observed in each sample, and so the crustal Pb component is determined. The concentration of crustal Pb in the Law Dome samples dated prior to 1890 AD varies between 0.02 and 0.06 pg/g, with an average of 0.04 pg Pb/g. This corresponds to an average crustal Pb contribution of ~12%, with crustal Pb contributions ranging from 5% to 32% of total natural Pb inputs. These findings of significant, but minor, crustal Pb contributions to Law Dome are in agreement with those of Hong et al. (1998).

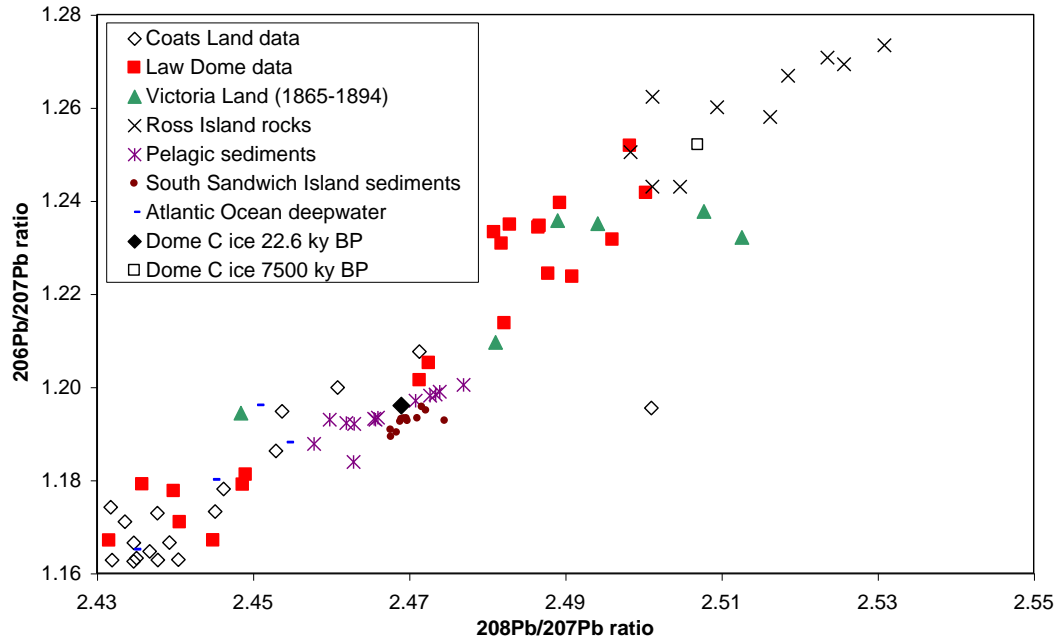


Figure 4.10. $^{206}\text{Pb}/^{207}\text{Pb}$ ratio vs $^{208}\text{Pb}/^{207}\text{Pb}$ ratio plot of pre-industrial Law Dome and early Coats Land and Victoria Land samples.

Natural Pb isotopic compositions observed in the Law Dome record are within the range $^{206}\text{Pb}/^{207}\text{Pb} = 1.225 \pm 0.025$, $^{208}\text{Pb}/^{207}\text{Pb} = 2.485 \pm 0.015$, $^{206}\text{Pb}/^{204}\text{Pb} = 19.1 \pm 0.8$. This data lies within the range of Pb isotopic signatures observed in Ross Island rocks (Sun and Hanson 1975), pelagic sediments from the South Atlantic Ocean (Chow and Patterson 1962) and South Sandwich Island sediments (Barreiro 1983), Atlantic Ocean deepwater (Alleman et al. 2001) and two samples of ancient ice from Dome C (Rosman et al. 1994, 1999), as shown in figure 4.10. The Pb isotope signature of Ross Island rocks are taken to be representative of Mount Erebus volcanic emissions and rock and soil dust emitted from ice-free regions of the Antarctic continent. Only two Pb isotopic signatures have been previously reported for pre-industrial Antarctic ice, both of these from Dome C. Lead isotopic compositions observed in ocean archives such as sediments and deepwaters are taken to be representative of the Pb isotopic signature of continental emission sources, including volcanism, wind-blown rock and soil dust and wild forest fires. It can be seen in figure 4.10 that the Pb isotopic signature of Ross Island rocks is within the range $^{206}\text{Pb}/^{207}\text{Pb} = 1.258 \pm 0.015$, $^{208}\text{Pb}/^{207}\text{Pb} = 2.515 \pm 0.015$, similar to that observed in the Dome C sample dated to 7,500 years BP. The sediment and deepwater data generally have less-radiogenic Pb isotopic signatures with $^{206}\text{Pb}/^{207}\text{Pb} < 1.22$ and

$^{208}\text{Pb}/^{207}\text{Pb} < 2.49$, which are similar to that seen in the Dome C ice sample dated to 22,600 years BP. From the distribution of natural Pb isotopic signatures observed in the Law Dome samples, it can be seen that a significant proportion of Pb in the samples has a signature similar to those of Ross Island rocks. As there are relatively few areas of exposed rock in East Antarctica (The TransAntarctic mountain area would probably be the dominant local source of rock and soil dust for the Antarctic continent), the emission of Pb from Mount Erebus is considered to be the dominant source of natural Pb to Law Dome. The contribution of Mount Erebus-type Pb to Law Dome can be calculated from the Pb isotopic signature observed in the samples dated prior to anthropogenic Pb inputs. The isotopic composition of Pb in each sample is treated as a binary mixture of Mount Erebus-type Pb ($^{206}\text{Pb}/^{207}\text{Pb} \sim 1.25$, $^{208}\text{Pb}/^{207}\text{Pb} = 2.50$) and continental dust-type Pb ($^{206}\text{Pb}/^{207}\text{Pb} \sim 1.20$, $^{208}\text{Pb}/^{207}\text{Pb} \sim 2.47$), from which the contribution of Mount Erebus-type emissions are found to comprise approximately $\sim 57\%$ of the total natural Pb input to Law Dome. This calculation does not take into account the Pb isotopic composition of other natural Pb sources such as marine aerosols, so it can only be used as an approximate evaluation of Mount Erebus-type contributions to the Law Dome record. Considering that Law Dome is a coastal site, it would also be expected that marine aerosol Pb inputs would comprise a significant proportion of natural Pb inputs, however no Pb isotope data are available to evaluate this potential Pb source.

Natural inputs of Pb and Ba to Coats Land cannot be accurately evaluated from the pollution record presented, as there is evidence of anthropogenic pollution in the earliest sample of the record, dated to 1834 AD. Of the samples dated prior to 1890, when significant levels of pollution are observed at Law Dome, those dated to 1846, 1851 and 1856 have the lowest observed Pb concentrations of 0.26, 0.20 and 0.16 pg/g and Pb/Ba ratios of 0.64, 0.55 and 0.58, respectively. These samples have $^{206}\text{Pb}/^{207}\text{Pb}$ ratios of 1.174, 1.166 and 1.195, which are less than those of the earliest samples dated from 1834 to 1843 ($^{206}\text{Pb}/^{207}\text{Pb}$ range: 1.186-1.208), however. From the Ba concentrations observed in the three samples dated from 1846 to 1856, it is calculated that crustal Pb contributes $\sim 50\%$ of the total Pb in the sample, while crustal Pb contributes $\sim 25\%$ of total Pb observed in the three earliest samples. Although the inputs of other natural Pb sources such as volcanism and marine aerosols cannot be assessed due to the lack of available proxy data and the Pb

observed in earliest Coats Land samples are affected by anthropogenic Pb inputs, the approximate proportions of crustal Pb contributions to Coats Land found here are in agreement with those of Wolff and Suttie (1994).

In the Victoria Land pollution record, natural inputs of Pb and Ba are observed in the earliest samples, from 1865 to 1883 (adjusted dates), as evidenced by stable $^{206}\text{Pb}/^{207}\text{Pb}$ ratios ~ 1.24 . Although Pb and Ba concentrations in these samples vary widely due to the variable quantities of rock and soil dust deposited in the snow, Pb/Ba ratios are observed to remain stable and constant at ~ 0.15 (range: 0.10-0.19). After 1883, lower $^{206}\text{Pb}/^{207}\text{Pb}$ ratios are regularly observed, suggesting the samples may be influenced by anthropogenic Pb inputs. Despite the presence of lower $^{206}\text{Pb}/^{207}\text{Pb}$ ratios, Pb/Ba ratios in samples dated from 1884 to 1894 are similar to those in earlier samples, averaging 0.12 and varying between 0.08 and 0.17. By 1895, significant inputs of anthropogenic Pb are observed, with Pb/Ba ratios ~ 0.46 and $^{206}\text{Pb}/^{207}\text{Pb}$ ratios ~ 1.12 . In the samples dated from 1865 to 1884, the crustal Pb contribution to the Victoria Land samples (calculated from a crustal Pb/Ba ratio of ~ 0.03) averages 24%, varying between 16% and 36%. These results are in good agreement with those of Barbante et al. (1997) who calculated a crustal Pb contribution of 20-30% for natural Pb inputs to Victoria Land. The Ba concentration observed in Victoria Land snow provides some indication of the quantity of dust deposited. As the average natural Ba concentrations observed at Victoria Land (~ 21 pg Ba/g) are significantly greater than those at Law Dome (1.3 pg Ba/g) and Coats Land (~ 3.5 pg Ba/g), it can be seen that dust inputs to Victoria Land are significantly greater than those to Law Dome or Coats Land. Given the proximity of Victoria Land to the TransAntarctic mountains, it is likely that the enhanced dust levels observed in the Victoria Land record are due to weathering of exposed rocks local to the sampling site.

Some indication of this predominant natural dust source can also be provided by evaluation of Pb isotopes. Lead isotopic compositions of the earliest Victoria Land samples are relatively radiogenic, with $^{206}\text{Pb}/^{207}\text{Pb} = 1.235 \pm 0.003$ and $^{208}\text{Pb}/^{207}\text{Pb} = 2.50 \pm 0.01$. These signatures are similar to those observed in pre-industrial Law Dome samples, and essentially range between the signatures associated with Ross Island rocks (Mount Erebus emissions, Antarctic rock and soil dust) and Southern

Ocean signatures (continental rock and soil dust). If the Pb isotopic composition observed in these Victoria Land samples ($^{206}\text{Pb}/^{207}\text{Pb} = 1.235 \pm 0.003$ and $^{208}\text{Pb}/^{207}\text{Pb} = 2.50 \pm 0.01$) is calculated as a binary mixture of Mount Erebus-type Pb ($^{206}\text{Pb}/^{207}\text{Pb} \sim 1.25$, $^{208}\text{Pb}/^{207}\text{Pb} = 2.50$) and continental dust-type Pb ($^{206}\text{Pb}/^{207}\text{Pb} \sim 1.20$, $^{208}\text{Pb}/^{207}\text{Pb} \sim 2.47$), the contribution from continental dust would vary from ~20% to ~29%. This is shown in Table 4.2. These values are in good agreement with the Victoria Land dust contributions as calculated from dust proxies. A dominant Mount Erebus-type Pb contribution of ~75%, as calculated here, is also in agreement with that calculated by Barbante et al. (1997) from SO_4 concentration data. From the significant proportions of inputs of crustal and volcanic Pb observed in the Victoria Land samples, there appears to be little influence from marine aerosol Pb at the sampling site. Considering the relative proximity of Taylor Dome to Victoria Land and Mount Erebus, it appears quite possible for the natural Pb signal at Taylor Dome to be completely dominated by Pb emissions from Mount Erebus. The proximity of the Taylor Dome site to Mount Erebus, a significant emitter of Pb, may limit the reliability of the Taylor Dome site as a representative site of Pb fluxes to Antarctica.

Table 4.2 Calculation of contributions of dust- and Mount Erebus-type Pb in Victoria Land samples, assuming a binary mixture.

Victoria Land Samples			% Contributions*	
Date	$^{206}\text{Pb}/^{207}\text{Pb}$	$^{208}\text{Pb}/^{207}\text{Pb}$	Dust	Mount Erebus
1887	1.232	2.513	28.6	71.4
1878	1.236	2.489	29.2	70.8
1874	1.235	2.494	29.1	71.0
1865	1.238	2.508	20.5	79.6

*Lead isotope compositions of dust and Mount Erebus sources assumed to be $^{206}\text{Pb}/^{207}\text{Pb}=1.20$, $^{208}\text{Pb}/^{207}\text{Pb}=2.47$ and $^{206}\text{Pb}/^{207}\text{Pb}=1.25$, $^{208}\text{Pb}/^{207}\text{Pb}=2.50$, respectively.

**4.6 RESEARCH ARTICLE: LEAD, Ba AND Bi IN ANTARCTIC LAW DOME
ICE CORRESPONDING TO THE 1815 AD TAMBORA ERUPTION: AN
ASSESSMENT OF EMISSIONS SOURCES USING Pb ISOTOPES.**

Submitted to *Earth and Planetary Science Letters* 7th August 2002

Accepted for publication 7th April 2003.

Currently in press

Lead, Ba and Bi in Antarctic Law Dome ice corresponding to the 1815 AD Tambora eruption: an assessment of emission sources using Pb isotopes.

P. Vallelonga^{1*}, J.-P. Candelone¹, K. Van de Velde¹, M.A.J. Curran², V.I. Morgan² and K.J.R. Rosman¹.

¹Department of Applied Physics, Curtin University of Technology, GPO Box U 1987, Perth 6845, Australia. Email: p.vallelonga@curtin.edu.au, Fax: 618 9266 2377.

²Antarctic CRC and Australian Antarctic Division, GPO Box 252-80, Hobart 7001, Australia.

*Author to whom correspondence should be addressed.

WORD COUNT (Main Text): 5280 words

ESTIMATED PAGE COUNT: 13 pages

KEY WORDS: lead isotopes, volcanism, Mount Erebus, barium, bismuth, thermal ionization mass spectrometry

Abstract

Lead, Ba and Bi concentrations and Pb isotopic compositions have been measured in Antarctic Law Dome (66.8°S, 112.4°E) ice dated from 1814 AD to 1819 AD by Thermal Ionization Mass Spectrometry to investigate the possible deposition of heavy metals from the 1815 AD eruption of Tambora volcano (8.5°S, 117.4°E) in Indonesia. Although volcanic S emissions from Tambora (observed as SO_4^{2-}) are present in the Antarctic ice core record, there are grounds to question the origin of the Pb and Bi also deposited at Law Dome from late-1817, as the Pb isotope data suggest this Pb originated from Mount Erebus (77.5°S, 167.2°E) on Ross Island, Antarctica. It is shown that at least 97% of any Pb and Bi emitted from Tambora was removed from the atmosphere within the 1.6 year period required to transport aerosols from Indonesia to Antarctica. Consequently, increased Pb and Bi concentrations observed in Law Dome ice about 1818 AD are attributed to either increased heavy metal emissions from Mount Erebus, or increased fluxes of heavy metals to the Antarctic ice sheet resulting from climate and meteorological modifications following the Tambora eruption. Elevated Ba concentrations, observed from mid-1816 to mid-1818, indicate increased atmospheric loading of rock and soil dust also occurred at the time.

1. Introduction

Investigations of the Antarctic ice sheet have revealed past and present atmospheric conditions and compositions [1] and supported calculations of metal emissions to the atmosphere from natural sources [2-4]. These emission sources include rock and soil dust, volcanism, sea-salt spray, forest fires and marine biogenic activity [5], with the relative significance of each varying with location and time.

While volcanogenic Pb inputs have been calculated for only three Antarctic sites, at Coats Land (77°34'S, 25°22'W and 77°15'S, 18°05'W [6]), Dome C (72°39'S, 124°10'E [7]) and Victoria Land (74°32'S, 162°56'E and 73°52'S, 163°42'E, [2]), quiescently-degassing volcanism has recently been evaluated as the primary source of Pb deposited in Antarctic ice [8] based on new global volcanic metal emissions data (0.86x10⁹ g Pb/y, 0.41x10⁹ g Bi/y [9]). Concentrations of Pb, Bi and other trace metals are known to be greatly enriched in volcanic plumes [10] compared to average crustal abundances. In volcanic plumes, Pb is attached to S aerosols [11] and emitted into the atmosphere in the form of fine particulates [12].

Two previous studies have reported Pb concentrations in polar ice corresponding to the deposition of debris emitted from volcanic eruptions. Hong et al. [13] investigated Pb, Cd, Cu and Zn in Greenland ice associated with the effusive (predominantly lava-flow) eruption of Laki, Iceland, in 1783 - 1784 AD and observed an increase in Pb concentrations three times above background levels. Although this enhancement could not be accurately verified due to the influence of anthropogenic Pb emissions from Europe at the time [14], they calculated that 0.9 tons of Pb emitted from Laki was deposited on the Greenland ice sheet. The Laki

eruption released approximately 15 km^3 of magma [15], and led to the production of about 2×10^{11} kg of H_2SO_4 aerosols [16].

Matsumoto and Hinkley [8] measured Pb isotopes and Pb, Cd, In and Tl concentrations in ancient ice from Taylor Dome ($77^\circ 48' \text{S}$, $158^\circ 43' \text{E}$) in Antarctica which contained a visible tephra layer deposited from an explosive volcanic eruption. The ice strata was dated to approximately 72.9 ky BP. Although Matsumoto and Hinkley observed a three-fold Pb concentration increase in the ice stratum they noted that this was accounted for by the Pb content in volcanic tephra, and so concluded that any excess metals that may have been present in the eruption cloud were lost prior to deposition of the tephra in the ice. This finding contradicted the conclusions of Nho et al. [17] who, in reporting SO_2 fluxes and Pb/ SO_2 and Bi/ SO_2 ratios for two Indonesian arc volcanoes, concluded that explosive volcanism was more important than effusive volcanism as a source of volcanogenic metals for long-range transport. Their conclusion was based on the reasoning that only explosive eruptions were capable of injecting large quantities of volcanogenic metals into the stratosphere, where long-range transport would be facilitated by the longer atmospheric residence time of aerosols.

The Tambora volcano erupted violently in April 1815 AD, ejecting 2×10^{14} kg of material and later producing $>10^{11}$ kg of SO_4 [18]. These emissions produced the 'year without a summer', 1816 AD, during which global temperatures decreased by $0.4\text{-}0.7^\circ\text{C}$ [19]. Enhancements of non-sea salt SO_4^{2-} (nssSO_4^{2-}) concentrations attributed to the eruption of Tambora have been identified in several Greenland [20, 21] and Antarctic [22-24] ice cores. At Law Dome, a nssSO_4^{2-} signal is observed from late-1816, with a 1.6-year time lag attributed to the relatively slow stratospheric transport of fine volcanic debris [23].

We present the first measurements of Pb, Ba and Bi concentrations and Pb isotopes corresponding to an identified volcanic signal in Antarctic ice. Previous analyses of Law Dome ice cores have established a reliable background for Pb and Ba concentrations and Pb isotopic compositions representative of normal Pb and Ba inputs [25]. At Law Dome, Pb and Ba concentrations are at background levels in the early 19th century, and we assume the same for Bi. Barium has been measured as a proxy for natural dust inputs [26], while enhancements in Bi are most likely due to volcanism [27].

2. Methods

2.1 Samples

Samples were obtained from the DSS-W20k firn/ice core (lat. 66°46'27" S, long. 112°21'26" E, altitude 1370 m a.s.l.) drilled on the Law Dome ice cap in Wilkes Land [28]. The locations of Law Dome in Antarctica and Tambora in Indonesia are shown in Figure 1. The 70.3 m long 8.2 cm diameter electromechanical core was drilled in December 1997, 20 km west of the Dome Summit South (DSS) ice core [23]. A 1 m length of the core was analysed, incorporating the years 1814 – 1818 AD. There appears to be little disturbance from katabatic winds at the site [29], for which the accumulation rate is about 160 kg/m²/y and the mean annual temperature is –21.8°C. Law Dome experiences mostly easterly airflow driven by Southern Ocean cyclonic systems which centre on 65°S.

The dating of the DSS-W20k ice core was based on a multi-parametric approach consisting of snow accumulation and densification rate calculations combined with intercomparisons of characteristic nssSO₄²⁻ signals observed in the

DSS-W20k and DSS [23] ice core records. The high accumulation rate (>600 kg/m²/y) and low surface winds and temperatures at the Law Dome summit contribute to the excellent preservation of seasonal $\delta^{18}\text{O}$ and chemical signals in the DSS ice core, however snow accumulation decreases to the west of the summit where the DSS-W20k site is located. While seasonal characteristics of chemical signals are retained at the DSS-W20k site, the lower snow accumulation rate precludes the preservation of seasonal $\delta^{18}\text{O}$ signals so dating of the DSS-W20k core by annual layer counting is not possible. Instead, the DSS-W20k core was initially dated using snow accumulation and densification data based on ice rheology calculations and later improved by trapped-gas measurements of the close-off depth (D. Etheridge, pers. comm.). The accumulation rate was confirmed after identification of the characteristic doublet of nssSO₄²⁻ signals attributed to eruptions of Tambora (1815 AD) and an unknown volcano (1809 AD) which were correlated with the doublet observed in the DSS core record. The times of arrival of these volcanic emission products at Law Dome have been established using accurate multiparameter multicore dating [23], for which the uncertainty is less than 0.5 years.

Chemical signals observed in the DSS-W20k core were used to identify annual layers of snow accumulation, based on observations of the seasonal deposition of chemicals at Law Dome [29]. Of the chemical species measured by ion chromatography (Cl⁻, Na⁺, K⁺, MSA, Mg²⁺, Ca²⁺, SO₄²⁻ and NO₃⁻), Cl⁻, Na⁺, K⁺ and Mg²⁺ all displayed distinct winter maxima. Uncertainty in the dating of the annual layers in the DSS-W20k core, based on seasonal chemical signals, is ± 0.5 years.

Fallout of volcanic debris was identified by measurements of electrical conductivity [30] and nssSO₄²⁻ concentrations. The nssSO₄²⁻ signals observed in the DSS-W20k ice core between 1808 and 1818 AD are shown in Figure 2. The nssSO₄²⁻

seasonal cycles between the volcanic events are attributed to seasonal biological production of SO_4^{2-} [29]. The nssSO_4^{2-} signal tentatively assigned to Tambora was observed between the depths of 41.98 m (about 1817.0) and 41.72 m (about 1818.5), while that tentatively assigned to an unidentified volcanic eruption of 1809 AD [22, 23] was observed between 43.01 m and 43.26 m.

2.2 Decontamination

Since the decontamination and mass spectrometry procedures used for this study are described by Vallelonga et al. [31], only a summary of those protocols is presented here. All apparatus used to handle the samples was made of polyethylene (PE), fluorinated ethylene propylene (FEP) Teflon or type 316L stainless steel, cleaned by immersion in a series of successively purer, heated acid baths prior to use. The decontamination procedure involves the chiselling of concentric layers of ice from the core, leaving a pristine inner core (IC) section free from any external contamination. The extent to which samples were contamination-free was assessed by measuring the concentrations in the profile from the exterior to the centre of the core, with a plateau in the innermost layers generally indicating a pristine inner core [32].

The samples were collected from two pieces of the DSS-W20k ice core, each piece being 50 cm in length. Prior to the decontamination of each piece, a bandsaw was used to remove a longitudinal slice for $\delta^{18}\text{O}$ and other chemical analyses. The concentric layers were chiselled and the inner core was then broken into several pieces that were each stored separately in polyethylene (PE) or perfluoroalkoxy (PFA) Teflon containers. The length and corresponding depth interval of each piece is shown in Figure 3. Fifteen inner core pieces were collected between depths 41.727

m and 42.644 m, of which 9 (designated 'IC1' to 'IC9') correspond to 2.5 years of deposition from 1816 - 1819 and 6 (designated 'IC10' to 'IC15') correspond to the preceding years 1814 - 1816, when normal nssSO_4^{2-} levels are observed.

Following the decontamination, the samples were weighed then melted and aliquotted into PE bottles. The samples were then frozen and transported across Australia from Hobart, Tasmania, to Curtin University of Technology in Perth, Western Australia, for analysis by Thermal Ionization Mass Spectrometry (TIMS).

2.3 Mass Spectrometry

All samples were prepared in a clean-room supplied with HEPA-filtered air. Approximately 10-15 g of sample was transferred to a preconditioned PFA Teflon beaker, to which were added concentrated HNO_3 , a silica gel- H_3PO_4 mixture and a $^{205}\text{Pb}/^{137}\text{Ba}$ mixed spike (approximately 3 pg Pb/64 pg Ba). The sample was then evaporated to dryness in a Teflon chamber under an IR lamp. The residue was transferred in a drop of silica gel- H_3PO_4 mixture onto a zone-refined acid-cleaned Re filament and evaporated slowly. It was then mounted in the mass-spectrometer.

All samples were measured by TIMS (model VG354, Fisons Instruments). For all of the samples, all isotopes were measured using a Daly detector. The TIMS sample turret allowed 16 filaments to be loaded at a time, so each batch of measurements consisted of 10 samples, 3 beaker blanks, 2 filament blanks and a 200 pg NIST SRM 981 (common Pb isotopic standard). Blanks contributed < 0.3 pg Pb and < 2 pg Ba [31].

Lead and Ba concentrations were determined by Isotope Dilution Mass Spectrometry (IDMS), using a $^{205}\text{Pb}/^{137}\text{Ba}$ spike added to each sample prior to evaporation. Since ^{205}Pb is not present in natural Pb this allows the Pb and Ba

concentrations and Pb isotopic composition to be obtained from one sample. Lead and Ba concentrations have been determined to an accuracy of $\pm 15\%$ (95% confidence interval), which is limited by the accuracy of the spike calibration and the dispensing of the spike into the sample.

2.4 Bismuth Measurements

Bismuth was measured by TIMS according to the technique described by Chisholm et al. [33], in which the $^{209}\text{Bi}/^{208}\text{Pb}$ ion current ratio was used to determine the amount of Bi present on the filament. For each sample, a calibration ratio of 11 ± 2 was used to correct for the higher thermal ionization efficiency of Bi compared to that of Pb. The presence of an interfering ion, $^{130}\text{BaPO}^{3+}$, at $m/z = 209$ was corrected by monitoring $^{134}\text{BaPO}^{3+}$ at $m/z = 213$, this correction being consistently less than 5% of the ^{209}Bi ion current. Lead, Ba and Bi were measured simultaneously in each sample, with Bi concentrations determined with an accuracy of approximately 50% (95% confidence interval). Bismuth blanks, evaluated to be less than 1 fg, were determined in the same manner as for those of Pb and Ba.

3. Results

3.1 Character of the data

Shown in Table 1 are Pb, Ba and Bi concentrations and Pb isotopic compositions of the 15 inner core pieces and also 9 samples corresponding to the external, chiselled layers. While the samples obtained from the deeper core section, between depths 42.224 m and 42.644 m, were all deposited prior to the influence of emissions from Tambora, they cannot all be considered representative of background atmospheric emissions due to elevated Pb/Ba and Bi/Ba ratios observed in samples

‘IC13’ to ‘IC15’. This enrichment appears to be due to the deposition of volcanic debris, possibly from Mt Erebus, however a synchronous increase in nsSO_4^{2-} is not observed. The average concentrations measured in IC samples 9 to 12 (corresponding to low Pb/Ba and Bi/Ba ratios between the two volcanic events) are 0.25 pg Pb/g, 1.2 pg Ba/g and 3 fg Bi/g. Although the Pb concentration is lower, Ba and Bi values are in agreement with previously measured concentrations in pre-industrial Law Dome ice (0.4 pg Pb/g, 1.3 pg Ba/g, 3 fg Bi/g) [25, 34].

The presence of contamination in samples was initially evaluated by identifying a plateau of concentrations across the profile of the core layers. The inner core concentration was taken as the sum of the IC pieces, each weighted by the proportion of the inner core it comprised. This is expressed in the equation:

$$\text{IC Concentration} = \sum_{i=1}^n \frac{\text{Piece Concentration}_i \times \text{Piece Length}_i}{\text{IC Length}}$$

for which the inner core consists of n pieces of uniform cross-section. Data pertaining to the three plateau profiles (designated ‘TOP’, ‘MID’ and ‘BOT’ according to the physical orientation of the core sections and so as not to be confused with the IC pieces) are included in Table 1. It can be seen that plateaus are established for Bi and Pb in all profiles, however for Ba, a plateau is not apparent in the section 41.927 m to 42.207 m, designated ‘MID’ in Table 1 and Figure 3. In this profile, Ba concentrations are similar to those seen only in the outer layers of other sections (designated ‘TOP’ and ‘BOT’). Contamination of the ‘MID’ section is unlikely as this part of the ice core section corresponds to a period of enhanced dust deposition, which would elevate Ba concentrations throughout the profile. Plateaus of Pb/Ba and Bi/Ba ratios, also observed in the ‘MID’ section, support this conclusion.

Evaluation of Pb isotopes also enables contaminated inner core pieces to be identified. In Figure 4, it can be seen that the Pb isotopic compositions of pieces ‘IC1’ ($^{206}\text{Pb}/^{207}\text{Pb}=1.156\pm 0.019$, $^{208}\text{Pb}/^{207}\text{Pb}=2.366\pm 0.027$) and ‘IC15’ ($^{206}\text{Pb}/^{207}\text{Pb}=1.160\pm 0.019$, $^{208}\text{Pb}/^{207}\text{Pb}=2.347\pm 0.022$) are distinct from those of the other samples ($^{206}\text{Pb}/^{207}\text{Pb}$: 1.176 – 1.303, $^{208}\text{Pb}/^{207}\text{Pb}$: 2.419 – 2.517). These low values for the isotopic ratios suggest that anthropogenic Pb was entrained in the core ends. In Table 1, the concentrations and Pb isotopic compositions of the contaminated pieces (‘IC1’ and ‘IC15’) are given as upper and lower limits, respectively. All other pieces lie within the range of Pb isotopic compositions of pre-industrial Law Dome ice, and so do not appear to be contaminated.

3.2 Lead, Ba and Bi concentrations

Figure 5a shows variations in Pb/Ba and Bi/Ba ratios and nssSO_4^{2-} concentrations, while Figure 5b compares Pb concentrations with $^{206}\text{Pb}/^{207}\text{Pb}$ isotopic compositions. The resolution at which the IC pieces have been sampled (5–7 cm per sample) is such that each sample integrates a quarter to a third of a year of snow deposition. At such resolution, irregularities in snow deposition at Law Dome may alter the Pb, Bi or Ba concentrations observed. However these potential variations in deposition will not alter element ratios or Pb isotopic compositions.

An increase in Pb/Ba and Bi/Ba ratios, observed about mid-1814 and apparently unrelated to the Tambora eruption, is likely due to the deposition of volcanogenic Pb and Bi from Mount Erebus. The Bi/Ba ratio in sample ‘IC14’ (31×10^{-3}) exceeds the threshold value (20×10^{-3}) given by Rosman et al. [34] for volcanic Bi in ice, but no great change in nssSO_4^{2-} concentration is observed. The Pb isotopic composition of the sample, which is indistinguishable from that of Mt

Erebus lava, lends further support for a volcanic contribution. The location of Mount Erebus on Ross Island in Antarctica is shown in Figure 1.

Following the volcanogenic Pb and Bi input at mid-1814, element concentrations and ratios are generally constant until mid-1816 AD. Marginally increasing Pb/Ba ratios and decreasing Bi/Ba ratios are observed from 1815 to early 1816, however these fluctuations may be due to seasonal variations in the deposition of Pb and Bi, and element concentrations approximate to background levels throughout.

Higher-than-normal Ba concentrations are observed from mid-1816 to mid-1818 ('IC8' to 'IC2'), indicating a period of elevated dust deposition at Law Dome. Increased levels of dust input are consistent with the lower Pb/Ba ratios (about 0.15) present in these samples, as the average Pb/Ba ratio found in the Earth's crust (about 0.03) is lower than that found in Law Dome ice (about 0.31) [25]. Decreasing Pb isotope ratios in these samples are further indication of a change in the proportions of Pb sources to Law Dome at the time. Concentrations of other dust indicators such as Ca^{2+} , Mg^{2+} and K^{+} did not increase but at Law Dome sea salt inputs of these ions usually prevail over terrestrial dust inputs due to the dominant influence of marine air at this coastal location.

Increased Pb/Ba and Bi/Ba ratios are again observed in the samples from late-1817 to mid-1818, coinciding with the nssSO_4^{2-} concentration peak attributed to the deposition of S aerosols erupted from Tambora. While the nssSO_4^{2-} peak is attributed to S emissions from Tambora [23], the Pb isotopic data presented here indicates the Pb to have mostly likely originated from Mount Erebus. The Bi/Ba ratios corresponding to peak nssSO_4^{2-} concentrations (19×10^{-3} , 36×10^{-3}) about 1818 AD match and exceed the threshold value (20×10^{-3}) given by Rosman et al. [34] for

volcanic Bi in ice. At the time of maximum nssSO_4^{2-} deposition (1818 AD) Pb and Bi are enriched about 5 times and about 17 times above background levels, respectively, which is greater than the volcanogenic Pb enhancements in ice sheets observed by Matsumoto and Hinkley [8] and Hong et al. [13]. Lead/S ratios of 0.1×10^{-4} and Bi/S ratios of 0.01×10^{-4} have been evaluated in the strata corresponding to maximum nssSO_4^{2-} concentrations. These values are below the ranges published by Hinkley et al. [9] and Nriagu [5] for Pb/S and Bi/S in volcanic emissions, and also lower than the Pb/S value observed in Greenland ice corresponding to the Laki eruption [13].

3.3 Lead isotopes

Lead isotopic compositions measured in Law Dome ice for the period 1814 – 1819 ($^{206}\text{Pb}/^{207}\text{Pb}$: 1.20 - 1.26, $^{208}\text{Pb}/^{207}\text{Pb}$: 2.44 – 2.50) generally fall within the range previously observed for pre-industrial Law Dome ice dated between 0 AD and 1890 AD ($^{206}\text{Pb}/^{207}\text{Pb} = 1.225 \pm 0.025$, $^{208}\text{Pb}/^{207}\text{Pb} = 2.48 \pm 0.02$ [25]). This data is displayed in Figure 4, a plot of $^{206}\text{Pb}/^{207}\text{Pb}$ versus $^{208}\text{Pb}/^{207}\text{Pb}$ isotope ratios which enables mixtures of Pb from sources with different Pb isotopic compositions to be evaluated [35]. Also included in Figure 4 are Pb isotopic signatures representative of relevant emission sources such as Mount Erebus [36], Tambora and other Indonesian island-arc volcanoes [37] and Pb isotopic signatures measured in pre-industrial Antarctic ice from Taylor Dome [8]. Samples deposited in 1818 ('IC2' and 'IC3': $^{206}\text{Pb}/^{207}\text{Pb}$ about 1.26, $^{208}\text{Pb}/^{207}\text{Pb}$ about 2.50) display Pb isotopic compositions which are more-radiogenic than those deposited in late-1816 AD ('IC6' and 'IC7': $^{206}\text{Pb}/^{207}\text{Pb}$ about 1.20, $^{208}\text{Pb}/^{207}\text{Pb}$ about 2.45), while other samples ('IC4', 'IC5' and 'IC8') display Pb isotopic compositions within these limits. Lead isotope ratios in

samples corresponding to the nssSO_4^{2-} signal attributed to the deposition of S aerosols from Tambora are similar to those of Mount Erebus lavas, while none of the samples deposited after 1815 AD ('IC1' – 'IC12') display a Pb isotopic composition similar to that of Tambora lava. Duplicate measurements of all inner core samples were in agreement with each other except for 'IC3', for which identical $^{208}\text{Pb}/^{207}\text{Pb}$ ratios (about 2.505) but different $^{206}\text{Pb}/^{207}\text{Pb}$ ratios (1.303 ± 0.010 and 1.265 ± 0.005) were measured. The different $^{206}\text{Pb}/^{207}\text{Pb}$ ratios are attributed to sample heterogeneity, possibly due to the presence of undissolved Pb-bearing particles in the sample.

4. Discussion

Two periods of enhanced inputs of Pb and Bi derived from volcanism can be observed in the Law Dome samples. The first, relatively brief, volcanic input event occurred in mid-1814, with Pb isotope ratios similar to those found in Mount Erebus lavas but no corresponding increase in nssSO_4^{2-} concentrations. The second period of volcanic input occurred from 1817 to mid-1818, coinciding with a sustained increase in dust deposition and including the nssSO_4^{2-} peak attributed to the deposition of S aerosols erupted from Tambora. Lead isotope ratios vary over the period 1817 to mid-1818, however Pb isotope ratios in samples corresponding to the deposition of S aerosols from Tambora are again similar to those in Mount Erebus lava.

The first volcanic event is observed in sample 'IC14' (mid-1814 AD), with elevated Pb/Ba and Bi/Ba ratios also present in the two adjacent inner-core pieces. There is no evidence to suggest this may be the result of contamination. The Pb and Bi deposited in the samples is attributed to volcanism even though there is no increase in nssSO_4^{2-} concentrations and no nssSO_4^{2-} signal is observed in Antarctic

ice cores about 1814 AD [22, 23]. The nssSO_4^{2-} signal for the unidentified 1809 AD eruption is observed earlier in the Law Dome ice core record at 1811 AD, as shown in Figure 2. Based on the Pb isotope data, the Pb deposited in 1814.5 is attributed to Mount Erebus, suggesting that Pb and Bi from Mount Erebus was deposited in East Antarctic ice without a corresponding increase in nssSO_4^{2-} levels. The absence of excess nssSO_4^{2-} in these samples may be due to the preferential scavenging of SO_4^{2-} (compared to Pb and Bi) by snow during atmospheric transport and/or high Pb/S and Bi/S emission ratios from Mount Erebus. Fluxes of SO_2 from Mount Erebus vary from 5.5×10^3 t/y to 84.0×10^3 t/y [38] and are much lower than those reported for Kilauea in Hawaii (0.73×10^6 t/y [9]) and Indonesian arc volcanoes (3.5×10^6 t/y [17]), but Pb/S and Bi/S data are not available for the Mount Erebus plume. A review by Wolff [39] notes that the preferential deposition of SO_4^{2-} compared to Pb aerosols has been observed in Antarctic snow.

Elevated Ba concentrations are observed from mid-1816 to 1818 and indicate a period of increased atmospheric dust levels but no data is available to link this dust event to the eruption of Tambora. The dust deposited between 1816 and mid-1817 does not appear to have a volcanic origin, as Bi/Ba levels remain consistently low in the corresponding samples. Additional evidence for the non-volcanic nature of the dust event is observed in the Pb isotopic ratios in these samples (IC4 – IC8: $^{206}\text{Pb}/^{207}\text{Pb}$ from 1.19 to 1.24, $^{208}\text{Pb}/^{207}\text{Pb}$ from 2.44 to 2.49), which are similar to average values reported for pre-industrial Law Dome ice ($^{206}\text{Pb}/^{207}\text{Pb} = 1.225 \pm 0.025$, $^{208}\text{Pb}/^{207}\text{Pb} = 2.48 \pm 0.02$ [25]). The available data suggests that although the quantity of dust deposited in Law Dome from 1816 to 1818 increased greatly, the origin of this dust did not appear to change. The eruption of Tambora greatly influenced global climate [19], so it is possible that the eruption led to, contributed to and/or

prolonged the enhancement of atmospheric dust levels observed from 1816, but further investigation is needed.

The sources of wind-blown dust deposited in Antarctica during the Holocene have not yet been determined and a characteristic Pb isotopic signature for this natural Pb source is yet to be established, so we provide a tentative evaluation of the Pb isotopic signature for continental dust transported to Antarctica based on the enhanced dust loading observed in 1816 and early-1817. Considering that Ba concentrations were greatly enhanced in the Law Dome samples, but no change in Pb isotope ratios was observed, we infer that the Pb isotopic signature for Southern Hemisphere wind-blown dust is not substantially different from that of the average Pb isotopic composition observed in Law Dome samples. Four inner core samples (IC5 - IC8) which featured high Ba concentrations but average Bi/Ba ratios (so as to minimise the isotopic influence from volcanogenic Pb) were selected to calculate the signature of this dust source. The average Pb isotope ratio calculated from these four IC samples is $^{206}\text{Pb}/^{207}\text{Pb} = 1.22$, $^{208}\text{Pb}/^{207}\text{Pb} = 2.46$ and $^{206}\text{Pb}/^{204}\text{Pb} = 17.8$. We attribute the spread of Pb isotopic signatures observed in Law Dome samples to changes in the proportions of crustal and volcanic Pb transported to Antarctica as well as changing sources of emission of crustal and volcanic Pb. Generally, Pb isotope ratios observed in Law Dome and Taylor Dome ice are located between our proposed Pb isotopic signature for crustal Pb and the Pb isotopic signature reported for Mount Erebus lavas, suggesting that Mount Erebus is the other main natural source of Pb deposited in Law Dome and Taylor Dome.

The second period of deposition of volcanic debris occurs from mid-1817 to mid-1818 and is denoted by increases in Pb/Ba and Bi/Ba ratios coincident with S inputs from Tambora, but the Pb isotope data suggest that Tambora was not the

emission source for Pb. In Figure 5, it can be seen that Pb/Ba and Bi/Ba ratios continue to increase after nssSO_4^{2-} inputs from Tambora have begun to decrease, suggesting that the Pb and Bi deposition is unassociated with that of S aerosols from Tambora. Ice core samples are not available above 41.717 m, so it cannot be established for how long Pb/Ba and Bi/Ba levels remained high after Ba and nssSO_4^{2-} concentrations return to normal levels about mid-1818. The Pb isotope data further supports the conclusion that Pb (and probably Bi) deposited in Law Dome did not originate from Tambora as Pb isotopic compositions observed in samples corresponding to the nssSO_4^{2-} concentration peak ('IC2', 'IC3': $^{206}\text{Pb}/^{207}\text{Pb}$ from 1.25 to 1.30, $^{208}\text{Pb}/^{207}\text{Pb}$ about 2.50) are similar to those reported for Mount Erebus lavas ($^{206}\text{Pb}/^{207}\text{Pb} > 1.25$, $^{208}\text{Pb}/^{207}\text{Pb} > 2.50$). From the data presented, we consider it most likely that the Pb and Bi enhancements observed in the Law Dome samples from mid-1817 to mid-1818 originate from the same volcanic source, that being Mount Erebus on Ross Island.

On the basis that Pb and Bi deposited in Law Dome between mid-1817 and mid-1818 originated from Mount Erebus rather than Tambora, we now consider the transport of volcanogenic Pb and Bi to Law Dome and the fate of any Pb and/or Bi aerosols that may have been emitted from Tambora eruption. While SO_2 fluxes or metal/ SO_4 ratios are not available for Tambora, such measurements have been reported for two other volcanoes in the Indonesian arc [17] and are taken as being representative of emissions from Tambora during its eruption in 1815 AD. Combining this data ($\text{Pb}/\text{S}=3.5 \times 10^{-4}$, $\text{Bi}/\text{S}=0.16 \times 10^{-4}$, as summarised in [9]) with the nssSO_4^{2-} concentration observed in Law Dome ice at the peak of the Tambora signal (190 ng/g), we calculate that approximately 22 pg Pb/g and 1 pg Bi/g should be present in sample 'IC3' if there was no loss of Pb or Bi during atmospheric transport

of aerosols from Tambora to Antarctica. Considering that the Pb and Bi concentrations observed in sample 'IC3' are 1.1 pg Pb/g and 34 fg Bi/g (including background contributions of 0.4 pg Pb/g and 3 fg Bi/g), we calculate that approximately 97% of any Pb and Bi that may have been emitted from Tambora was removed before the air-mass(es) reached Antarctica. If the eruption of Tambora did produce excess emissions of Pb and Bi, these were most likely lost from the atmosphere by coagulation and sedimentation processes [19].

On the balance of the data presented, the elevated Pb/Ba and Bi/Ba ratios observed in Law Dome ice from 1817 to 1818 AD are attributed to either increased emissions of Pb and Bi from Mount Erebus, or changes in the deposition of Pb, Ba and Bi resulting from climate changes induced by the eruption of Tambora. A better understanding of heavy metals emissions from Mount Erebus and the climatic alterations induced by large volcanic eruptions are required in order to draw further conclusions from the data presented here.

5. Conclusions

Lead and Bi enrichments, relative to Ba, observed in Law Dome ice indicate deposition of volcanic debris in Antarctica at mid - 1814 and from 1817 to mid - 1818 AD. While Pb isotopic compositions in dated core samples from that site indicate that both episodes are primarily due to emissions from Mount Erebus, the nssSO_4^{2-} signal in those core samples was observed in other Antarctic ice cores from 1817 to early-1818 and has been associated with the Tambora eruption. The data presented here suggests that any Pb and Bi aerosols that might be emitted into the stratosphere from large equatorial eruptions are removed from the atmosphere before

they can be transported to the Antarctic ice sheet. The period of atmospheric transport was taken to be the time delay between the eruption date and the observation of a nssSO_4^{2-} signal in Antarctic ice, this being about 1.6 years for the Tambora signal observed at Law Dome. While the isotopic evidence suggests that enhanced deposition of Pb and Bi to Law Dome observed about 1818 AD was not due to Pb emissions from Tambora, it has still to be established if this Pb and Bi enhancement was due to eruption-induced modifications to Antarctic meteorology and climate, or increased emissions from Mount Erebus. In contrast, the deposition of Pb and Bi in Law Dome snow dated to mid-1814 (and assigned to emissions from Mount Erebus) featured no corresponding increase in nssSO_4^{2-} , suggesting that the quiescently-emitted Pb and Bi were not attached to S aerosols or that Mount Erebus emissions contain relatively high proportions of Pb and Bi relative to S. More work is required to determine if excess metals are released during explosive volcanic eruptions, to characterise the metal-containing aerosols emitted into the atmosphere from quiescent and explosive volcanism and to identify the different mechanisms controlling the residence time and fate of these metal-containing aerosols when they are injected into the atmosphere at different altitudes.

Elevated Ba concentrations are observed from mid-1816 to mid-1818 and indicate enhanced inputs of rock and soil dust to the samples. While no evidence is available to associate enhanced atmospheric loading of rock and soil dust to the eruption of Tambora, this phenomenon is also worthy of further study on account of the potential climate-forcing resulting from the presence of greater-than-normal amounts of rock and soil dust in the atmosphere at that time.

These data indicate that major volcanic eruptions, such as that of Tambora, are not likely to have a great effect on the fluxes of heavy metals to the polar ice

sheets, on account of the coagulation and sedimentation processes which occur during the atmospheric transport of any aerosols emitted and the slow poleward transport of those aerosols in the stratosphere. It is necessary to further investigate emissions of heavy metals and S from Mount Erebus, and to accurately evaluate its contributions to the Antarctic ice sheet as the most significant source of volcanogenic aerosols in the Antarctic atmosphere. Similar studies of Pb isotopes should be undertaken for other volcanic SO₄ signals commonly identified in ice cores but occurring prior to the influence of industrial Pb emissions, such as Kuwae (1452) and Krakatau (1883). Such data will help to verify the extent to which volcanic eruptions influence Pb fluxes to Antarctica and enable Pb isotope-based evaluations of the sources of Pb deposited in the Antarctic ice sheet during these eruptions.

Acknowledgements

This research has been supported by grants from the Australian Research Council (A39938047) and the Antarctic Science Advisory Committee (No. 1092) in the Glaciology Section. We thank the reviewers, R. Flegal and C. Dick, for their comments which greatly improved the manuscript and T. Hinkley for advice regarding volcanic metal emissions. We also thank colleagues and students of the John de Laeter Centre of Mass Spectrometry - TIMS Laboratory and particularly D. Nelson, G. Burton and R. Loss for their helpful discussions. At the Antarctic CRC, we thank T. van Ommen, B. Smith, C. Dick, N. Petrie, A. Palmer and L. Robertson for their assistance and advice. The assistance of D. Mackey and J. O'Sullivan at the CSIRO Marine Laboratories, Hobart, and Viorel Paraschivoiu at the University of Adelaide is also acknowledged.

References

- [1] J.R. Petit, J. Jouzel, D. Raynaud, N.I. Barkov, J.-M. Barnola, I. Basile, M. Bender, J. Chappelaz, M. Davis, G. Delaygue, M. Delmotte, V.M. Kotlyakov, M. Legrand, V.Y. Lipenkov, C. Lorius, L. Pepin, C. Ritz, E. Saltzman, M. Stievenard, Climate and atmospheric history of the past 420,000 years from the Vostok ice core, Antarctica, *Nature* 399 (1999) 429-436.
- [2] C. Barbante, C. Turetta, G. Capodaglio, G. Scarponi, Recent decrease in the lead concentration of Antarctic snow, *Int. J. Environ. Anal. Chem.* 68 (1997) 457-477.
- [3] C.F. Boutron, C.C. Patterson, C. Lorius, V.N. Petrov, N.I. Barkov, Atmospheric lead in Antarctic ice during the last climatic cycle, *Ann. Glaciol.* 10 (1988) 5-9.
- [4] S. Hong, C.F. Boutron, R. Edwards, V.I. Morgan, Heavy Metals in Antarctic Ice from Law Dome: Initial Results, *Environ. Res.* 78 (1998) 94-103.
- [5] J.O. Nriagu, A global assessment of natural sources of atmospheric trace metals, *Nature* 338 (1989) 47-49.
- [6] E.W. Wolff, E.D. Suttie, Antarctic snow record of southern hemisphere lead pollution, *Geophys. Res. Lett.* 21 (1994) 781-784.
- [7] C.F. Boutron, C.C. Patterson, Lead concentration changes in Antarctic ice during the Wisconsin/Holocene transition, *Nature* 323 (1986) 222-225.
- [8] A. Matsumoto, T.K. Hinkley, Trace metal suites in Antarctic pre-industrial ice are consistent with emissions from quiescent degassing of volcanoes worldwide, *Earth Planet. Sci. Lett.* 186 (2001) 33-43.
- [9] T.K. Hinkley, P.J. Lamothe, S.A. Wilson, D.L. Finnegan, T.M. Gerlach, Metal emissions from Kilauea, and a suggested revision of the estimated worldwide metal

output by quiescent degassing of volcanoes, *Earth Planet. Sci. Lett.* 170 (1999) 315-325.

[10] T.K. Hinkley, M.F. Le Cloarec, G. Lambert, Fractionation of families of major, minor, and trace metals across the melt-vapor interface in volcanic exhalations, *Geochim. Cosmochim. Acta* 58 (1994) 3255-3263.

[11] C.C. Patterson, D.M. Settle, Magnitude of lead flux to the atmosphere from volcanoes, *Geochim. Cosmochim. Acta* 51 (1987) 675-681.

[12] T.K. Hinkley, Distribution of metals between particulate and gaseous forms in a volcanic plume, *Bull. Volcanol.* 53 (1991) 395-400.

[13] S. Hong, J.-P. Candelone, C.F. Boutron, Deposition of atmospheric heavy metals to the Greenland ice sheet from the 1783-1784 volcanic eruption of Laki, Iceland, *Earth Planet. Sci. Lett.* 144 (1996) 605-610.

[14] J.-P. Candelone, S. Hong, C. Pellone, C.F. Boutron, Post-Industrial Revolution changes in large-scale atmospheric pollution of the northern hemisphere by heavy metals as documented in central Greenland snow and ice, *J. Geophys. Res.* 100 (1995) 16605-16616.

[15] T. Thordarson, S. Self, The Laki (Skaftar Fires) and Grimsvötn eruptions in 1783-1785, *Bull. Volcanol.* 55 (1993) 233-263.

[16] T. Thordarson, S. Self, Atmospheric and environmental effects of the 1783-1784 Laki eruption: A review and reassessment, *J. Geophys. Res.* 108(D1) (2003) doi: 10.1029/2001JD002042.

[17] E.-Y. Nho, M.F. Le Cloarec, B. Ardouin, W.S. Tjetjep, Source strength assessment of volcanic trace elements emitted from the Indonesian arc, *J. Volcanol. Geotherm. Res.* 74 (1996) 121-129.

- [18] D.M. Pyle, Sizes of volcanic eruptions, in: H. Sigurdsson (Ed.), *Encyclopedia of Volcanoes*, Academic Press, Sydney, 2000, pp. 263-269.
- [19] M.J. Mills, Volcanic aerosol and global atmospheric effects, in: H. Sigurdsson (Ed.), *Encyclopedia of Volcanoes*, Academic Press, Sydney, 2000, pp. 931- 943.
- [20] C.U. Hammer, H.B. Clausen, W. Dansgaard, Greenland ice sheet evidence of post-glacial volcanism and its climatic impact, *Nature* 288 (1980) 230-235.
- [21] H.B. Clausen, C.U. Hammer, C.S. Hvidberg, D. Dahl-Jensen, J.P. Steffensen, A comparison of the volcanic records over the past 4000 years from the Greenland Ice Core Project and Dye 3 Greenland ice cores, *J. Geophys. Res.* 102 (1997) 26707-26723.
- [22] J. Cole-Dai, E. Mosley-Thompson, L.G. Thompson, Annually resolved southern hemisphere volcanic history from two Antarctic ice cores., *J. Geophys. Res.* 102 (1997) 16761-16771.
- [23] A.S. Palmer, T.D. van Ommen, M.A.J. Curran, V. Morgan, J.M. Souney, P.A. Mayewski, High precision dating of volcanic events (A.D. 1301-1995) using ice cores from Law Dome, Antarctica, *J. Geophys. Res.* 106 (2001) 28089-28095.
- [24] R. Udisti, S. Becagli, E. Castellano, R. Mulvaney, J. Schwander, S. Torcini, E. Wolff, Holocene electrical and chemical measurements from the EPICA-Dome C ice core, *Ann. Glaciol.* 30 (2000) 20-26.
- [25] P. Vallelonga, K. Van de Velde, J.-P. Candelone, V.I. Morgan, C.F. Boutron, K.J.R. Rosman, The lead pollution history of Law Dome, Antarctica, from isotopic measurements on ice cores: 1500 AD to 1989 AD, *Earth Planet. Sci. Lett.* 204 (2002) 291-306.

- [26] C.C. Patterson, D.M. Settle, Review of data on eolian fluxes of industrial and natural lead to the lands and seas in remote regions on a global lead scale, *Mar. Chem.* 22 (1987) 137-162.
- [27] C.P. Ferrari, S. Hong, K. Van de Velde, C.F. Boutron, S.N. Rudniev, M. Bolshov, W. Chisholm, K.J.R. Rosman, Natural and anthropogenic bismuth in Central Greenland, *Atmos. Environ.* 34 (2000) 941-948.
- [28] V. Morgan, C.W. Wookey, J. Li, T.D. van Ommen, W. Skinner, M.F. Fitzpatrick, Site information and initial results from deep ice drilling on Law Dome, Antarctica, *J. Glaciol.* 43 (1997) 3-10.
- [29] M.A.J. Curran, T.D. van Ommen, V. Morgan, Seasonal characteristics of the major ions in the high-accumulation Dome Summit South ice core, Law Dome, Antarctica, *Ann. Glaciol.* 27 (1998) 385-390.
- [30] C.U. Hammer, Acidity of polar ice cores in relation to absolute dating, past volcanism, and radio-echoes, *J. Glaciol.* 25 (1980) 359-372.
- [31] P. Vallelonga, K. Van de Velde, J.-P. Candelone, C. Ly, K.J.R. Rosman, C.F. Boutron, V.I. Morgan, D.J. Mackey, Recent advances in measurement of Pb isotopes in Polar ice and snow at sub-picogram per gram concentrations using Thermal Ionisation Mass Spectrometry, *Anal. Chim. Acta* 453 (2002) 1-12.
- [32] J.-P. Candelone, S. Hong, C.F. Boutron, An improved method for decontaminating polar snow or ice cores for heavy metal analysis, *Anal. Chim. Acta* 299 (1994) 9-16.
- [33] W. Chisholm, K.J.R. Rosman, J.-P. Candelone, C.F. Boutron, M.A. Bolshov, Measurement of bismuth at pg g^{-1} concentrations in snow and ice samples by thermal ionisation mass spectrometry, *Anal. Chim. Acta* 347 (1997) 351-358.

- [34] K.J.R. Rosman, W. Chisholm, C.F. Boutron, S. Hong, R. Edwards, V. Morgan, P.N. Sedwick, Lead isotopes and selected metals in ice from Law Dome, Antarctica, *Ann. Glaciol.* 27 (1998) 349-354.
- [35] K.J.R. Rosman, Natural isotopic variations in lead in polar snow and ice as indicators of source regions, in: S. Caroli, P. Cescon, D.W.H. Walton (Eds.), *Environmental contamination in Antarctica: A challenge to analytical chemistry*, Elsevier Science B.V., New York, 2001, pp. 87-106.
- [36] S.S. Sun, G.H. Hanson, Origin of Ross Island Basanitoids and Limitations upon the Heterogeneity of Mantle Sources for Alkali Basalts and Nephelinites, *Contrib. Mineral. Petrol.* 52 (1975) 77-106.
- [37] S. Turner, J. Foden, U, Th and Ra disequilibria, Sr, Nd and Pb isotope and trace element variations in Sunda arc lavas: predominance of a subducted sediment component, *Contrib. Mineral. Petrol.* 142 (2001) 43-57.
- [38] G. Zreda-Gostynska, P.R. Kyle, D. Finnegan, Chlorine, fluorine, and sulfur emissions from Mount Erebus, Antarctica and estimated contributions to the Antarctic atmosphere, *Geophys. Res. Lett.* 20 (1993) 1959-1962.
- [39] E.W. Wolff, Signals of atmospheric pollution in polar snow and ice, *Antarctic Sci.* 2 (1990) 189-205.

Table 1. Concentrations of non-sea salt SO_4^{2-} , Ba, Bi and Pb and Pb isotope ratios measured in Law Dome ice core sections. The 'TOP' profile corresponds to inner core pieces IC1-IC4, the 'MID' profile corresponds to inner core pieces IC5-IC9 and 'BOT' profile corresponds to inner core pieces IC10-IC15.

	middle depth	nsSSO_4^{2-} conc (ng/g)	Ba conc ($\mu\text{g/g}$)	Bi conc (fg/g)	Pb conc (pg/g)	$^{206}\text{Pb}/^{207}\text{Pb}$ 95% C.I.	$^{208}\text{Pb}/^{207}\text{Pb}$ 95% C.I.	$^{206}\text{Pb}/^{204}\text{Pb}$ 95% C.I.	Pb/Ba	Bi/Ba (x1000)		
TOP External layer		28.40	132193	53.69	1.176	0.004	2.420	0.002	18.4	0.1	1.89	4654
TOP 2nd layer		6.72	61	3.14	1.169	0.004	2.416	0.033	17.9	0.3	0.47	9
TOP 3rd layer		2.97	107	1.06	1.218	0.010	2.460	0.017	18.8	0.3	0.36	36
TOP Weighted average Inner Core		2.32	42	0.80	1.234		2.459		19.4		0.34	18
MID External layer		4.34	2642	4.73	1.191	0.005	2.430	0.018	18.5	0.2	1.09	609
MID 2nd layer		3.51	15	0.56	1.212	0.010	2.445	0.028	18.1	1.9	0.16	4
MID 3rd layer		6.30	11	0.41	1.216	0.012	2.476	0.017	19.3	0.7	0.06	2
MID Weighted average Inner Core		3.77	11	0.49	1.224		2.475		18.1		0.13	3
BOT External Layer		5.63	48434	24.05	1.179	0.001	2.424	0.007	18.4	0.1	4.27	8604
BOT 2nd layer		4.97	383	1.72	1.173	0.005	2.418	0.013	18.2	0.3	0.35	77
BOT 3rd layer		0.86	6	0.46	1.211	0.011	2.451	0.019	19.4	0.7	0.54	7
BOT Weighted average Inner Core		0.92	7	0.31	1.203		2.440		18.9		0.34	7
IC1 (~1818.5)	41.752	113	1.09	39	< 0.69	0.019	> 2.366	0.027	> 18.3	2.4	< 0.63	36
IC2 (~1818)	41.802	155	3.00	57	0.81	0.015	2.508	0.028	19.6	1.3	0.27	19
IC3 (~1817.8)	41.847	190	2.61	34	1.03	0.010	2.502	0.012	20.5	0.4	0.40	13
IC3 (~1817.8)	41.847	190	2.81	35	1.25	0.005	2.500	0.013	19.7	0.5	0.45	12
IC4 (~1817.5)	41.897	194	2.59	18	0.55	0.014	2.462	0.015	19.2	2.1	0.21	7
IC5 (~1817.2)	41.947	143	8.22	30	0.79	0.009	2.475	0.005	18.6	0.4	0.10	4
IC6 (~1817)	41.992	77	3.56	4	0.48	0.009	2.450	0.011	18.2	1.0	0.14	1
IC7 (~1816.8)	42.042	63	3.77	15	0.45	0.005	2.439	0.040	16.0	1.9	0.12	4
IC8 (~1816.5)	42.102	45	3.88	11	0.44	0.015	2.485	0.021	18.5	0.5	0.11	3
IC9 (~1816.2)	42.172	40	1.01	1	0.34	0.008	2.502	0.037	18.7	1.1	0.33	1
IC10 (~1815.8)	42.259	14	1.51	4	0.38	0.007	2.419	0.027	16.9	1.2	0.25	3
IC11 (~1815.5)	42.329	7	1.65	5	0.14	0.018	2.440	0.012	19.6	1.6	0.09	3
IC12 (~1815)	42.399	16	0.71	4	0.15	0.028	2.443	0.031	21.5	2.9	0.21	6
IC13 (~1814.8)	42.469	36	0.47	3	0.24	0.014	2.472	0.038	19.8	1.7	0.50	6
IC14 (~1814.5)	42.539	12	0.75	23	0.69	0.008	2.517	0.035	18.9	1.9	0.92	31
IC15 (~1814.2)	42.609	16	0.41	2	< 0.21	0.019	> 2.347	0.022	> 16.9	0.9	< 0.50	5

Figure captions.

Figure 1. Location of Law Dome where the DSS-W20k ice core was drilled (66.8°S, 112.4°E), the Mount Erebus volcano (77.5°S, 167.2°E) on Ross Island, Antarctica, and the Tambora volcano (8.5°S, 117.4°E) on Flores Island, Indonesia. The equator is shown as a dotted line.

Figure 2. Changes in nssSO_4^{2-} concentration with depth in the DSS-W20k ice core. The start of each year of snow deposition is shown as a vertical downward arrow, and is based on the DSS core dating [23]. The signal observed at 1811-1812 AD corresponds to the unidentified volcanic eruption of 1809, while that at 1817-1818 AD corresponds to deposition of SO_4^{2-} resulting from the eruption of Tambora in April 1815 AD.

Figure 3. The depths (in metres) corresponding to each piece of the inner core (numbered 1 to 15) obtained from the DSS-W20k ice core. Concentric layer profiles collected are designated 'TOP', 'MID' and 'BOT', as shown. Locations of winter maxima of various chemical ions (Cl^- , Na^+ , K^+ and Mg^{2+}) are also indicated. Samples numbered 1...15 correspond to those designated IC1...IC15 in the text and Figure 5.

Figure 4. $^{206}\text{Pb}/^{207}\text{Pb}$ vs $^{208}\text{Pb}/^{207}\text{Pb}$ isotope ratios measured in Law Dome ice. Also shown are Pb isotopic signatures for relevant source materials such as pre-industrial Law Dome samples [25], Mount Erebus lavas [36], Indonesian island-arc lavas [37] and Taylor Dome ice [8]. Error bars shown are 95% confidence intervals. Samples numbered 1...15 correspond to those designated IC1...IC15 in the text and Figure 5.

Figure 5. a) Variations in Pb/Ba (x20) and Bi/Ba ratios and nssSO_4^{2-} concentrations with depth in the DSS-W20k ice core. Elevated nssSO_4^{2-} concentrations are clearly discernible between 41.77 m and 41.98 m. b) Variations in Pb concentrations and $^{206}\text{Pb}/^{207}\text{Pb}$ isotope ratios with depth. Samples were obtained from a 1 m length of ice broken into two pieces at 42.217 m depth, indicated by a bold dotted line. Concentrations are quoted to an accuracy of $\pm 15\%$ for Pb and Ba and $\pm 50\%$ for Bi. Error bars shown for $^{206}\text{Pb}/^{207}\text{Pb}$ ratios are 95% confidence intervals. Samples designated IC1...IC15 correspond to those numbered 1...15 in Figures 3 and 4.

Figure 1

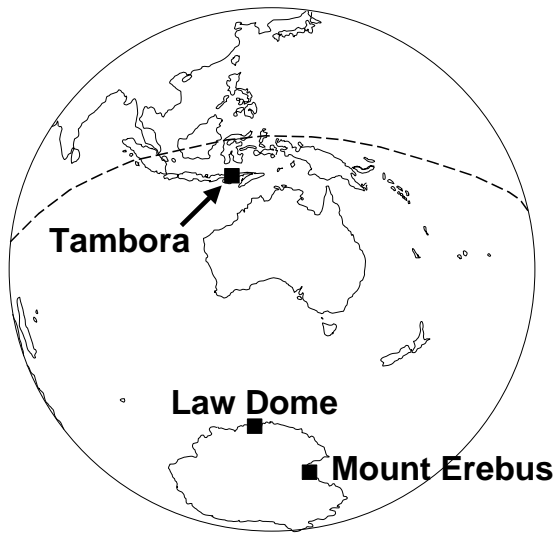


Figure 2

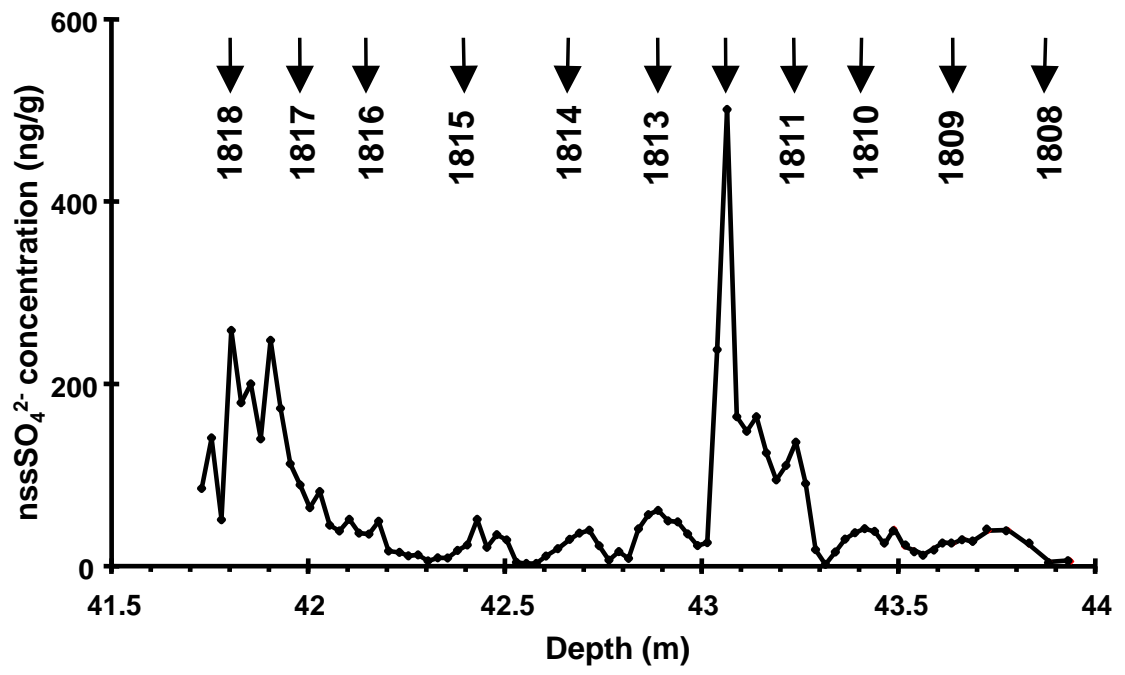


Figure 3

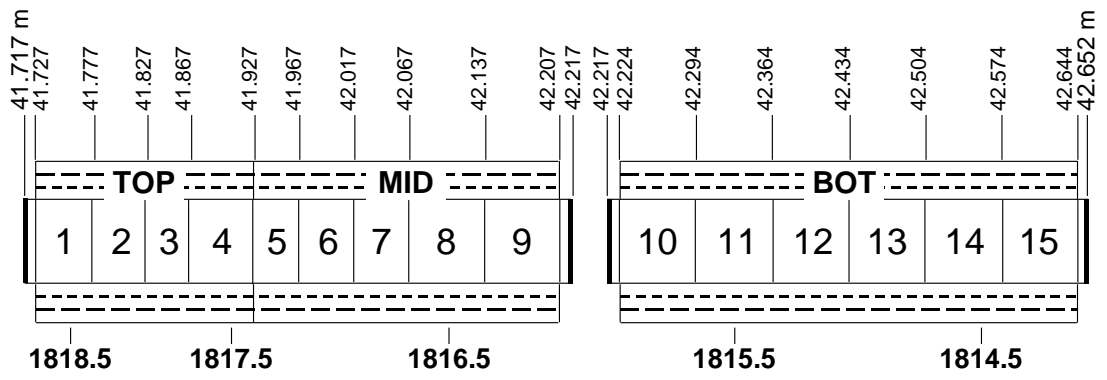


Figure 4

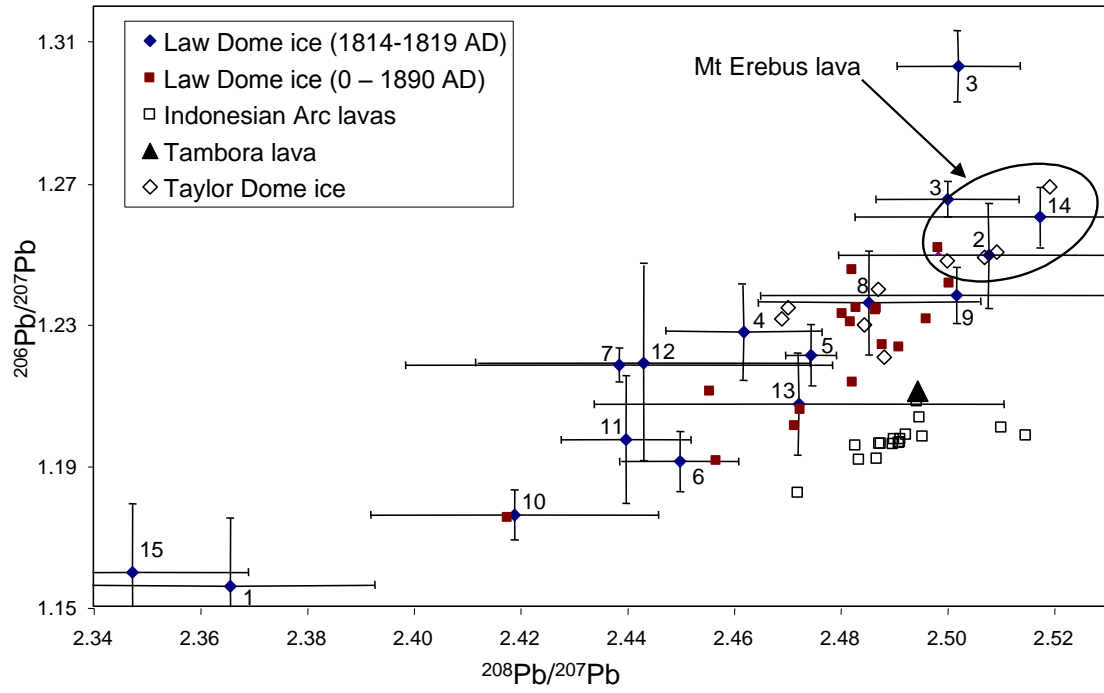
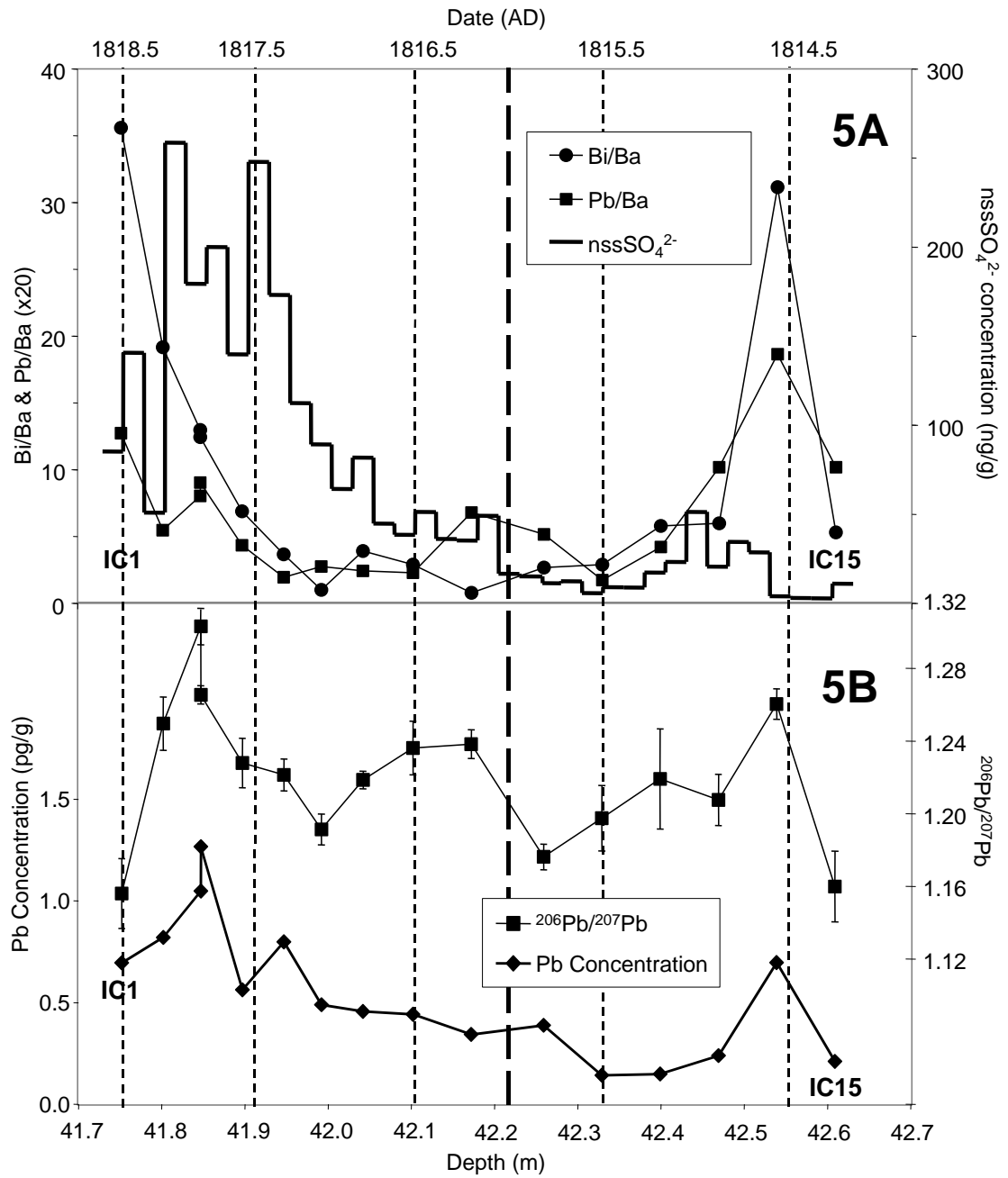


Figure 5



4.7 Natural Pb deposition in Antarctica, and the influence of Mount Erebus.

Across Antarctica, the variability observed in Pb fluxes derived from natural sources is primarily due to presence of local Pb emission sources. Evaluations of proxies for various natural emission sources of Pb (such as Na^+ for marine aerosols and SO_4^{2-} for volcanism) have shown that coastal locations are generally more susceptible to Pb inputs from marine aerosols, while other sites, such as those in Victoria Land, are more influenced by volcanic Pb emissions from Mount Erebus. While there appears to be no significant influence of marine aerosol Pb at Dome C, the two Pb isotopic compositions available from that location represent inputs from rock and soil dust as well as volcanism. Of the available Pb isotope data, Coats Land is the only site where a Pb isotopic signal consistent with that of Mount Erebus has not been identified, however all of the Coats Land samples were influenced by anthropogenic Pb. Until a reliable value for the Coats Land background Pb isotopic composition have been established, the influence of Mount Erebus at that location is unknown. Wolff and Suttie (1994) calculated a volcanic Pb contribution of ~19% for the Coats Land site, however it is yet to be established if that volcanic contribution derives from Mount Erebus, or from other southern hemisphere sources. From evaluations of the Pb isotopic compositions observed in various Victoria Land and Law Dome samples, the contribution of Pb emissions from Mount Erebus have been calculated at ~75% (~ 0.45 pg Pb/g) and ~57% (~0.21 pg Pb/g) of natural Pb inputs to Victoria Land and Law Dome, respectively. It is apparent that Pb emissions from Mount Erebus can be observed in the Pb isotopic records of Dome C and Law Dome, however samples predating anthropogenic Pb inputs will be required to establish if Mount Erebus is a significant source of natural Pb inputs to Coats Land. In order to establish the full extent of the influence of Mount Erebus' Pb emissions to the Antarctic ice sheet, it would be of value to obtain ice core records from the south pole as well as from the opposite side of Antarctica (longitudes in the vicinity of 0°), such as Dome Fuji or Princess Elizabeth Land.

Table 4.3 shows a summary of the calculated crustal Pb inputs to various sites in Antarctica. From the table, it can be seen that the crustal Pb inputs calculated for Victoria Land and Coats Land in this study are quite different to previous estimates,

however the proportion of crustal Pb to natural Pb calculated is in agreement with those previous calculated. Crustal Pb inputs to Victoria Land and Taylor Dome are generally greater in quantity than at other Antarctic locations, probably due to the input of rock and soil dust from weathering of local exposed rock outcrops and/or from sedimentary deposits. Other Antarctic locations, located far from the TransAntarctic mountains, generally have lower crustal Pb inputs <0.4 pg Pb/g.

Table 4.3 Summary of crustal Pb inputs at various locations in Antarctica.

Location	Crustal Pb input	
	(pg/g)	% of total
Coats Land		
Wolff and Suttie (1994)	0.4	~19%
This study (data, Planchon et al. 2002b)	0.15	~25-50%
Victoria Land		
Barbante et al. (1997)	0.07	20-30%
This study (data, pers. comm. K. Rosman)	0.62	16-36%
Taylor Dome		
Matsumoto and Hinkley (2001)	<0.45	<5%
Law Dome		
Hong et al. (1996)	<0.1	1-20%
This study (Vallelonga et al. 2002b)	0.04	5-32%
Dome C		
Boutron and Patterson (1986)	0.2	50%

Do fluxes of Pb and Ba to Law Dome vary seasonally, does the Pb isotope signal at Law Dome display seasonal variability?

4.8 Seasonal variations of Pb in Law Dome snow, 1980 – 1985 AD.

The Law Dome site presents an excellent location for the investigation of seasonal variations in the deposition of Pb and Ba. For seasonal studies to be reliable and accurate, the location should feature a high snow accumulation rate and should experience regular snowfall throughout the year. Such conditions occur at Law Dome, where the annual meteorology and snowfall characteristics have been monitored in detail since the early 1990's, and high-resolution measurements of seasonal variations in major ions, peroxide and $\delta^{18}\text{O}$ are available for many years. From these data, it has been shown that snowfall over the Law Dome summit is dominated by cyclonic systems which form over the Southern Ocean at latitudes $\sim 65^\circ$ S, with relatively little influence from inland katabatic winds (Morgan et al. 1997). Recently, "drought" events have been observed, in which winter accumulation decreases significantly, but normally, snow accumulation at Law Dome is regular throughout the year (McMorrow et al. 2002). The snow accumulation rate at the Law Dome summit is also particularly high, ~ 600 kg/m²/yr, equivalent to over a metre of snowfall each year. Overall, these characteristics enable seasonal studies to be undertaken with confidence that the observed variations in metal deposition are related to seasonal effects, and that there is sufficient snow deposited to enable the accurate measurement of Pb in samples corresponding to as short a time as a month.

Six sections of the DSS-W2k core, drilled in 1990 approximately 2 km west of the DSSmain drilling site, were obtained for seasonal analyses of Pb isotopes and Pb and Ba concentrations. These were decontaminated using the same procedure as that adopted for the high-resolution sampling of the DSS-W20k core sections corresponding to the Tambora eruption. Evaluations of the core decontamination plateaus indicate that pristine inner core samples were obtained in all cases. Data pertaining to these samples are included in Appendix 2. The collected samples represent snowfall at Law Dome from Spring 1981 (18.1 m) to Winter 1983 (15.67 m), Spring 1983 (15.35 m) to Autumn 1984 (14.9 m) and from Autumn 1985 (14 m) to Spring 1985 (12.9 m). The samples were collected at differing resolutions, with 21

samples obtained for the period Autumn 1985 – Spring 1985 (~6 cm/sample), only 4 samples obtained from Spring 1983 to Autumn 1984 (~12 cm/sample), and 32 samples obtained from Spring 1981 to Winter 1983 (6-10 cm/sample). Overall, the periods Spring 1981 – Winter 1983 and Autumn 1985 – Spring 1985 have been sampled with sufficient resolution to enable an in-depth analysis of Pb and Ba deposition at Law Dome. The density of sampling, and inclusion of Pb isotopes measurements enables the Law Dome seasonal record presented here to be the most detailed seasonal record of Pb deposition in polar snow. The dating of the samples has been established by high-resolution measurements of $\delta^{18}\text{O}$ values in the samples, also included in Appendix 2, which have been referenced to those values observed in the DSS-W0k and DSSmain ice cores (see Figure 4.11). $\delta^{18}\text{O}$ data are not available for DSS-W2k core #16 (13.61m – 14.65 m), so the seasonal dating applied to this depth interval has been taken from the DSS-W0k core. From figure 4.11, it can be seen that there is good correspondence between the $\delta^{18}\text{O}$ signals observed in the two snow records, so a limited section of the DSS-W0k core $\delta^{18}\text{O}$ record can be used to accurately represent that of the DSS-W2k core.

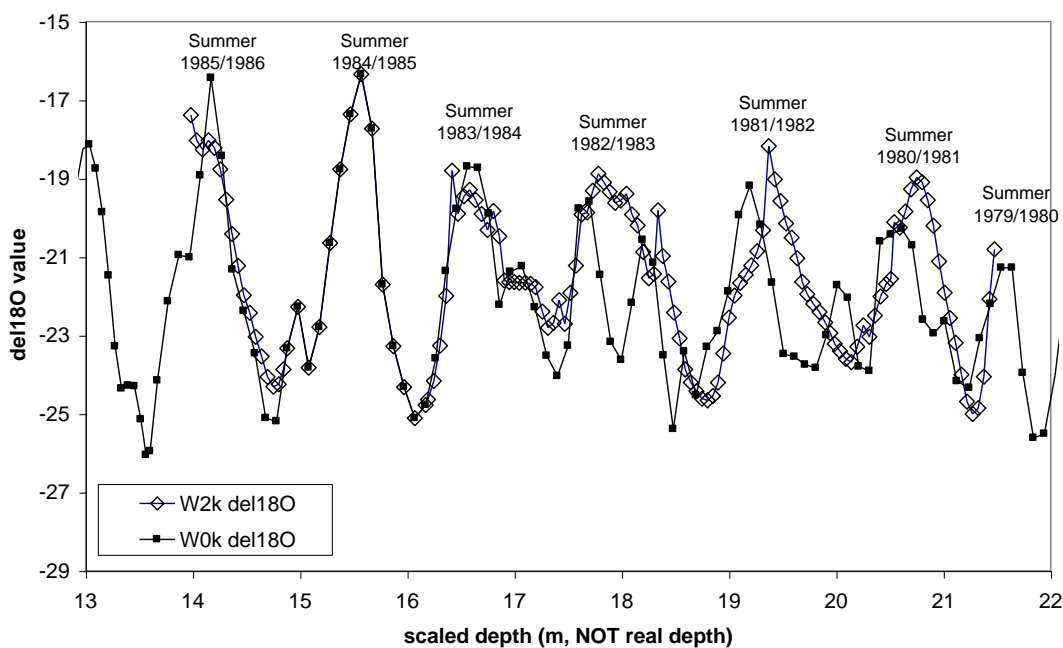


Figure 4.11. $\delta^{18}\text{O}$ values for two Law Dome Summit cores, DSS-W2k and DSS-W0k over the period summer 1979/1980 to summer 1985/1986.

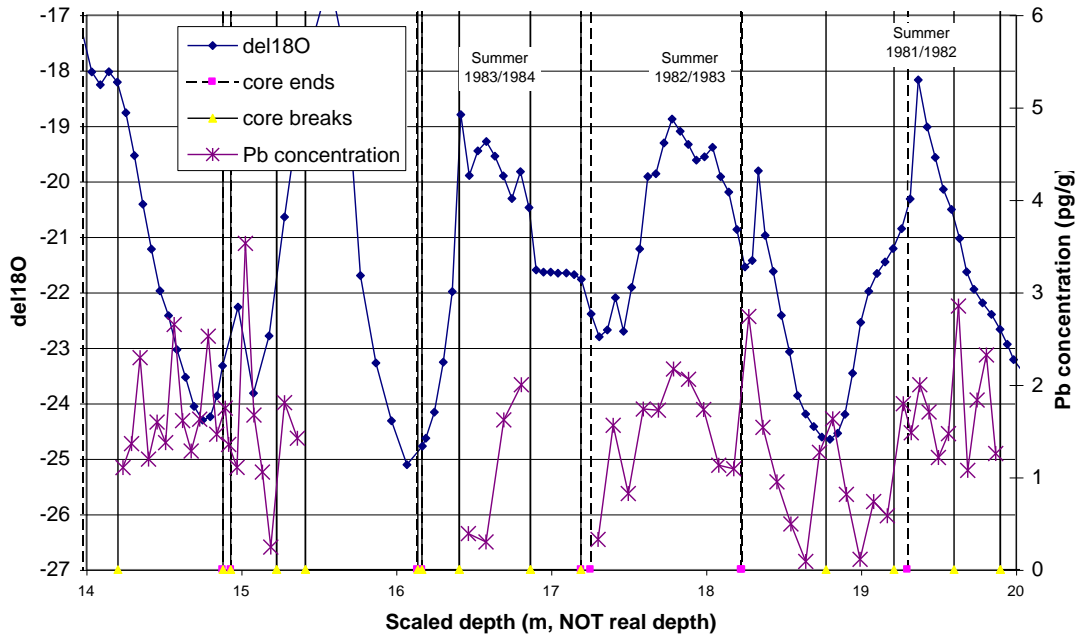


Figure 4.12. $\delta^{18}\text{O}$ values and Pb concentrations measured in DSS-W2k core sections dating from summer 1979/1980 to summer 1985/1986.

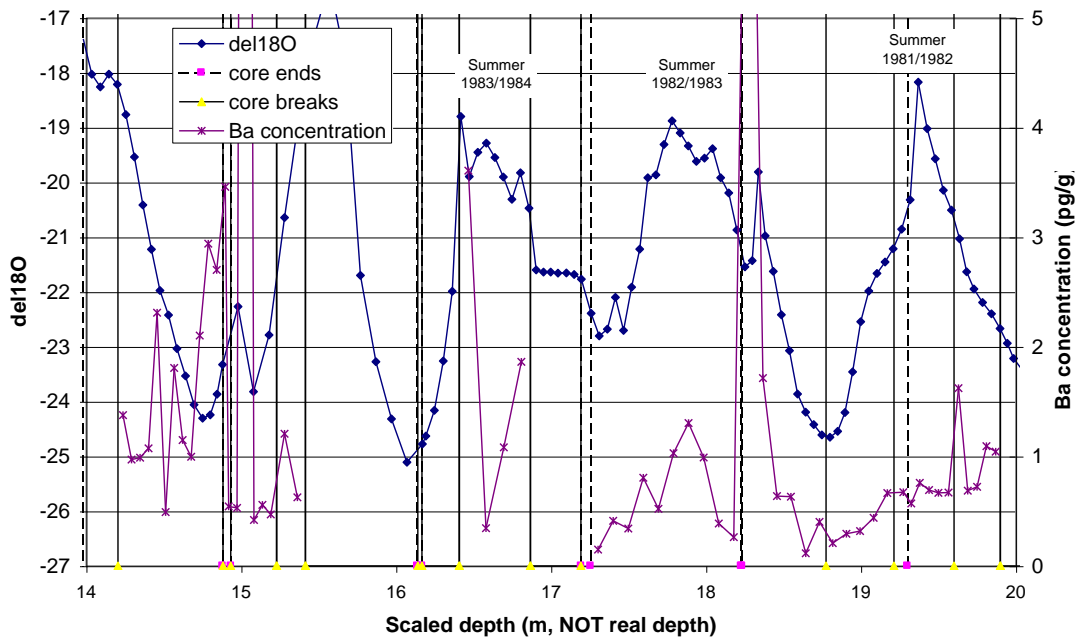


Figure 4.13. $\delta^{18}\text{O}$ values and Ba concentrations measured in DSS-W2k core sections dating from summer 1979/1980 to summer 1985/1986.

The seasonal record of Pb and Ba deposition is shown in Figures 4.12 and 4.13. In figure 4.12, it can be seen that the Pb concentration varies from ~ 0.1 pg/g (Winter 1982) to ~ 3.5 pg/g (Autumn/Winter 1985), with an overall average concentration of

1.5 pg Pb/g. Generally, it can be seen that Pb levels are high during the Summers of 1981/82 and 1982/83, with lower concentrations during Autumn and Spring of 1982. Lower Pb concentrations occur in the Autumn/Winter of 1983 and Summer of 1983/84. In Winter 1985, the Pb concentrations are systematically higher than those observed in previous winters. Low Pb concentrations are briefly occur in the Autumn of 1985, however. Generally, it appears that Pb concentrations in Law Dome precipitation are high in Summer, with lower Pb concentrations during Autumn and Spring. Relatively high Pb concentrations occur in Winter 1985, however. Short-lived episodes of high Pb concentration, likely to represent inputs of anthropogenic Pb from continental sources, occur in Spring of 1981 (2.85 pg/g) and Spring of 1982 (2.74 pg/g) and on three occasions during Winter/Spring of 1985 (3.5, 2.6 and 2.5 pg/g). Generally similar trends occur for Ba (figure 4.13) as for Pb, with higher concentrations during Summer 1981/82 and 1982/83 and lower Pb concentrations during the winters of 1982 and 1983. Once again, the opposite trend occurs in 1985, with higher Ba concentrations during the winter. On four occasions, extremely high Ba concentrations were observed, which may represent relatively direct transport of continental dust from southern hemisphere landmasses to Law Dome. In these four samples, crustal Pb does not contribute more than 55% of total Pb in the sample, and Pb isotopic compositions are not dissimilar to other samples, indicating that these significant dust inputs are neither frequent nor significant relative to other anthropogenic and natural sources of Pb. Dust inputs are least significant during summer, with crustal Pb contributions ~1.5% of total Pb, while during the Autumn/Spring season, the crustal Pb contribution increases to 3-6%. During the period Autumn-Spring in 1985, Ba concentrations were higher than during the period Winter 1981 - Winter 1983. Figure 4.14 shows seasonal changes in Pb/Ba ratios at Law Dome. Generally the Pb/Ba ratios are lower in Autumn and Spring than in Summer, however there is significant variability in the data. Systematically high Pb/Ba ratios occur in Summer 1981/1982 and Autumn/Winter 1983. Lower Pb/Ba values occur in Autumn and Spring of 1982 and Summer 1982/1983. In 1985, high Pb/Ba ratios occur in Autumn and Spring, with low values in winter, however the data vary greatly.

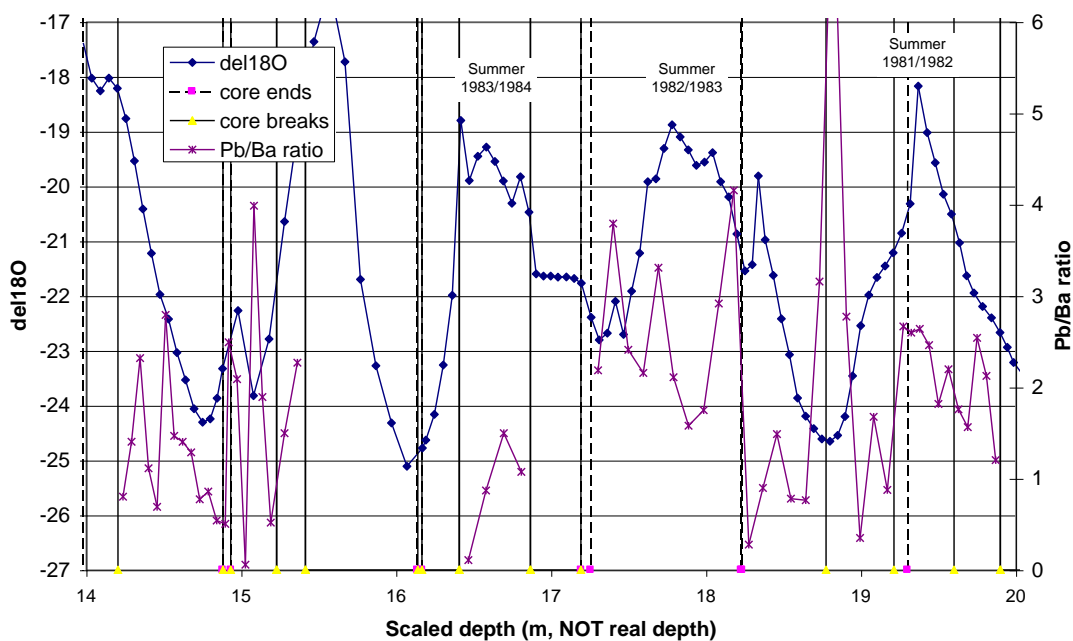


Figure 4.14. $\delta^{18}\text{O}$ values and Pb/Ba ratios measured in DSS-W2k core sections dating from summer 1979/1980 to summer 1985/1986.

Overall, the Pb and Ba concentration data collected for seasonal variations suggest that crustal dust inputs are more significant during Autumn and Spring seasons, while higher Pb concentrations occur in the Summer. The presence of crustal Pb during Autumn and Spring corresponds with the storm events and lower-latitude cyclonic air masses which pass over Law Dome during the winter months (McMorrow et al. 2002). During summer months, maxima of SO_4^{2-} and MSA concentrations have been observed at Law Dome (Curran et al. 1998). These chemicals are indicators of marine biogenic activity and volcanic activity, which are likely sources of natural Pb inputs to Law Dome, particularly considering that crustal Pb regularly contributes less than 32% of total natural Pb inputs to Law Dome. Our observations of higher Pb concentrations in summer compared to winter contradict those of Hong et al (1998) at Law Dome and those of (Suttie and Wolff, 1992) on the Antarctic Peninsula. While it is likely that the samples analysed by Hong et al. (1998) were affected by contamination, it appears that the pattern of Pb deposition at the Antarctic Peninsula is different to that observed at Law Dome. The data presented here clearly shows the variability in Pb and Ba deposition at Law Dome through several annual cycles. In particular, it can be seen that the signal is regularly punctuated by episodes of high Pb and/or Ba concentration, representing deposition

from individual air masses or storm systems. The Law Dome data is more detailed than any other seasonal evaluation of Antarctic Pb fluxes, however it is still limited by the absence of detailed snow accumulation data. More data are needed to explain why the patterns of Pb and Ba deposition during Autumn-Spring 1984 are not consistent with those observed from Winter 1981 to Winter 1983.

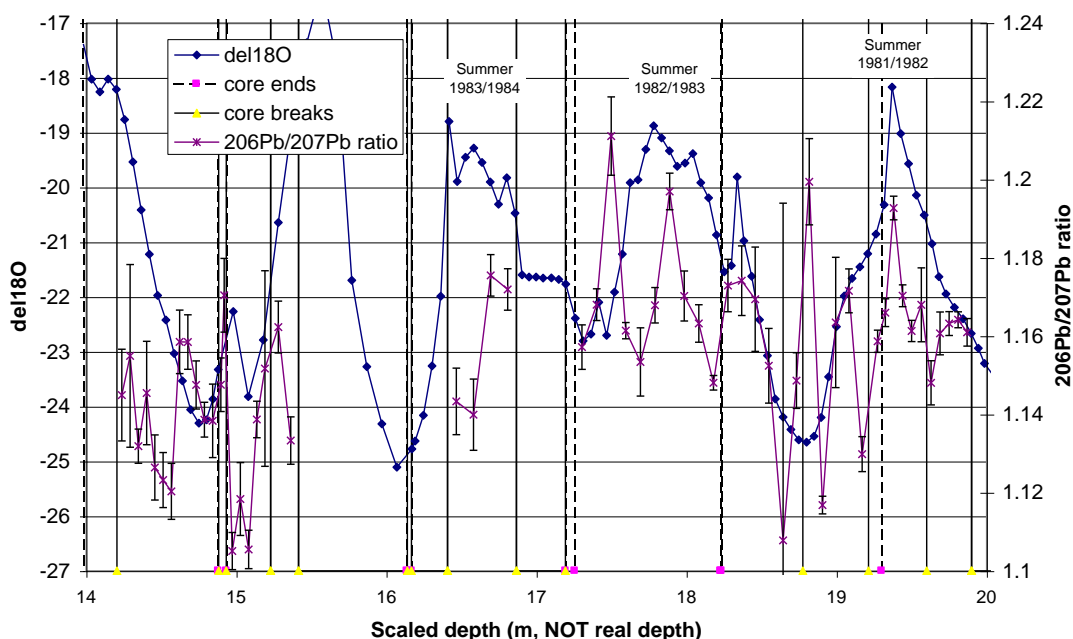


Figure 4.15. $\delta^{18}\text{O}$ values and $^{206}\text{Pb}/^{207}\text{Pb}$ ratios measured in DSS-W2k core sections dating from summer 1979/1980 to summer 1985/1986. Uncertainties shown are 95% confidence intervals.

A more satisfactory understanding of the varying seasonal fluxes of anthropogenic and natural Pb to Law Dome is provided by an examination of the Pb isotopes. In Figure 4.15, $^{206}\text{Pb}/^{207}\text{Pb}$ ratios are shown, indicating the variation in sources of Pb to Law Dome over time. Figure 4.16 shows $^{206}\text{Pb}/^{207}\text{Pb}$ and $^{208}\text{Pb}/^{207}\text{Pb}$ ratios for the Law Dome snow samples, as well as pre-industrial Law Dome ice and signatures representative of potential southern hemisphere Pb emission sources, including circum-Antarctic seawater (Flegal et al. 1993), Ross Island rocks (Sun and Hanson 1975), South Atlantic Ocean pelagic sediments (Chow and Patterson 1962), South Sandwich Island sediments (Barreiro 1983) and various aerosols collected in the Southern Hemisphere during the 1990's (Bollhöfer and Rosman 2000). In Figure 4.16 it can be seen that all of the Law Dome snow samples are displaced from the

signatures of pre-industrial Law Dome ice, indicating the dominance of anthropogenic Pb emissions to Law Dome during the early 1980's. The Pb isotopic composition of recent Law Dome snow (1980-1985 AD) is in good agreement with those observed in circum-Antarctic seawaters collected in 1987/88 (Flegal et al. 1993). In figure 4.15, it can be seen that between Winter/Spring 1981 and Winter 1983, $^{206}\text{Pb}/^{207}\text{Pb}$ ratios are usually ~ 1.16 , but are consistently lower during 1984. During the period Winter/Spring 1981 – Winter 1983, it appears that variations in $^{206}\text{Pb}/^{207}\text{Pb}$ ratio are relatively short-lived, and can vary from sample-to-sample. This variability from sample-to-sample is most prominent during the Autumn/Winter period of 1982, when $^{206}\text{Pb}/^{207}\text{Pb}$ ratios vary from ~ 1.12 to ~ 1.20 and then back to ~ 1.11 in less than a few months' time. Samples with low $^{206}\text{Pb}/^{207}\text{Pb}$ ratios (indicating significant anthropogenic Pb inputs) usually also have low Pb concentrations, while those with high $^{206}\text{Pb}/^{207}\text{Pb}$ ratios usually also have high Pb concentrations. It is of interest that the average $^{206}\text{Pb}/^{207}\text{Pb}$ ratio observed at Law Dome during this period, ~ 1.16 , is similar to the signature of "background" Antarctic Pb described by Rosman et al. (1994) and the average $^{206}\text{Pb}/^{207}\text{Pb}$ ratio observed by Flegal et al. (1993) in circum-Antarctic seawater collected in 1987 and 1988. This signature is likely to represent a mixture of Pb emitted from various countries in the southern hemisphere, which each consumed different mixtures of US Mississippi valley-type Pb ($^{206}\text{Pb}/^{207}\text{Pb} \sim 1.3$) and Australian and Canadian Pb ($^{206}\text{Pb}/^{207}\text{Pb} \sim 1.06$). During the 1990's, lower $^{206}\text{Pb}/^{207}\text{Pb}$ ratios (< 1.10) were observed in more southern cities, such as Villa Rica, Puerto Natales and Punta Arenas (Chile), Harare (Zimbabwe), East London, Reunion Island, Pretoria and Cape Town (South Africa), Perth, Melbourne, Sydney and Hobart (Australia) and Christchurch and Auckland (New Zealand). The "background" Antarctic $^{206}\text{Pb}/^{207}\text{Pb}$ ratio (~ 1.16) is generally similar to $^{206}\text{Pb}/^{207}\text{Pb}$ values observed in some South American cities during the 1990's, including Quito (Ecuador), Buenos Aires and Rio Gallegos (Argentina), Santiago (Chile) and Rio de Janeiro and Sao Paulo (Brazil). Statistics indicate that South America was the greatest consumer of alkyllead gasoline additives in the Southern Hemisphere from 1962 to 1992 (Barbante et al. 1997).

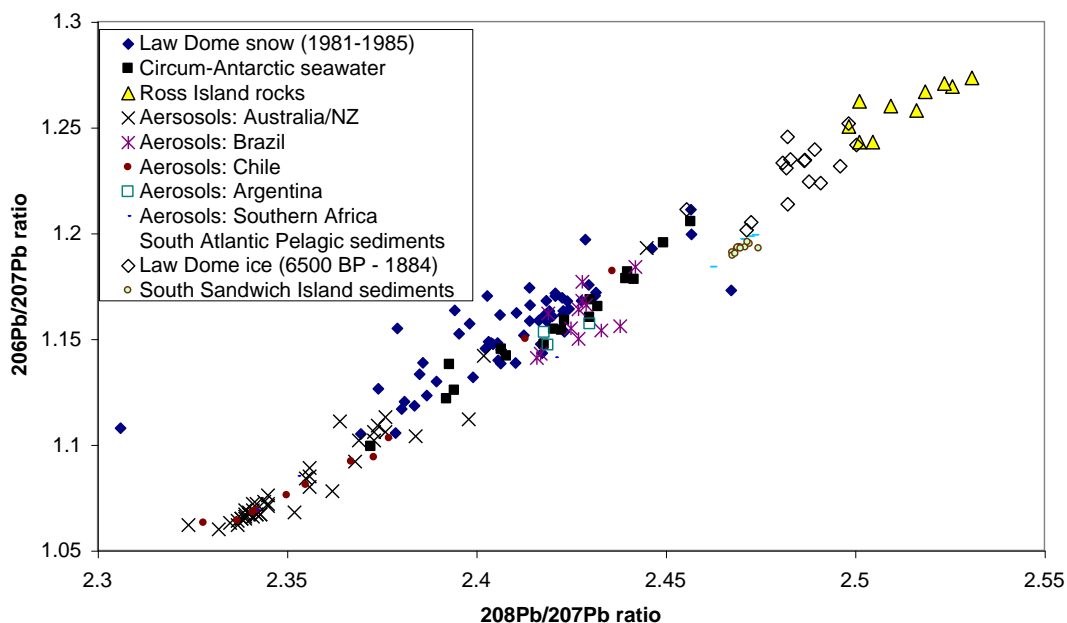


Figure 4.16. $^{206}\text{Pb}/^{207}\text{Pb}$ ratio vs $^{208}\text{Pb}/^{207}\text{Pb}$ ratio plot of Law Dome DSS-W2k samples dating from 1980 to 1985 and pre-industrial Law Dome ice. Also shown are Pb isotopic compositions of various Southern Hemisphere aerosols, rocks, seawater and sediments.

During the period Autumn – Spring 1995, however, $^{206}\text{Pb}/^{207}\text{Pb}$ ratios were usually lower than the Antarctic “background” of ~ 1.16 , indicating significant inputs of anthropogenic Pb. An episode of particularly low $^{206}\text{Pb}/^{207}\text{Pb}$ ratios ~ 1.11 are observed during Autumn 1985, while another episode ($^{206}\text{Pb}/^{207}\text{Pb} \sim 1.12$) is observed in Spring 1985. $^{206}\text{Pb}/^{207}\text{Pb}$ ratios varied less during the winter, but did decrease from from 1.17 (Autumn/winter) to 1.14 (mid-winter) and then increase again to 1.16 (winter/spring). These episodes of low $^{206}\text{Pb}/^{207}\text{Pb}$ values are correlated with high Pb concentrations, and are likely to represent transport of polluted air masses from continental areas to Law Dome.

Overall, the data presented here shows that deposition of Pb and Ba at Law Dome does undergo seasonal variations, with higher concentrations of Pb and Ba usually observed during Summers and lower concentrations of Pb and Ba usually observed during Autumn and Spring. These findings contradict those of Hong et al. (1998) and Suttie and Wolff (1992), who observed Antarctic winter peaks of Pb concentration. $^{206}\text{Pb}/^{207}\text{Pb}$ ratios ~ 1.16 , observed during the period Spring 1981 – Winter 1983, are

similar to those observed in Antarctic seawater collected in 1987/88 (Flegal et al. 1993) and the “background” value of Antarctic Pb described by Rosman et al. (1994). During Autumn-Spring 1985, however, significant variations in Pb and Ba concentrations are observed and the seasonal pattern is apparently reversed, with high concentrations during the Autumn and Spring seasons. This data is in agreement with that of Suttie and Wolff (1992), who sampled snow deposited during 1984 and 1985. During 1985, significant inputs of Ba and anthropogenic Pb are also observed. These data show that at Law Dome, broad patterns of seasonal Pb and Ba deposition are punctuated by short-term events, or may even be composed of a series of short-term events. The variability inherent in the data presented here gives some indication of the complexity of the meteorological systems contributing to the deposition of Pb and Ba at Law Dome, and probably Antarctica in general. The problem of distinguishing anthropogenic source regions in the Southern Hemisphere is complicated by the similarity of $^{206}\text{Pb}/^{207}\text{Pb}$ ratios in southern cities of Australia, Africa and South America. Overall, this data demonstrates that the studies of seasonal variations in heavy metals deposition reported by Suttie and Wolff (1992) and Hong et al. (1998) can only be evaluated in a very limited sense due to the significant variability in the Antarctic meteorological system. Accurate evaluations of seasonal variations in heavy metals deposition to any Antarctic site should be supported by additional data such as high-resolution $\delta^{18}\text{O}$ values, major ion concentrations, snow accumulation and meteorological conditions.

Chapter 5: Conclusions& recommendations

The preceding chapters have provided a history of the progression in techniques for the analysis of Pb and determination of Pb isotopic compositions in polar snow and ice and have reported the findings of an evaluation of a 500-year record of Pb and Ba concentrations and Pb isotopic compositions from Law Dome in East Antarctica.

Special precautions were undertaken to ensure the minimisation of Pb contamination entrained in the samples prior to their measurement by thermal ionisation mass spectrometry (TIMS). This involved quantification of the Pb blank associated with the 'chiselling' mechanical decontamination procedure first described by Candelone et al. (1994), via the use of artificial ice cores prepared from pre-analysed ultrapure water. Particular attention was also turned to the cleaning of polyethylene bottles used for the storage of samples and the evaluation of the rate at which bottles released Pb at various stages of cleaning. Techniques were also developed to reliably analyze Pb isotopic compositions in Antarctic samples containing sub-picogram per gram concentrations of Pb. From these evaluations, the Pb blank contribution to the samples was determined to be smaller than previously reported evaluations of Pb in Antarctica, with a contribution of ~5.2 pg Pb to the total sample analyzed.

A detailed record of Pb and Ba concentrations and Pb isotopic compositions in Law Dome ice was produced, enabling an evaluation of the variations in natural and anthropogenic Pb inputs to Antarctica since 1530 AD. Natural Pb inputs to Law Dome were observed prior to ~1884 AD, with Pb concentrations ~ 0.4 pg/g and Pb isotopic compositions varying within the range $^{206}\text{Pb}/^{207}\text{Pb} = 1.20$ to 1.25 and $^{208}\text{Pb}/^{207}\text{Pb} = 2.46$ to 2.50. Between ~1884 and 1908, a major pollution event was observed, with a significant decrease in $^{206}\text{Pb}/^{207}\text{Pb}$ ratios and an increase in Pb concentrations at Law Dome. This pollution event was attributed to the respective mining and smelting of Pb ores in Broken Hill and Port Pirie, in Australia. Through the 20th century, anthropogenic inputs were most significant between ~1900 and ~1910 (~1.5 pg Pb/g) and between ~1960 and ~1980 (~1.8 pg Pb/g). $^{206}\text{Pb}/^{207}\text{Pb}$ ratios varied from ~1.14 during the period 1980-1900 and ~1.18 between 1908 and 1939 to ~1.16 during the 1970's and 1980's.

Based on statistics of non-ferrous metal production and use, anthropogenic emissions prior to ~1950 were attributed primarily to emissions from mining and production of

non-ferrous metals, while emissions after ~1950 AD were dominated by consumption of alkyllead additives in gasoline. The statistics of alkyllead consumption indicate that during and after the 1960's, emissions from South America, particularly Brazil, dominated over emissions from South Africa, Australia and New Zealand. These changes in the sources of anthropogenic Pb emissions are consistent with the Pb isotope data observed in Antarctica, and the available reported Pb isotopic compositions in urban aerosols and Pb ores.

From comparison of the Law Dome record with those made available for Coats Land and Victoria Land, it was observed that anthropogenic Pb inputs to Coats Land occur much earlier than at Law Dome, from at least ~1830 AD. Assuming that this pollution was due to Pb production in South America, this data suggested that Coats Land is more sensitive to pollution emissions from South America. In contrast, the Victoria Land record indicated higher levels of Ba compared to Law Dome and Coats Land, and so natural Pb inputs to the site were likely dominated by emission of rock and soil dust and/or volcanogenic Pb particles from local sources. All three locations clearly recorded the c.1900 (Broken Hill) pollution event and also displayed similar trends in Pb isotopic compositions and Pb concentrations during the 20th century.

Natural Pb inputs to Law Dome, and most other Antarctic locations for which data are available, appear to be dominated by volcanism and rock and soil dust while, at coastal locations, the influence of Pb from marine aerosols also appears to be important. At Law Dome, the average Pb contribution from rock and soil dust was about 12% (determined from Ba concentrations) while volcanogenic Pb inputs were approximately 57%. This evaluation of volcanic Pb inputs was made using Pb isotope systematics and assuming that marine Pb inputs to Law Dome were not important, so it is, at best, approximate. In Antarctic coastal locations, marine aerosols have been reported to contribute between 6 and 40% of total natural Pb inputs, while rock and soil dust inputs vary from 1 to 50% of total natural Pb inputs. The influence of volcanogenic Pb varies more than coastal or marine Pb, with inputs varying between 19% (at Coats Land) and >95% (at Taylor Dome) of total natural Pb inputs. The Pb isotopic signature attributed to volcanic Pb sources was identical to that observed in Mount Erebus lavas. Mount Erebus appears to be a significant source of Pb emission in the Antarctic environment, but the extent of Pb contributions from Mount Erebus to the Antarctic ice sheet is still to be evaluated.

It was found that Pb and Ba at Law Dome do exhibit seasonal variations in deposition, with higher concentrations of Pb and Ba usually observed during Summer and lower concentrations of Pb and Ba usually observed during Autumn and Spring. During Autumn-Spring 1985, however, this seasonal pattern was apparently reversed, with higher concentrations during the Autumn and Spring seasons. At Law Dome, it appears that broad patterns of seasonal Pb and Ba deposition are punctuated by short-term events, or may even be composed of a series of short-term events. There is significant variability in the data, however, so it appears that the meteorological systems contributing to the deposition of Pb and Ba at Law Dome, and probably Antarctica in general, are much more complex than those reported for Greenland. This complexity is likely to limit the possibility of elucidating anthropogenic emission sources from Antarctic snow and ice data.

From this research, it is recommended that the Law Dome record be extended to the present, preferably from the high-resolution sampling of a snow pit collecting samples from the present to ~1970 AD. Law Dome has never been sampled at high resolution for Pb or Pb isotopes from a snow pit. This data would be valuable as the Law Dome summit features a high snow accumulation rate that is regular throughout the year and suffers from minimal wind remobilization. It would offer a superior record to those currently available from Coats Land and Victoria Land, and could be correlated with automatic weather stations and chemical data previously collected for the Law Dome summit. It has been seen that evaluations of high-resolution records are significantly enhanced by the availability of meteorological, chemical and oxygen isotope data for the samples, allowing a complete understanding of the various natural and anthropogenic inputs to the site to be achieved. The availability of satellite data for tracking air masses, offers another potential for evaluating continental Pb emission sources, which should be further exploited.

Chapter 6: References

- Alleman, L. Y., Church, T. M., Ganguli, P., Véron, A. J., Hamelin, B. and Flegal, A. R. 2001, 'Role of oceanic circulation on contaminant lead distribution in the South Atlantic', *Deep-Sea Research II*, vol. 48, pp.2855-2876.
- Barbante, C., Bellomi, T., Mezzadri, G., Cescon, P., Scarponi, G., Morel, C., Jay, S., Van de Velde, K., Ferrari, C. and Boutron, C. F. 1997a, 'Direct determination of heavy metals at picogram per gram levels in Greenland and Antarctic snow by double focusing inductively coupled plasma mass spectrometry', *Journal of Analytical Atomic Spectrometry*, vol. 12, pp.925-931.
- Barbante, C., Turetta, C., Capodaglio, G. and Scarponi, G. 1997b, 'Recent decrease in the lead concentration of Antarctic snow', *International Journal of Environmental Analytical Chemistry*, vol. 68, no.4, pp.457-477.
- Barbante, C., Veysseyre, A., Ferrari, C., Van de Velde, K., Morel, C., Capodaglio, G., Cescon, P., Scarponi, G. and Boutron, C. 2001a, 'Greenland Snow Evidence of Large Scale Atmospheric Contamination for Platinum, Palladium, and Rhodium.', *Environmental Science and Technology*, vol. 35, no.5, pp.835-839.
- Barbante, C., Veysseyre, A., Ferrari, C., Van de Velde, K., Morel, C., Capodaglio, G., Cescon, P., Scarponi, G. and Boutron, C. 2001b, 'Greenland snow evidence of large scale atmospheric contamination for platinum, palladium, and rhodium', *Environmental Science & Technology*, vol. 35, no.5, pp.835-839.
- Basile, I., Grousset, F. E., Revel, M., Petit, J. R., Biscaye, P. E. and Barkov, N. I. 1997, 'Patagonian origin of glacial dust deposited in East Antarctica (Vostok and Dome C) during glacial stages 2, 4 and 6', *Earth and Planetary Science Letters*, vol. 146, pp.573-589.
- Bluth, G. S. J., Schnetzler, C. C., Krueger, A. J. and Wlaser, L. S. 1993, 'The contribution of explosive volcanism to global atmospheric sulphur dioxide concentrations', *Nature*, vol. 366, pp.327-329.
- Bollhöfer, A. F. and Rosman, K. J. R. 2000, 'Isotopic source signatures for atmospheric lead: The Southern Hemisphere', *Geochimica et Cosmochimica Acta*, vol. 64, pp.3251-6362.
- Bollhöfer, A. F. and Rosman, K. J. R. 2001, 'Isotopic source signatures for atmospheric lead: The Northern Hemisphere', *Geochimica et Cosmochimica Acta*, vol. 65, no.11, pp.1727-1740.

- Bollhöfer, A. F. and Rosman, K. J. R. 2002, 'The temporal stability of lead isotopic signatures at selected sites in the Southern and Northern Hemispheres', *Geochimica et Cosmochimica Acta*, vol. 66, no.8, pp.1375-1386.
- Bory, A. J.-M., Biscaye, P. E., Svensson, A. and Grousset, F. E. 2002, 'Seasonal variability in the origin of recent atmospheric mineral dust at NorthGRIP, Greenland', *Earth and Planetary Science Letters*, vol. 196, pp.123-134.
- Boutron, C., Görlach, U., Candelone, J.-P., Bolshov, M. A. and Delmas, R. J. 1991, 'Decrease in anthropogenic lead, cadmium and zinc in Greenland snows since the late 1960's', *Nature*, vol. 353, pp.153-156.
- Boutron, C. F. 1990, 'A clean laboratory for ultralow concentration heavy metal analysis', *Fresenius' Journal of Analytical Chemistry*, vol. 337, pp.482-491.
- Boutron, C. F. and Lorius, C. 1979, 'Trace metals in Antarctic snows since 1914', *Nature*, vol. 277, pp.551-554.
- Boutron, C. F. and Patterson, C. C. 1983, 'The occurrence of lead in Antarctic recent snow, firn deposited over the last two centuries and prehistoric ice', *Geochimica et Cosmochimica Acta*, vol. 47, pp.1355-1368.
- Boutron, C. F. and Patterson, C. C. 1986, 'Lead concentration changes in Antarctic ice during the Wisconsin/Holocene transition', *Nature*, vol. 323, pp.222-225.
- Boutron, C. F. and Patterson, C. C. 1987, 'Relative levels of natural and anthropogenic lead in recent Antarctic snow', *Journal of Geophysical Research*, vol. 92, no.D7, pp.8454-8464.
- Boutron, C. F., Patterson, C. C., Lorius, C., Petrov, V. N. and Barkov, N. I. 1988, 'Atmospheric lead in Antarctic ice during the last climatic cycle', *Annals of Glaciology*, vol. 10, pp.5-9.
- Boutron, C. F., Rudniev, S. N., Bolshov, M. A., Koloshnikov, V. G., Patterson, C. C. and Barkov, N. I. 1993, 'Changes in cadmium concentrations in Antarctic ice and snow during the past 155,000 years', *Earth and Planetary Science Letters*, vol. 117, pp.431-441.
- Boyle, E. A., Sherrell, R. M. and Bacon, M. P. 1994, 'Lead variability in the western North Atlantic Ocean and central Greenland ice: Implications for the search for decadal trends in anthropogenic emissions', *Geochimica et Cosmochimica Acta*, vol. 58, no.15, pp.3227-3238.
- Brimblecombe, P. and Hunter, K. A. 1977, 'Rock volatility and aerosol composition', *Nature*, vol. 265, pp.761-762.

- Cameron, A. E., Smith, D. H. and Walker, R. L. 1969, 'Mass spectrometry of nanogram-size samples of lead', *Analytical Chemistry*, vol. 41, no.3, pp.525-526.
- Candelone, J.-P., Hong, S. and Boutron, C. F. 1994, 'An improved method for decontaminating polar snow or ice cores for heavy metal analysis', *Analytica Chimica Acta*, vol. 299, pp.9 -16.
- Candelone, J.-P., Hong, S., Pellone, C. and Boutron, C. F. 1995, 'Post-Industrial Revolution changes in large-scale atmospheric pollution of the northern hemisphere by heavy metals as documented in central Greenland snow and ice', *Journal of Geophysical Research*, vol. 100, no.D8, pp.16605-16616.
- Candelone, J.-P., Jaffrezo, J.-L., Hong, S., Davidson, C. I. and Boutron, C. F. 1996, 'Seasonal variations in heavy metals concentrations in present day Greenland snow', *The Science of the Total Environment*, vol. 193, pp.101-110.
- Chisholm, W., Rosman, K. J. R., Boutron, C. F., Candelone, J.-P. and Hong, S. 1995, 'Determination of lead isotopic ratios in Greenland and Antarctic snow and ice at picogram per gram concentrations', *Analytica Chimica Acta*, vol. 311, pp.141-151.
- Chisholm, W., Rosman, K. J. R., Candelone, J.-P., Boutron, C. F. and Bolshov, M. A. 1997, 'Measurement of bismuth at pg g^{-1} concentrations in snow and ice samples by thermal ionisation mass spectrometry', *Analytica Chimica Acta*, vol. 347, pp.351-358.
- Chow, T. J. (1978) 'Lead in natural waters' In *The biogeochemistry of lead in the environment. Part A. Ecological cycles*, (Ed, Nriagu, J. O.), Elsevier/North-Holland Biomedical Press, New York, pp. 185-218.
- Chow, T. J. and Patterson, C. C. 1962, 'The occurrence and significance of lead isotopes in pelagic sediments', *Geochimica et Cosmochimica Acta*, vol. 26, pp.263-308.
- Chow, T. J., Snyder, C. B. and Earl, J. L. (1975) Isotope ratios of lead as pollutant source indicators, in *United Nations FAO and International Atomic Energy Association Symposium. (IAEA-SM-191/4)* Vienna, Austria, pp. 95-108.
- Chylek, P., Lesins, G. and Lohmann, U. 2001, 'Enhancement of dust source area during past glacial periods due to changes of the Hadley circulation', *Journal of Geophysical Research*, vol. 106, no.D16, pp.18477-18485.

- Cross, W. G. 1951, 'Two directional focussing of charged particles and a sector-shaped uniform magnetic field', *Reviews of scientific instruments*, vol. 22, no.10, pp.717-722.
- Curran, M. A. J., van Ommen, T. D. and Morgan, V. 1998, 'Seasonal characteristics of the major ions in the high-accumulation Dome Summit South ice core, Law Dome, Antarctica', *Annals of Glaciology*, vol. 27, pp.385-390.
- Davidson, C. I., Chu, L., Grimm, T. C., Nasta, M. A. and Qamoos, M. P. 1981, 'Wet and dry deposition of trace elements onto the Greenland ice sheet', *Atmospheric Environment*, vol. 15, no.8, pp.1429-1437.
- de Laeter, J. R. (2001) *Applications of Inorganic Mass Spectrometry*, Wiley-Interscience, New York.
- Dempster, A. J. 1918, *Physics Reviews*, vol. 11, pp.316.
- Dick, A. L. 1991, 'Concentrations and sources of metals in the Antarctic Peninsula aerosol', *Geochimica et Cosmochimica Acta*, vol. 55, pp.1827-1836.
- Duce, R. A., Hoffman, G. L. and Zoller, W. H. 1975, 'Atmospheric Trace Metals at Remote Northern and Southern Hemisphere Sites: Pollution or Natural?', *Science*, vol. 187, pp.59-61.
- Faure, G. (1986) *Principles of isotope geology*, Wiley, New York.
- Ferrari, C. P., Hong, S., Van de Velde, K., Boutron, C. F., Rudniev, S. N., Bolshov, M., Chisholm, W. and Rosman, K. J. R. 2000, 'Natural and anthropogenic bismuth in Central Greenland', *Atmospheric Environment*, vol. 34, pp.941-948.
- Flegal, A. R. 1998, 'Clair Patterson's Influence on Environmental Research', *Environmental Research*, vol. 78, no.A, pp.65-70.
- Flegal, A. R., Maring, H. and Niemeyer, S. 1993, 'Anthropogenic lead in Antarctic sea water', *Nature*, vol. 365, pp.242-244.
- Gerstenberger, H. and Haase, G. 1997, 'A highly effective emitter substance for mass spectrometric Pb isotope ratio determinations', *Chemical Geology*, vol. 136, pp.309-312.
- Greenwood, N. N. and Earnshaw, A. (1984) *Chemistry of the elements*, Pergamon, Oxford.
- Grousset, F. E., Biscaye, P. E., Revel, M., Petit, J. R., Pye, K., Joussaume, S. and Jouzel, J. 1992, 'Antarctic (Dome C) ice-core dust at 18 k.y. B.P.: Isotopic constraints on origins', *Earth and Planetary Science Letters*, vol. 111, pp.175-182.

- Herron, M. M., Langway, C. C., Jr, Weiss, H. V. and Cragin, J. H. 1977, 'Atmospheric trace metals and sulfate in the Greenland Ice Sheet', *Geochimica et Cosmochimica Acta*, vol. 41, pp.915-920.
- Hildreth, W. and Moorbath, S. 1988, 'Crustal contributions to arc magmatism in the Andes of Central Chile', *Contributions to Mineralogy and Petrology*, vol. 98, pp.455-489.
- Hinkley, T. K. 1991, 'Distribution of metals between particulate and gaseous forms in a volcanic plume', *Bulletin of Volcanology*, vol. 53, pp.395-400.
- Hinkley, T. K., Lamothe, P. J., Wilson, S. A., Finnegan, D. L. and Gerlach, T. M. 1999, 'Metal emissions from Kilauea, and a suggested revision of the estimated worldwide metal output by quiescent degassing of volcanoes', *Earth and Planetary Science Letters*, vol. 170, pp.315-325.
- Hinkley, T. K., Le Cloarec, M.-F. and Lambert, G. 1994, 'Fractionation of families of major, minor, and trace metals across the melt-vapor interface in volcanic exhalations', *Geochimica et Cosmochimica Acta*, vol. 58, no.15, pp.3255-3263.
- Hong, S., Boutron, C. F., Edwards, R. and Morgan, V. I. 1998, 'Heavy Metals in Antarctic Ice from Law Dome: Initial Results', *Environmental Research*, vol. 78, no.Section A, pp.94-103.
- Hong, S., Candelone, J.-P. and Boutron, C. F. 1996a, 'Deposition of atmospheric heavy metals to the Greenland ice sheet from the 1783-1784 volcanic eruption of Laki, Iceland', *Earth and Planetary Science Letters*, vol. 144, pp.605-610.
- Hong, S., Candelone, J.-P., Patterson, C. C. and Boutron, C. F. 1994, 'Greenland Ice Evidence of Hemispheric Lead Pollution Two Millennia Ago by Greek and Roman Civilisations', *Science*, vol. 265, pp.1841-1843.
- Hong, S., Candelone, J.-P., Turetta, C. and Boutron, C. F. 1996b, 'Changes in natural lead, copper, zinc and cadmium concentrations in central Greenland ice from 8250 to 149,100 years ago: their association with climatic changes and resultant variations of dominant source contributions', *Earth and Planetary Science Letters*, vol. 143, pp.233-244.
- Joussame, S. 1993, 'Paleoclimatic tracers: an investigation using an atmospheric general circulation model under ice age conditions 1. desert dust', *Journal of Geophysical Research*, vol. 98, pp.2767-2805.

- Kessinger, G. F., Huett, T. and Delmore, J. E. 2001, 'Ag ion formation mechanisms in molten glass ion emitters', *International Journal of Mass Spectrometry*, vol. 208, pp.37-57.
- Kuehner, E. C., Alvarez, R., Paulsen, P. J. and Murphy, T. J. 1972, 'Production and analysis of special high-purity acids purified by subboiling distillation', *Analytical Chemistry*, vol. 44, no.12, pp.2050-2056.
- Lambert, G., Le Cloarec, M.-F. and Pennisi, M. 1988, 'Volcanic output of SO₂ and trace metals: A new approach', *Geochimica et Cosmochimica Acta*, vol. 52, pp.39-42.
- Lambert, G., Polian, G., Sanak, J., Buisson, A., Ardouin, B. and Jegou, A. 1982, 'Volcanic output of long-lived radon daughters', *Journal of Geophysical Research*, vol. 87, pp.11103-11108.
- Landy, M. P. 1980, 'An evaluation of differential pulse anodic stripping voltammetry at a rotating glassy carbon electrode for the determination of cadmium, copper, lead and zinc in Antarctic snow samples', *Analytica Chimica Acta*, vol. 121, pp.39-49.
- Landy, M. P. and Peel, D. A. 1981, 'Short-term fluctuations in heavy metal concentrations in Antarctic snow', *Nature*, vol. 291, pp.144-146.
- Legrand, M., Jouzel, J. and Raynaud, D. (1994) 'Past climate and trace gas content of the atmosphere inferred from polar ice cores' In *ERCA Vol. 1: Topics in Atmospheric and interstellar physics and chemistry*, (Ed, Boutron, C.), Les Editions de Physique, Les Ulis, France, pp. 453-477.
- Levin, I. and Hesshaimer, V. 1996, 'Refining of Atmospheric Transport Model Entries by the Globally Observed Passive Tracer Distributions of ⁸⁵Krypton and Sulfur Hexafluoride (SF₆)', *Journal of Geophysical Research*, vol. 101, no.D11, pp.16745-16755.
- Loss, R. D. (1986) *Mobility of the fission valley elements from the Oklo fossil reactors*, Ph.D. thesis, *Department of Physics*, The University of Western Australia, Perth, 322.
- Loss, R. D. and Rosman, K. J. R. (1987) *Femtolab - Metal free clean room.*, School of Physics and Geosciences, Curtin University of Technology, Internal report SPG 464/1987/AP143, Perth, Australia., pp. 50.

- Maggi, V. and Petit, J.-R. 1998, 'Atmospheric dust concentration record from the Hercules Névé firn core, northern Victoria Land, Antarctica', *Journal of Glaciology*, vol. 27, pp.355-359.
- Matsumoto, A. and Hinkley, T. K. 1997, 'Determination of lead, cadmium, indium, thallium and silver in ancient ices from Antarctica by isotope dilution-thermal ionization mass spectrometry', *Geochemical Journal*, vol. 31, pp.175 - 181.
- Matsumoto, A. and Hinkley, T. K. 2001, 'Trace metal suites in Antarctic pre-industrial ice are consistent with emissions from quiescent degassing of volcanoes worldwide', *Earth and Planetary Science Letters*, vol. 186, pp.33-43.
- McMorrow, A. J., Curran, M. A. J., van Ommen, T. D., Morgan, V. I. and Allison, I. 2002, 'Features of meteorological events preserved in a high resolution Law Dome snow pit', *Annals of Glaciology*, vol. 35, pp.In press.
- Monna, F., Aiuppa, A., Varrica, D. and Dongarra, G. 1999, 'Pb Isotope Composition in Lichens and Aerosols from Eastern Sicily: Insights into the Regional Impact of Volcanoes on the Environment', *Environmental Science and Technology*, vol. 33, pp.2517-2523.
- Moody, J. R. 1982, 'NBS Clean Laboratories for Trace Element Analysis', *Analytical Chemistry*, vol. 54, no.13, pp.1358A-1376A.
- Moody, J. R. and Lindstrom, R. M. 1977, 'Selection and Cleaning of Plastic Containers for Storage of Trace Element Samples', *Analytical Chemistry*, vol. 49, no.14, pp.2264-2267.
- Morgan, V., Wookey, C. W., Li, J., van Ommen, T. D., Skinner, W. and Fitzpatrick, M. F. 1997, 'Site information and initial results from deep ice drilling on Law Dome, Antarctica', *Journal of Glaciology*, vol. 43, no.143, pp.3-10.
- Murozumi, M., Chow, T. J. and Patterson, C. C. 1969, 'Chemical concentrations of pollutant lead aerosols, terrestrial dusts and sea salts in Greenland and Antarctic snow strata', *Geochimica et Cosmochimica Acta*, vol. 33, pp.1247-1294.
- Ng, A. and Patterson, C. C. 1981, 'Natural concentrations of lead in ancient Arctic and Antarctic ice', *Geochimica et Cosmochimica Acta*, vol. 45, pp.2109-2121.
- Nriagu, J. O. (1978) 'Lead in the atmosphere' In *The biogeochemistry of lead in the environment. Part A. Ecological cycles*, (Ed, Nriagu, J. O.), Elsevier/North-Holland Biomedical Press, New York, pp. 137-184.
- Nriagu, J. O. 1979, 'Global inventory of natural and anthropogenic emissions of trace metals to the atmosphere', *Nature*, vol. 279, pp.409-411.

- Nriagu, J. O. (1983) *Lead and lead poisoning in antiquity*, John Wiley & Sons, New York.
- Nriagu, J. O. 1989, 'A global assessment of natural sources of atmospheric trace metals', *Nature*, vol. 338, pp.47-49.
- Nriagu, J. O. 1990, 'The rise and fall of leaded gasoline', *The Science of the Total Environment*, vol. 92, pp.13-28.
- Nriagu, J. O. 1996, 'A History of Global Metal Pollution', *Science*, vol. 272, pp.223-224.
- Nriagu, J. O. 1998, 'Clair Patterson and Robert Kehoe's Paradigm of "Show Me the Data" on Environmental Lead Poisoning', *Environmental Research*, vol. 78, no.A, pp.71-78.
- Nriagu, J. O., Blankson, M. L. and Ocran, K. 1996, 'Childhood lead poisoning in Africa: a growing public health problem', *The Science of the Total Environment*, vol. 181, pp.93-100.
- Nriagu, J. O. and Pacyna, J. M. 1988, 'Quantitative assessment of worldwide contamination of air, water and soils by trace metals', *Nature*, vol. 333, pp.134-139.
- Palmer, A. S., van Ommen, T. D., Curran, M. A. J., Morgan, V., Souney, J. M. and Mayewski, P. A. 2001, 'High precision dating of volcanic events (A.D. 1301-1995) using ice cores from Law Dome, Antarctica', *Journal of Geophysical Research*, vol. 106, no.D22, pp.28089-28095.
- Patterson, C. C. 1965, 'Contaminated and Natural Lead Environments of Man', *Archives of Environmental Health*, vol. 11, pp.344-360.
- Patterson, C. C. and Settle, D. M. (1976) 'The reduction of orders of magnitude errors in lead analyses of biological materials and natural waters by evaluating and controlling the extent and sources of industrial lead contamination introduced during sample collection, handling and analysis' In *Accuracy in Trace Analysis: Sampling, Sample Handling and Analysis*, (Ed, LaFleur, P. D.), U.S. Bureau of Standards Special Publication, Washington D.C., pp. 321-351.
- Patterson, C. C. and Settle, D. M. 1987, 'Magnitude of lead flux to the atmosphere from volcanoes', *Geochimica et Cosmochimica Acta*, vol. 51, pp.675-681.
- Peel, D. A. 1986, 'Is lead pollution of the atmosphere a global problem?', *Nature*, vol. 323, pp.200.

- Peterson, J. T. and Junge, C. E. (1971) 'Sources of Particulate Matter in the Atmosphere' In *Man's Impact on the Climate*, (Eds, Matthews, W. H., Kellogg, W. W. and Robinson, G. D.), M.I.T. Press, Cambridge, Massachusetts, pp. 310-320.
- Petit, J. R., Jouzel, J., Raynaud, D., Barkov, N. I., Barnola, J.-M., Basile, I., Bender, M., Chappelaz, J., Davis, M., Delaygue, G., Delmotte, M., Kotlyakov, V. M., Legrand, M., Lipenkov, V. Y., Lorius, C., Pepin, L., Ritz, C., Saltzman, E. and Stievenard, M. 1999, 'Climate and atmospheric history of the past 420,000 years from the Vostok ice core, Antarctica', *Nature*, vol. 399, pp.429-436.
- Planchon, F. A. M., Boutron, C. F., Barbante, C., Cozzi, G., Gaspari, V., Wolff, E. W., Ferrari, C. P. and Cescon, P. 2002a, 'Changes in heavy metals in Antarctic snow from Coats Land since the mid-19th to the late-20th century', *Earth and Planetary Science Letters*, vol. 200, pp.207-222.
- Planchon, F. A. M., Boutron, C. F., Barbante, C., Wolff, E. W., Cozzi, G., Gaspari, V., Ferrari, C. P. and Cescon, P. 2001, 'Ultrasensitive determination of heavy metals at the sub-picogram per gram level in ultraclean Antarctic snow samples by inductively coupled plasma sector field mass spectrometry', *Analytica Chimica Acta*, vol. 450, no.1-2, pp.193-205.
- Planchon, F. A. M., Van de Velde, K., Rosman, K. J. R., Wolff, E. W., Ferrari, C. P. and Boutron, C. F. 2002b, 'A 150 year record of lead isotopes in Antarctic snow from Coats Land', *Geochimica et Cosmochimica Acta*, vol. In press.
- Rabinowitz, M. B. and Wetherill, G. W. 1972, 'Identifying sources of Pb contamination by stable isotope techniques', *Environmental Science & Technology*, vol. 6, pp.705-709.
- Rosman, K. J. R. (2001) 'Natural isotopic variations in lead in polar snow and ice as indicators of source regions' In *Environmental contamination in Antarctica: A challenge to analytical chemistry*, (Eds, Caroli, S., Cescon, P. and Walton, D. W. H.), Elsevier Science B.V., New York, pp. 87-106.
- Rosman, K. J. R., Chisholm, W., Boutron, C. F. and Candelone, J.-P. 1999, 'Lead Isotopes as Tracers of Pollution in Snow and Ice', *Korean Journal of Polar Research*, vol. 10, no.2, pp.53-58.
- Rosman, K. J. R., Chisholm, W., Boutron, C. F., Candelone, J.-P. and Görlach, U. 1993, 'Isotopic evidence for the source of lead in Greenland snows since the late 1960's.', *Nature*, vol. 362, pp.333.

- Rosman, K. J. R., Chisholm, W., Boutron, C. F., Candelone, J.-P. and Hong, S. 1994a, 'Isotopic evidence to account for changes in the concentration of lead in Greenland snow between 1960 and 1988', *Geochimica et Cosmochimica Acta*, vol. 58, no.15, pp.3265-3269.
- Rosman, K. J. R., Chisholm, W., Boutron, C. F., Candelone, J.-P., Jaffrezo, J.-L. and Davidson, C. I. 1998a, 'Seasonal variations in the origin of lead in snow at Dye 3, Greenland', *Earth and Planetary Science Letters*, vol. 160, pp.383-389.
- Rosman, K. J. R., Chisholm, W., Boutron, C. F., Candelone, J.-P. and Patterson, C. C. 1994b, 'Anthropogenic lead isotopes in Antarctica', *Geophysical Research Letters*, vol. 21, no.24, pp.2669-2672.
- Rosman, K. J. R., Chisholm, W., Boutron, C. F., Hong, S., Edwards, R., Morgan, V. and Sedwick, P. N. 1998b, 'Lead isotopes and selected metals in ice from Law Dome, Antarctica', *Annals of Glaciology*, vol. 27, pp.349-354.
- Rosman, K. J. R., Chisholm, W., Hong, S., Candelone, J.-P. and Boutron, C. F. 1997, 'Lead from Carthaginian and Roman Spanish mines isotopically identified in Greenland ice dated from 600 B.C. to 300 A.D.', *Environmental Science and Technology*, vol. 31, no.12, pp.3413-3416.
- Rosman, K. J. R., Ly, C. V., Van de Velde, K. P. and Boutron, C. F. 2000, 'A two century record of lead isotopes in high altitude alpine snow and ice', *Earth and Planetary Science Letters*, vol. 176, pp.413-424.
- Rosman, K. J. R. and Taylor, P. D. P. 1998, 'Isotopic compositions of the elements 1997', *Journal of Physical and Chemical Reference Data*, vol. 27, no.6, pp.1275-1287.
- Sangster, D. F., Outridge, P. M. and Davis, W. J. 2000, 'Stable lead isotope characteristics of lead ore deposits of environmental significance', *Environ. Rev.*, vol. 8, pp.115 - 147.
- Savarino, J., Boutron, C. F. and Jaffrezo, J.-L. 1994, 'Short-term variations of Pb, Cd, Zn and Cu in recent Greenland snow', *Atmospheric Environment*, vol. 28, no.10, pp.1731-1737.
- Settle, D. M. and Patterson, C. C. 1980, 'Lead in Albacore: Guide to Lead Pollution in Americans', *Science*, vol. 207, pp.1167 - 1176.
- Sherrell, R. M., Boyle, E. A., Falkner, K. K. and Harris, N. R. 2000, 'Temporal variability of Cd, Pb, and Pb isotope deposition in central Greenland snow', *Geochemistry Geophysics Geosystems*, vol. 1.

- Shirahata, H., Elias, R. W., Patterson, C. C. and Koide, M. 1980, 'Chronological variations in concentrations and isotopic compositions of anthropogenic atmospheric lead in sediments of a remote subalpine pond', *Geochimica et Cosmochimica Acta*, vol. 44, pp.149-162.
- Stenni, B., Caprioli, R., Cimino, L., Cremisini, C., Flora, O., Gagnani, R., Longinelli, A., Maggi, V. and Torcini, S. 1999, '200 years of isotope and chemical records in a firn core from Hercules N ev , northern Victoria Land, Antarctica', *Annals of Glaciology*, vol. 29, pp.106-112.
- Stenni, B., Serra, F., Frezzotti, M., Maggi, V., Traversi, R., Becagli, S. and Udisti, R. 2000, 'Snow accumulation rates in northern Victoria Land, Antarctica, by firn-core analysis', *Journal of Glaciology*, vol. 46, no.155, pp.541-552.
- Suttie, E. D. and Wolff, E. W. 1992, 'Seasonal input of heavy metals to Antarctic snow', *Tellus*, vol. 44B, pp.351-357.
- Suttie, E. D. and Wolff, E. W. 1993, 'The local deposition of heavy metal emissions from point sources in Antarctica', *Atmospheric Environment*, vol. 27A, no.12, pp.1833-1841.
- Svensson, A., Biscaye, P. E. and Grousset, F. E. 2000, 'Characterization of late glacial continental dust in the Greenland Ice Core Project ice core', *Journal of Geophysical Research*, vol. 105, no.D4, pp.4637-4656.
- Tatsumoto, M. and Patterson, C. C. 1963, 'Concentrations of common lead in some Atlantic and Mediterranean waters and in snow', *Nature*, vol. 199, pp.350-352.
- Tong, S., von Schirnding, Y. E. and Prapamontol, T. 2000, 'Environmental lead exposure: a public health problem of global dimensions.', *Bulletin of the World Health Organisation*, vol. 78, no.9, pp.1068-1077.
- Vallelonga, P., Van de Velde, K., Candelone, J.-P., Ly, C., Rosman, K. J. R., Boutron, C. F., Morgan, V. I. and Mackey, D. J. 2002a, 'Recent advances in measurement of Pb isotopes in Polar ice and snow at sub-picogram per gram concentrations using Thermal Ionisation Mass Spectrometry', *Analytica Chimica Acta*, vol. 453, pp.1-12.
- Vallelonga, P., Van de Velde, K., Candelone, J.-P., Morgan, V. I., Boutron, C. F. and Rosman, K. J. R. 2002b, 'The lead pollution history of Law Dome, Antarctica, from isotopic measurements on ice cores: 1500 AD to 1989 AD', *Earth and Planetary Science Letters*, vol. In press.

- Veyseyre, A. M., Bollhöfer, A. F., Rosman, K. J. R., Ferrari, C. P. and Boutron, C. F. 2001, 'Tracing the origin of pollution in French Alpine snow and aerosols using lead isotopic ratios', *Environmental Science & Technology*, vol. 35, no.22, pp.4463-4469.
- Webster, R. K. (1960) 'Mass spectrometric isotopic dilution analysis' In *Methods in geochemistry*, (Eds, Smales, A. A. and Wager, L. R.), Interscience, New York, pp. 202-246.
- White, F. A. and Wood, G. M. (1986) *Mass Spectrometry. Applications in Science and Engineering*, Wiley, New York.
- Wolff, E. W. 1990, 'Signals of atmospheric pollution in polar snow and ice', *Antarctic Science*, vol. 2, no.3, pp.189-205.
- Wolff, E. W. (2000) 'History of the Atmosphere from Ice cores' In *ERCA Vol. 4: From weather forecasting to exploring the solar system*, (Ed, Boutron, C.), EDP Sciences, Les Ulis, France, pp. 147-177.
- Wolff, E. W., Landy, M. P. and Peel, D. A. 1981, 'Preconcentration of Cadmium, Copper, Lead, and Zinc in Water at the 10^{-12} g/g Level by Adsorption onto Tungsten Wire Followed by Flameless Atomic Absorption Spectrometry', *Analytical Chemistry*, vol. 53, no.11, pp.1566-1570.
- Wolff, E. W. and Peel, D. A. 1985a, 'Closer to a true value for heavy metal concentrations in recent Antarctic snow by improved contamination control', *Annals of Glaciology*, vol. 7, pp.61-69.
- Wolff, E. W. and Peel, D. A. 1985b, 'The record of global pollution in polar snow and ice', *Nature*, vol. 313, pp.535-540.
- Wolff, E. W. and Suttie, E. D. 1994, 'Antarctic snow record of southern hemisphere lead pollution', *Geophysical Research Letters*, vol. 21, no.9, pp.781-784.
- Wolff, E. W., Suttie, E. D. and Peel, D. A. 1999, 'Antarctic snow record of cadmium, copper, and zinc content during the twentieth century', *Atmospheric Environment*, vol. 33, pp.1535-1541.
- Zreda-Gostynka, G. and Kyle, P. R. 1997, 'Volcanic gas emissions from Mount Erebus and their impact on the Antarctic environment', *Journal of Geophysical Research*, vol. 102, no.B7, pp.15039-15055.

Appendix 1. Law Dome, Coats Land and Victoria Land data

Law Dome.

The Law Dome data presented here were determined using the methods described in Chapter 2 (methods). The various data shown represent three data sets. The first set is the overall pollution record in Law Dome (6500 BP to 1989 AD). The second set are the Law Dome samples collected corresponding to the 1815 AD eruption of Tambora covering the period 1814 to 1818 AD. The last set is the data from the high-resolution sampling of the DSS-W2k core to observe seasonal variations (1980 to 1985 AD).

This data has been corrected for instrumental mass fractionation, and for the analytical blank, which varied from 0.1 to 0.3 pg Pb and from 1.5 to 3 pg Ba, depending on the concentration of the silica gel ionisation enhancer solution loaded with the sample. It is included in the following form to allow the data within each data set to be evaluated with relative ease. Following the three data sets will be a complete set of all of the Law Dome samples analyzed, including uncorrected Pb isotope ratios and uncorrected amounts of Pb and Ba. The Pb and Ba blanks evaluated for each measurement are included in the last two columns of the tables, and included in the caption of each table is the Pb isotopic composition evaluated for the procedural blank, to enable the final isotopic composition of the samples to be determined independently.

Coats Land.

Coats Land data was obtained from Planchon et al. (2002b), through personal communication with K. Rosman. This data is summarized in two tables which follow the Law Dome data.

Sample Designation	Date	$^{206}\text{Pb}/^{207}\text{Pb}$	\pm	$^{208}\text{Pb}/^{207}\text{Pb}$	\pm	$^{206}\text{Pb}/^{204}\text{Pb}$	\pm	Pb Conc. (pg/g)	Ba Conc. (pg/g)	Pb/Ba (g/g at.wt.)
DSS-W2k 9	1990	1.100	0.002	2.369	0.006	17.7	0.2	7.00	4.68	1.50
DSS-W2k 17	1983	1.168	0.007	2.428	0.016	18.1	0.7	0.88	1.72	0.51
DSS-W20k 7	1977	1.163	0.006	2.422	0.012	18.1	0.2	1.60	1.22	1.31
DSS-W20k 9	1971	1.163	0.004	2.425	0.009	18.2	0.5	2.46	2.42	1.01
DSS-W20k 10	1967	1.145	0.005	2.408	0.014	17.6	0.3	1.33	2.02	0.66
DSS-W20k 11	1964	1.150	0.005	2.408	0.010	17.3	1.5	1.51	3.47	0.43
DSS-W20k 12	1960	1.165	0.005	2.429	0.006	18.3	0.2	2.89	2.98	0.97
DSS-W20k 13	1956	1.144	0.007	2.404	0.011	17.9	0.4	1.27	3.75	0.34
DSS-W20k 15	1948	1.171	0.005	2.441	0.008	18.2	0.2	1.08	1.84	0.59
DSS-W20k 16	1942	1.167	0.006	2.432	0.013	18.3	0.4	0.59	2.01	0.29
DSS99 36	1939	1.179	0.005	2.449	0.010	18.4	0.3	0.79	1.08	0.73
DSS-W20k 18	1933	1.179	0.006	2.436	0.030	17.8	1.5	1.72	2.16	0.80
DSS99 40	1932	1.178	0.005	2.440	0.016	17.8	0.5	1.10	6.67	0.16
DSS99 51	1919	1.181	0.004	2.449	0.005	18.5	0.4	1.24	1.11	1.11
DSS99 60	1908	1.167	0.006	2.445	0.008	18.5	0.7	1.69	1.72	0.98
DSS99 68	1898	1.123	0.006	2.395	0.006	17.5	0.2	1.42	1.49	0.95
DSS99 75	1890	1.179	0.007	2.425	0.020	17.4	1.1	0.63	2.03	0.31
DSS99 79	1884	1.205	0.010	2.473	0.012	18.4	0.8	0.45	1.10	0.41
DSS99 84	1877	1.224	0.006	2.491	0.015	19.1	0.3	0.41	0.67	0.62
DSS99 95	1860	1.234	0.007	2.487	0.008	19.0	0.6	0.32	0.90	0.36
DSS-W20k 35	1858	1.214	0.019	2.482	0.018	18.9	2.4	0.21	1.02	0.21
DSS99 103	1852	1.231	0.005	2.482	0.015	19.2	0.5	0.28	1.02	0.27
DSS-W20k 41	1831	1.252	0.002	2.498	0.009	19.9	0.4	0.45	0.90	0.50
DSS-W20k 46	1807	1.224	0.019	2.488	0.027	19.1	2.2	0.36	1.98	0.18
DSS-W20k 50	1790	1.235	0.006	2.487	0.022	18.5	1.3	0.47	1.50	0.31
DSS-W20k 55	1767	1.201	0.010	2.471	0.029	19.0	0.5	0.36	1.81	0.20
DSS-W20k 62	1729	1.235	0.013	2.483	0.024	19.2	1.7	0.27	0.75	0.36
DSS-W20k 70	1692	1.232	0.007	2.496	0.012	19.9	0.6	0.33	1.40	0.24
BHD 132	1650	1.239	0.007	2.489	0.027	18.9	1.6	0.48	1.37	0.35
DSS 218	1605	1.233	0.006	2.481	0.025	19.1	1.3	0.33	1.30	0.25
DSS 257	1530	1.242	0.005	2.500	0.009	18.9	0.5	0.30	0.68	0.44
DSS 790	68 AD	1.245	0.007	2.482	0.012	19.1	0.4	0.42	1.83	0.23
DSS 1129	4500 BC	1.211	0.008	2.456	0.016	19.1	1.2	0.31	3.21	0.09

The data used to evaluate the Pb and Ba record at Law Dome, from 6500 BP to 1989 AD.

	middle depth	nssSO ₄ ²⁻ conc	Ba conc	Bi conc	Pb conc	²⁰⁶ Pb/ ²⁰⁷ Pb	95% C.I.	²⁰⁸ Pb/ ²⁰⁷ Pb	95% C.I.	²⁰⁶ Pb/ ²⁰⁴ Pb	95% C.I.	Pb/Ba	Bi/Ba
	m	ng/g	pg/g	fg/g	pg/g								(x1000)
TOP External layer			28.40	132193	53.69	1.176	0.004	2.420	0.002	18.4	0.1	1.89	4654
TOP 2nd layer			6.72	61	3.14	1.169	0.004	2.416	0.033	17.9	0.3	0.47	9
TOP 3rd layer			2.97	107	1.06	1.218	0.010	2.460	0.017	18.8	0.3	0.36	36
TOP Weighted average Inner Core			2.32	42	0.80	1.234		2.459		19.4		0.34	18
MID External layer			4.34	2642	4.73	1.191	0.005	2.430	0.018	18.5	0.2	1.09	609
MID 2nd layer			3.51	15	0.56	1.212	0.010	2.445	0.028	18.1	1.9	0.16	4
MID 3rd layer			6.30	11	0.41	1.216	0.012	2.476	0.017	19.3	0.7	0.06	2
MID Weighted average Inner Core			3.77	11	0.49	1.224		2.475		18.1		0.13	3
BOT External Layer			5.63	48434	24.05	1.179	0.001	2.424	0.007	18.4	0.1	4.27	8604
BOT 2nd layer			4.97	383	1.72	1.173	0.005	2.418	0.013	18.2	0.3	0.35	77
BOT 3rd layer			0.86	6	0.46	1.211	0.011	2.451	0.019	19.4	0.7	0.54	7
BOT Weighted average Inner Core			0.92	7	0.31	1.203		2.440		18.9		0.34	7
IC1 (~1818.5)	41.752	113	1.09	39	<0.69	> 1.156	0.019	> 2.366	0.027	> 18.3	2.4	< 0.63	36
IC2 (~1818)	41.802	155	3.00	57	0.81	1.250	0.015	2.508	0.028	19.6	1.3	0.27	19
IC3 (~1817.8)	41.847	190	2.61	34	1.03	1.303	0.010	2.502	0.012	20.5	0.4	0.40	13
IC3 (~1817.8)	41.847	190	2.81	35	1.25	1.265	0.005	2.500	0.013	19.7	0.5	0.45	12
IC4 (~1817.5)	41.897	194	2.59	18	0.55	1.228	0.014	2.462	0.015	19.2	2.1	0.21	7
IC5 (~1817.2)	41.947	143	8.22	30	0.79	1.221	0.009	2.475	0.005	18.6	0.4	0.10	4
IC6 (~1817)	41.992	77	3.56	4	0.48	1.191	0.009	2.450	0.011	18.2	1.0	0.14	1
IC7 (~1816.8)	42.042	63	3.77	15	0.45	1.219	0.005	2.439	0.040	16.0	1.9	0.12	4
IC8 (~1816.5)	42.102	45	3.88	11	0.44	1.236	0.015	2.485	0.021	18.5	0.5	0.11	3
IC9 (~1816.2)	42.172	40	1.01	1	0.34	1.238	0.008	2.502	0.037	18.7	1.1	0.33	1
IC10 (~1815.8)	42.259	14	1.51	4	0.38	1.176	0.007	2.419	0.027	16.9	1.2	0.25	3
IC11 (~1815.5)	42.329	7	1.65	5	0.14	1.198	0.018	2.440	0.012	19.6	1.6	0.09	3
IC12 (~1815)	42.399	16	0.71	4	0.15	1.219	0.028	2.443	0.031	21.5	2.9	0.21	6
IC13 (~1814.8)	42.469	36	0.47	3	0.24	1.208	0.014	2.472	0.038	19.8	1.7	0.50	6
IC14 (~1814.5)	42.539	12	0.75	23	0.69	1.260	0.008	2.517	0.035	18.9	1.9	0.92	31
IC15 (~1814.2)	42.609	16	0.41	2	<0.21	> 1.160	0.019	> 2.347	0.022	> 16.9	0.9	< 0.50	5

The data used to evaluate the Pb, Ba and Bi fluxes to Law Dome from 1814 to 1818 AD, during the eruption of the Tambora volcano.

Core designation	middle depth (m)	206Pb/207Pb	±	208Pb/207Pb	±	206Pb/204Pb	±	Pb conc (pg/g)	Ba conc (pg/g)	Pb/Ba (by wt)
DSS-W2k 15#1	14.2375	1.145	0.012	2.407	0.014	18.2	0.8	1.10	1.38	0.80
DSS-W2k 15#2	14.2925	1.155	0.023	2.379	0.032	16.1	1.3	1.36	0.97	1.40
DSS-W2k 15#3	14.3475	1.132	0.004	2.399	0.007	17.6	0.3	2.29	0.99	2.32
DSS-W2k 15#4	14.4025	1.145	0.013	2.402	0.022	17.2	1.0	1.20	1.07	1.11
DSS-W2k 15#5	14.4575	1.126	0.008	2.374	0.034	17.0	0.7	1.60	2.31	0.69
DSS-W2k 15#6	14.5125	1.123	0.007	2.387	0.030	16.7	0.7	1.37	0.49	2.79
DSS-W2k 15#7	14.5675	1.120	0.007	2.381	0.017	17.2	0.2	2.65	1.81	1.47
DSS-W2k 15#8	14.6225	1.159	0.008	2.419	0.032	17.4	1.1	1.61	1.15	1.40
DSS-W2k 15#9	14.6775	1.158	0.007	2.414	0.025	18.1	0.7	1.28	1.00	1.29
DSS-W2k 15#10	14.7325	1.148	0.006	2.404	0.018	17.6	0.5	1.63	2.10	0.77
DSS-W2k 15#11	14.7875	1.139	0.004	2.410	0.021	17.4	0.6	2.53	2.94	0.86
DSS-W2k 15#12	14.8425	1.138	0.009	2.406	0.012	17.3	0.8	1.46	2.70	0.54
DSS-W2k 15#13	14.8975	1.148	0.007	2.417	0.018	17.5	1.5	1.75	3.46	0.51
DSS-W2k 16#1	14.9195	1.170	0.009	2.431	0.014	18.1	0.5	1.35	0.54	2.49
DSS-W2k 16#2	14.9735	1.105	0.005	2.370	0.030	17.0	0.9	1.11	0.53	2.09
DSS-W2k 16#3	15.0275	1.118	0.009	2.384	0.005	17.3	0.1	3.53	61.25	0.06
DSS-W2k 16#4	15.0825	1.105	0.005	2.379	0.014	16.7	1.3	1.67	0.42	3.99
DSS-W2k 16#5	15.137	1.139	0.005	2.386	0.031	17.8	1.0	1.06	0.56	1.89
DSS-W2k 16#6	15.191	1.152	0.025	2.413	0.015	17.9	1.5	0.24	0.47	0.52
DSS-W2k 16#7	15.28025	1.162	0.007	2.411	0.004	18.4	0.6	1.81	1.21	1.50
DSS-W2k 16#8	15.36275	1.133	0.006	2.385	0.012	17.4	0.6	1.42	0.63	2.27
DSS-W2k 17#1	16.4665	1.143	0.009	2.417	0.032	18.1	1.0	0.39	3.61	0.11
DSS-W2k 17#2	16.5805	1.140	0.009	2.406	0.015	17.8	0.6	0.30	0.34	0.87
DSS-W2k 17#3	16.695	1.176	0.005	2.430	0.012	18.3	0.4	1.62	1.08	1.50
DSS-W2k 17#4	16.8085	1.172	0.005	2.432	0.007	18.1	0.7	2.00	1.86	1.07

The data used to evaluate seasonal variations in Pb and Ba at Law Dome from 1980 to 1985 AD, table 1/2.

Core designation	middle depth (m)	206Pb/207Pb	±	208Pb/207Pb	±	206Pb/204Pb	±	Pb conc (pg/g)	Ba conc (pg/g)	Pb/Ba (by wt)
DSS-W2k 18#1	17.3037369	1.157	0.006	2.398	0.025	17.1	1.0	0.33	0.15	2.19
DSS-W2k 18#2	17.4010707	1.168	0.004	2.418	0.005	17.8	0.6	1.56	0.41	3.79
DSS-W2k 18#3	17.4984045	1.211	0.010	2.457	0.014	18.1	1.5	0.82	0.34	2.41
DSS-W2k 18#4	17.5957383	1.161	0.002	2.423	0.014	17.7	0.5	1.74	0.81	2.16
DSS-W2k 18#5	17.6930721	1.153	0.009	2.423	0.003	17.8	0.3	1.72	0.52	3.31
DSS-W2k 18#6	17.7904059	1.168	0.005	2.424	0.012	18.0	0.3	2.17	1.03	2.11
DSS-W2k 18#7	17.8877397	1.197	0.005	2.429	0.020	18.9	0.8	2.06	1.30	1.58
DSS-W2k 18#8	17.9850735	1.170	0.006	2.421	0.005	17.8	0.5	1.73	0.99	1.75
DSS-W2k 18#9	18.0824073	1.163	0.005	2.423	0.003	18.2	0.4	1.13	0.39	2.92
DSS-W2k 18#10	18.1797411	1.148	0.002	2.404	0.009	17.8	0.2	1.09	0.26	4.16
DSS-W2k 19#1	18.2765	1.173	0.007	2.467	0.032	18.3	0.2	2.74	9.85	0.28
DSS-W2k 19#2	18.36785	1.174	0.009	2.414	0.014	18.1	0.7	1.54	1.71	0.90
DSS-W2k 19#3	18.45805	1.169	0.013	2.423	0.091	17.8	2.5	0.95	0.64	1.49
DSS-W2k 19#4	18.54825	1.152	0.010	2.395	0.046	16.1	0.9	0.49	0.63	0.78
DSS-W2k 19#5	18.64395	1.108	0.086	2.306	0.097	16.1	2.3	0.09	0.12	0.76
DSS-W2k 19#6	18.73305	1.149	0.007	2.403	0.016	17.4	0.5	1.27	0.40	3.16
DSS-W2k 19#7	18.8183	1.199	0.011	2.457	0.023	18.0	0.6	1.63	0.21	7.83
DSS-W2k 19#8	18.9063	1.117	0.002	2.380	0.008	17.4	0.2	0.81	0.29	2.77
DSS-W2k 19#9	18.9943	1.163	0.017	2.394	0.031	18.2	1.6	0.11	0.32	0.35
DSS-W2k 19#10	19.0823	1.172	0.006	2.421	0.010	18.1	0.3	0.74	0.44	1.68
DSS-W2k 19#11	19.1703	1.130	0.004	2.389	0.009	17.5	0.3	0.58	0.67	0.88
DSS-W2k 19#12	19.27365	1.159	0.003	2.417	0.007	17.9	0.1	1.79	0.67	2.67
DSS-W2k 20#1	19.325	1.166	0.004	2.414	0.004	17.8	0.4	1.48	0.57	2.60
DSS-W2k 20#2	19.38	1.193	0.003	2.446	0.007	18.6	0.3	2.00	0.76	2.64
DSS-W2k 20#3	19.44	1.170	0.003	2.403	0.005	17.0	0.9	1.71	0.69	2.46
DSS-W2k 20#4	19.5	1.161	0.003	2.406	0.009	17.5	0.4	1.21	0.67	1.82
DSS-W2k 20#5	19.565	1.168	0.009	2.428	0.051	18.2	0.8	1.47	0.67	2.20
DSS-W2k 20#6	19.6295	1.148	0.006	2.406	0.023	17.3	0.6	2.85	1.62	1.76
DSS-W2k 20#7	19.6895	1.161	0.005	2.420	0.010	17.6	0.5	1.07	0.69	1.56
DSS-W2k 20#8	19.75	1.163	0.003	2.419	0.008	17.9	0.3	1.83	0.72	2.54
DSS-W2k 20#9	19.81	1.164	0.002	2.424	0.003	17.8	0.2	2.32	1.09	2.12
DSS-W2k 20#10	19.87	1.161	0.004	2.418	0.010	17.9	0.3	1.26	1.04	1.20

The data used to evaluate seasonal variations in Pb and Ba at Law Dome from 1980 to 1985 AD, table 2/2.

NAME	CORE SECTION	206/207	err	208/207	err	206/204	err	Amount Pb (pg)	err	Amount Ba (pg)	err	Vol analysed. mL	Pb (pg)	err	Filament Blank Ba (pg)	err
BHD 132/2	OUTER2	1.1060	0.0035	2.3684	0.0029	16.859	0.223	234.33	2.19	26.26	4.74	11.8	0.29	0.05	1.7	0.2
BHD 132/2	OUTER3	1.2137	0.0009	2.4581	0.0223	17.915	0.947	10.81	0.03	12.15	1.92	11	0.29	0.05	1.7	0.2
BHD 132/2	OUTER4	1.2223	0.0085	2.4690	0.0383	18.216	1.307	13.87	0.12	26.88	9.72	26.1	0.29	0.05	1.7	0.2
BHD 132/2	IC TOP	1.2273	0.0267	2.4683	0.1601	17.498	3.447	13.50	1.80	22.31	19.34	24.5	0.29	0.05	1.7	0.2
BHD 132/2	IC TOP	1.2378	0.0055	2.4820	0.0236	18.870	1.276	8.03	0.14	17.03	1.00	11.4	0.29	0.05	1.7	0.2
BHD 132/2	IC BOT	1.2404	0.0074	2.4743	0.0291	18.438	1.869	10.86	0.30	31.60	7.46	21.5	0.29	0.05	1.7	0.2
BHD192	OUTER 1, CORE 1	1.0891	0.0090	2.3535	0.0012	16.657	0.023	4654.83	22.88	1179.96	47.58	9.1	0.29	0.05	1.7	0.2
BHD192	OUTER 2 CORE 1	1.1117	0.0029	2.3724	0.0021	17.022	0.151	322.25	5.70	35.85	5.56	10.4	0.29	0.05	1.7	0.2
BHD192	OUTER 3, CORE 1	1.1302	0.0023	2.3900	0.0055	17.217	0.054	20.28		51.99		12.1	0.29	0.05	1.7	0.2
BHD192	INNER, CORE1	1.2093	0.0116	2.4613	0.0133	20.746	2.037	2.99	0.02	10.52	0.29	11.6	0.29	0.05	1.7	0.2
BHD192	INNER, CORE 1	1.2027	0.0143	2.4457	0.1041	21.081	5.099	7.18	0.35	38.10	9.99	32.3	0.2	0.05	1.3	0.2
BHD192	OUTER 1, CORE 2	1.1304	0.0484	2.3781	0.0036	17.125	0.168	4205.82	5.12	1060.73	106.19	7.3	0.29	0.29	0.29	0.29
BHD192	OUTER 2 CORE 2	1.0854	0.0039	2.3496	0.0038	16.490	0.121	69.42	0.19	13.07	0.30	13.1	0.29	0.29	0.29	0.29
BHD192	OUTER 3, CORE 2	1.1479	0.0231	2.3969	0.0389	24.818	4.327	7.22	0.15	8.58	0.53	10.4	0.29	0.05	1.7	0.2
BHD192	INNER, CORE 2	1.1717	0.0131	2.4127	0.0322	17.664	1.588	6.38	0.07	11.12	0.93	12.1	0.29	0.05	1.7	0.2
BHD272	INNER TOP	1.1479	0.0069	2.3919	0.0244	17.261	1.500	15.26	1.32	64.35	3.03	20.3	0.29	0.05	1.7	0.2
BHD272	INNER BOTTOM	1.1030	0.0027	2.3653	0.0097	16.717	0.765	39.64	0.28	18.64	1.43	20	0.29	0.05	1.7	0.2
BHD272	OUTER4	1.0953	0.0116	2.3605	0.0038	16.776	0.402	245.55	1.03	64.84	13.20	11.3	0.29	0.05	1.7	0.2
BHD272	OUTER3	1.0980	0.0007	2.3644	0.0255	16.739	0.137	132.14	1.20	39.98	7.18	11.6	0.29	0.05	1.7	0.2
BHQ260	INNER TOP	1.2168	0.0244	2.3731	0.0412	14.573	1.979	5.29	0.34	45.01	#DIV/0!	21.4	0.29	0.05	1.7	0.2
BHQ260	INNER MID	1.2119	0.0081	2.4361	0.0745	15.405	2.496	5.45	4.06	65.26	192.99	21.4	0.29	0.05	1.7	0.2
BHQ260	INNER BOTTOM	1.2098	0.0162	2.4551	0.0576	16.067	1.804	2.25	0.04	15.01	0.50	11.7	0.29	0.05	1.7	0.2
BHQ260	INNER LAYER3	1.1399	0.0057	2.3582	0.0339	14.043	2.825	8.00	0.46	21.13	5.93	11.3	0.29	0.05	1.7	0.2
BHC1 135	IC TOP	1.2177	0.0147	2.4786	0.0118	18.710	0.934	35.86	1.64	431.00	21.62	11.5	0.29	0.05	1.7	0.2
BHC1 135	IC MID	1.2204	0.0049	2.4752	0.0119	18.426	0.478	27.96	1.62	249.61	7.58	7.3	0.29	0.05	1.7	0.2
BHC1 135	IC BOT	1.2007	0.0069	2.4562	0.0172	18.130	0.266	28.77	1.55	439.91	18.45	10.9	0.29	0.05	1.7	0.2
W2K 9	INNER T2/28/4	1.0977	0.0008	2.3582	0.0036	16.875	0.054	186.26	0.80	91.42	7.55	11.8	0.25	0.05	2.4	0.5
W2K 9	INNER T2/26/2	1.1630	0.0029	2.4274	0.0079	18.200	0.331	13.33	0.02	19.99	0.71	9.7	0.25	0.05	2.4	0.5
W2K 9	OUTER3	1.1029	0.0067	2.3631	0.0227	16.931	0.357	94.68	1.90	34.16	0.39	11.9	0.25	0.05	2.4	0.5
W2K 9	OUTER2	1.1302	0.0090	2.3844	0.0108	17.460	0.114	218.38	2.03	84.46	19.66	12.5	0.23	0.05	2.4	0.5
W2K 9	OUTER1	1.1642	0.0014	2.4045	0.0040	18.088	0.101	353.85	2.77	43.81	1.69	9.5	0.23	0.05	2.4	0.5
W2k 17	OUTER4	1.1654	0.0052	2.4106	0.0089	17.610	0.325	52.96	1.18	26.94	1.60	33.2	0.23	0.05	2.4	0.5
W2k 17	IC TOP?	1.1452	0.0079	2.4078	0.0306	17.812	0.975	4.32	0.24	40.63	30.97	10.6	0.23	0.05	2.4	0.5
W2k 17	IC top-mid	1.1417	0.0083	2.3959	0.0135	17.498	0.564	3.30	0.02	5.95	1.10	10.3	0.23	0.05	2.4	0.5
W2k 17	IC mid-bot	1.1777	0.0052	2.4229	0.0116	18.192	0.376	19.00	0.18	14.95	1.11	11.6	0.23	0.05	2.4	0.5
W2k 17	IC bottom	1.1745	0.0052	2.4253	0.0066	17.991	0.711	37.95	5.67	37.60	2.61	18.9	0.23	0.05	2.4	0.5

Law Dome data table 1/9, Procedural Blank Pb isotopic composition used was

$$^{206}\text{Pb}/^{207}\text{Pb} = 1.13 \pm 0.02, \quad ^{208}\text{Pb}/^{207}\text{Pb} = 2.34 \pm 0.02 \quad \text{and} \quad ^{206}\text{Pb}/^{204}\text{Pb} = 14 \pm 1.$$

NAME	CORE SECTION	206/207	err	208/207	err	206/204	err	Amount Pb (pg)	err	Amount Ba (pg)	err	Vol analysed, mL	Pb (pg)	err	Filament Blank Ba(pg)	err
W20K 007/2	OUTER1	1.1334	0.0032	2.3850	0.0076	17.411	0.151	123.25	0.54	289.30	3.45	9.1	0.22	0.05	2.2	0.05
W20K 007/2	OUTER2	1.1687	0.0114	2.4181	0.0131	18.010	0.256	30.51	0.09	17.13	2.42	11.2	0.22	0.05	2.2	0.05
W20K 007/2	OUTER3	1.1716	0.0058	2.4257	0.0121	17.859	0.664	21.34	0.10	13.31	1.72	12.2	0.09	0.03	1.3	0.5
W20K 007/2	INNER BOTTOM	1.1658	0.0040	2.4141	0.0058	18.038	0.164	47.87	0.28	25.97	0.34	21.1	0.09	0.03	1.3	0.5
W20K 007/2	INNER TOP	1.1568	0.0143	2.4074	0.0216	17.478	0.505	36.61	0.34	29.38	3.84	20	0.09	0.03	1.3	0.5
W20K 007/2	INNER TOP	1.1649	0.0074	2.4188	0.0175	18.052	0.287	27.77	0.31	22.87	0.63	16.7	0.15	0.03	1.7	0.05
W20K 9	INNER TOP	1.1617	0.0072	2.4206	0.0105	18.035	0.494	50.88	0.89	46.59	1.63	16.5	0.15	0.03	1.7	0.05
W20K 9	INNER BOTTOM	1.1695	0.0014	2.4177	0.0077	18.224	0.576	49.27	1.54	37.57	4.18	16.7	0.21	0.05	2.1	0.3
W20K 9	OUTER3	1.1672	0.0042	2.4201	0.0138	17.982	0.776	33.47	0.61	42.05	1.18	16.6	0.21	0.05	2.1	0.3
W20K 9	OUTER2	1.1723	0.0050	2.4290	0.0066	17.862	0.556	30.60	0.33	38.54	2.55	9.3	0.23	0.05	2.2	0.5
W20K 9	OUTER1	1.1379	0.0108	2.3923	0.0399	17.589	0.753	510.19	12.57	3940.98	1181.37	9.8	0.23	0.05	2.2	0.5
W20K 10	INNER TOP	1.1581	0.0135	2.4041	0.0167	17.577	0.320	42.89	0.19	39.64	1.80	17.2	0.23	0.05	2.2	0.5
W20K 10	INNER TOP	1.1451	0.0033	2.4001	0.0066	17.496	0.108	34.39	0.10	50.43	3.05	17	0.23	0.05	2.4	0.3
W20K 10	INNER BOTTOM	1.1519	0.0074	2.4031	0.0213	17.443	0.560	19.07	0.19	20.44	1.43	15.1	0.23	0.05	2.2	0.5
W20K 10	OUTER3	1.1513	0.0198	2.4167	0.0604	18.050	5.699	24.00	21.30	16.81	18.95	11	0.2	0.03	2.2	0.05
W20K 10	OUTER2	1.1514	0.0064	2.4039	0.0054	17.685	0.253	25.30	0.09	26.01	0.85	10.9	0.2	0.03	2.2	0.05
W20K 10	OUTER1	1.1774	0.0018	2.4148	0.0142	18.166	0.199	1218.77	99.74	1311.71	165.73	10.9	0.2	0.03	2.2	0.05
W20K 11	INNER TOP	1.1641	0.0103	2.4197	0.0120	18.271	0.563	48.95	1.40	101.83	9.04	19.1	0.2	0.03	2.2	0.05
W20K 11	INNER TOP	1.1543	0.0043	2.3986	0.0087	17.349	0.739	30.97	0.87	60.86	1.75	12.5	0.23	0.03	2.4	0.3
W20K 11	INNER BOTTOM	1.1488	0.0049	2.4065	0.0112	17.093	2.275	20.80	0.17	40.32	2.64	16.8	0.2	0.03	2.2	0.05
W20K 11	OUTER3	1.1550	0.0083	2.4143	0.0102	17.596	0.636	27.85	0.32	70.31	1.91	15.4	0.2	0.03	2.2	0.05
W20K 11	OUTER2	1.1490	0.0008	2.4013	0.0033	17.767	0.217	26.88	0.17	46.81	0.76	10.8	0.2	0.03	2.2	0.05
W20K 11	OUTER1	1.1219	0.0079	2.3881	0.0033	17.240	0.817	362.57	9.03	266.28	12.46	11.3	0.2	0.03	2.2	0.05
W20K 12#2	INNER TOP	1.1573	0.0031	2.4126	0.0052	17.994	0.130	64.93	0.26	67.85	0.91	15.6	0.25	0.05	2.4	0.5
W20K 12#2	INNER BOTTOM	1.1814	0.0068	2.4363	0.0072	18.301	0.239	45.14	0.32	29.44	1.27	15.3	0.25	0.05	2.4	0.5
W20K 12#2	OUTER3	1.1818	0.0043	2.4375	0.0140	18.416	0.502	41.05	0.56	40.74	0.44	12.4	0.25	0.05	2.4	0.5
W20K13	INNER TOP	1.1507	0.0086	2.4023	0.0165	17.969	0.426	20.11	0.14	40.51	0.56	14.7	0.25	0.03	2.5	0.3
W20K13	INNER BOTTOM	1.1442	0.0052	2.3946	0.0051	17.628	0.382	30.26	0.33	86.65	3.89	17.1	0.25	0.03	2.5	0.3
W20K13	OUTER3	1.1494	0.0209	2.4137	0.0255	19.777	5.680	28.92	1.11	51.65	1.61	20	0.45	0.1	2.4	0.3
W20K13	OUTER 2	1.1375	0.0086	2.3939	0.0173	17.594	0.131	59.29	1.47	121.54	17.92	12.4	0.25	0.03	2.5	0.3
W20K13	OUTER 1	1.1317	0.0045	2.3814	0.0121	17.301	0.484	614.30	24.04	1038.35	152.36	10.8	0.25	0.03	2.5	0.3
W20K 15#2	INNER	1.1733	0.0045	2.4338	0.0077	18.064	0.182	23.05	0.27	34.15	0.99	17.3	0.25	0.05	2.4	0.5
W20K 15#2	INNER	1.1695	0.0082	2.4473	0.0315	20.545	8.981	21.00	1.06	47.60	12.20	18.8	0.23	0.05	2.4	0.5
W20K 15#2	OUTER3	1.1548	0.0105	2.4072	0.0143	17.481	0.353	5.48	0.08	30.31	2.72	12.2	0.25	0.05	2.4	0.5
W20K 15#2	OUTER3	1.2362	0.0039	2.4536	0.0158	20.109	1.049	5.14	0.03	30.36	1.51	10.9	0.23	0.05	2.4	0.5
W20K 15#2	OUTER3	1.2063	0.0102	2.4154	0.0117	17.934	1.612	9.60	0.55	42.21	2.11	23.5	0.23	0.05	2.4	0.5
W20K 15#2	OUTER3	1.2371	0.0205	2.4136	0.0081	18.344	1.400	10.17	0.57	41.15	1.04	18.2	0.23	0.05	2.4	0.5
W20K 15#2	OUTER3	1.2146	0.0125	2.3985	0.0144	17.887	0.453	14.63	1.46	45.39	1.52	10.6	0.23	0.05	2.4	0.5
W20K 15#2	OUTER2	1.1634	0.0094	2.4171	0.0099	17.484	0.686	20.58	1.33	17.43	0.13	13	0.23	0.05	2.4	0.5
W20K 15#2	OUTER1	1.1430	0.0021	2.3919	0.0090	17.524	0.093	156.97	1.23	58.61	5.81	10.6	0.23	0.05	2.4	0.5

Law Dome data table 2/9, Procedural Blank Pb isotopic composition used was

$$^{206}\text{Pb}/^{207}\text{Pb} = 1.13 \pm 0.02, \quad ^{208}\text{Pb}/^{207}\text{Pb} = 2.34 \pm 0.02 \quad \text{and} \quad ^{206}\text{Pb}/^{204}\text{Pb} = 14 \pm 1.$$

NAME	CORE SECTION	206/207	err	208/207	err	206/204	err	Amount Pb (pg)	err	Amount Ba (pg)	err	Vol analysed. mL	Pb (pg)	err	Filament Blank Ba(pg)	err
W20K 16#2	INNER	1.1688	0.0061	2.4236	0.0127	18.140	0.416	9.84	0.07	29.13	0.91	13.3	0.25	0.05	2.4	0.5
W20K 16#2	OUTER3	1.1595	0.0065	2.4136	0.0175	17.414	0.818	9.14	0.08	22.73	0.64	12.2	0.25	0.05	2.4	0.5
W20K 16#2	OUTER2	1.1432	0.0069	2.3972	0.0186	16.944	1.006	11.79	0.09	19.56	0.77	11.1	0.25	0.05	2.4	0.5
W20K 16#2	OUTER1	1.1336	0.0027	2.3819	0.0060	17.001	0.445	52.19	1.47	44.56	0.89	8.4	0.25	0.05	2.4	0.5
W20K18	OUTER4	1.1840	0.0073	2.4309	0.0096	18.039	0.319	50.17	1.31	70.57	2.76	22.1	0.18	0.05	2.4	0.3
W20K18	IC TOP	1.1834	0.0076	2.4307	0.0178	17.756	1.084	52.92	3.54	62.24	2.21	19.4	0.18	0.05	2.4	0.3
W20K18	IC TOP-IMD	1.1880	0.0074	2.4348	0.0069	17.605	1.006	71.96	2.21	66.02	5.40	20.3	0.18	0.05	2.4	0.3
W20K18	IC MID-BOT	1.1538	0.0192	2.3882	0.0700	16.662	0.847	20.20	1.46	19.60	0.99	27.9	0.18	0.05	2.4	0.3
W20K18	IC MID-BOT	1.1671	0.0083	2.4230	0.0090	18.013	0.526	15.31	0.38	17.42	1.67	16.3	0.18	0.05	2.4	0.3
W20K18	IC BOT	1.1735	0.0095	2.3931	0.1615	16.431	2.321	24.28	4.50	37.55	14.69	23.8	0.18	0.05	2.4	0.3
W20K18	IC BOT	1.1709	0.0015	2.4175	0.0865	17.709	3.204	19.15	3.62	25.22	4.06	15.1	0.18	0.05	2.4	0.3
W20K 35/2	OUTER1	1.1599	0.0085	2.4019	0.0107	17.950	0.235	1330.30	19.15	1053.00	56.58	13.1	0.1	0.02	1.4	0.2
W20K 35/2	OUTER2	1.1696	0.0319	2.4112	0.1517	17.452	1.581	14.18	1.02	14.28	0.11	12.2	0.1	0.02	1.4	0.2
W20K 35/2	OUTER2	1.1611	0.0040	2.4283	0.0084	17.790	0.299	39.29	56.61	77.90	442.52	10.9	0.22	0.05	2.2	0.05
W20K 35/2	OUTER3	1.2134	0.0117	2.4456	0.0136	18.481	3.193	4.78	0.01	12.17	0.78	12.5	0.1	0.02	1.4	0.2
W20K 35/2	OUTER3	1.2007	0.0355	2.4763	0.0270	18.418	1.962	6.95	0.13	42.96	0.15	20.3	0.15	0.02	1.7	0.05
W20K 35/2	INNER BOTTOM	1.2192	0.0220	2.4581	0.0438	20.695	1.812	5.41	0.10	19.88	1.23	13.4	0.1	0.02	1.4	0.2
W20K 35/2	INNER BOTTOM	1.2165	0.1821	2.5168	0.0299	18.642	1.502	12.33	0.85	43.17	13.31	33.3	0.1	0.02	1.4	0.2
W20K 35/2	INNER BOTTOM	1.2149	0.0128	2.4793	0.0066	19.122	0.888	9.88	0.29	39.20	5.79	26.6	0.23	0.05	2.4	0.5
W20K 35/2	INNER TOP	1.2047	0.0102	2.4549	0.0260	27.934	40.198	2.58	0.16	10.23	1.05	12.6	0.1	0.02	1.4	0.2
W20K 35/2	INNER TOP	1.2044	0.0250	2.4552	0.0657	18.380	0.431	6.56	0.10	225.66	205.29	34.5	0.1	0.02	1.4	0.2
W20K 35/2	INNER TOP	1.2114	0.0231	2.4552	0.0269	18.111	3.678	4.59	0.12	21.20	1.19	28.5	0.23	0.05	2.4	0.5
W20K 41	INNER	1.2526	0.0015	2.4897	0.0089	19.691	0.428	13.17	0.15	23.48	5.28	23.3	0.23	0.05	2.4	0.5
W20K 41	OUTER3	1.2532	0.0055	2.4938	0.0154	19.587	0.497	13.38	0.19	31.13	2.24	25	0.23	0.05	2.4	0.5
W20K 46	INNER	1.1953	0.0108	2.4379	0.0342	18.634	1.121	4.46	0.15	38.62	4.87	32	0.23	0.05	2.4	0.5
W20K 46	INNER	1.2257	0.0183	2.4796	0.0271	18.898	2.209	14.47	0.15	67.11	8.78	32.7	0.23	0.05	2.4	0.5
W20K 46	INNER	1.2228	0.0228	2.4630	0.0434	17.402	1.791	15.91	0.55	53.90	2.50	39.7	0.23	0.05	2.4	0.5
W20K 46	OUTER3	1.1903	0.0070	2.4384	0.0104	18.237	0.761	19.21	0.37	112.13	22.08	31.7	0.23	0.05	2.4	0.5
W20K50	INNER TOP	1.2329	0.0072	2.4709	0.0131	18.241	0.867	11.14	0.13	22.44	1.36	16	0.45	0.1	2.4	0.3
W20K50	INNER BOTTOM	1.2408	0.0159	2.4917	0.0455	18.943	1.678	11.66	0.22	47.06	7.88	20	0.45	0.1	2.4	0.3
W20K50	INNER BOTTOM	1.2363	0.0051	2.4846	0.0302	18.328	1.653	14.69	0.28	55.91	1.62	30.5	0.23	0.03	2.4	0.3
W20K50	OUTER3	1.2501	0.0155	2.5042	0.0262	19.775	1.854	6.47	0.18	89.34	33.24	23.5	0.25	0.05	2.4	0.3
W20K50	OUTER2	1.2216	0.0076	2.4369	0.1347	16.238	2.556	8.92	0.26	14.77	6.15	11.7	0.25	0.05	2.4	0.3
W20K50	OUTER1	1.1232	0.0025	2.3769	0.0138	17.225	0.211	259.47	6.70	115.27	7.80	13.6	0.25	0.05	2.4	0.3
W20K55	INNER TOP	1.1910	0.0113	2.4263	0.0078	18.427	0.506	12.60	1.31	94.49	18.68	23.2	0.23	0.05	2.4	0.5
W20K 55	INNER BOTTOM	1.2226	0.0043	2.4805	0.0070	18.436	0.572	12.74	0.48	45.57	4.72	32	0.23	0.05	2.4	0.5
W20K 55	INNER MIX	1.2028	0.0100	2.4629	0.0286	18.848	0.455	11.17	0.10	47.35	6.92	24.9	0.23	0.05	2.4	0.5
W20K 55	OUTER3	1.1739	0.0032	2.4067	0.0206	17.803	0.251	16.71	0.40	44.48	3.17	30.4	0.23	0.05	2.4	0.5
W20K 55	OUTER2	1.1463	0.0246	2.3797	0.0426	16.781	0.954	10.47	0.20	13.02	2.05	11.6	0.23	0.05	2.4	0.5
W20K 55	OUTER1	1.1083	0.0107	2.3446	0.0345	16.722	0.397	316.60	38.51	230.23	8.08	10	0.23	0.05	2.4	0.5

Law Dome data table 3/9, Procedural Blank Pb isotopic composition used was

$$^{206}\text{Pb}/^{207}\text{Pb} = 1.13 \pm 0.02, \quad ^{208}\text{Pb}/^{207}\text{Pb} = 2.34 \pm 0.02 \quad \text{and} \quad ^{206}\text{Pb}/^{204}\text{Pb} = 14 \pm 1.$$

NAME	CORE SECTION	206/207	err	208/207	err	206/204	err	Amount Pb (pg)	err	Amount Ba (pg)	err	Vol analysed. mL	Pb (pg)	err	Filament Blank Ba (pg)	err
W20K62	INNER (bottom)	1.2504	0.0102	2.4968	0.0205	19.817	0.874	15.57	0.48	22.20	0.94	17.3	0.25	0.05	2.4	0.3
W20K62	INNER (bottom)	1.2488	0.0863	2.5110	0.1905	19.217	2.920	6.41	0.54	20.81	63.82	18.6	0.25	0.05	2.4	0.3
W20K62	INNER (bottom)	1.2399	0.0109	2.4727	0.0208	18.279	1.197	10.44	0.22	21.96	1.91	28.7	0.23	0.03	2.4	0.3
W20K62	INNER cont. top	1.2287	0.0136	2.4724	0.0255	19.383	0.841	5.10	0.05	11.82	0.50	16.4	0.22	0.05	2.4	0.3
W20K62	INNER mixed	1.1365	0.0394	2.3799	0.0308	15.042	41.706	4.68	17.99	39.02	99.87	15	0.22	0.05	2.4	0.3
W20K62	OUTER2	1.2258	0.0107	2.4802	0.0213	18.698	1.138	5.49	0.01	46.27	30.48	11.5	0.22	0.05	2.4	0.3
W20K62	OUTER1	1.1418	0.0071	2.3977	0.0271	17.776	0.428	74.45	1.61	23.12	3.56	11.8	0.22	0.05	2.4	0.3
W20K62	OUTER3	1.2412	0.0155	2.4851	0.0123	19.453	2.771	7.29	0.03	17.18	1.74	19	0.18	0.05	2.4	0.3
W20K70	INNER TOP	1.2219	0.0054	2.4724	0.0094	19.846	0.686	3.89	0.11	10.23	0.61	17.1	0.23	0.03	2.2	0.3
W20K70	INNER BOTTOM	1.2348	0.0080	2.4902	0.0131	19.265	0.456	10.68	0.45	43.07	8.43	17.5	0.23	0.03	2.2	0.3
W20K70	OUTER3	0.9749	0.1470	1.8386	0.3391	13.604	11.889	9.52	1.66	54.28	39.83	34	0.23	0.03	2.2	0.3
W20K70	OUTER2	1.2173	0.0163	2.4303	0.0559	18.017	1.611	5.35	0.31	19.00	1.13	12.8	0.23	0.03	2.2	0.3
DSS99-36	INNER TOP	1.1892	0.0052	2.4469	0.0099	18.364	0.183	24.96	0.08	14.88	0.40	23.5	0.25	0.05	2.4	0.5
DSS99-36	INNER BOTTOM	1.1716	0.0037	2.4356	0.0100	18.188	0.352	21.51	0.25	42.27	3.46	24.4	0.25	0.05	2.4	0.5
DSS99-36	OUTER3	1.1403	0.0021	2.4023	0.0045	17.500	0.216	21.59	0.06	20.19	4.01	11.7	0.23	0.05	2.4	0.5
DSS99-36	OUTER2	1.1465	0.0023	2.3984	0.0466	17.541	0.366	24.44	1.01	36.04	0.70	14.2	0.23	0.05	2.4	0.5
DSS99-36	OUTER1	1.1212	0.0043	2.3781	0.0078	17.116	0.306	56.70	0.43	83.18	2.51	9.9	0.23	0.05	2.4	0.5
DSS99-40	INNER TOP	1.1428	0.0030	2.3831	0.0297	16.357	0.618	4.31	0.33	53.46	3.36	11.1	0.23	0.05	2.4	0.5
DSS99-40	INNER TOP-MID	1.2166	0.0041	2.4550	0.0079	18.414	0.383	18.94	0.12	48.39	4.79	12.4	0.23	0.05	2.4	0.5
DSS99-40	INNER MID-BOTT	1.1770	0.0045	2.4389	0.0140	17.829	0.885	19.20	0.51	98.51	10.76	11.7	0.23	0.05	2.4	0.5
DSS99-40	INNER BOTTOM	1.1599	0.0086	2.4195	0.0094	17.825	0.190	22.20	4.37	121.23	28.06	11.7	0.23	0.05	2.4	0.5
DSS99-51	INNER TOP	1.2033	0.0106	2.4638	0.0211	18.642	0.322	25.83	0.05	27.06	1.00	17.2	0.18	0.05	2.4	0.3
DSS99-51	INNER TOP	1.1981	0.0054	2.4593	0.0066	18.596	0.664	19.18	0.10	21.38	0.42	12.3	0.25	0.05	2.4	0.3
DSS99-51	INNER BOTTOM	1.1680	0.0020	2.4240	0.0022	18.045	0.126	21.20	0.06	11.80	0.79	14.1	0.23	0.03	2.2	0.3
DSS99-51	OUTER3 (inner)	1.1820	0.0046	2.4465	0.0089	18.293	0.090	22.16	0.11	25.42	0.74	13.8	0.23	0.03	2.2	0.3
DSS99-60	INNER TOP	1.1729	0.0096	2.4463	0.0040	18.474	0.640	27.59	0.79	18.77	5.80	17.2	0.23	0.03	2.2	0.3
DSS99-60	INNER BOTTOM	1.1675	0.0021	2.4335	0.0122	18.307	0.851	39.78	0.78	40.61	18.19	15.5	0.23	0.03	2.2	0.3
DSS99-60	OUTER3 (inner)	1.1650	0.0052	2.4334	0.0102	18.054	0.181	38.66	0.60	26.53	4.45	16.5	0.23	0.03	2.2	0.3
DSS99-68	INNER TOP	1.1088	0.0043	2.3754	0.0022	16.905	0.227	46.32	0.35	26.71	0.82	24.4	0.25	0.05	2.4	0.5
DSS99-68	INNER BOTTOM	1.1461	0.0080	2.4041	0.0090	17.910	0.195	31.12	0.87	41.07	3.11	19.5	0.25	0.05	2.4	0.5
DSS99-68	INNER3	1.1148	0.0074	2.3836	0.0116	17.538	0.288	26.12	1.03	27.80	5.29	12.3	0.25	0.05	2.4	0.5
DSS99-68	OUTER3	1.0756	0.0077	2.2257	0.0690	11.038	2.640	21.76	4.83	15.77	0.39	10.9	0.25	0.05	2.4	0.5
DSS99-68	OUTER3	1.1015	0.0061	2.3538	0.0081	16.414	0.413	31.52	0.26	19.22	0.87	11	0.25	0.05	2.4	0.5
DSS99-68	OUTER2	1.0976	0.0021	2.3555	0.0164	16.596	0.312	34.69	0.24	21.13	0.94	10.7	0.25	0.05	2.4	0.5
DSS99-75	IC TOP	1.1737	0.0182	2.3125	0.0514	14.087	4.642	4.00	0.42	17.06	2.51	17.9	0.2	0.02	2.5	0.1
DSS99-75	IC TOP	1.2106	0.0093	2.4116	0.0147	18.044	1.454	4.73	0.35	16.34	0.43	14.1	0.2	0.02	2.5	0.1
DSS99-75	IC MID-TOP	1.1870	0.0435	2.4146	0.0552	16.148	10.52	8.71	9.80	9.80	0.79	18.4	0.15	0.02	1.5	0.1
DSS99-75	IC MID-TOP	1.1847	0.0050	2.4163	0.0136	17.117	0.450	10.14	0.20	11.98	1.02	17.3	0.2	0.02	2.5	0.1
DSS99-75	IC MID-BOTTOM	1.1836	0.0037	2.4245	0.0313	17.345	1.548	15.73	0.34	26.68	0.90	11.8	0.15	0.02	1.5	0.1
DSS99-75	IC BOTTOM	1.1702	0.0319	2.4088	0.0862	15.970	3.251	13.75	0.37	45.94	8.62	17.1	0.15	0.02	1.5	0.1
DSS99-75	IC BOTTOM	1.1644	0.0097	2.4102	0.0176	17.019	0.994	8.68	0.11	24.86	1.47	9.6	0.2	0.02	2.5	0.1
DSS99-75	Inner3	1.1873	0.0095	2.4304	0.0263	17.189	1.116	23.25	0.56	41.48	0.69	23.1	0.2	0.02	2.5	0.1
DSS99-75	Outer3	1.1642	0.0034	2.4151	0.0090	17.440	0.418	16.01	0.06	20.17	1.00	11.1	0.2	0.02	2.5	0.1

Law Dome data table 4/9, Procedural Blank Pb isotopic composition used was

$$^{206}\text{Pb}/^{207}\text{Pb} = 1.13 \pm 0.02, \quad ^{208}\text{Pb}/^{207}\text{Pb} = 2.34 \pm 0.02 \quad \text{and} \quad ^{206}\text{Pb}/^{204}\text{Pb} = 14 \pm 1.$$

NAME	CORE SECTION	206/207	err	208/207	err	206/204	err	Amount Pb (pg)	err	Amount Ba (pg)	err	Vol analysed, mL	Pb (pg)	err	Filament Blank Ba (pg)	err
DSS99-79	OUTER3	1.2093	0.0060	2.4714	0.0207	18.032	0.908	11.46	0.27	20.16	0.25	19.5	0.25	0.05	2.4	0.5
DSS99-79	IC Bottom	1.2067	0.0033	2.4714	0.0094	18.579	0.123	10.28	0.16	23.36	0.25	15.8	0.25	0.05	2.4	0.5
DSS99-79	IC Bott/mid	1.2032	0.0060	2.4769	0.0109	18.500	0.193	11.10	0.17	26.14	0.25	19.3	0.25	0.05	2.4	0.5
DSS99-79	IC Mid/Top	1.2143	0.0329	2.4487	0.0628	17.433	2.185	8.50	0.32	16.84	0.25	19.1	0.25	0.05	2.4	0.5
DSS99-79	IC Mid/Top	1.2089	0.0205	2.4497	0.0092	17.101	2.321	6.13	0.63	11.59	0.25	11.6	0.25	0.05	2.4	0.5
DSS99-79	IC Top	1.2043	0.0083	2.4504	0.0152	18.288	0.547	8.53	0.08	19.61	0.25	16.6	0.25	0.05	2.4	0.5
DSS99-84	INNER TOP	1.2234	0.0666	2.4815	0.0227	20.714	5.483	15.37	0.08	27.66	0.23	26.7	0.23	0.05	2.4	0.5
DSS99-84	INNER TOP	1.2244	0.0042	2.4861	0.0169	18.759	0.353	15.50	0.16	24.90	0.23	31.4	0.23	0.05	2.4	0.5
DSS99-84	INNER TOP	1.2240	0.0049	2.4842	0.0069	19.541	1.380	15.37	0.08	27.66	0.23	26.7	0.23	0.05	2.4	0.5
DSS99-84	INNER BOTTOM	1.2256	0.0077	2.4794	0.0124	19.131	0.327	13.68	0.05	18.09	0.24	25.5	0.24	0.05	2.4	0.5
DSS99-84	OUTER3	1.2255	0.0041	2.4773	0.0072	19.052	0.259	8.15	0.95	21.74	0.24	12.5	0.24	0.05	2.4	0.5
DSS99-95	INNER TOP	1.2360	0.0046	2.4892	0.0010	19.229	0.551	12.37	0.07	31.61	0.23	25.7	0.23	0.05	2.4	0.5
DSS99-95	INNER BOTTOM	1.2330	0.0088	2.4606	0.0137	18.379	0.701	8.42	0.07	19.36	0.23	25.4	0.23	0.05	2.4	0.5
DSS99-95	INNER3	1.2016	0.0079	2.4272	0.0269	17.981	0.806	5.71	0.03	16.94	0.23	11	0.23	0.05	2.4	0.5
DSS99-95	OUTER3	1.1370	0.0090	2.3864	0.0190	17.403	0.215	20.29	0.29	19.98	0.23	11.6	0.23	0.05	2.4	0.5
DSS99-95	OUTER2	1.1150	0.0069	2.3725	0.0105	17.067	0.199	120.52	1.76	154.27	0.23	10.8	0.23	0.05	2.4	0.5
DSS99-103	INNER TOP	1.3001	0.3272	2.6979	0.9751	-9.602	#####	13.51	0.35	17.95	0.23	26.1	0.23	0.05	2.4	0.5
DSS99-103	INNER TOP	1.2302	0.0198	2.4878	0.0890	19.423	2.437	21.69	0.87	69.81	0.23	32.8	0.23	0.05	2.4	0.5
DSS99-103	INNER TOP	1.2188	0.0040	2.4442	0.0179	18.456	0.804	6.96	0.04	30.53	0.23	30.1	0.23	0.05	2.4	0.5
DSS99-103	INNER BOTTOM	1.2376	0.0051	2.4870	0.0116	19.426	0.223	12.96	0.09	32.92	0.23	27.7	0.23	0.05	2.4	0.5
DSS99-103	OUTER3	1.2361	0.0040	2.4957	0.0148	19.334	0.499	5.39	0.03	12.89	0.24	11	0.24	0.05	2.4	0.5
DSS 218	INNER BOTTOM	1.2423	0.0031	2.4881	0.0324	19.407	1.208	10.90	0.33	32.09	0.23	30.1	0.23	0.05	2.4	0.5
DSS 218	INNER BOTTOM	1.2126	0.0243	2.4230	0.0347	17.244	1.347	14.89	0.51	22.90	0.23	35	0.23	0.05	2.4	0.5
DSS 218	INNER TOP	1.1761	0.0051	2.4357	0.0074	17.737	0.577	30.69	0.33	52.12	0.23	30.7	0.23	0.05	2.4	0.5
DSS 218	INNER TOP	1.2251	0.0074	2.4568	0.0167	18.463	1.333	5.25	0.14	20.22	0.23	11.1	0.23	0.05	2.4	0.5
DSS 218	OUTER 3	1.2066	0.0038	2.4500	0.0152	18.394	0.457	12.97	0.10	26.95	0.23	24.9	0.23	0.05	2.4	0.5
DSS 257	INNER TOP	1.2493	0.0045	2.5029	0.0128	18.774	0.635	13.03	0.17	26.84	0.23	32.7	0.23	0.05	2.4	0.5
DSS 257	INNER BOTTOM	1.2346	0.0042	2.4782	0.0037	18.573	0.406	11.57	0.07	22.85	0.23	33.9	0.23	0.05	2.4	0.5
DSS 257	OUTER3	1.2506	0.0135	2.4862	0.0226	19.219	0.449	9.83	0.02	15.61	0.23	26.4	0.23	0.05	2.4	0.5
DSS main 790	OUTER4	1.2535	0.0055	2.4968	0.0127	19.705	0.343	15.88	0.08	85.17	0.23	31.7	0.23	0.05	2.4	0.5
DSS main 790	INNER BOTTOM	1.2650	0.0062	2.4928	0.0172	19.114	0.373	21.38	0.09	26.76	0.23	30.4	0.23	0.05	2.4	0.5
DSS main 790	INNER TOP	1.2179	0.0118	2.4461	0.0147	18.831	0.792	10.55	0.17	89.90	0.23	27.8	0.23	0.05	2.4	0.5
DSS main 790	INNER TOP	1.2101	0.0084	2.4369	0.0066	18.731	0.448	9.71	0.10	81.40	0.23	27.6	0.23	0.05	2.4	0.5
DSS main 1129	INNER	1.2125	0.0074	2.4476	0.0154	18.956	1.199	12.09	0.83	104.55	0.23	31.8	0.23	0.05	2.4	0.5
DSS main 1129	OUTER4	1.1922	0.0104	2.4408	0.0100	18.297	0.780	12.04	0.08	97.58	0.23	26.2	0.23	0.05	2.4	0.5

Law Dome data table 5/9, Procedural Blank Pb isotopic composition used was

$$^{206}\text{Pb}/^{207}\text{Pb} = 1.13 \pm 0.02, \quad ^{208}\text{Pb}/^{207}\text{Pb} = 2.34 \pm 0.02 \quad \text{and} \quad ^{206}\text{Pb}/^{204}\text{Pb} = 14 \pm 1.$$

NAME	CORE SECTION	206/207	err	208/207	err	206/204	err	Amount Pb (pg)	err	Amount Ba (pg)	err	Vol analysed, mL	Pb (pg)	err	Filament Blank Ba(pg)	err
W2k 15	TOP-OUTER3	1.1429	0.0029	2.3808	0.0210	16.986	0.719	22.36	0.28	20.64	5.33	11.3	0.23	0.05	2.4	0.5
W2k 15	BOTTOM-OUTER3	1.1429	0.0034	2.4034	0.0026	17.529	0.297	45.02	1.04	32.07	6.19	12.3	0.23	0.05	2.4	0.5
W2k 16	OUTER3	1.1328	0.0011	2.3769	0.0097	16.973	0.796	21.03	0.40	33.61	1.52	12.2	0.23	0.05	2.4	0.5
W2k 15/2	TOP IC1	1.1486	0.0115	2.4022	0.0140	18.104	0.747	13.04	0.37	18.36	1.32	11.6	0.23	0.05	2.4	0.5
W2k 15/2	TOP IC1	1.1200	0.5067	2.3300	0.9468	17.441	8.547	13.73	3.26	13.48	0.90	12.1	0.23	0.05	2.4	0.5
W2k 15/2	TOP IC2	1.1562	0.1512	2.4146	0.2060	17.227	1.946	19.77	18.82	15.31	10.00	10.6	0.23	0.05	2.4	0.5
W2k 15/2	TOP IC2	1.1583	0.0230	2.3749	0.0311	16.049	1.255	16.58	0.46	14.05	1.27	12	0.23	0.05	2.4	0.5
W2k 15/2	TOP IC3	1.1352	0.0042	2.3943	0.0064	17.521	0.257	23.39	1.31	12.38	0.90	10.1	0.23	0.05	2.4	0.5
W2k 15/2	TOP IC4	1.1344	0.0310	2.3727	0.0333	16.234	2.252	10.80	0.67	12.07	6.36	10	0.23	0.05	2.4	0.5
W2k 15/2	TOP IC4	1.1491	0.0129	2.3981	0.0211	17.145	0.977	13.26	0.40	14.10	1.43	10.9	0.23	0.05	2.4	0.5
W2k 15/2	TOP IC5	1.1300	0.0081	2.3699	0.0337	16.917	0.660	18.11	0.14	28.27	1.00	11.2	0.23	0.05	2.4	0.5
W2k 15/2	TOP IC6	1.1271	0.0068	2.3828	0.0296	16.629	0.694	14.79	0.12	7.61	1.95	10.6	0.23	0.05	2.4	0.5
W2k 15/2	BOTTOM IC1	1.1236	0.0071	2.3761	0.0170	17.155	0.224	32.58	0.27	24.44	0.41	12.2	0.23	0.05	2.4	0.5
W2k 15/2	BOTTOM IC2	1.1616	0.0080	2.4133	0.0321	17.353	1.133	25.85	0.87	20.66	0.55	15.9	0.23	0.05	2.4	0.5
W2k 15/2	BOTTOM IC3	1.1623	0.0027	2.4351	0.0268	18.057	1.344	16.35	0.42	613.02	179.09	11.5	0.23	0.05	2.4	0.5
W2k 15/2	BOTTOM IC3	1.1619	0.0067	2.4095	0.0250	17.945	0.666	14.34	0.56	13.36	4.92	11	0.23	0.05	2.4	0.5
W2k 15/2	BOTTOM IC4	1.1509	0.0060	2.3997	0.0175	17.458	0.506	17.96	0.19	25.32	0.53	10.9	0.23	0.05	2.4	0.5
W2k 15/2	BOTTOM IC5	1.1418	0.0043	2.4052	0.0209	17.308	0.560	27.51	0.38	34.16	0.95	10.8	0.23	0.05	2.4	0.5
W2k 15/2	BOTTOM IC6	1.1419	0.0092	2.4018	0.0114	17.210	0.809	17.36	0.20	34.00	1.08	11.7	0.23	0.05	2.4	0.5
W2k 15/2	BOTTOM IC7	1.1465	0.0155	2.4066	0.0041	17.728	0.582	19.95	0.49	18.36	2.14	10.9	0.23	0.05	2.4	0.5
W2k 15/2	BOTTOM IC7	1.1509	0.0067	2.4121	0.0176	17.441	1.529	18.40	0.10	38.37	1.21	10.4	0.23	0.05	2.4	0.5
W2k 16/1	IC1	1.1736	0.0092	2.4263	0.0135	17.950	0.509	17.29	0.45	9.24	0.36	12.6	0.23	0.05	2.4	0.5
W2k 16/1	IC2	1.1092	0.0045	2.3657	0.0297	16.885	0.847	14.50	0.10	9.23	0.63	12.9	0.23	0.05	2.4	0.5
W2k 16/1	IC3	1.1218	0.0035	2.3803	0.0086	17.262	0.377	39.59	0.38	439.72	7.71	12.8	0.23	0.05	2.4	0.5
W2k 16/1	IC3	1.1216	0.0092	2.3786	0.0049	17.255	0.020	35.88	0.67	621.03	8.11	10.1	0.23	0.05	2.4	0.5
W2k 16/1	IC4	1.1091	0.0048	2.3741	0.0137	16.629	1.262	21.80	0.10	7.81	0.98	12.9	0.23	0.05	2.4	0.5
W2k 16/1	IC5	1.1426	0.0043	2.3822	0.0307	17.659	0.986	11.63	0.05	8.42	1.44	10.8	0.23	0.05	2.4	0.5
W2k 16/1	IC6	1.1311	0.0298	2.3826	0.0340	18.240	3.304	1.61	0.03	7.68	0.71	8.1	0.23	0.05	2.4	0.5
W2k 16/1	IC6	1.1570	0.0233	2.4108	0.0132	17.685	1.331	4.21	0.09	10.06	0.67	16.3	0.23	0.05	2.4	0.5
W2k 16/2	IC7	1.1655	0.0065	2.4057	0.0037	18.309	0.627	19.37	0.49	15.18	0.96	10.6	0.23	0.05	2.4	0.5
W2k 16/2	IC8	1.1370	0.0058	2.3808	0.0119	17.253	0.578	15.29	0.15	9.04	0.70	10.6	0.23	0.05	2.4	0.5

Law Dome data table 6/9, Procedural Blank Pb isotopic composition used was

$$^{206}\text{Pb}/^{207}\text{Pb} = 1.2 \pm 0.07, \quad ^{208}\text{Pb}/^{207}\text{Pb} = 2.48 \pm 0.1 \text{ and } ^{206}\text{Pb}/^{204}\text{Pb} = 16 \pm 7.$$

NAME	CORE SECTION	206/207	err	208/207	err	206/204	err	Amount Pb (pg)	err	Amount Ba (pg)	err	Vol analysed, mL	Pb (pg)	err	Filament Blank Ba(pg)	err
W2K 18	BOTTOM-OUTER1	1.1101	0.0038	2.3730	0.0148	17.074	0.060	8706.70	511.76	3454.09	286.93	12.1	0.3	0.05	3	0.5
W2K 18	BOTTOM-OUTER2	1.1260	0.0003	2.3825	0.0044	17.298	0.052	665.75	25.65	397.36	7.84	10.4	0.25	0.05	2.5	0.5
W2K 18	BOTTOM-OUTER3	1.1395	0.0011	2.3983	0.0074	17.558	0.139	131.30	0.76	50.37	2.32	19.3	0.25	0.05	2.5	0.5
W2K 18	BOTTOM-OUTER4	1.1524	0.0037	2.4009	0.0068	17.709	0.354	32.84	0.78	23.83	3.19	22.2	0.25	0.05	2.5	0.5
W2K 18	TOP-OUTER1	1.1140	0.0010	2.3742	0.0011	17.107	0.038	825.83	10.90	1326.52	30.70	9.8	0.3	0.05	3	0.5
W2K 18	TOP-OUTER2	1.1650	0.0051	2.4183	0.0114	17.909	0.251	16.51	1.12	14.88	0.40	9.4	0.25	0.05	2.5	0.5
W2K 18	TOP-OUTER3	1.1626	0.0075	2.4111	0.0176	17.804	0.276	40.06	0.68	15.50	0.51	24.6	0.25	0.05	2.5	0.5
W2K 18	TOP-OUTER4	1.1754	0.0057	2.4319	0.0076	18.048	0.024	36.15	0.42	13.24	0.69	20.7	0.25	0.05	2.5	0.5
W2K 18	IC (A1*)	1.1613	0.0049	2.3955	0.0236	17.013	0.941	7.22	0.03	5.69	0.18	21.3	0.25	0.05	2.5	0.5
W2K 18	IC (A2*)	1.1711	0.0039	2.4132	0.0047	17.702	0.595	31.32	0.38	10.69	0.13	19.9	0.25	0.05	2.5	0.5
W2K 18	IC (A3*)	1.2138	0.0098	2.4512	0.0134	18.028	1.479	15.89	0.27	8.99	1.55	19	0.25	0.05	2.5	0.5
W2K 18	IC (A4*)	1.1644	0.0019	2.4175	0.0136	17.566	0.529	33.25	1.05	17.80	1.33	19	0.25	0.05	2.5	0.5
W2K 18	IC (A4#)	1.1565	0.0086	2.4179	0.0026	17.719	0.331	34.22	0.43	12.77	1.68	19.7	0.25	0.05	2.5	0.5
W2K 18	IC (B1*)	1.1708	0.0044	2.4186	0.0117	17.871	0.259	44.09	0.47	23.28	0.97	20.2	0.25	0.05	2.5	0.5
W2K 18	IC (B2*)	1.1998	0.0046	2.4233	0.0203	18.790	0.760	41.85	1.07	28.84	22.26	20.2	0.25	0.05	2.5	0.5
W2K 18	IC (B3*)	1.1732	0.0063	2.4156	0.0051	17.663	0.449	34.36	0.19	22.00	1.59	19.7	0.25	0.05	2.5	0.5
W2K 18	IC (B4*)	1.1663	0.0047	2.4177	0.0027	18.081	0.380	28.82	0.31	12.29	0.66	25.3	0.25	0.05	2.5	0.5
W2K 18	IC (B4#)	1.1513	0.0016	2.3990	0.0083	17.688	0.167	24.78	0.25	8.40	1.20	22.5	0.25	0.05	2.5	0.5
W2K 19	TOP-OUTER2	1.1402	0.0046	2.3918	0.0058	17.415	0.061	245.54	13.36	137.21	1.71	11.4	0.3	0.05	3	0.5
W2K 19	TOP-OUTER3	1.1581	0.0033	2.4123	0.0150	17.570	0.420	33.48	1.30	40.00	7.84	15.5	0.3	0.05	3	0.5
W2K 19	TOP-OUTER4	1.1597	0.0055	2.4001	0.0080	17.911	0.351	19.11	0.07	37.09	1.82	13.8	0.3	0.05	3	0.5
W2K 19	BOTTOM-OUTER2	1.1350	0.0024	2.3899	0.0034	17.415	0.094	142.25	1.86	75.32	0.97	19.9	0.3	0.05	3	0.5
W2K 19	BOTTOM-OUTER3	1.1332	0.0019	2.3876	0.0029	17.430	0.080	371.69	4.08	151.68	2.23	20.2	0.3	0.05	3	0.5
W2K 19	BOTTOM-OUTER4	1.1530	0.0040	2.4038	0.0053	17.626	0.267	35.20	0.32	36.03	7.18	22.9	0.3	0.05	3	0.5
W2K 19	IC (A1*)	1.1759	0.0066	2.4615	0.0323	18.180	0.201	57.25	3.96	207.85	59.38	20.8	0.3	0.05	3	0.5
W2K 19	IC (A2*)	1.1772	0.0088	2.4089	0.0142	18.011	0.720	31.70	0.84	37.96	1.78	20.4	0.3	0.05	3	0.5
W2K 19	IC (A3*)	1.1726	0.0131	2.4178	0.0897	17.655	2.453	21.28	1.59	17.10	2.47	22.1	0.3	0.05	3	0.5
W2K 19	IC (A4*)	1.1564	0.0090	2.3923	0.0443	15.986	0.847	10.67	0.30	16.28	2.02	21	0.3	0.05	3	0.5
W2K 19	IC (A4#)	1.1201	0.0767	2.3199	0.0855	15.996	1.928	2.78	0.26	6.25	1.73	28.1	0.3	0.05	3	0.5
W2K 19	IC (A4#)	1.0156	0.1572	1.9120	0.9016	12.928	18.102	3.16	0.96	7.23	0.25	23.7	0.3	0.05	3	0.5
W2K 19	IC (bkr)	1.1518	0.0070	2.3982	0.0158	17.323	0.507	33.66	1.69	13.57	1.57	26.3	0.3	0.05	3	0.5
W2K 19	IC (B1*)	1.2023	0.0109	2.4512	0.0226	17.905	0.592	34.39	2.07	7.35	0.66	20.9	0.3	0.05	3	0.5
W2K 19	IC (B2*)	1.1210	0.0017	2.3765	0.0073	17.255	0.198	16.66	0.13	8.90	0.53	20.1	0.3	0.05	3	0.5
W2K 19	IC (B3*)	1.1719	0.0075	2.4038	0.0196	17.773	0.560	1.81	0.02	7.30	0.51	13.5	0.3	0.05	3	0.5
W2K 19	IC (B4*)	1.1749	0.0053	2.4163	0.0099	17.931	0.255	15.39	0.16	12.00	0.92	20.5	0.3	0.05	3	0.5
W2K 19	IC (B4#)	1.1342	0.0040	2.3861	0.0080	17.391	0.253	12.54	0.03	16.97	0.10	21	0.3	0.05	3	0.5
W2K 19	IC (Piece 3)	1.1618	0.0027	2.4114	0.0068	17.761	0.130	31.34	0.15	14.64	0.80	17.3	0.3	0.05	3	0.5

Law Dome data table 7/9, Procedural Blank Pb isotopic composition used was

$$^{206}\text{Pb}/^{207}\text{Pb} = 1.2 \pm 0.07, \quad ^{208}\text{Pb}/^{207}\text{Pb} = 2.48 \pm 0.1 \quad \text{and} \quad ^{206}\text{Pb}/^{204}\text{Pb} = 16 \pm 7.$$

NAME	CORE SECTION	206/207	err	208/207	err	206/204	err	Amount Pb (pg)	err	Amount Ba (pg)	err	Vol analysed, mL	Pb (pg)	Filament Blank Ba(pg)	err
W2K 20	TOP - OUT2	1.1561	0.0023	2.4056	0.0095	17.745	0.075	80.62	0.52	24.69	0.68	9.8	0.3	0.05	3
W2K 20	TOP - OUT3	1.1698	0.0010	2.4144	0.0071	17.990	0.440	23.99	0.18	14.66	0.28	10	0.3	0.05	3
W2K 20	TOP - OUT4	1.1739	0.0023	2.4150	0.0056	17.962	0.237	16.98	0.07	16.24	0.47	10.3	0.3	0.05	3
W2K 20	BOTTOM - OUT2	1.1331	0.0016	2.3917	0.0092	17.410	0.134	462.17	10.96	280.61	10.90	11	0.3	0.05	3
W2K 20	BOTTOM - OUT3	1.1665	0.0035	2.4158	0.0057	17.947	0.147	41.07	0.24	20.93	1.93	10.4	0.3	0.05	3
W2K 20	BOTTOM - OUT4	1.1638	0.0020	2.4116	0.0086	17.921	0.164	31.29	0.13	15.41	1.92	10.9	0.3	0.05	3
W2K 20	IC (A1*)	1.1691	0.0033	2.4093	0.0036	17.651	0.363	24.44	0.24	12.29	0.15	16.3	0.3	0.05	3
W2K 20	IC (A2*)	1.1956	0.0029	2.4408	0.0063	18.460	0.265	41.90	0.20	18.76	0.40	20.8	0.3	0.05	3
W2K 20	IC (A3*)	1.1734	0.0026	2.3980	0.0050	16.901	0.861	30.48	0.71	15.26	0.31	17.7	0.3	0.05	3
W2K 20	IC (A4*)	1.1645	0.0025	2.4015	0.0092	17.369	0.410	25.17	0.45	16.68	0.17	20.5	0.3	0.05	3
W2K 20	IC (A4#)	1.1711	0.0093	2.4226	0.0501	18.063	0.785	27.07	2.01	15.18	3.60	18.2	0.3	0.05	3
W2K 20	IC (B1*)	1.1511	0.0056	2.4004	0.0232	17.244	0.604	49.35	1.71	30.90	1.49	17.2	0.3	0.05	3
W2K 20	IC (B2*)	1.1641	0.0052	2.4154	0.0099	17.455	0.507	17.48	0.22	13.99	0.43	16	0.3	0.05	3
W2K 20	IC (B3*)	1.1663	0.0029	2.4141	0.0077	17.794	0.303	33.50	0.37	16.07	0.26	18.1	0.3	0.05	3
W2K 20	IC (B4*)	1.1672	0.0018	2.4191	0.0020	17.701	0.145	43.71	0.35	23.43	0.27	18.7	0.3	0.05	3
W2K 20	IC (B4#)	1.1642	0.0033	2.4131	0.0100	17.770	0.304	22.02	0.28	21.05	7.98	17.3	0.3	0.05	3

Law Dome data table 8/9, Procedural Blank Pb isotopic composition used was

$$^{206}\text{Pb}/^{207}\text{Pb} = 1.2 \pm 0.07, \quad ^{208}\text{Pb}/^{207}\text{Pb} = 2.48 \pm 0.1 \quad \text{and} \quad ^{206}\text{Pb}/^{204}\text{Pb} = 16 \pm 7.$$

NAME	CORE SECTION	206/207	err	208/207	err	206/204	err	Amount Pb (pg)	err	Amount Ba (pg)	err	Bi/Pb ratio	Amount Bi (pg)	Vol analysed. mL	Pb (pg)	Filament Blank Ba (pg)	err	
W20K 43	Piece 1 Top OUTER1	1.1791	0.0035	2.4139	0.0020	18.275	0.040	454.65	209.16	211.37	6.02	25.587	1057.547	7.4	0.3	0.05	3	0.5
W20K 43	Piece 1 Bottom OUTER1	1.1935	0.0050	2.4245	0.0176	18.374	0.222	58.76	1.67	49.47	0.97	5.342	28.536	10.8	0.3	0.05	3	0.5
W20K 43	Piece 2 OUTER1	1.1822	0.0010	2.4186	0.0065	18.278	0.114	324.79	6.09	68.85	0.91	19.356	571.526	11.8	0.3	0.05	3	0.5
W20K 43	Piece 1 Top OUTER2	1.1725	0.0038	2.4107	0.0328	17.769	0.333	40.57	1.76	77.58	7.23	0.184	0.680	11.2	0.3	0.05	3	0.5
W20K 43	Piece 1 Bottom OUTER2	1.2145	0.0089	2.4409	0.0268	17.890	0.823	7.44	0.09	41.63	3.37	0.251	0.170	11.1	0.3	0.05	3	0.5
W20K 43	Piece 2 OUTER2	1.1759	0.0052	2.4135	0.0123	18.055	0.227	20.81	0.10	54.19	2.46	2.105	3.982	10.4	0.3	0.05	3	0.5
W20K 43	Piece 1 Top OUTER3	1.2201	0.0095	2.4544	0.0164	18.654	0.232	13.75	0.14	35.65	0.95	0.955	1.194	11.1	0.3	0.05	3	0.5
W20K 43	Piece 1 Bottom OUTER3	1.2175	0.0101	2.4708	0.0145	19.032	0.506	5.26	0.11	69.18	1.37	0.242	0.115	10.6	0.3	0.05	3	0.5
W20K 43	Piece 2 OUTER3	1.2236	0.0106	2.4577	0.0121	18.699	0.986	5.89	0.18	67.56	3.70	0.169	0.090	10.9	0.3	0.05	3	0.5
W20K 43	IC (A1*)	1.2132	0.0100	2.4468	0.0177	19.108	0.601	5.77	0.05	11.84	1.11	0.122	0.064	10.4	0.3	0.05	3	0.5
W20K 43	IC (A1*)	1.1603	0.0184	2.3644	0.0258	18.161	2.315	8.24	0.36	13.61	0.75	0.509	0.381	9.8	0.3	0.05	3	0.5
W20K 43	IC (A1*)	1.1845	0.0224	2.4360	0.0100	17.458	2.975	8.76	0.30	47.06	2.92	0.150	0.119	10.6	0.3	0.05	3	0.5
W20K 43	IC (A2*)	1.2511	0.0141	2.5012	0.0273	19.363	1.222	10.44	0.66	34.52	2.82	0.649	0.616	10.6	0.3	0.05	3	0.5
W20K 43	IC (A3*)	1.3039	0.0097	2.4958	0.0110	20.288	0.320	13.86	0.42	31.71	1.88	0.302	0.380	11.1	0.3	0.05	3	0.5
W20K 43	IC (A3*)	1.2671	0.0047	2.4938	0.0129	19.553	0.482	14.47	0.21	29.70	1.46	0.260	0.342	9.6	0.3	0.05	3	0.5
W20K 43	IC (A4)	1.2463	0.0100	2.4745	0.0449	19.957	1.849	7.12	0.10	29.72	0.54	0.287	0.186	10.4	0.3	0.05	3	0.5
W20K 43	IC (A4)	1.2318	0.1425	2.4702	0.3604	21.330	9.089	7.21	1.86	23.49	3.72	0.332	0.217	10.7	0.3	0.05	3	0.5
W20K 43	IC (A4)	1.2296	0.0127	2.4570	0.0134	19.014	1.998	7.22	0.20	20.70	1.93	0.238	0.156	10.2	0.3	0.05	3	0.5
W20K 43	IC (Bkr1)	1.2235	0.0082	2.4689	0.0033	18.466	0.324	10.07	0.30	88.52	4.51	0.363	0.332	10.5	0.3	0.05	3	0.5
W20K 43	IC (Bkr1)	1.2221	0.0187	2.4730	0.0262	19.570	0.907	7.33	0.75	56.37	8.29	0.104	0.069	8.7	0.3	0.05	3	0.5
W20K 43	IC (Bkr2)	1.1945	0.0074	2.4457	0.0094	18.050	0.849	6.52	0.01	41.51	1.19	0.067	0.039	10.9	0.3	0.05	3	0.5
W20K 43	IC (Bkr3)	1.2204	0.0025	2.4352	0.0375	15.883	1.802	5.62	0.18	40.35	1.29	0.290	0.148	10	0.3	0.05	3	0.5
W20K 43	IC (A4*)	1.2003	0.0408	2.3418	0.0504	13.218	1.653	7.51	0.13	52.06	2.18	0.145	0.099	15.1	0.3	0.05	3	0.5
W20K 43	IC (A4*)	0.9769	0.1213	1.7864	0.3742	10.755	5.028	6.35	0.22	62.28	5.20	0.354	0.204	10.3	0.3	0.05	3	0.5
W20K 43	IC (A4*)	1.2377	0.0140	2.4794	0.0197	18.331	0.387	8.50	0.16	64.13	8.75	0.231	0.179	15.9	0.3	0.05	3	0.5
W20K 43	IC (A4#)	1.2393	0.0068	2.4951	0.0346	18.482	0.963	6.34	0.47	18.12	4.18	0.021	0.012	15.1	0.3	0.05	3	0.5
W20K 43	IC (B1*)	1.1799	0.0062	2.4158	0.0256	16.742	1.105	7.63	0.06	27.20	1.15	0.094	0.065	16.2	0.3	0.05	3	0.5
W20K 43	IC (B2*)	1.1437	0.1213	2.2092	0.2861	11.748	6.313	3.31	0.06	22.08	6.91	0.165	0.050	20.4	0.3	0.05	3	0.5
W20K 43	IC (B2*)	1.2004	0.0158	2.4375	0.0082	19.243	1.359	3.94	0.08	38.76	10.54	0.291	0.104	21.9	0.3	0.05	3	0.5
W20K 43	IC (B3*)	1.2100	0.0617	2.3656	0.1995	13.929	7.480	2.56	0.05	7.79	0.65	0.071	0.016	15.5	0.3	0.05	3	0.5
W20K 43	IC (B3*)	4.1707	0.0332	1.9703	0.0027	75.194	2.273	4.87	0.04	11.98	0.72	0.063	0.028	20.8	0.3	0.05	3	0.5
W20K 43	IC (B3*)	1.2199	0.0239	2.4416	0.0262	20.833	2.478	3.00	0.11	13.91	0.70	0.233	0.064	15.6	0.3	0.05	3	0.5
W20K 43	IC (B4)	1.2099	0.0125	2.4672	0.0356	19.448	1.555	4.87	0.08	10.64	0.47	0.104	0.046	16.4	0.3	0.05	3	0.5
W20K 43	IC (B4*)	1.2405	0.0298	2.4714	0.0467	18.317	1.141	9.42	0.13	10.27	1.36	0.134	0.115	14.9	0.3	0.05	3	0.5
W20K 43	IC (B4*)	1.2616	0.0078	2.5105	0.0336	18.702	1.873	10.29	0.30	12.12	2.30	0.306	0.286	12.3	0.3	0.05	3	0.5
W20K 43	IC (B4#)	1.1546	0.0307	2.3303	0.0489	17.201	10.783	3.64	0.10	8.63	1.64	0.079	0.026	15.2	0.3	0.05	3	0.5
W20K 43	IC (B4#)	1.1362	0.0215	2.3037	0.0107	14.719	1.602	4.23	0.17	9.35	0.34	0.100	0.038	16.9	0.3	0.05	3	0.5
W20K 43	IC (B4#)	1.1655	0.0173	2.3518	0.0186	16.760	0.662	4.08	0.06	9.32	0.51	0.091	0.034	15.4	0.3	0.05	3	0.5

Law Dome data table 9/9, Procedural Blank Pb isotopic composition used was

$$^{206}\text{Pb}/^{207}\text{Pb} = 1.2 \pm 0.07, \quad ^{208}\text{Pb}/^{207}\text{Pb} = 2.48 \pm 0.1 \quad \text{and} \quad ^{206}\text{Pb}/^{204}\text{Pb} = 16 \pm 7.$$

Date	206/207	err	208/207	err	Pb conc (pg/g)	Ba conc (pg/g)	Pb/Ba
1990.6	1.1328	0.0058	2.3885	0.0081	1.38	1.40	0.98
1990.4	1.1377	0.0056	2.3935	0.0130	0.51	5.47	0.09
1990.1	1.1470	0.0070	2.4053	0.0170	0.33	0.95	0.34
1989.7	1.1647	0.0212	2.4075	0.0422	0.13	1.17	0.11
1989.4	1.1014	0.0344	2.2435	0.0912	0.10	1.64	0.06
1986.2	1.1286	0.0028	2.3941	0.0102	6.21	2.93	2.12
1985.8	1.1173	0.0031	2.3816	0.0056	2.66	0.94	2.81
1985.5	1.1292	0.0020	2.3941	0.0029	6.99	2.07	3.37
1985.3	1.1547	0.0029	2.4152	0.0064	11.22	6.01	1.87
1984.2	1.1394	0.0139	2.4046	0.0229	5.75	2.00	2.87
1983.9	1.1579	0.0044	2.4265	0.0223	6.08	3.31	1.83
1983.6	1.1543	0.0055	2.4217	0.0106	6.08	4.54	1.34
1983.3	1.1394	0.0047	2.4046	0.0055	3.34	1.11	3.00
1983	1.1345	0.0046	2.3986	0.0131	5.66	1.11	5.09
1979.1	1.1549	0.0039	2.4215	0.0088	2.61	1.44	1.82
1978.7	1.1348	0.0024	2.4019	0.0119	2.65	0.74	3.57
1978.4	1.1456	0.0054	2.4104	0.0087	3.64	1.30	2.79
1978.1	1.1625	0.0028	2.4347	0.0035	6.67	1.92	3.47
1977	1.1634	0.0088	2.4280	0.0198	3.03	9.71	0.31
1976.8	1.1522	0.0016	2.4167	0.0043	9.21	3.86	2.39
1976.7	1.1557	0.0047	2.4150	0.0100	5.41	3.51	1.54
1976.6	1.1473	0.0021	2.4080	0.0063	3.64	2.08	1.75
1976.4	1.1564	0.0016	2.4155	0.0096	5.73	4.34	1.32
1976.3	1.1358	0.0040	2.3927	0.0143	2.68	1.82	1.48
1976.1	1.1347	0.0041	2.4022	0.0129	2.05	0.45	4.52
1975.9	1.1247	0.0073	2.3965	0.0119	2.25	0.46	4.93
1975	1.1607	0.0019	2.4254	0.0059	5.11	3.43	1.49
1974.7	1.1481	0.0017	2.4172	0.0051	11.44	8.35	1.37
1974.3	1.1493	0.0022	2.4137	0.0054	10.92	7.11	1.54
1974	1.1342	0.0031	2.4040	0.0101	6.17	3.51	1.76
1973.9	1.1319	0.0057	2.3982	0.0093	4.80	1.77	2.72
1972.6	1.1328	0.0064	2.4054	0.0107	2.35	1.73	1.36
1972.3	1.1369	0.0022	2.4051	0.0057	6.81	3.58	1.90
1972.1	1.1393	0.0035	2.4010	0.0089	4.23	8.63	0.49
1971.9	1.1473	0.0081	2.4117	0.0036	4.55	5.49	0.83
1971.6	1.1346	0.0033	2.4008	0.0099	0.72	0.94	0.77
1971.3	1.1525	0.0043	2.4115	0.0233	0.58	0.97	0.59
1971	1.1374	0.0066	2.4070	0.0245	1.03	0.94	1.10
1969.6	1.1345	0.0020	2.4079	0.0089	7.36	4.55	1.62
1969.3	1.1335	0.0041	2.4049	0.0094	7.38	3.45	2.14
1968.8	1.1326	0.0023	2.4102	0.0072	7.05	2.84	2.48
1968.4	1.1373	0.0009	2.4111	0.0047	5.23	2.59	2.02
1967.3	1.1377	0.0056	2.4095	0.0104	0.63	4.43	0.14
1967	1.1308	0.0013	2.4045	0.0046	2.96	3.08	0.96
1966.8	1.1421	0.0045	2.4182	0.0104	3.07	10.48	0.29
1966.6	1.1507	0.0053	2.4270	0.0098	5.85	7.27	0.81
1966.3	1.1378	0.0023	2.4113	0.0070	10.81	12.63	0.86
1965.9	1.1407	0.0063	2.4077	0.0091	2.69	2.02	1.33

Coats Land data, table 1/2.

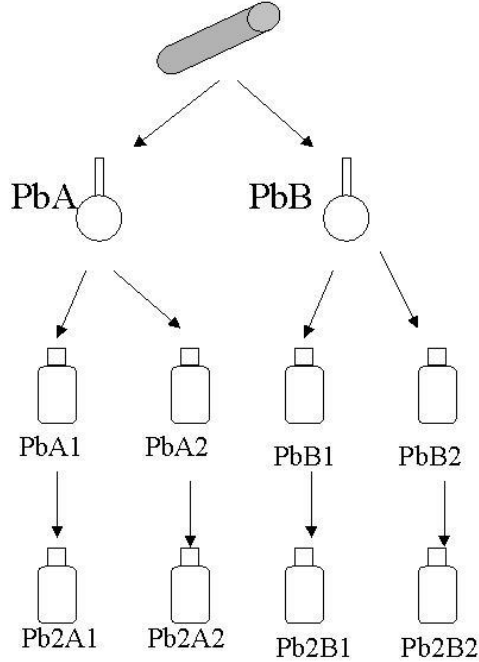
Date	206/207	err	208/207	err	Pb conc (pg/g)	Ba conc (pg/g)	Pb/Ba
1964.9	1.1380	0.0046	2.4141	0.1430	4.98	5.14	0.97
1964.7	1.1138	0.0124	2.3852	0.0055	1.31	1.09	1.20
1964.4	1.1383	0.0042	2.4030	0.0054	2.83	3.34	0.85
1964	1.1145	0.0023	2.3836	0.0041	2.51	1.89	1.33
1963.7	1.1334	0.0020	2.4091	0.0062	4.70	4.49	1.05
1964	1.1374	0.0017	2.4108	0.0025	4.41	3.86	1.14
1962	1.1255	0.0045	2.3956	0.0139	0.99	0.84	1.19
1962	1.1344	0.0059	2.4045	0.0113	2.70	3.34	0.81
1962	1.1323	0.0106	2.4038	0.0070	5.10	6.39	0.80
1961.2	1.1306	0.0048	2.3966	0.0129	5.95	4.77	1.25
1959.9	1.1491	0.0090	2.4237	0.0083	1.55	1.50	1.03
1959.3	1.1429	0.0065	2.4035	0.0132	0.82	0.45	1.83
1958.9	1.1226	0.0057	2.3962	0.0024	3.59	5.97	0.60
1958.6	1.1435	0.0108	2.4174	0.0158	2.62	6.95	0.38
1951.8	1.1551	0.0039	2.4280	0.0094	1.42	2.75	0.51
1951.5	1.1710	0.0069	2.4336	0.0089	1.58	3.84	0.41
1951.1	1.1632	0.0064	2.4351	0.0118	1.50	5.97	0.25
1950.8	1.1999	0.0041	2.4608	0.0097	3.02	7.16	0.42
1950.4	1.1628	0.0066	2.4320	0.0089	1.92	6.09	0.32
1944	1.1484	0.0041	2.4180	0.0080	1.60	2.72	0.59
1943.6	1.1518	0.0064	2.4171	0.0112	0.84	3.65	0.23
1943.1	1.1449	0.0068	2.4197	0.0067	2.70	7.85	0.34
1942.7	1.1736	0.0063	2.4266	0.0097	0.57	2.96	0.19
1923.5	1.1412	0.0088	2.4157	0.0087	5.59	3.50	1.60
1923	1.1185	0.0037	2.3885	0.0076	1.73	2.79	0.62
1922.6	1.1781	0.0077	2.4462	0.0070	8.22	4.72	1.74
1922.1	1.1729	0.0078	2.4378	0.0222	4.78	2.57	1.86
1920.8	1.1647	0.0031	2.4368	0.0098	3.23	4.31	0.75
1919.9	1.1576	0.0026	2.4317	0.0126	2.87	4.70	0.61
1914.382	1.1521	0.0099	2.4349	0.0067	2.48	6.70	0.37
1911.261	1.1629	0.0017	2.4405	0.0046	6.50	5.51	1.18
1910.04	1.1628	0.0047	2.4378	0.0046	1.85	5.94	0.31
1908.101	1.1665	0.0033	2.4348	0.0076	1.74	4.60	0.38
1906.674	1.1348	0.0040	2.4087	0.0137	4.21	2.35	1.79
1905.671	1.1527	0.0027	2.4207	0.0057	2.13	5.15	0.41
1898.926	1.1071	0.0071	2.3805	0.0220	3.43	3.47	0.99
1897.051	1.0955	0.0057	2.3721	0.0136	0.94	2.32	0.41
1890.533	1.1348	0.0085	2.4110	0.0208	1.05	4.01	0.26
1888.496	1.1590	0.0165	2.4096	0.0211	0.44	3.26	0.14
1872.017	1.1732	0.0221	2.4452	0.0133	1.01	6.93	0.15
1856.776	1.1955	0.0635	2.5010	0.0851	0.16	2.76	0.06
1851.137	1.1666	0.0125	2.4393	0.0195	0.20	3.67	0.05
1846.104	1.1742	0.0217	2.4318	0.0308	0.26	4.05	0.06
1843.141	1.1863	0.0066	2.4529	0.0728	0.47	4.03	0.12
1838.83	1.1948	0.0127	2.4537	0.0284	0.68	5.14	0.13
1834.155	1.2076	0.0058	2.4713	0.0066	1.05	10.18	0.10

Coats Land data, table 2/2.

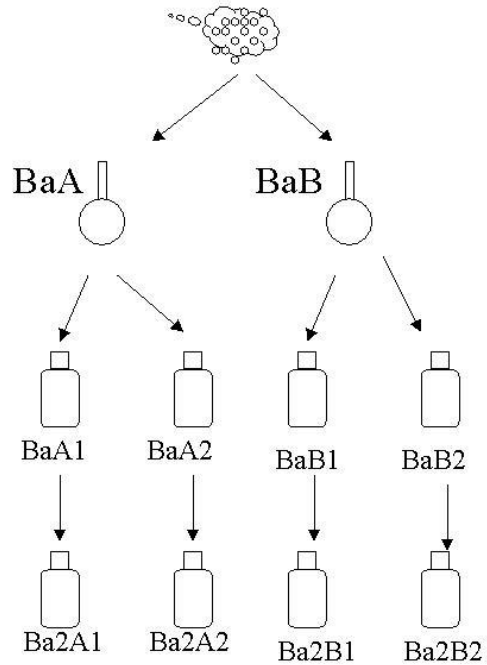
Appendix 2. Lead and Barium isotopic tracer solution calibration

Isotope dilution is a technique used to determine the amount of an element in a sample from the change in isotopic composition induced by the addition of a known quantity of tracer with a known isotopic composition. The accuracy of the technique relies on an accurate calibration of the tracer solution to be added to the sample, which in this case was a mixed solution of $^{205}\text{Pb}/^{137}\text{Ba}$. The concentration of ^{205}Pb in the solution was determined by its addition to a gravimetrically prepared solution of high purity Pb metal (NIST SRM 981 common Pb isotopic standard), while the concentration of ^{137}Ba was determined by its addition to a gravimetrically prepared solution of high purity $\text{Ba}(\text{NO}_3)_2$ powder. In order for pg quantities to be dispensed with a micropipette, the concentration of the tracer solution was ~ 0.5 ng/g, however, so the primary standard solutions were to be greatly diluted if only a small amount of tracer was to be used for the calibration. The dilutions were undertaken in two stages. Four independent primary solutions were prepared, two of Pb (PbA, PbB) and two of Ba (BaA, BaB), which had concentrations of ~ 1.1 mg Pb/g and ~ 0.6 mg Ba/g, respectively. From each of these solutions, two dilutions were then made (PbA1, PbA2, PbB1, PbB2 and BaA1, BaA2, BaB1, BaB2) with concentrations ~ 7 μg Pb/g and ~ 4 μg Ba/g. From each of these secondary solutions, another dilution was made (Pb2A1, Pb2A2, Pb2B1, Pb2B2 and Ba2A1, Ba2A2, Ba2B1, Ba2B2) with concentrations ~ 30 ng Pb/g and ~ 20 ng Ba/g. An aliquot of each of the eight final Pb and Ba solutions were then mixed with aliquots of the tracer solution to determine the tracer concentrations of Pb and Ba. As can be seen, these have been evaluated as 0.384 ± 0.005 ng Pb/g and 10.56 ± 0.14 ng Ba/g. Included below is a flowchart indicating the preparation of each of the standard solutions from their source materials, tables indicating the calculation of the concentrations of the standard solutions, and a summary of the spike/standard mixture data and spike concentration calculations.

NIST SRM 981 Pb



99.99% Ba(NO₃)₂ powder



Preparation of Pb standard solutions from NIST 981 metal 1/2.

Pb standard dissolution (using NIST 981 common Pb isotopic SRM)

PbA	weight of flask	weight of flask + lid	weight of flask + lid + NIST 981	PbB	weight of flask	weight of flask + lid	weight of flask + lid + NIST 981
	41.3317	43.3256	43.4263		52.9381	54.9971	55.0927
		43.3259	43.4263			54.9971	55.0923
	added to PbA:	7.96 g MQ			added to PbB:	11.72 g MQ	
	+	4.53 g conc HNO ₃			+	5.49 g conc HNO ₃	
	wt NIST 981 Pb in PbA:		0.1005 g		wt NIST 981 Pb in PbB:		0.0954 g
dilution		wt of flask + lid + NIST 981 +				wt of flask + lid + NIST 981 + HNO ₃	
		129.4002 g				139.0800 g	
		129.4004 g				139.0791 g	
						139.0786 g	
PbA	Amt NIST 981:	0.1005 g Pb		PbB:	NIST 981:	0.0954 g Pb	
	Amt HNO ₃ :	86.0746 g			Amt HNO ₃ :	84.0825 g	
	PbA conc:	1.1682 mg/g Pb			PbB conc:	1.1346 mg/g Pb	

Preparation of Pb standard solutions from NIST 981 metal 2/2.

Pb standard dilutions

PbA conc:		1.1682 mg/g Pb			PbA1		PbA1		
weight of PE bottle+lid	wt of bottle + lid+ PbA soln	wt of bottle + lid+ PbA soln+HNO3		weight of PE bottle+lid	wt of bottle + lid+ PbA1 soln	wt of bottle + lid+ PbA1			
19.5574	20.3574	123.2335		19.8110	20.3384	128.9682			
PbA1	Amt NIST 981: Amt HNO3:	0.9345 mg 103.6761 g		PbA1	Amt NIST 981: Amt HNO3:	4.7540 ug 109.1572 g			
PbA1 conc:	9.0140 ug/g Pb			PbA1 conc:	43.5518 ng/g Pb				
PbA conc:		1.1682 mg/g Pb			PbA2		PbA2		
weight of PE bottle+lid	wt of bottle + lid+ PbA soln	wt of bottle + lid+ PbA soln+HNO3		weight of PE bottle+lid	wt of bottle + lid+ PbA2 soln	wt of bottle + lid+ PbA2 soln+HNO 3			
19.7780	20.3719	124.3662		19.7082	20.2326	129.9195			
PbA2	Amt NIST 981: Amt HNO3:	0.6938 mg 104.5882 g		PbA2	Amt NIST 981: Amt HNO3:	3.4786 ug 110.2113 g			
PbA2 conc:	6.6334 ug/g Pb			PbA2 conc:	31.5627 ng/g Pb				
PbB conc:		1.1346 mg/g Pb			PbB1		PbB1		
weight of PE bottle+lid	wt of bottle + lid+ PbB soln	wt of bottle + lid+ PbB soln+HNO3		weight of PE bottle+lid	wt of bottle + lid+ PbB1soln	wt of bottle + lid+ PbB1 soln+HNO 3			
19.7681	20.3451	125.3566		19.6054	20.1303	130.5432			
PbB1	Amt NIST 981: Amt HNO3:	0.6547 mg 105.5885 g		PbB1	Amt NIST 981: Amt HNO3:	3.2545 ug 110.9378 g			
PbB1 conc:	6.2002 ug/g Pb			PbB1 conc:	29.3359 ng/g Pb				
PbB conc:		1.1346 mg/g Pb			PbB2		PbB2		
weight of PE bottle+lid	wt of bottle + lid+ PbB soln	wt of bottle + lid+ PbB soln+HNO3		weight of PE bottle+lid	wt of bottle + lid+ PbB2 soln	wt of bottle + lid+ PbB2 soln+HNO 3			
19.6918	20.2074	129.7295		15.9923	16.4964	130.1990			
PbB2	Amt NIST 981: Amt HNO3:	0.5850 mg 110.0377 g		PbB2	Amt NIST 981: Amt HNO3:	2.6800 ug 114.2067 g			
PbB2 conc:	5.3164 ug/g Pb			PbB2 conc:	23.4660 ng/g Pb				

Preparation of Ba standard solutions from Johnson Matthey Specpure Ba(NO₃)₂ powder.

Ba(NO₃)₂ powder dissolution

BaA	weight of flask	weight of flask + lid	weight of flask + lid + Ba(NO ₃) ₂	BaB	weight of flask	weight of flask + lid	weight of flask + lid + Ba(NO ₃) ₂
	47.4440	49.3578	49.4516		46.5948	48.4438	48.5717
	47.4438	49.3575	49.4512		46.5942	48.4438	48.5714
			49.4510				
	mol.wt Ba	137.3270 g/mol			mol.wt Ba	137.3270 g/mol	
	mol.wt N	14.0067 g/mol			mol.wt N	14.0067 g/mol	
	mol.wt O	15.9940 g/mol			mol.wt O	15.9940 g/mol	
	% Ba in Ba(NO ₃) ₂	52.5544 %			% Ba in Ba(NO ₃) ₂	52.5544 %	
	wt Ba in BaA	0.0492 g			wt Ba in BaB	0.0671 g	
	dilution	wt of flask + lid + Ba + HNO ₃			dilution	wt of flask + lid + Ba + HNO ₃	
		132.0138 g				142.4816 g	
		132.0132 g				142.4810 g	
		132.0127 g				142.4807 g	
BaA	Amt Ba:	0.0492 g Ba		BaB	Amt Ba:	0.0671 g Ba	
	Amt HNO ₃ :	82.6553 g			Amt HNO ₃ :	94.0371 g	
	BaA conc:	0.5952 mg/g Ba			BaB conc:	0.7140 mg/g Ba	

Preparation of Ba standard solutions from Johnson Matthey Specpure Ba(NO₃)₂ powder.

Ba standard dilutions

		BaA conc: 0.5952 mg/g Ba							
BaA1	weight of PE bottle+lid	wt of bottle + lid+ BaA soln	wt of bottle + lid+ BaA soln+HNO ₃		Ba2A1	weight of PE bottle+lid	wt of bottle + lid+ BaA1 soln	wt of bottle + lid+ BaA1 soln+HNO ₃	
	19.7529	20.4844	127.9723			16.1595	16.7144	124.4476	
BaA1		Amt Ba:	0.4354 mg		Ba2A1		Amt Ba:	2.2326 ug	
		Amt HNO ₃ :	108.2194 g				Amt HNO ₃ :	108.2881 g	
BaA1 conc:		4.0235 ug/g Ba			Ba2A1 conc:		20.6174 ng/g Ba		
		BaA conc: 0.5952 mg/g Ba							
BaA2	weight of PE bottle+lid	wt of bottle + lid+ BaA soln	wt of bottle + lid+ BaA soln+HNO ₃		Ba2A2	weight of PE bottle+lid	wt of bottle + lid+ BaA2 soln	wt of bottle + lid+ BaA2 soln+HNO ₃	
	19.7558	20.2929	131.5800			19.7762	20.2996	130.6456	
BaA2		Amt Ba:	0.3197 mg		Ba2A2		Amt Ba:	1.4964 ug	
		Amt HNO ₃ :	111.8242 g				Amt HNO ₃ :	110.8694 g	
BaA2 conc:		2.8590 ug/g Ba			Ba2A2 conc:		13.4969 ng/g Ba		
		BaB conc: 0.7140 mg/g Ba							
BaB1	weight of PE bottle+lid	wt of bottle + lid+ BaB soln	wt of bottle + lid+ BaB soln+HNO ₃		Ba2B1	weight of PE bottle+lid	wt of bottle + lid+ BaB1 soln	wt of bottle + lid+ BaB1 soln+HNO ₃	
	19.7742	20.5805	131.8499			19.7897	20.3091	131.5321	
BaB1		Amt Ba:	0.5757 mg		Ba2B1		Amt Ba:	2.6678 ug	
		Amt HNO ₃ :	112.0757 g				Amt HNO ₃ :	111.7424 g	
BaB1 conc:		5.1364 ug/g Ba			Ba2B1 conc:		23.8748 ng/g Ba		
		BaB conc: 0.7140 mg/g Ba							
BaB2	weight of PE bottle+lid	wt of bottle + lid+ BaB soln	wt of bottle + lid+ BaB soln+HNO ₃		Ba2B2	weight of PE bottle+lid	wt of bottle + lid+ BaB2 soln	wt of bottle + lid+ BaB2 soln+HNO ₃	
	19.7807	20.3956	130.3410			19.7967	20.3377	131.6747	
BaB2		Amt Ba:	0.4390 mg		Ba2B2		Amt Ba:	2.1482 ug	
		Amt HNO ₃ :	110.5603 g				Amt HNO ₃ :	111.8780 g	
BaB2 conc:		3.9708 ug/g Ba			Ba2B2 conc:		19.2012 ng/g Ba		

Summary of Pb spike concentration analyses:

	Wt.Spike added (g)	Amount of NIST (ng)	Spike conc. (ng/g)
Pb2A1	0.3898	10.500	0.3834
Pb2A2	0.3880	6.634	0.3821
Pb2B1	0.3913	6.521	0.3807
Pb2B2	0.3482	4.987	0.3876
		average	0.3835
		95%CI	0.0047

Pb spike concentration data 1/2

1

Nuclidic Mass	203.973 204	204.974 205	205.974 206	206.976 207	207.977 208	Sum
Spike Ratios	0.00002	1.00000	0.05295	0.00045	0.00101	1.05443
Abund	0.00002	0.94838	0.05022	0.00042	0.00096	1.00000
Abund*Mi	0.00416	194.39276	10.34398	0.08735	0.19968	205.02793
Mixture Ratios	1.0483	1.0000	17.7494	16.2010	38.3516	74.3502
M-S	1.0482	0.0000	17.6964	16.2005	38.3505	73.2958
Abund (Sample)	0.0143		0.2414	0.2210	0.5232	1.0000
Abund * Mi	2.9171	0.0000	49.7301	45.7479	108.8198	207.2149
Atomic Wt Spike	205.028		Wt Std	0.2411 g		
Atomic Wt Pb std	207.215		Conc Std	43.55 ng/g		
			Wt Sp Soln	0.3898 g		
			Conc Sp	0.3834		

2

Nuclidic Mass	203.973 204	204.974 205	205.974 206	206.976 207	207.977 208	Sum
Spike Ratios	0.00002	1.00000	0.05295	0.00045	0.00101	1.05443
Abund	0.00002	0.94838	0.05022	0.00042	0.00096	1.00000
Abund*Mi	0.00416	194.39276	10.34398	0.08735	0.19968	205.02793
Mixture Ratios	0.6651	1.0000	11.3350	10.3196	24.4240	47.7437
M-S	0.6651	0.0000	11.2821	10.3192	24.4230	46.6893
Abund (Sample)	0.0142		0.2416	0.2210	0.5231	1.0000
Abund * Mi	2.9055	0.0000	49.7719	45.7455	108.7918	207.2147
Atomic Wt Spike	205.0279276		Wt Std	0.2102 g		
Atomic Wt Pb std	207.214717		Conc Std	31.56 ng/g		
			Wt Sp Soln	0.388 g		
			Conc Sp	0.3821		

Pb spike concentration data 2/2

3

Nuclidic Mass	203.973 204	204.974 205	205.974 206	206.976 207	207.977 208	
Spike Ratios	0.00002	1.00000	0.05295	0.00045	0.00101	1.05443
Abund	0.00002	0.94838	0.05022	0.00042	0.00096	1.00000
Abund*Mi	0.00416	194.39276	10.34398	0.08735	0.19968	205.02793
Mixture Ratios	0.6529	1.0000	11.0990	10.0932	23.8821	46.7272
M-S	0.6529	0.0000	11.0461	10.0928	23.8810	45.6728
Abund (Sample)	0.0143		0.2419	0.2210	0.5229	1.0000
Abund * Mi	2.9157	0.0000	49.8154	45.7376	108.7455	207.2141
Atomic Wt Spike	205.0279276		Wt Std	0.2223 g		
Atomic Wt Pb std	207.214133		Conc Std	29.34 ng/g		
			Wt Sp Soln	0.3913 g		
			Conc Sp	0.3807		

4

Nuclidic Mass	203.973 204.00000	204.974 205.00000	205.974 206.00000	206.976 207.00000	207.977 208.00000	
Spike Ratios	0.00002	1.00000	0.05295	0.00045	0.00101	1.05443
Abund	0.00002	0.94838	0.05022	0.00042	0.00096	1.00000
Abund*Mi	0.00416	194.39276	10.34398	0.08735	0.19968	205.02793
Mixture Ratios	0.5565	1.0000	9.3935	8.5190	20.1355	39.6045
M-S	0.5564	0.0000	9.3405	8.5186	20.1345	38.5500
Abund (Sample)	0.0144		0.2423	0.2210	0.5223	1.0000
Abund * Mi	2.9441	0.0000	49.9068	45.7366	108.6252	207.2127
Atomic Wt Spike	205.0279276		Wt Std	0.2125 g		
Atomic Wt Pb std	207.2126902		Conc Std	23.47 ng/g		
			Wt Sp Soln	0.3482 g		
			Conc Sp	0.3876		

Summary of Ba spike concentration analyses:

	Spike(g)	NIST (ng)	Spike amount (ng)	Spike conc (ng/g)
Ba2A1	0.4247	4.800	4.444	10.465
Ba2A2	0.4349	3.023	4.576	10.522
Ba2B1	0.4151	5.477	4.414	10.634
Ba2B2	0.4356	4.374	4.634	10.638
		average	4.517	10.565
		95%CI	0.167	0.136

Ba spike concentration data

1	0.4247g stock spike + 0.2328g Ba2A1 std				FRACTIONATION CORRECTED
	201/200	95%err	203/205	95%err	201/200
	1.0048	0.0059	0.0103	0.0076	1.0072
	4.4444 ng spike		10.4649 ng/g spike conc		
2	0.4349g stock spike + 0.2240g Ba2A2 std				
	201/200	95%err	203/205	95%err	201/200
	0.7233	0.0004	0.0218	0.0047	0.7250
	4.5761 ng spike		10.5222 ng/g spike conc		
3	0.4151g stock spike + 0.2294g Ba2B1 std				
	201/200	95%err	203/205	95%err	201/200
	1.1054	0.0011	0.0076	0.0009	1.1081
	4.4142 ng spike		10.6341 ng/g spike conc		
4	0.4356g stock spike + 0.2278g Ba2B2 std				
	201/200	95%err	203/205	95%err	201/200
	0.9166	0.0006	0.0187	0.0094	0.9188
	4.6337 ng spike		10.6375 ng/g spike conc		

Appendix 3. Research Article: Lead fluxes and Pb isotopic compositions from Masaya Volcano, Nicaragua.

The following manuscript has been submitted to *Atmospheric Environment*. The research described does not have a formal place in the thesis structure, but has relevance to the validation of volcanoes as a source of Pb emissions traceable by Pb isotopic analyses. The paper describes an evaluation of the Pb isotopic composition on aerosol filters sampling the plume of Masaya volcano in Nicaragua, with reference to the Pb isotopic composition of the volcanic lava. Currently, volcanic Pb signals observed in Antarctic ice cores are attributed to emissions from Mount Erebus, based on the assumption that the Pb isotopic signature in the volcano lava is identical to that in the volcanic gas plume. This paper provides a preliminary assessment of that assumption.

Lead fluxes and Pb isotopic compositions from Masaya Volcano, Nicaragua.

P. Vallelonga^{1*} and T. A. Mather²

¹ Department of Applied Physics, Curtin University of Technology, GPO Box U 1987, Perth 6845, Australia. Current address: Department of Environmental Sciences, University Ca'Foscari of Venice, Dorsoduro 2137, 30123 Venice, Italy. Email: vallelon@unive.it, Fax: +39 041 234 8549.

² Department of Earth Sciences, University of Cambridge, Downing Street, Cambridge, CB2 3EQ, UK.

*Author to whom correspondence should be addressed.

Abstract

We report Pb concentrations and isotopic compositions measured in plume aerosol and Pele's hair (lava) samples collected from Masaya volcano, Nicaragua, to provide the first data of Pb emissions from the Central American volcanic arc. Lead isotopic compositions measured in the Pele's hair samples were $^{206}\text{Pb}/^{207}\text{Pb}\sim 1.196$, $^{208}\text{Pb}/^{207}\text{Pb}\sim 2.46$ and $^{206}\text{Pb}/^{204}\text{Pb}\sim 18.6$. Evaluation of Pb isotopic compositions on the exposed filters indicated that the Pb collected consisted of a mixture of magmatic Pb and contaminant Pb. Contamination represented a maximum of 15% of Pb collected on the fine aerosol filters

(< 2.5 μm diameter), with the majority of the volcanogenic Pb present in this fine aerosol (96% in the daytime plume and 68% in the night-time plume). Total Pb fluxes from Masaya were corrected for these contamination effects using isotope systematics and were calculated to be a mean of 1.0 ton Pb yr⁻¹, with a mean plume Pb/S_(g) ratio of 1.2 x 10⁻⁵.

Key Words: Pele's hair, aerosols, filter sampling, lead contamination, sulphur emissions

1. Introduction

Volcanoes constitute one of the most important natural sources of pollution to the atmosphere both through occasional (and often explosive) eruptions and through continuous emissions (see tables compiled in Mather et al., 2003). These emissions will often experience extended lifetimes compared to anthropogenic pollution due to the comparative altitude of their release: many volcanoes degas into the free troposphere, whereas anthropogenic emissions are generally entrained in the planetary boundary layer where species' lifetimes are reduced (Graf et al., 1998; Stevenson et al., 2003). As well as emitting large quantities of gases such as CO₂ and SO₂, volcanoes also release prodigious quantities of volatile heavy metals into the atmosphere and for some species (including Pb) volcanoes may be the largest natural emission source (e.g. Nriagu, 1989).

Two methods have been adopted to estimate volcanic metal fluxes. The first approach is to estimate the metal/sulfur ratio of volcanic emissions, and then use the known emission rates of sulfur to estimate the metal flux. This has been used to constrain individual metal fluxes from a few volcanoes (e.g. Erebus, Zreda-Gostynska et al., 1997; Etna, Gauthier and Le Cloarec, 1998; Stromboli, Allard et al., 2000), as well as to estimate global emission rates (e.g. Nriagu, 1989; Hinkley et al., 1999). The second approach is to use the flux of a radioactive volatile metal (²¹⁰Po) as the normalizing factor (e.g. Lambert et al., 1988). While there are still relatively few ²¹⁰Po/S ratios measured in volcanic emanations, the metal:sulfur ratios estimated using this technique (e.g. Lambert et al., 1988; Le Cloarec and Marty, 1991) are nonetheless consistent with the estimates derived by Nriagu (1989) and Hinkley et al. (1999) using the first method. The accuracy

of global volcanogenic metal emissions budgets are limited by, amongst other things, the small number of volcanic systems where trace metal degassing has been constrained. The recent evaluation by Hinkley et al. (1999) was essentially based upon the data collected from Kilauea volcano in Hawaii and two Indonesian arc volcanoes (Merapi and Papandayan) and highlighted the need to extend the available collection of volcanogenic metal emissions data to include the east-African rift-system and volcanic systems in the mid-Pacific islands, Central America and the Aleutian islands from which heavy metal degassing is essentially unconstrained.

Here we present the first reported Pb/S_(g) ratios and Pb fluxes from Masaya volcano, Nicaragua, providing preliminary data of Pb emissions from the Central American volcanic arc. The isotopic composition of Pb both from the volcanic plume (assumed to be entirely in the particulate phase; Hinkley, 1991) and in samples of Pele's hair (fine, brittle strands of fresh basaltic glass extruded from the lava by escaping plume gases) were also measured in order to evaluate the Pb isotope composition of the plume and in the magma at approximately the same time. There have been relatively few evaluations of Pb isotopic compositions in volcanic plumes, despite the application of Pb isotope analysis to investigation of long-range atmospheric transport of pollutants (e.g. Rosman et al., 1997; Bollhöfer and Rosman, 2001). Recently however Pb isotope data (Matsumoto and Hinkley, 2001; Vallelonga et al., 2002) have been used to evaluate Mount Erebus, on Ross Island, as a source of the Pb deposited to Antarctica, based, in the absence of Pb isotope data from the Erebus plume itself, upon the Pb isotopic composition of Mount Erebus lavas reported by Sun and Hanson (1975). These evaluations assumed that negligible Pb isotopic fractionation occurs during transport

across the magma-air interface. Monna et al. (1999) measured Pb isotope compositions in plume particles collected at Mt. Etna and found them to be indeed similar to signatures previously reported for Mt. Etna volcanics suggesting the validity of this assumption. Here we test this assumption with near simultaneous measurements of magma and plume isotopic composition and also use isotope systematics to correct our volcanic Pb fluxes for contamination effects.

2. Methods

Samples were obtained from Masaya (11.984°N, 86.161°W), a basaltic shield volcano, of elevation 635 m a.s.l, situated 25 km south-east of Managua, Nicaragua on 12th and 20th December 2001. Masaya has exhibited several episodes of passive degassing since 1852, with the present degassing crisis starting in mid-1993. Filter samples were collected in the plume on the crater rim using a Nucleopore 12 µm polycarbonate (PC) filter in series with a 1 µm Whatman polytetrafluoroethylene (PTFE) filter, followed by 2 stages of filters designed to collect acidic gas species (55 mm Whatman 41 ashless circles impregnated with NaHCO₃ (10% m/v) and glycerol (10%) in 1:1 methanol/deionized water). The filters were exposed to the plume and sampled for approximately 30 minutes using a pump with a flow rate of 1.8 m³ h⁻¹. The PC filter retained 2.5 µm particles with 50% efficiency, with retention efficiency increasing for larger particle sizes (e.g. Allen et al., 2000). One set of filter samples (12/AAFP/010) was collected from the dry midday plume of Masaya, while another set (20/AAFP/039) was collected from the condensed night-time plume. The filters were stored in the manufacturer's packaging and only

opened on site. After sampling, they were kept refrigerated in multiple sealed plastic bags in a sealed plastic box. Pele's hair lava samples were obtained near the sampled Masaya plume. These were stored in an airtight polyethylene bag. After collection, the samples were transported to Cambridge and stored for 4 months. A 120° section of each filter and a portion of the lava sample were taken for Pb analyses. These were transported to Perth in multiple airtight polyethylene bags.

The analytical procedures used for TIMS analysis of Pb on aerosol-filter samples were those established by Bollhöfer et al. (1999). Samples were prepared in a clean room supplied with HEPA-filtered air. All chemistry was undertaken using Millipore MQ water and ultra-clean HCl, HNO₃, HF and HBr acids. The filter samples were leached in dilute HBr acid and purified in anion (Dowex AG 1-X8) exchange columns prior to TIMS analysis. The Pele's hair sample (total weight: 0.246 g) was initially leached with dilute HBr to remove any surface contamination, and then digested using a concentrated HCl/HF solution. The Pb was separated by anion exchange column chemistry prior to TIMS analysis. Aliquots of all samples were taken for the determination of Pb concentrations by Isotope Dilution Mass Spectrometry (IDMS) (Webster, 1960) using a ²⁰⁴Pb spike. The accuracy of the determined concentrations are ~5%, with the greatest uncertainty arising from the aliquotting process.

All samples were measured manually by TIMS (Fisons Instruments VG354) with most filter samples and all Pele's hair samples measured using a Faraday collector array. Samples were measured at a filament temperature of ~1300°C, with approximately 60 sets of isotope ratios collected for each sample. Mass fractionation was monitored by the repeated analysis of a 150 ng sample of NIST SRM 981 common Pb isotopic standard. A

more detailed description of the measurement procedure is given by Chisholm et al. (1995). Analytical blanks were determined using the methods described by Bollhöfer et al. (1999). Filament blanks varied between 18 pg and 34 pg while column blanks varied between 30 pg and 90 pg. A procedural blank of 102 pg Pb was found to be consistent with the sum of the column and filament blanks.

Other 120° sections of the same particle filters and the alkali impregnated filters in their entirety were extracted (0.25 cm³ of propan-2-ol and 9.75 cm³ of distilled deionized water for the hydrophobic teflon filters and 10 cm³ of distilled deionized water for the other filter types). Concentrations of soluble SO₄²⁻ were then determined by Dionex ion chromatography using gradient analysis with distilled deionised water and 0.1 M sodium hydroxide as eluents.

3. Results

Table 1 shows the results of Pb analyses on Pele's hair samples, sampled filter sections and blank filters. From the Pele's hair sample, the HBr leach removed 236 ng Pb and the HF digestion recovered 1032 ng Pb. As the Pb isotopic composition of the two samples were identical (²⁰⁶Pb/²⁰⁷Pb ~ 1.1965, ²⁰⁸Pb/²⁰⁷Pb ~ 2.46, ²⁰⁶Pb/²⁰⁴Pb~18.6), addition of these amounts gives a total Pb concentration of 5.15 µg g⁻¹. These magmatic compositions are in agreement with those reported for other Nicaraguan volcanic lavas (Patino et al., 2000, M.J. Carr data files from <http://www-rci.rutgers.edu/~carr/index.html>). Unused PC and PTFE filters were also analysed and found to contain ~120 pg Pb and ~410 pg Pb, respectively, with a Pb isotopic

composition of $^{206}\text{Pb}/^{207}\text{Pb}=1.14\pm 0.01$, $^{208}\text{Pb}/^{207}\text{Pb}=2.41\pm 0.01$ and $^{206}\text{Pb}/^{204}\text{Pb}=17.5\pm 0.3$. The Pb isotopic compositions observed in these blank filters were not compatible with those corresponding to their places of manufacture: the PTFE filters were made in Japan while the PC filters were produced in the US (pers. comm. Whatman Corp.). This discrepancy provided the first indication that the filters had been contaminated.

3.1 Contaminant Pb

Figure 1 shows the deviation between Pb signatures observed in the Pele's hair samples, the sampled filters and the blank filters. In the figure, the filter samples form a line deviating from the Pele's hair samples in the direction of the blank filters, indicating that they were influenced in varying quantities by Pb originating from the same source as that present on the blank filters. Most of the exposed filter samples displayed Pb isotopic compositions similar to those of the Pele's hair despite the influence of contamination. This was however not the case for the night-time-collected PC filter (12 μm , 20/AAFP/039) which showed a Pb isotopic composition more similar to those of the blank filters. A disproportionately large quantity of Pb was also measured on this filter compared to the daytime-collected PC filter sample further suggesting a larger proportion of contaminant Pb to be present on this filter. The Pb detected on the blank filters could have derived from the filter material, filter manufacturing processes and also Pb entrained on the filters during their storage. Additional Pb contamination could have been introduced when the sampled filters were cut into sections at Cambridge and during their subsequent transport to Australia. To represent the Pb signatures originating from these

various potential contamination sources, the Pb isotopic compositions of aerosols collected in Japan and the United States (Bollhöfer and Rosman, 2001), the United Kingdom (Bollhöfer et al., 1999) and Perth in Western Australia (Bollhöfer and Rosman, 2000) have been included in Figure 1.

In Figure 1, an input of Pb with a signature distinct from that observed in the Pele's hair samples will be observed as an isotopic deviation toward the Pb isotopic composition of that input (Rosman, 2001). Thus, a binary mixture of two isotopically different Pb sources will appear as a straight line between the two sources, with the location of a mixture on that line determined by the relative amount of each source within the mixture. As the quantity of contaminant Pb present on the filter increases, the Pb isotopic composition measured on the filter will become more like that of the contaminant Pb. The isotopic composition of all the exposed filters used to sample the plume fall approximately on a line between the Pele's hair samples and the blank filters suggesting that their Pb composition can be described as a binary mixture of magmatic and contaminant Pb. This is in accordance with previous assumptions that negligible Pb isotopic fractionation occurs upon the emission of volatile Pb from the magma or in plume processes thereafter. These isotopic systematics can be applied to the data to correct for the presence of contamination and so produce an accurate evaluation of the Pb fluxes from Masaya, assuming that the Pb contamination source is adequately characterised.

3.2 Corrected Pb fluxes

On the basis that the Pb present on the filters is a binary combination of contaminant Pb (with a signature identical to that observed in the blank filters) and Pb in the Pele's hair samples, isotope systematics were used to calculate the quantities of Pb originating from the Masaya plume. The results of these calculations are shown in Table 2 and confirm that contamination of the night-time-collected PC filter (20/AAFP/039) was much greater than that of the other filters. Note that these calculations are based on the evaluation that the Pb isotopic composition of the contamination input is identical to that found on the blank filters ($^{206}\text{Pb}/^{207}\text{Pb}$ ratio of 1.145). If the filters were in part contaminated during storage and sectioning in the UK or during transport to Australia, the $^{206}\text{Pb}/^{207}\text{Pb}$ signature of the contamination would be lower, between 1.06 and 1.12. To evaluate the effect of such a contamination source, potential Pb emissions from Masaya have also been calculated for a contaminant $^{206}\text{Pb}/^{207}\text{Pb}$ ratio of 1.08, as shown in Table 2.

Comparison of the proportions of volcanic Pb and SO_4^{2-} in the coarse and fine phase aerosol for each contamination scenario (shown in Table 3) suggest that contamination with Pb of composition $^{206}\text{Pb}/^{207}\text{Pb} = 1.145$ dominates. With this correction there is good consistency between the comparative Pb and SO_4^{2-} proportions in the coarse and fine grade aerosol in the daytime and night-time plume (daytime: 96% Pb and 97% SO_4^{2-} in fine; night-time: 68% Pb and 76% SO_4^{2-} in fine, Table 3). With the other contaminant correction the agreement is much worse for the night-time plume where major contamination corrections had to be made for the PC filter (night-time: 46% Pb and 76% SO_4^{2-} in fine, Table 3). The larger proportion of Pb and SO_4^{2-} collected on the 12 μm PC filter from the condensed night-time plume of Masaya, compared to that collected in the daytime can be explained as being due to enhanced particle growth in the condensed

(much more cloud-like in appearance) night-time plume. Hence more Pb and SO_4^{2-} bearing particles are in the $> 2.5 \mu\text{m}$ particle size fraction by the point of measurement at night.

These masses of volcanogenic Pb (corrected for contamination) were used in conjunction with the amounts of SO_2 present on the gas filters to calculate the $\text{Pb}/\text{S}_{(\text{g})}$ ratios and Pb fluxes presented in Table 3. A mean $\text{Pb}/\text{S}_{(\text{g})}$ ratio of 1.2×10^{-5} (contaminant evaluated as $^{206}\text{Pb}/^{207}\text{Pb} = 1.145$) was calculated. Sulphur dioxide flux measurements made during the same field campaign were approximately 5 kg s^{-1} (McGonigle et al., 2002) yielding a mean Pb flux from Masaya of approximately $3.1 \times 10^{-5} \text{ kg s}^{-1}$ (1.0 ton yr^{-1}).

4. Discussion

Lead isotopic compositions measured in the Masaya plume and in Pele's hair samples are generally similar and also agree with previously reported Pb isotopic compositions in Central American volcanics (from M.J. Carr data files from <http://www-rci.rutgers.edu/~carr/index.html>). Isotopic analysis of Pb in the lava and plume from Masaya volcano, Nicaragua, has shown that the deviations of aerosol Pb from that of the magma can be accounted for by inputs of Pb contamination with an isotopic signature similar to that observed in the filter blanks. This enabled an evaluation of the contaminant Pb present in the filter samples. The results showed that up to 28% of the total Pb found on the filters might be due to contamination (calculated from Table 2) and highlighted the importance of maintaining protocols for the minimisation of sample contamination when sampling aerosols for Pb analyses. The Pb isotopic signatures observed in the filter

blanks were primarily attributed to the filter material/manufacturing process, for which a $^{206}\text{Pb}/^{207}\text{Pb}$ ratio of 1.145 was assigned. It has been shown that even if a substantial proportion of contamination occurred during the storage, sectioning and measurement of the filters, for which a more representative $^{206}\text{Pb}/^{207}\text{Pb}$ ratio would be between 1.06 and 1.12, the volcanic Pb fluxes reported here would have been underestimated by a maximum of approximately 30%.

Volcanogenic lead fluxes from Masaya, determined from the contamination-corrected aerosol filter results, are 1.0 ton yr^{-1} . These fluxes are lower but comparable to the reported emissions from Kilauea, Hawaii, of 12 ton yr^{-1} (Hinkley et al., 1999) and represent between about 0.02 and 0.13 % of the estimated annual volcanic flux (calculated from the range of flux estimates, $0.9 - 4.1 \text{ kton yr}^{-1}$, compiled in Mather et al., 2003). We have shown that the majority of the Pb (96% in the daytime plume and 68% in the night-time plume) is carried in the finer aerosol fraction which (especially if it is in the accumulation mode $\sim 0.1 - 2 \mu\text{m}$) will tend to have an elevated atmospheric lifetime. The $\text{Pb}/\text{S}_{(\text{g})}$ ratio quoted for Kilauea is 3.3×10^{-5} which is not very different to that from Masaya (mean: 1.2×10^{-5}) suggesting that it is the lower SO_2 flux from Masaya that accounts for the lower Pb flux calculated ($\sim 5 \text{ kg s}^{-1}$ for Masaya, McGonigle et al. 2002, compared to the SO_2 flux used by Hinkley et al., 1999 of $\sim 20 \text{ kg s}^{-1}$ for Kilauea). Other volcanoes in the Central American arc can be very significant emitters of volatiles to the atmosphere (e.g. Popocatépetl volcano, Mexico, with SO_2 flux at times recorded to be as high as 150 kg s^{-1} ; Delgado-Granados et al., 2001) and so may also emit large amounts of Pb. The data reported here should serve as a preliminary evaluation of the Pb flux from

volcanoes in the Central American arc, but it will be necessary to conduct similar studies on other volcanoes in order to evaluate a representative Pb flux from the entire arc.

Acknowledgements

The Australian Research Council (grant A39938047) supported this research. PV thanks K.J.R. Rosman, G. Burton and colleagues in the TIMS laboratory of the John de Laeter Centre of Mass Spectrometry. TM thanks D. M. Pyle, for helpful discussion and his assistance in the field, C. Oppenheimer, A. G. Allen and A. J. S. McGonigle for help collecting the samples and the Natural Environment Research Council UK for financial support. This work was initiated following discussions at the 2002 European Research Course on Atmospheres in Grenoble and the authors gratefully thank C.F. Boutron and M. Poinsoot for their organisation and sustenance of ERCA. We also thank T. K. Hinkley for his constructive criticism of an earlier version of this manuscript.

References

- Allard, P., A. Aiuppa, H. Loyer, F. Carrot, A. Gaudry, G. Pinte, A. Michel, G. Dongarrà, 2000. Acid gas and metal emission rates during long-lived basalt degassing at Stromboli volcano, *Geophys. Res. Lett.*, *27*, 1207-1210.
- Allen, A.G., Baxter, P.J., Ottley, C.J., 2000. Gas and particle emissions from Soufrière Hills Volcano, Montserrat, West Indies: characterization and health hazard assessment. *Bulletin of Volcanology* *62*, 8-19.
- Bollhöfer, A., Chisholm, W., Rosman, K.J.R., 1999. Sampling aerosols for lead isotopes on a global scale. *Analytica Chimica Acta* *390*, 227-235.
- Bollhöfer, A.F., Rosman, K.J.R., 2000. Isotopic source signatures for atmospheric lead: The Southern Hemisphere. *Geochimica et Cosmochimica Acta* *64*, 3251-3262.

Bollhöfer, A.F., Rosman, K.J.R., 2001. Isotopic source signatures for atmospheric lead: The Northern Hemisphere. *Geochimica et Cosmochimica Acta* 65, 1727-1740.

Chisholm, W., Rosman, K.J.R., Boutron, C.F., Candelone, J.-P., Hong, S., 1995. Determination of lead isotopic ratios in Greenland and Antarctic snow and ice at picogram per gram concentrations. *Analytica Chimica Acta* 311, 141-151.

Delgado-Granados, H., Cardenas Gonzalez, L., Piedad Sanchez, N., 2001. Sulfur dioxide emissions from Popocatepetl volcano (Mexico): case study of a high-emission rate, passively degassing erupting volcano. *Journal of Volcanology and Geothermal Research* 108, 107-120.

Gauthier, P. J., M-F. Le Cloarec, 1998. Variability of alkali and heavy metal fluxes released by Mt Etna volcano, Sicily, between 1991 and 1995, *J. Volcanol. Geotherm. Res.*, 81, 311 – 326.

Graf, H-F., B. Langmann, J. Feichter, 1998. The contribution of Earth degassing to the atmospheric sulfur budget, *Chem. Geol.*, 147, 131-145.

Hinkley, T.K., 1991. Distribution of metals between particulate and gaseous forms in a volcanic plume. *Bulletin of Volcanology* 53, 395-400.

Hinkley, T.K., Lamothe, P.J., Wilson, S.A., Finnegan, D.L., Gerlach, T.M., 1999. Metal emissions from Kilauea, and a suggested revision of the estimated worldwide metal output by quiescent degassing of volcanoes. *Earth and Planetary Science Letters* 170, 315-325.

Lambert, G., M-F. Le Cloarec, M. Pennisi, 1988. Volcanic output of SO₂ and trace metals: a new approach, *Geochim. Cosmochim. Acta*, 52, 39-42.

Le Cloarec, M-F., B. Marty, 1991. Volatile fluxes from volcanoes, *Terra Nova*, 3, 17-27.

Mather, T.A., Pyle, D.M., Oppenheimer, C., 2003. *Tropospheric Volcanic Aerosol in Volcanism and the Earth's Atmosphere*, Geophysical Monograph (in press).

Matsumoto, A., Hinkley, T.K., 2001. Trace metal suites in Antarctic pre-industrial ice are consistent with emissions from quiescent degassing of volcanoes worldwide. *Earth and Planetary Science Letters* 186, 33-43.

McGonigle, A.J.S., Oppenheimer, C., Galle, B., Mather, T.A., Pyle, D. M., 2002. Walking traverse and scanning DOAS measurements of volcanic gas emission rates. *Geophysical Research Letters*, 29(20), 46-1 - 46-4, doi: 10.1029/2002GL015827.

Monna, F., Aiuppa, A., Varrica, D., Dongarra, G., 1999. Pb Isotope Composition in Lichens and Aerosols from Eastern Sicily: Insights into the Regional Impact of Volcanoes on the Environment. *Environmental Science and Technology* 33, 2517-2523.

Nriagu, J.O., 1989. A global assessment of natural sources of atmospheric trace metals. *Nature* 338, 47-49.

Patino, L.C., Carr, M.J., Feigenson, M.D., 2000. Local and regional variations in Central American arc lavas controlled by variations in subducted sediment input. *Contributions to Mineralogy and Petrology* 138, 265-283.

Rosman, K.J.R., Chisholm, W., Hong, S., Candelone, J.-P., Boutron, C. F., 1997. Lead from Carthaginian and Roman Spanish mines isotopically identified in Greenland ice dated from 600 B.C. to 300 A.D. *Environmental Science and Technology* 31, 3413-3416.

Rosman, K.J.R., 2001. Natural isotopic variations in lead in polar snow and ice as indicators of source regions, in: *Environmental contamination in Antarctica: A challenge to analytical chemistry* (Eds. Caroli, S., Cescon, P., and Walton, D. W. H.), pp.87-106. Elsevier Science B.V., New York.

Stevenson, D. S., C. E. Johnson, W. J. Collins, R. G. Derwent, The tropospheric sulphur cycle and the role of volcanic SO₂, in *Volcanic Degassing* edited by C. Oppenheimer, D. M. Pyle and J. Barclay, *Geol. Soc. Lond. Spec. Pub.*, 213, in press, 2003.

Sun, S.S., Hanson, G.H., 1975. Origin of Ross Island Basanitoids and Limitations upon the Heterogeneity of Mantle Sources for Alkali Basalts and Nephelinites. *Contributions to Mineralogy and Petrology* 52, 77-106.

Vallelonga, P., Van de Velde, K., Candelone, J.-P., Morgan, V.I., Boutron, C.F., Rosman, K.J.R., 2002. The lead pollution history of Law Dome, Antarctica, from isotopic measurements on ice cores: 1500 AD to 1989 AD. *Earth and Planetary Science Letters* 204, 291-306.

Webster, R.K., 1960. Mass spectrometric isotope dilution analysis, in: *Methods in geochemistry* (Eds. Smales, A. A. and Wager, L. R.), pp.202-246. Interscience, New York.

Zreda-Gostynska, G., P. R. Kyle, D. L. Finnegan, K. M. Prestbo, 1997. Volcanic gas emissions from Mount Erebus and their impact on the Antarctic environment, *J Geophys. Res.*, 102, 15039-15055.

Table 1. Results of TIMS analysis of Pele's hair and filter samples from Masaya volcano.

The results have been corrected for procedural blanks as described in the text.

	$^{206}\text{Pb}/^{207}\text{Pb}$	\pm^a	$^{208}\text{Pb}/^{207}\text{Pb}$	\pm^a	$^{206}\text{Pb}/^{204}\text{Pb}$	\pm^a	Total Pb (ng)	Lead concentration ^b
Pele's Hair ^c								(ng g ⁻¹)
HBr leach	1.1959	0.0006	2.4618	0.0013	18.59	0.03	236	956
HF digestion	1.1970	0.0006	2.4635	0.0012	18.61	0.02	1032	4191
Teflon filters								(ng m ⁻³)
PTFE Filter 010	1.1908	0.0006	2.4584	0.0013	18.55	0.03	21.1	70
PTFE Filter 039	1.1891	0.0008	2.4514	0.0017	18.31	0.03	6.0	20
Polycarbonate filters								(ng m ⁻³)
PC Filter 010	1.1880	0.0009	2.4468	0.0019	18.33	0.03	0.96	3.2
PC Filter 039	1.1577	0.0006	2.4302	0.0013	18.06	0.03	9.7	32
Blank Filters								
PC Filter	1.146	0.007	2.403	0.012	17.57	0.27	0.14	
PC Filter	1.135	0.039	2.396	0.010	17.27	0.02	0.12	
PTFE Filter	1.153	0.002	2.420	0.010	17.80	0.07	0.62	
PTFE Filter	1.146	0.001	2.412	0.004	17.65	0.02	0.21	

^aUncertainties in the isotope ratios are 95% confidence intervals.

^bLead concentrations were determined to an accuracy of 5%.

^cThe mass of the analysed Pele's hair sample was 0.246 g.

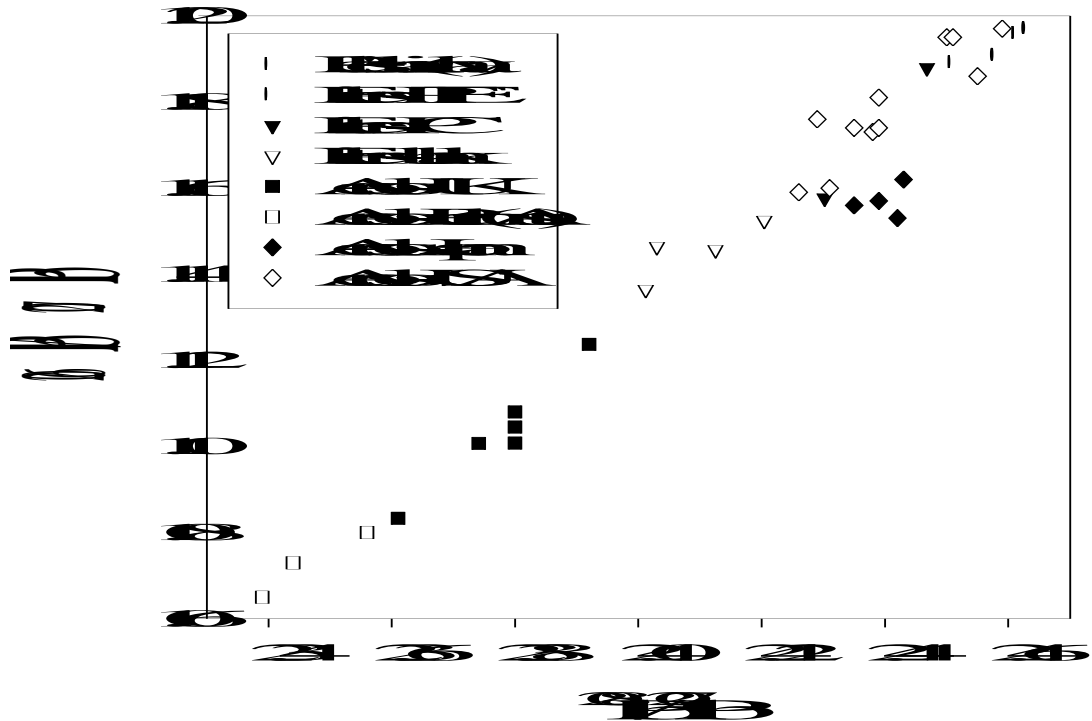
Table 2. Evaluation of the quantities of volcanic Masaya Pb and contaminant Pb present on polytetrafluoroethylene (PTFE) and polycarbonate (PC) filter samples using Pb isotope systematics. This calculation assumes the measured filter values represent a binary mixture of Masaya Pb ($^{206}\text{Pb}/^{207}\text{Pb}=1.196$) and contaminant Pb ($^{206}\text{Pb}/^{207}\text{Pb}=1.145$ as measured on blank filters or $^{206}\text{Pb}/^{207}\text{Pb}=1.08$ representing contamination during storage and measurement).

Sample	Measured values		Contamination $^{206}\text{Pb}/^{207}\text{Pb} = 1.145$				Contamination $^{206}\text{Pb}/^{207}\text{Pb} = 1.08$			
			Contaminant Pb		Volcano Pb		Contaminant Pb		Volcano Pb	
	Total Pb (ng)	$^{206}\text{Pb}/^{207}\text{Pb}$	Amount (ng)	% of total Pb	Amount (ng)	Conc. in air (ng m ⁻³)	Amount (ng)	% of total Pb	Amount (ng)	Conc. in air (ng m ⁻³)
PTFE Filter 010	21.1	1.1905	2.3	11	18.8	63	1.0	5	20.1	67
PTFE Filter 039	6.0	1.1882	0.9	15	5.1	17	0.4	7	5.6	19
PC Filter 010	0.96	1.1860	0.2	20	0.8	2.6	0.1	9	0.9	3
PC Filter 039	9.7	1.1577	7.3	75	2.4	8.0	3.2	33	6.5	22

Table 3. Lead/S ratios in plume emissions and Pb fluxes from Masaya, based on the Masaya SO₂ flux value of approximately 5 kg s⁻¹ reported by McGonigle et al. (2002). Aerosols collected on the 12 μm PC filters are evaluated as the >2.5 μm particle size fraction (C), while aerosols collected on the 2.5 μm PTFE filters are evaluated as the <2.5 μm particle size fraction (F).

Sample	Contamination ²⁰⁶ Pb/ ²⁰⁷ Pb = 1.145					Contamination ²⁰⁶ Pb/ ²⁰⁷ Pb = 1.08						
	% Pb		% SO ₄ ²⁻		Pb/S _(g)	Pb Flux / kg s ⁻¹	% Pb		% SO ₄ ²⁻		Pb/S _(g)	Pb Flux / kg s ⁻¹
	C	F	C	F			C	F	C	F		
Daytime filters (010)	4	96	3	97	1.0 x 10 ⁻⁵	2.4 x 10 ⁻⁵ (0.8 ton yr ⁻¹)	4	96	3	97	1.0 x 10 ⁻⁵	2.6 x 10 ⁻⁵ (0.8 ton yr ⁻¹)
Night-time filters (039)	32	68	24	76	1.5 x 10 ⁻⁵	3.7 x 10 ⁻⁵ (1.2 ton yr ⁻¹)	54	46	24	76	2.4 x 10 ⁻⁵	6.0 x 10 ⁻⁵ (1.9 ton yr ⁻¹)
Mean					1.2 x 10⁻⁵	3.1 x 10⁻⁵ (1.0 ton yr⁻¹)					1.7 x 10⁻⁵	4.3 x 10⁻⁵ (1.3 ton yr⁻¹)

Figure 1. Lead isotopic compositions measured on aerosol filters used to sample the Masaya volcano plume, Pele's hair (lava) samples also from Masaya and blank filters. Also included are Pb isotopic compositions for aerosols collected in the United States and Japan (Bollhöfer and Rosman, 2001), the United Kingdom (Bollhöfer et al., 1999) and Perth in Western Australia (Bollhöfer and Rosman, 2000). The influence of contamination is most clearly evident in one of the polycarbonate (PC) filters, for which the Pb isotopic composition is similar to those observed in the blank filters.



Memo

To: The PhD Supervisor (Professor K.J.R. Rosman)
The PhD Committee Chairperson (Dr. R.D. Loss)

I have updated my submitted PhD thesis following receipt of the examiners' comments, the changes being described in the following pages. As the thesis was passed Unconditionally, I have chosen to not follow some of the recommendations of the examiners. In these cases, I provide an explanation for doing so.

Yours sincerely,

Paul Travis Vallelonga

Changes made to the thesis following examiners' comments:

Examiner 1

No changes made

Examiner 2

General changes:

All usage of the words 'lead' and 'Pb' have been amended to follow the convention that 'Pb' is normally used in the text, with the exception that 'Lead' is used at the beginning of a sentence. Where an element is first mentioned, its chemical symbol is given in parentheses. This usage has been adopted for all references to elements in the thesis as it is used in the publications.

Notes have been added on pages vi and vii to indicate the current status of research articles that were in submission or in press at the time of writing the thesis.

Chapter 2 – The location of the methods section has not been changed. This section was placed before the literature review so as to emphasise the various technical procedures required to reliably evaluate Pb concentrations and Pb isotopic compositions in Antarctic snow and ice. A knowledge of the current procedures and considerations is of benefit to fully appreciating the enormous improvements in this field which occurred during the past four decades.

All in-text references to figures have been, where necessary, changed to a capital 'F'.

Chapter 3 – The literature review is admittedly extensive. In consideration of Examiner 3's response to the literature review, I do not think that any changes to the section, beyond typographical corrections, are warranted. The structure and content of the literature review was, in part, a result of the dearth of review articles in the literature adequately reporting the historical development of this particular field of science.

Chapter 4 – The *exact same* questions posed in the results and discussion section have been incorporated into the conclusion of the literature review. The questions included at the conclusion of the literature review were intended to summarise the main research topics that are still to be properly addressed, while those given in the results and discussion were intended to focus the discussion, as noted by the examiner. As such, there remain more questions at the end of the literature review than could be addressed by this thesis.

The Coats Land data from Planchon et al. (2002) was not included in the literature review because it was the subject of an unpublished PhD thesis at the time when this thesis was written. As such, it would have been inappropriate to include the work in the literature as it had not been peer-reviewed and hence had not been accepted into the body of scientific literature. The sources of the data for Coats Land and Victoria Land and the conditions under which they were included in the thesis are described in the thesis preamble (page vi). It was the preference of Planchon et al. (2002) to use a three point moving average to indicate trends in the Coats Land data.

Barium concentrations do vary prior to 1900 AD, between 0.67 pg/g and 3.21 pg/g, as described in section 4.5. The principal source of Ba in Antarctica is the deposition of wind-blown rock and soil dust, so this variation represents natural fluctuations in the efficiency with which dust particles are transported from the continents of the Southern Hemisphere to Law Dome. Natural fluctuations are also observed in the concentration of Pb. The period observed in detail, from 1530 to 1989 AD, was not sufficiently long to determine the extent to which dust inputs have varied throughout the Holocene, but was intended to incorporate a sufficiently long time period so as to allow reliable ‘background’ Pb and Ba concentrations and Pb isotopic compositions to be established for comparison to more recent, polluted, Pb concentrations and Pb isotopic compositions. As described in section 1.3 of the introduction, there are various natural sources of Pb, so Ba is the more reliable indicator of dust inputs to Law Dome. It is also noted that the reliability of Ba as an indicator of crustal inputs has been previously demonstrated by Patterson and Settle (1987, *Mar. Chem.* v.22 pp.137-162).

Chapter 5 – The conclusions section has been altered. The structure has been modified to more closely reflect the various research objectives described in section 1.7. Particularly, additional information has been given regarding the sample preparation procedures developed, and the evaluation of various natural sources of Pb deposited in Antarctica.

Minor corrections:

Page i – no change has been made in regard to this comment. To elaborate the sources contributing to the ion source would require description and definition of the filament blank and sample preparation procedure. I consider such changes to be inappropriately detailed for the thesis abstract.

Page 5 – recommended change made (Bollhöfer).

Page 7 – ‘are been’ was changed to ‘have been’

Page 8 – recommended changes made (Bollhöfer).

Page 17 – The use of O isotope variations to date ice cores is described in the introduction, section 1.5 (pages 10 and 11)

Page 19 – recommended change made (accuracy).

Page 20 – recommended change made (changed)

Page 21 – recommended changes made.

Page 22 – recommended changes made.

Page 23 – It is noted in the text that seasonal variations in Pb concentrations may bias results if a full-year of deposition is not collected for each sample. It follows, then, that if a collected sample contains two winter depositions of snow and one summer deposition of snow, then the

concentration measured in each sample will be biased toward the concentration of snow in the winter. This does not appear to be a great problem in Antarctica, but it can produce significant biases in Greenland, where the predominant continental sources of aerosols deposited in the snow varies seasonally. This problem was first recognized by Murozumi et al. (1969).

Page 24 – the term “approximately similar” has been changed to “standardised”, to indicate that the collection of each core section was similar by design.

Page 25 - recommended change made.

Page 27 – A sentence has been added to note that the polyethylene bridge was cleaned in the same manner as the other ‘high cleaning-priority’ apparatus, such as the collecting scoops.

Page 28 -The recommended change has been made (positive pressure) and the sentence has been modified.

Page 29 – the recommended change has been made.

Page 31 – The term ‘Laboratory water’ has been changed to ‘Filtered deionised water’ and the sentence has been altered for clarity. The use of an IBIS RO system and an USFilter water polishing system for the femtolab ultrapure water supply has been elucidated.

Page 32 – The acronym UPW has been defined at the end of page 31.

Page 33 – It has been noted in the text that a two-decimal place electronic balance was used to weigh the aliquotted samples.

Page 34 – As described in the research article, it was observed that the storage of acidified UPW in a polyethylene bottle leads to an increase in the Pb concentration in the solution, rather than a decrease, indicating that the Pb is preferentially retained in the liquid matrix rather than the plastic polymer matrix. I think it most likely that the Pb ions are bound to free nitrate ions in the acidified solution, but have not investigated this process further.

Page 35 – The term ‘sector magnet’ has been changed to ‘magnetic sector’. Approximate filament temperatures used during degas and measurement were also added.

Page 36 – The first part of the sentence has been rewritten. It now reads ‘In the VG354, ions are liberated from the solid sample by thermal ionisation...’.

Page 37 – The first sentence of the last paragraph has been changed to ‘...accelerated through an electric potential...’. The following sentence has also been changed to ‘...energy E imparted to the ions...’. The possibility of relativistic effects occurring to the ions in the flight chamber had not been considered.

Page 38 – Due to the symmetry of the ion optics of the VG354, the size of the ion beam when it enters the magnetic sector is equal to its size when it leaves the magnetic sector. Hence, the geometry of the VG354 allows a larger beam (allowing better counting statistics) to be analysed compared to that offered by other (earlier) mass spectrometer geometry configurations of similar resolving power.

Page 39 – The recommended changes have been made.

Page 40 – The sentence regarding the use of the Daly collector to measure small ion currents has been moved closer to the start of the paragraph. In response to the aside, the accelerating potential is not changed during measurement as this would introduce biases into the measurement, such as variations in the ion beam shape. Instrumental mass fractionation has been described in more detail.

Page 41- The recommended change has been made (amu to u). The sentence regarding measurement precision has been clarified.

Page 43 – The sentence has been modified to accommodate the examiner’s comments (ion currents). The word ‘the’ has been added in the middle of the first paragraph. The IDMS technique is recognised by the US National Institute of Standards and Technology (NIST) and described by them as a ‘definitive’ analytical technique. This description means that it is highly accurate and that all uncertainties involved in the technique are fully traceable. The word ‘naturally’ has been added to the last sentence on the page.

Page 58 – The second sentence has been altered. ‘Earth’ has been capitalised.

Page 63 – The recommended changes have been made.

Page 64 – For IDMS, the isotope with the smallest natural abundance is preferred if one must use a naturally occurring isotope of the element to be measured, but it is not essential. Financial constraints are just one of the many potential factors that influence the eventual choice of what tracer isotope is used. The recommended changes lower down the page have been made.

Page 76 – This is the first time LGM is used.

Page 82 – The recommended changes have been made.

Page 87 – The recommended changes have been made. The sentence regarding the emission of Pb and S from volcanoes has been modified.

Page 88 – Where necessary ‘tons’ has been changed to the intended, metric, ‘tonnes’. The SI-approved unit of radioactive decay is the Becquerel (Bq), which is measured as s^{-1} . The term ‘dpm’, decays per minute, is therefore not a SI-approved unit, but is often used. The Curie (Ci) is another commonly used, non-SI approved measure of radioactive decay, where 1 Ci is equal to 3.7×10^{10} Bq.

Page 89 – The text has been corrected as recommended. The mechanism hypothesised for the emission of Pb from the oceans has been elaborated. Elevated Pb concentrations in the surface layers of the oceans are due to atmospheric fallout of anthropogenic Pb.

Pages 95+ - I do not understand what change the examiner is suggesting.

Page 96 – The recommended change has been made

Page 98 – The different symbols used in the plot have been defined.

Page 100 – The recommended change was made

Page 101 – The full reference has been given. The sentence regarding Pb isotopes has been rewritten and the other recommended changes have been made.

Page 102 – This sentence has been altered for clarity.

Page 105 – The sentence has been modified.

Page 108 – The recommended modifications have been made.

Page 113 – ‘Antarctic’ has been changed to ‘Arctic’.

Page 114 – The final statement has been clarified.

Page 115 – The table has been updated.

Page 134 – Peroxide is used as a dating tool. The concentration of peroxide in snow can be related to the quantity of sunlight (UV radiation) in the polar environment, and so it varies with maxima in winter and minima in summer. I am not sure if MSA is oxidised by peroxide, but I do not think that this poses a major problem to the integrity of the snow/firn core records.

Page 140 – The figures have been corrected.

Page 146 – Recommended change made.

Page 156 – Recommended changes made.

Page 158 – Additional explanation of Table 3.5 has been included on page 157.

Page 164 – The symbols have been defined in the caption of Figure 3.32.

Page 202 – This paper has now been published, the error was corrected during publication. It is too late to correct the comment regarding Mont Blanc.

Page 224 – The figures were not changed – in the final version of the thesis they will be printed in colour, in which the most recent part of the record is clearer.

Page 229 – The sentences have been corrected.

Page 234 – I have received limited information regarding the dating of the Victoria Land samples. All of the available information has been included in the thesis.

Page 235+ - The figure legends have been corrected.

Page 245 – recommended change made.

Page 258 – ‘normal background levels of volcanism’ means those levels of volcanogenic Pb input which are normally observed throughout the Holocene – those usually due to quiescent degassing of volcanoes. It means that the samples were not affected by the volcanic activity observed earlier at about mid-1814 and later after 1816 AD. Current research (Such as that carried out on the Vostok and Dome C ice cores) indicates that there are several climatic interrelationships potentially occurring during the glacial-interglacial transitions, such as iron fertilisation of the oceans from

increased dust content in the air, increased dust content in the air related to aridification and variations in climate and vegetation and the possibility of climate and vegetation variation due to climate change, which can occur from carbon drawdown of the oceans as a response to iron fertilisation from dust... of course this is a circular argument but the point I am trying to emphasise is that the potential geochemical/climatic/atmospheric variations resulting from a three-fold increase in atmospheric dust content cannot be easily guessed at and are best not speculated upon within the context of the article.

Page 259 – The samples analysed in the Tambora study were sampled at high resolution (considering it was a manual ‘chiselling’ technique) so this decontamination procedure was definitely unroutine. The Pb isotope data do indicate that there is a good chance that these samples were contaminated, even though they do not contain particularly high Pb concentrations. Preliminary ICP-MS results indicate that the samples were contaminated for other elements also.

Page 272 – The text has been checked and the 2- charge has been appended to Sulphate ions.

Page 274 – The text in all cases has been changed to ‘yr’.

Examiner 3

P20 – recommended change made. The type of analytical grade reagent has been specified as BDH AnalaR[®] grade analytical reagent.

P26 – recommended change made

P31 – IBIS and USFilter are both trademarks and have been labelled as such. They have been further described as Reverse Osmosis water purification and water polishing systems, respectively.

P32 – all references to Teflon have been capitalised.

P52 – Yes, the paper has already been published so it cannot, unfortunately, be changed.

P63 – recommended correction made.

P90 – Where they appear, a space has been put between the ‘less than equal’ symbol and the following number.

P229 – The recommended change has been made.